DENSELY PACKED YEAST:
A TOOL TO STUDY EVOLUTION OF GROUP DYNAMICS AND TO ENHANCE BIOMANUFACTURING.

A Dissertation
Presented to
The Academic Faculty

by

Jordan Gulli

In Partial Fulfillment
of the Requirements for the Doctor of Philosophy in Biology
in the School of Biological Sciences

Georgia Institute of Technology
December 2019

DENSELY PACKED YEAST:
A TOOL TO STUDY EVOLUTION OF GROUP DYNAMICS AND TO ENHANCE BIOMANUFACTURING.

Approved by:

Dr. Frank Rosenzweig, Advisor
School of Biology
Georgia Institute of Technology

Dr. Francesca Storici
School of Biology
Georgia Institute of Technology

Dr. William Ratcliff
School of Biology
Georgia Institute of Technology

Dr. Peter Yunker
School of Physics
Georgia Institute of Technology

Dr. Brian Hammer
School of Biology
Georgia Institute of Technology

Dr. Arthur Kruckeberg
Senior Research Scientist
Trait Biosciences

Date Approved: August 03, 2019

To my parents, who always knew I could do it. And to Alex, who helped me get there.

ACKNOWLEDGEMENTS

I would like to first thank all those who have provided me with exemplary scientific training over the years, including mentors Dr. Amy Schmid, Dr. Alexander Pavlov, Dr. William Ratcliff, and Dr. Frank Rosenzweig, as well as less formal sources of instruction, including Kriti Sharma, Jennifer Pentz, Shane Jacobeen, and Emily Cook. I would also like to express gratitude for my sources of funding, including NSF Graduate Research Predoctoral Fellowship DGE-1148903, NSF iCorps 1743464 and the Georgia Research Alliance (GRA.Vl18.B16).

Last, but not least, I would like to thank all those whose support has been less tangible, though no less important: my parents Mick and Karen Gulli, my godparents Buzz and Rho Griffin, Alexander Radek, and, of course, Emma.

TABLE OF CONTENTS

ACKNOWLEDGEMENTS **iv**

LIST OF TABLES **ix**

LIST OF FIGURES **x**

LIST OF SYMBOLS AND ABBREVIATIONS **xii**

SUMMARY **xiv**

CHAPTER 1. Introduction **1**
1.1 Group formation **1**
1.2 A brief history of gasoline and ethanol production **5**
1.3 Current gasoline and ethanol demand **8**
1.4 An overview of modern ethanol production **9**
1.5 Cellulosic ethanol **11**
1.6 Political regulations impact ethanol production **13**
1.7 Technical difficulties associated with cellulosic ethanol production **14**
1.8 Project goals **16**

CHAPTER 2. Evolution of altruistic cooperation among nascent multicellular organisms Error! Bookmark not defined.
2.1 Introduction **17**
2.2 Methods **21**
2.2.1 Yeast culture 21
2.2.2 Aggregate discovery and creation of t227b.15 21
2.2.3 Evolving aggregate formation from an ancestral snowflake yeast 24
2.2.4 Measuring cluster size 25
2.2.5 Measuring cell death 25
2.2.6 Aggregate formation, cell death, and cluster size in ancestral strains 25
2.2.7 Heritability of aggregate formation 26
2.2.8 Aggregate composition 26
2.2.9 Cell death and aggregate formation 27
2.2.10 Divergent selection experiment 28
2.2.11 Settling speed 29
2.2.12 Aggregate formation and survival 29
2.2.13 Determining if aggregates discriminate against unicellular yeast 30
2.2.14 Determining if aggregate formation is a common good 30
2.3 Results **31**
2.3.1 Snowflake yeast evolved a novel form of cooperation under strong settling-rate selection 31
2.3.2 De novo evolution of aggregation 35
2.3.3 Aggregates form in snowflake yeast with high levels of cell death 35
2.3.4 Heritability of aggregate formation 36

2.3.5 Proteins are the main structural component of aggregates 39
2.3.6 Aggregates result from cell death 39
2.3.7 Aggregate formation is advantageous when fast settling is favoured 41
2.3.8 Aggregates settle faster than individual clusters, increasing survival 43
2.3.9 Aggregates are a common good 45
2.4 Discussion 46

CHAPTER 3. Diverse conditions support near-zero growth in yeast: implications for the study of cell lifespan 51
3.1 Introduction 51
3.2 Chronological aging in starved planktonic cultures 53
3.3 Chronological aging in yeast colonies 55
3.3.1 Cells in a colony display slower growth, and higher viability than aging planktonic cells 55
3.3.2 Yeast in aging colonies become physiologically-differentiated 57
3.3.3 Cell stratification benefits some cell types at the expense of others, contributing to colony longevity 60
3.3.4 Giant colonies as a model to study aging and cancer 62
3.4 Chronological aging in continuous culture: the retentostat 63
3.4.1 Retentostat growth and viability 64
3.4.2 Transcriptomics 64
3.4.3 Proteomics 66
3.4.4 Starvation vs. caloric restriction 67
3.4.5 Yeast retentostats as a model for the study of chronological aging 69
3.5 Chronological aging in continuously-fed immobilized cell reactors 70
3.5.1 Industrial applications 71
3.5.2 Potential for social interactions among encapsulated yeast 72
3.5.3 Physiology and transcriptomics 73
3.5.4 Proteomics and metabolomics 78
3.5.5 ICRs for the identification of anti-aging compounds 79
3.5.6 Encapsulated, continuously-fed yeast as a model for studying chronological lifespan 80
3.6 Conclusions and Future Directions 81

CHAPTER 4. Matrices (re)loaded: Durability, viability and fermentative capacity of yeast encapsulated in beads of different composition during long-term fed-batch culture 84
4.1 Introduction 84
4.2 Materials and Methods 88
4.2.1 Strains and culture conditions 88
4.2.2 Preparation of encapsulation matrices and cell encapsulation 89
4.2.3 Estimation of Young's modulus, viscosity, and bead size via Universal Testing Machine 91
4.2.4 Estimation of wet weight bead mass 92
4.2.5 Fermentative capacity 92
4.2.6 Cell enumeration and cell viability 93
4.2.7 Heat shock tolerance 95

4.2.8 Statistical analyses 96
4.3 Results and Discussion 96
4.3.1 Young's modulus and viscosity of alginate beads declined over time 96
4.3.2 Bead size and mass increased over time 102
4.3.3 Ethanol yield (g/g) from dextrose varied among treatments 104
4.3.4 Following outgrowth, total cell number was similar across encapsulated and planktonic cultures 107
4.3.5 Cell escape increased over time, except in Pr beads 109
4.3.6 Cell viability declined over time in both encapsulated and planktonic cell cultures 111
4.3.7 Encapsulated cells are more heat-shock resistant than planktonic cells, but no one matrix confers greater heat-shock resistance than another 115
4.3.8 Encapsulation matrices vary in cost 117
4.4 Conclusions 119

CHAPTER 5. Encapsulation increases genome stability of yeast dikaryons produced via protoplast fusion 120
5.1 Introduction 120
5.2 Materials and Methods 123
5.2.1 Strains and culture conditions 123
5.2.2 Protoplast formation and fusion 126
5.2.3 Verification of dikaryons using PI staining 127
5.2.4 Verification of dikaryons using DAPI staining 128
5.2.5 Preparation of encapsulation matrices and cell encapsulation 128
5.2.6 Cell enumeration, viability, and population dynamics 130
5.2.7 Fermentation parameters 132
5.2.8 Statistical analyses 133
5.3 Results and Discussion 133
5.3.1 Verification of dikaryons 134
5.3.2 Encapsulation impacts cell viability over repeated fed-batch culture 134
5.3.3 Encapsulation reduces the accumulation of biomass 136
5.3.4 Encapsulation enhances genetic stability 138
5.3.5 Encapsulation increases ethanol production on a per-cell basis 142
5.4 Conclusions 146

CHAPTER 6. Discussion 148
6.1 Overview 148
6.2 Aggregate formation is temporary 149
6.3 Aggregates are unlikely to represent a new level of selection 150
6.4 Aggregates lack a mechanism of fitness alignment 152
6.5 Suggestions for future work with aggregates 153
6.6 Feasibility of using encapsulated yeast at industry scales 155
6.7 Suggestions for future experiments on the use of encapsulated yeast for conventional ethanol production 158
6.8 Genome instability: the problem 160
6.9 Encapsulation as a means of improving genome stability 163
6.10 Encapsulated dikaryons for cellulosic ethanol production 163

6.11 Suggestions for future experiments utilizing encapsulated dikaryons 164
6.12 General Conclusions 165

REFERENCES 168

LIST OF TABLES

Table 1. Selective regime and aggregate production of yeast strains 34
Table 2. Types of matrices utilized in this manuscript.. 90
Table 3. Differences in Young's modulus over time 98
Table 4. Differences in viscosity over time. 99
Table 5. Chemical composition of different alginates. 100
Table 6. Differences in bead size (mm) over time. 101
Table 7. Differences in bead mass (g) over time. 103
Table 8. Differences in ethanol yield (g/g) from dextrose over time. 105
Table 9. A comparison of total cell number across different bead types over time. 108
Table 10. Differences in viability over time 112
Table 11. Differences in heat shock resistance over time. 116
Table 12. Strains of yeast used in this chapter. 125

LIST OF FIGURES

Figure 1. A schematic of modern ethanol production. 6
Figure 2. US ethanol production. 7
Figure 3. A correlation between the cost of corn and conventional ethanol production 11
Figure 4. Cellulosic and conventional ethanol production: goals vs. reality.. 14
Figure 5. A typical aggregate formed by strain *t227b.15* after 24 h of growth. 20
Figure 6. Evolution of proteinaceous aggregates that bind many multicellular clusters 32
Figure 7. Across-strain relationship between cluster size, cell death and aggregate production. 37
Figure 8. Proteins provide structural integrity to aggregates. 38
Figure 9. Hydrogen peroxide exposure results in extensive programmed cell death. 40
Figure 10. Apoptosis promotes proteinaceous aggregate formation. 42
Figure 11. Proteinaceous aggregates are adaptive under strong selection for rapid settling, but are a common good. 44
Figure 12. Chronological lifespan of non-dividing yeast 56
Figure 13. Yeast colonies transition through alkali (pH ~6.8) and acidic (pH ~5.2) phases 59
Figure 14. Yeast microcolonies form in alginate-encapsulated beads packed in immobilized cell reactors. 71
Figure 15. Alginate-encapsulated yeast cultured in continuously-fed bioreactors exhibit a stable pattern of gene expression 75
Figure 16. Levels of citric acid cycle metabolites in continuously-fed encapsulated yeast differ from planktonic yeast in exponential and stationary phases. 79
Figure 17. Calculating Young's modulus and viscosity. 92
Figure 18. Relation of cell number to optical density. 94
Figure 19. The modulus of rigidity as a function of the average length of G-Blocks. 96
Figure 20. Bead durability and swelling.. 97
Figure 21. Ethanol yield over time in planktonic and encapsulated cultures 104
Figure 22. Encapsulated populations have similar cell numbers to planktonic populations. 106
Figure 23. Cell escape over time. 110
Figure 24. Survivorship of encapsulated and planktonic cells at 50°C. 114
Figure 25. Yeast species and growth methods assayed in this experiment. 124
Figure 26. A schematic of protoplast fusion.. 126
Figure 27. Verification of protoplast fusion via flow cytometry. 132
Figure 28. Verification of protoplast fusion via DAPI. 133
Figure 29. Viability was similar among all cultures over time. 134
Figure 30. Viability by PI staining was higher in encapsulated cultures over time. . 135
Figure 31. Encapsulation reduces biomass accumulation. 137
Figure 32. Encapsulation stabilizes fusants, plasmids, and strain ratio in mixed cultures. 139
Figure 33. Fusant stability as determined by PI staining. 140

Figure 34. Encapsulation did not affect overall ethanol production. 142
Figure 35. Encapsulation increases ethanol production on a per cell basis. 143
Figure 36. Fermentation kinetics.....145
Figure 37. Factors influencing function loss in synthetic circuits.. 160

LIST OF SYMBOLS AND ABBREVIATIONS

ANOVA	Analysis of variance
ATP	Adenosine triphosphate
CFU	Colony forming unit
CLS	Chronological lifespan
CR	Caloric restriction
CTB	Cell Tracker Blue dye
DAPI	4,6-diamidino-2-phenylindole dye
DDGs	Dried distillers grains
EDTA	Ethylenediamine tetraacetic
ER	Ethanol Red yeast
G	α-L-guluronic
GHG	Greenhouse gas
ICR	Immobilized cell reactor
LiAC	Lithium acetate
M	β-D-mannuronic
MCF	Micro-centrifuge
MTBE	Methyl tertiary butyl ether
NaAlg	Sodium alginate
NaAlgCh	Sodium alginate cross-linked with chitosan
PBS	Phosphate-buffered saline
PCD	Programmed cell death
PEG	Polyethylene glycol
PI	Propidium iodide dye

Pr	Protanal
PrCh	Protanal cross-linked with chitosan
QS	Quorum sensing
RLS	Replicative lifespan
SC	Synthetic complete (medium)
SDC	Synthetic dextrose complete
TCA	Tricarboxylic acid
YPD	Yeast peptone dextrose (medium)
YPDX	Yeast peptone dextrose xylose (medium)

SUMMARY

Yeast can thrive in dense assemblages of its own, or our making, resulting in patterns of behavior that differ markedly from that of single planktonic cells. We first studied unicellular yeast that create their own assemblage upon selection for rapid settling in liquid medium. In these experiments, large clonal clusters, composed of hundreds to thousands of cells, began to form even larger macroscopic aggregates composed of hundreds of potentially unrelated clusters. The matrix of these aggregates includes extracellular proteins, and is likely produced via apoptosis. We found that such aggregates increase survival in environments that favor fast settling, but are evolutionarily unstable because they do not discriminate between aggregate-producers and non-producers. Next, we examined unicellular yeast maintained at high density via immobilization in a Ca^{2+}-alginate matrix. Immobilization uncouples reproduction from metabolism, resulting in metabolically active but growth-arrested cells. Because immobilized yeast allocates little substrate to biomass, we investigated its potential to enhance ethanol production under biorefinery-like conditions. We found that over a 7-week course of fed-batch culture immobilized yeast is able to produce more ethanol from the same amount of substrate than planktonic yeast. We further tested the resilience of different immobilization matrices to support long-term, fed-batch cultures, and determined that Protanal alginate has the lowest rates of cell escape and the highest ethanol yields. Lastly, we tested whether immobilization, by inducing replication arrest, could stabilize the genomes of dikaryons created by protoplast fusion of different yeast species: Saccharomyces cerevisiae and Pichia stipitis. In the absence of selection, planktonic dikaryons quickly revert to their parental genotypes via nuclear segregation during replication. We discovered that genome

content of growth-arrested immobilized dikaryons is stable in 19-day, fed-batch cultures, and that stable dikaryons retain the metabolic capacity of different the fused species to ferment 6-carbon and 5-carbon sugars. Taken together, our results demonstrate the utility of densely-packed yeasts to address issues related to the evolution of group dynamics as well as to enhance efficiency and longevity in biomanufacturing.

CHAPTER 1: INTRODUCTION

This work will primarily focus on two somewhat disparate topics: 1) group formation from clonal yeast clusters, and 2) the use of encapsulated yeast to improve the fermentation step of conventional ethanol production, and 3) the use of encapsulation to improve genomic stability. Though these topics may seem unrelated, all involve densely packed yeast. In the first case, experimental selection for rapid settling through liquid media led to yeast developing self-imposed assemblages in the form of densely packed clusters consisting of hundreds of cells, and, later, the formation of aggregates consisting of hundreds of clusters. In the second case, a matrix consisting of a Ca^{2+}-alginate was experimentally imposed around yeast cells, forcing them to remain at high densities in order to more efficiently produce ethanol from glucose, and, later, to stabilize the genomes of dikaryons.

This chapter will begin by discussing the many types of group formation, and their advantages and disadvantages. In particular, group formation requiring sacrifice on the part of one or more members will be discussed, and toward the end of this section the stability of these groups and how they initially form will be analyzed as well. The second part of this chapter will focus on ethanol production from both conventional and non-conventional substrates. Currently implemented technologies and challenges in these fields will be discussed, as well as their relation to US government policies and the environment.

1.1 Group formation

Group formation is a common solution to conditions under which individual survival would otherwise be low. Group formation has been observed among such diverse forms of

life as *Streptococcus* bacteria (X. Huang et al., 2017), ammonia-oxidizing archaea (Sabba, Terada, Wells, Smets, & Nerenberg, 2018), *Candida albicans* yeast (Desai & Mitchell, 2015), locusts (Cox & Carlton, 1991), penguins (C. Gilbert, Robertson, Le Maho, Naito, & Ancel, 2006), and large predators (Cassidy, Mech, MacNulty, Stahler, & Smith, 2017) and in response to such diverse challenges as pH homeostasis (X. Huang et al., 2017), locally concentrated nutrient supply (Sabba et al., 2018), exposure to toxins (Desai & Mitchell, 2015), drought (Cox & Carlton, 1991), extreme cold (C. Gilbert et al., 2006), low survival of offspring, and competition for territory (Cassidy et al., 2017). Group formation, then, is as ubiquitous as its benefits are numerous.

The benefits of group formation are clear in some cases. For example, more social baboons have higher rates of infant survival than their less social counterparts (Silk, Alberts, & Altmann, 2003), fish in schools are less likely to be eaten than lone fish (Herbert-Read et al., 2017), and groups of wolves can bring down large prey that lone wolves cannot (Herbert-Read et al., 2017). Most often, the benefits of group formation have associated costs, as well. For example, more social baboons do benefit from higher rates of infant survival, but at the cost of higher parasitism than solitary animals (Lutermann, Bennett, Speakman, & Scantlebury, 2013). Similarly, fish in schools enjoy such benefits as more efficient movement and greater ease in finding a mate, but at the cost of a higher migration requirement and more vulnerability to low oxygen and accumulated toxins than lone fish (Domenici, Steffensen, & Marras, 2017). Even wolves, long a quintessential example of the successes of group formation, sometimes choose to leave the safety of the pack to increase their chances for reproduction, since only one male and female typically mate (Cafazzo, Lazzaroni, & Marshall-Pescini, 2016).

In some cases, the costs associated with group formation are quite high. Eusocial organisms, such as termites, ants, bees and naked mole rats all feature large numbers of workers who are biologically unable to reproduce, (unlike the wolf pack, whose members are capable of reproduction but may lack the opportunity) and instead aid directly or indirectly in the rearing of their siblings (Kapheim, Nonacs, Smith, Wayne, & Wcislo, 2015). This sacrifice is considerable, and was recently characterized as a "high-risk, high-reward" strategy (F. Fu, Kocher, & Nowak, 2015); indeed, eusociality appears to have successfully evolved only a dozen or so times, even though eusocial insects comprise nearly half of all the insect biomass in the world (Edward O Wilson, 1971). Another example of costly group formation is the evolution of cellular adhesion as a mechanism to form microbial aggregates (Garcia, Doulcier, & De Monte, 2015). Adhesion requires costly, continual production of adhesive proteins, though aggregates typically persist long enough to positively affect the members within (Jiang, Levine, & Glazier, 1998), providing them with such benefits as improved resource utilization efficiency (Gresham, 2013), and resistance to drugs, dehydration, UV stress, and host immune system attacks (Santos et al., 2018). Despite these benefits, adhesion is so costly that less-adhesive mutants frequently arise in microbial aggregates and threaten their long-term stability (Garcia et al., 2015)

Group formation, then, is often temporary; stable group formation is less likely to evolve, and more likely to require high levels of group relatedness (Herre, Knowlton, Mueller, & Rehner, 1999; Trivers, 1971; Vautrin & Vavre, 2009). Indeed, nearly all of the examples of group formation discussed here are temporary, with the exception of groups that alter the level of selection (Krupp, 2016), changing the unit upon which natural selection acts. Some consider eusociality to be just such a change (Nowak, Tarnita, &

Wilson, 2010), altering the level of selection from individual worker to the colony as a whole, particlularly the queen. Studies of a facultatively eusocial bee indicate that such a transition may be genetically-aided (B. M. Jones, Kingwell, Wcislo, & Robinson, 2017), though exactly how this transition ocurred is a matter of much debate (Blacher, Huggins, & Bourke, 2017; Gadagkar, 2016).

More recently, group formation drove the development of a new level of selection within the unicellular yeast *Saccharomyces cerevisiae* (Ratcliff, Denison, Borrello, & Travisano, 2012). Ratcliff *et al*. demonstrated that by selecting for rapid settling through liquid media, unicellular yeast quickly evolved a simple mutation (Ratcliff, Fankhauser, Rogers, Greig, & Travisano, 2015) that caused them to form clonal clusters which either survived or perished as a group. They further went on to continue to select for increasingly faster settling, and documented not only a further increase in the number of cells per cluster, but also an increase in the size of those cells and the rates of apoptosis within large clusters, which facilitated smaller, faster-growing propagules than clusters with low apoptosis (Ratcliff, Pentz, & Travisano, 2013; Ratcliff & Travisano, 2014). These 'snowflake yeast' further developed a primitive division of labor (Eric Libby, Ratcliff, Travisano, & Kerr, 2014), an elongated shape that allowed cells to pack more tightly (Jacobeen et al., 2017) and other features that locked them in to a multicellular lifestyle, making reversion to unicellularity less likely (E. Libby, Conlin, Kerr, & Ratcliff, 2016; Eric Libby & Ratcliff, 2014). Further studies, discussed in Chapter 2, detail the continuing transition from individual clusters to groups of clusters dubbed aggregates.

Group formation, then, is a common, usually temporary, solution to individually low fitness across all forms of life, and can have profound consequences. Indeed, all life

was at one point unicellular, and group formation was almost certainly a pre-requisite for the complex, multicellular life that has so dramatically reshaped our planet's surface (Fisher, Cornwallis, & West, 2013). For our research, we utilized *S. cerevisiae* snowflake yeast that formed large, clonal clusters and selected them to settle even more rapidly through liquid media. We expected that they would either 1) become larger in size, in response to the new settling requirement, or 2) become smaller or perhaps even revert back to unicellularity altogether in a bid to reproduce as rapidly as possible, effectively ignoring selection. We observed yeast clusters come together to form aggregates composed of hundreds of clusters, dramatically increasing their survival in an environment that favored rapid settling. However, the high cost imposed by aggregate formation (>2% apoptosis) was ultimately untenable; aggregates evolved, and then were lost, in two separate experiments.

1.2 A brief history of gasoline and ethanol production

Gasoline has been the primary transportation fuel for over 100 years. The global dominance of gasoline in the transportation industry begins, unusually enough, with kerosene. The use of this oil for both lighting and fuel extends to at least the 9th century (Bikadi, 1995), though it wasn't until 1859 that the first well was dug by Edwin Drake in Pennsylvania (Administration, 2017). During distillation to produce kerosene, gasoline was produced as well, but discarded as there was no practical use for it. Kerosene was widely needed and used, leading to a rapid expansion in the number and size of wells. Gasoline continued to be discarded until 1892, when the invention of the automobile led to its recognition as a potential fuel source (Melaina, 2007). Cars were adapted to utilize gasoline from the beginning because it was a cheap, readily available by-product from kerosene production.

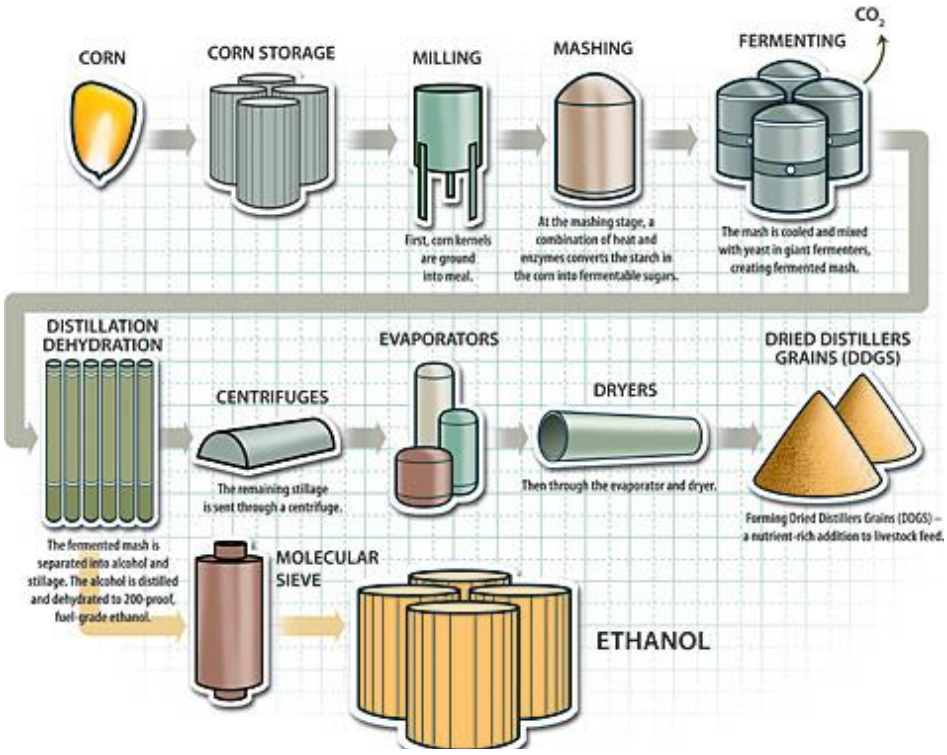

Figure 1. A schematic of modern ethanol production. Reproduced from http://me1065.wikidot.com/ethanol-as-a-fuel-source.

By 1920, there were over 9 million gasoline-powered vehicles on the road, requiring a growing number of stations to service them.

Ethanol's history is even older; it was first isolated from wine around 1100 AD, and was able to be distilled to nearly pure ethanol within 100 years (University, 2010). Historically, ethanol has been used for both lamp oil and cooking, though its value as a fuel was realized as well. Both Samuel Morey in 1826 and Nikolaus Otto in 1860 used ethanol in early combustion engines. However, to fund the Civil War, ethanol became highly taxed in 1862 and again in 1864 (Carolan, 2009). The tax on gasoline was much lower, cementing its dominance as the primary fuel for combustion engines. Gasoline's first mover advantage has endured to this day; gasoline is still the primary fuel for 'horseless carriages' all over the world. Over 143 billion gallons were consumed in 2017 by the United States alone, as

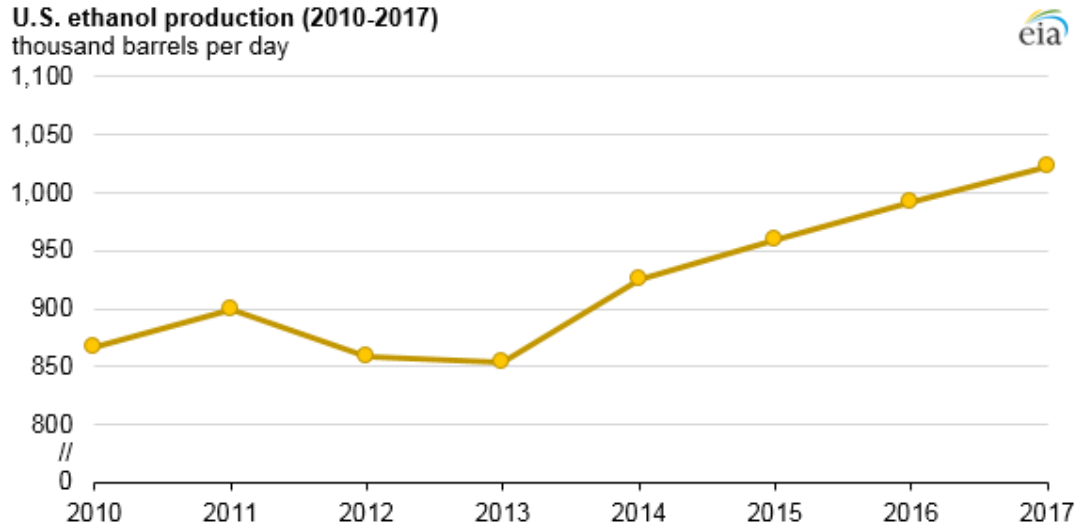

Figure 2. US ethanol production. Reproduced from the United States Energy Information Administration.

compared to around 10 billion gallons of ethanol (Administration, 2017), which is mostly used as a blended fuel.

Ethanol was produced as a fuel additive beginning in the late 1970s, but it was not until the early 2000s that production began to rise rapidly (Carolan, 2009). This increased demand for ethanol was based on the discovery that the oxygenate additive for gasoline fuel being used at the time, methyl tertiary butyl ether (MTBE), was causing significant groundwater contamination (Goettemoeller & Goettemoeller, 2007). Use of MTBE in fuel was widespread at this point because its addition to gasoline reduced carbon monoxide emissions as directed by the Clean Air Act of 1992. Unfortunately, in the attempt to reduce air pollution, use of MTBE inadvertently increased water pollution. The response was swift; by 2006, over 20 states had banned MTBE, and the nation was increasingly using ethanol as a ready replacement.

Ethanol production today is a mature industry that is both efficient and renewable. A series of well-refined steps, shown in Figure 1, demonstrate the modern methods for transforming corn sugars into ethanol. This process is complemented by technological increases in agricultural sciences, which have ensured a steady over-supply of cheap corn in the last decade, further fueling ethanol's growth (Figure 2).

1.3 Current gasoline and ethanol demand

Fuel supply is a significant problem not only in the United States, the world's largest consumer of gasoline (IndexMundi, 2017), but around the world. As countries like China (Xinhua, 2016) and India (Bike, 2016) rapidly increase their per capita consumption to fuel the growing demand for personal cars and industry, this problem will only worsen. Each year, readily accessible sources of crude oil dwindle, forcing industry workers to attempt to extract oil from more increasingly less desirable areas, often in the ocean floor (Faucon, 2013) or tar sands (Denchak, 2015).

Along with diminishing supply, gasoline use is undesirable for its negative environmental effects as well, accounting for 27% of all greenhouse gas emissions (Agency, 2017), and causing untold environmental damage from spills like the Deepwater Horizon of 2010 (Damage Assessment, 2010) and the infamous Valdez spill of 1989 (Restoration, 2013). However, relieving the demand for gasoline, while almost universally desired, is non-trivial. The entire transportation network relies on the well-developed infrastructure that takes crude oil from the ground, refines it, and distributes it to 168,000 gas stations nationwide (News, 2004). While electric vehicles may someday help to solve

this problem, they currently have little in the way of charging infrastructure and comprise less than 1% of cars on the road (Nanalyze, 2017).

Ethanol is a readily available fuel source that can help relieve immediate demand on gasoline via blending. Currently, all 2001 and newer vehicles, which comprise 97% of vehicles on the road, can safely use up to 15% ethanol blends (E15) (Wojdyla, 2013). Ethanol is preferable over gasoline because it can be renewably sourced from corn, has an increased octane rating, and emits 19-48% fewer greenhouse gases (Center, 2017). The advantages of ethanol are recognized to the degree that government mandates ensure that gasoline in the United States is at least a 10% blend with ethanol, which has helped spur a dramatic increase in ethanol production in the last decade (Figure 2).

1.4 An overview of modern ethanol production

Nearly all ethanol in the United States is derived from corn kernels, though wheat is also used to a lesser extent (Figure 1) (Goettemoeller & Goettemoeller, 2007). After grain is brought to the ethanol production plant, it is first milled (Nichols & Bothast, 2008). The purpose of milling is to break up the grains into small enough pieces so that they can be penetrated by water in the cooking step. There is disagreement about the optimal size of milled grain; some advocate grinding the pieces as small as possible, whereas others say that this damages the starch and diminishes final yields. After milling, the grains are cooked (sometimes called mashing), generally from 58-72°C, during which the milled grains are mixed with water and rendered into a mash ready for fermentation. The purposes of cooking include: 1) sterilization, 2) solubilization of sugars, 3) release of chains of sugars, and 4) reduction in viscosity of the grains (Jacques, 2003). During cooking, enzymes (often

the endoenzyme α−amylase and the exoenzymes glucoamylase) are used to convert the starches present into glucose, which can be readily used by yeasts. Cooking systems can be either batch or continuous.

After cooking, the fermentation step begins, which will be the focus of research discussed in Chapters 4 and 5. During the fermentation step, yeast turn the exposed sugars into ethanol (Jacques, 2003). Many different types of yeast are used, and they can be pitched directly, or grown first in a propagator to high density before introduction to the cooked mash. The temperature at which fermentations occur also varies; though 30°C is often optimal for yeast, if simultaneous saccharification and fermentation is being utilized (during which the enzymes expose the sugar and the yeast turn the sugar into ethanol in one step) a higher temperature, often 35°C, is chosen as a compromise between the yeasts' optimal temperature and the enzymes' optimal temperatures (often 45°C +). As more thermotolerant strains are created, this number is expected to climb. Larger facilities often use batch production systems for fermentation, which are less efficient than continuous production systems, but also less susceptible to contamination.

Excess proteins and undigested products from the fermentation are turned into animal feed, known in the industry as dried distiller's grains (DDGs). After fermentation, ethanol is distilled to concentrate it, generally to 192 proof (Jacques, 2003). Briefly, since ethanol evaporates faster than water, upon the addition of heat it rises through a tube and condenses in another chamber. This process is often repeated several times. Following distillation, a molecular sieve may be used to further remove water from the mixture via adsorption. After production is complete, ethanol is transported to its final destination (usually a blending facility to be mixed with gasoline), often by truck or rail.

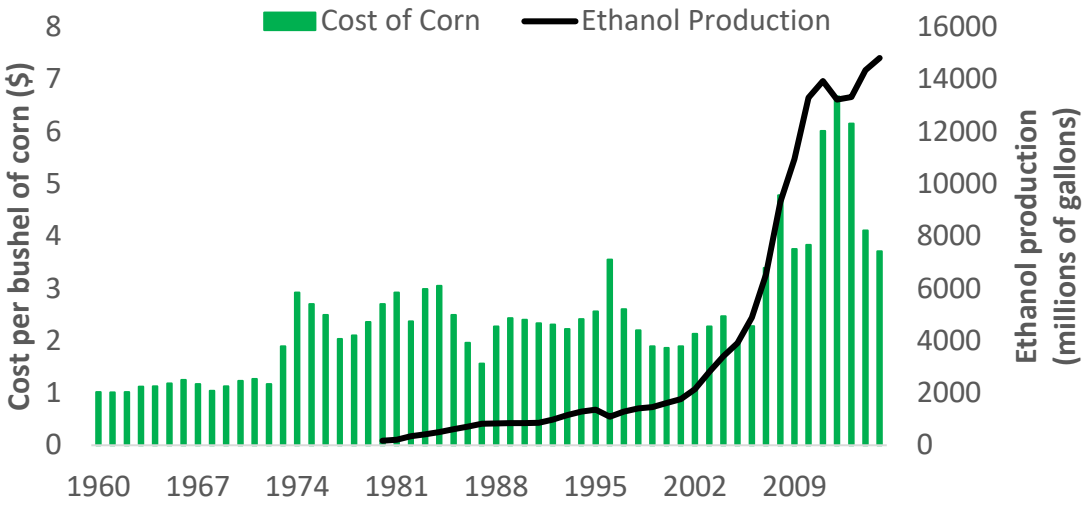

Figure 3. A correlation between the cost of corn and conventional ethanol production. Data obtained from Goettemoeller and Goettemoeller (2007)

1.5 Cellulosic ethanol

Whereas conventional ethanol is derived from corn kernel or wheat (or sugar beet elsewhere in the world), cellulosic ethanol is sourced from agricultural by-products like corn stalks, tree tops, or other agricultural residues, and is thus less pollutive in its refining processes than conventional ethanol due to its utilization of waste materials (Dwivedi et al., 2015). Further, it does not compete with food crops like conventional ethanol production (Erickson, 2018).

Increased use of fuel ethanol may have increased demand for corn (Figure 3), and, in turn, caused food prices to rise (Pimentel, 1991), in part because corn by-products like high fructose corn syrup are ubiquitous in many modern diets. The United States is the largest producer of corn in the world, producing 40% of the world's supply, and exporting approximately 13% of its annual yield, according to the USDA. Worldwide, over 3 billion people live on less than $2.50 a day according to the World Bank, so even a small increase

in food prices in the United States can translate to more malnourished individuals around the world.

There are also negative environmental effects associated with corn ethanol production; many, though not all, are lessened by cellulosic ethanol production. The Intergovernmental Panel on Climate Change recently found conventional ethanol production to be, at-best, neutral in terms of greenhouse gas (GHG) emissions. They claimed, "Biofuels have direct, fuel-cycle GHG emissions that are typically 30–90% lower than those for gasoline or diesel fuels. However, since for some biofuels indirect emissions—including from land use change—can lead to greater total emissions than when using petroleum products, policy support needs to be considered on a case by case basis.(*Intergovernmental Panel on Climate Change*, 2013)" Other sources (Hertel et al., 2010) agree with this assessment, though many maintain that conventional ethanol still leads to an overall reduction in GHG emissions (Liska et al., 2009).

It is generally agreed upon that cellulosic ethanol is less pollutive than conventional ethanol, reducing direct GHG emissions by 57-156% as compared to gasoline production (Dwivedi et al., 2015), whereas conventional ethanol, only reduces direct GHG emissions by 21-46% as compared to gasoline (Chavez-Rodriguez & Nebra, 2010), depending on the source materials used and the production facilities. Cellulosic ethanol is also uncompetitive with food production. Billions of tons of unused agricultural waste could now be used for fuel rather than food crops. In addition, since there is already a huge excess of supply of substrate, such as corn stalks, no new land would have to be cleared or farmed for its production, alleviating land-use change concerns.

1.6 Political regulations impact ethanol production

Despite the advantages associated with cellulosic ethanol production, among the 14.6 billion gallons of ethanol produced in 2015, only about 2.2 million gallons produced were cellulosic ethanol. Political regulations impact ethanol production. Within the United States, the driving force that continues to build demand for ethanol is the Renewable Fuel Standard (RFS) program. Most of the gasoline in the United States contains about 10% ethanol, due in large part to regulation based around the RFS program. A proposed change to this regulation is to increase the percentage of ethanol present in gasoline from 10% up to 15%; however, there has been pushback from political (oil) lobbyists on this matter and it is currently stalled, though year-round E15 has been made available (Eller, 2018). Outside of the United States, the European Union and certain South American countries, such as Brazil, encourage even greater percentages of ethanol for use in gasoline. Consequently, oil refiners (e.g., Chevron, ExxonMobil, and Valero) as well as oil importers will continue to depend on the supply of ethanol to satisfy these regulations.

Notably, the U.S. government does not indicate whether first generation (i.e., corn-based) or second generation (i.e., cellulosic, algae, etc.) ethanol is required to satisfy the RSF mandates. This is because first generation and second generation ethanol have nearly identical chemical compositions, and therefore can be interchangeably used. As such, competition in the ethanol space has largely depended on price, with the current cheapest mechanism for ethanol production being corn-based, allowing it to dominate the industry. Due to high production costs, second generation ethanol is often priced higher than corn-

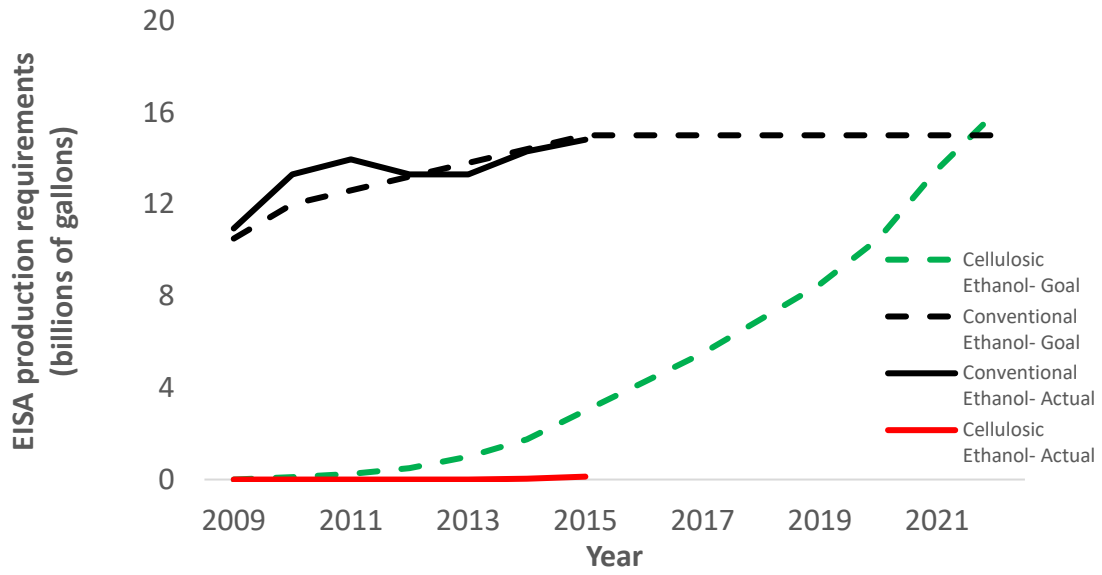

based ethanol. Price sensitivity is thus an enormous challenge for the second generation

Figure 4. Cellulosic and conventional ethanol production: goals vs. reality. Data obtained from the Environmental Protection Agency.

ethanol industry.

The 2007 Energy Independence and Security Act helped to fill this regulatory gap. It mandated that increasing amounts of ethanol be produced from cellulosic feedstocks in the United States, with the goal of producing just as much cellulosic as conventional ethanol by 2020 (Figure 4). Unfortunately, actual production has fallen, and continues to fall, far short of these goals. Part of this is due to the unexpectedly difficult technical challenge associated with cellulosic ethanol production.

1.7 Technical difficulties associated with cellulosic ethanol production

Cellulosic ethanol is more difficult to produce than conventional ethanol at nearly every step of production. The wide variety of source materials used is often seasonal, and vary greatly in terms of hemicellulose, cellulose, and lignin content (Jacques, 2003). Further

complicating matters, these materials also all differ in the proportion of 5-carbon (pentose) sugars like xylose to 6-cargon (hexose) sugars like glucose. Due to the recalcitrance of hemicellulose and cellulose, cellulosic substrates require more intense, more expensive pre-treatment than corn, as well as more numerous and more expensive enzymes to expose the contained sugars (L. R. Lynd et al., 2017).

Even once the sugars are exposed, a major difficulty in cellulosic ethanol production is fermentation, the subject of our research in Chapter 5. Corn kernels contain almost exclusively hexose sugars, which can be efficiently fermented into ethanol by the widely used industrial ethanologen *Saccharomyces cerevisiae* (J. E. McGhee, G. S. Julian, R. W. Detroy, & R. J. Bothast, 1982a). *S. cerevisiae*, however, is incapable of metabolizing pentose sugars; indeed, no naturally-occurring organisms exist that are capable of co-fermenting both 5- and 6-carbon sugars. Some organisms, like *Pichia stipitis*, can ferment both, but typically preferentially utilize the 6-carbon sugars before digesting 5-carbon sugars, a process which is uneconomically slow (Delgenes, Moletta, & Navarro, 1988). This technical difficulty has been researched by many for decades (F. K. Agbogbo & G. Coward-Kelly, 2008; Bechara, Gomez, Saint-Antonin, Schweitzer, & Marechal, 2016; Chen, 2011; Chen, Wu, Zhu, Zhang, & Wei, 2018; I. De Bari et al., 2013; Dien, Nichols, O'bryan, & Bothast, 2000; J. Lee, 1997), but current cellulosic processes remain less efficient and less competitive in the American fuel economy than corn ethanol production processes.

Despite these technical difficulties, the market for cellulosic ethanol is forecasted to expand in the coming years as the technology matures and production costs drop. A handful of cellulosic ethanol plants capable of producing >10 million gallons per year have

been opened in the last decade by conventional ethanol leaders like DuPont and POET (Lee R. Lynd et al., 2017). These new plants will be able to help cellulosic ethanol production at larger scales mature as a technology, and in turn help the United States reach its energy goals as outlined by the Energy Independence and Security Act of 2007.

1.8 Project goals

The goal of Chapters 4 and 5 was to improve the fermentation step of ethanol production by using a form of cell immobilization. Cellular immobilization is a decades-old technology; one form, encapsulation, is well-known to improve product yields by reducing biomass accumulation, and thus increasing substrate utilization efficiency (Baruch & Machluf, 2006; Burgain, Gaiani, Linder, & Scher, 2011; Cha, Kim, Jin, & Kong, 2012). In Chapter 4, we seek to determine if encapsulated yeast 'beads' can be re-used long enough to make it economically viable for large-scale use, and, if so, what type of encapsulation matrix is most suited to such long-term use. In Chapter 5, we utilize encapsulation as a method for stabilizing protoplast fusants and plasmids to make the fermentation step of cellulosic ethanol production more efficient.

CHAPTER 2. EVOLUTION OF ALTRUISTIC COOPERATION AMONG NASCENT MULTICELLULAR ORGANISMS

Cooperation is a classic solution to hostile environments that limit individual survival. In extreme cases this may lead to the evolution of new types of biological individuals (e.g., eusocial super-organisms). We examined the potential for inter-individual cooperation to evolve via experimental evolution, challenging nascent multicellular 'snowflake yeast' with an environment in which solitary multicellular clusters experienced low survival. In response, snowflake yeast evolved to form cooperative groups composed of thousands of multicellular clusters that typically survive selection. Group formation occurred through the creation of protein aggregates, only arising in strains with high (>2%) rates of cell death. Nonetheless, it was adaptive and repeatable, though ultimately evolutionarily unstable. Extracellular protein aggregates act as a common good, as they can be exploited by cheats that do not contribute to aggregate production. These results highlight the importance of group formation as a mechanism for surviving environmental stress, and underscore the remarkable ease with which even simple multicellular entities may evolve—and lose—novel social traits.

2.1 Introduction

Group formation is a common adaptation to environmental stress, permitting survival under conditions in which solitary individuals would otherwise perish. Group formation provides diverse benefits, including thermal insulation (Alberts, 1978), increased predation efficiency (Berleman, Chumley, Cheung, & Kirby, 2006), protection from predation (Brock & Riffenburgh, 1960), improved dispersal ability (Joan E. Strassmann, Zhu, &

Queller, 2000), and the ability to thrive in environments with patchily-distributed resources (Silva, Nogueira, & De Marco, 2016; Edward O. Wilson & Hölldobler, 2005).

The evolution of group formation can also be driven by selective mortality (as opposed to selection on growth rate or random mortality as in Brockhurst, Habets, Libberton, Buckling, & Gardner, 2010). Truncation selection for rapid sedimentation in liquid suspension, for example, has driven the evolution of undifferentiated multicellularity in yeast (Ratcliff et al., 2012) and in the green alga *Chlamydomonas* (W. C. Ratcliff et al., 2013). Selective mortality in the form of predation has driven experimental populations of *Chlamydomonas* (Becks, Ellner, Jones, & Hairston, 2012; Herron, Zamani-Dahaj, & Ratcliff, 2018) and another green alga, *Chlorella* (Boraas, Seale, & Boxhorn, 1998), to evolve multicellular structures.

In some cases, the benefits of group formation come at high individual cost. For example, the production of stalked fruiting bodies in *Dictylostelium* requires the altruistic sacrifice of the cells forming the stalk, but allows for improved spore dispersal for non-stalk cells (Queller & Strassmann, 2009). Similarly, caste-based division of labor within eusocial organisms requires that workers sacrifice opportunities for direct reproduction, and instead perform functions (e.g., foraging, brood rearing, colony maintenance and defense) that help the queen reproduce more efficiently (Bull, 1999; Folse & Roughgarden, 2010; Jarvis, O'Riain, Bennett, & Sherman, 1994; Thorne, 1997; Edward O. Wilson & Hölldobler, 2005).

In this paper, we explore the de novo evolution of cooperative group formation in snowflake yeast, a nascent multicellular organism. Snowflake yeast previously evolved

from unicellular yeast in an environment where individuals had little chance of surviving: strong selection for fast sedimentation through liquid media. Within a matter of weeks, fast-settling clonal groups of cells had evolved and displaced their unicellular ancestors (Ratcliff et al., 2012).

Snowflake yeast possess many attributes that facilitate adaptive evolution of cluster-level traits. One such attribute is an emergent life cycle in which groups of cells grow until physical forces cause the group to fracture (Jacobeen et al., 2018; E. Libby et al., 2016), producing small propagules which then grow back to their parent cluster's approximate size before fragmenting themselves. Due to their branching growth form (William C. Ratcliff et al., 2013), each propagule goes through a unicellular genetic bottleneck, even if it ends up containing multiple cells (Ratcliff, Fankhauser, et al., 2015). This ensures that mutations are rapidly segregated between cellular groups (Ratcliff, Fankhauser, et al., 2015), allowing selection to act on emergent multicellular traits that arise as a consequence of novel mutations (Ratcliff, Herron, Conlin, & Libby, 2017). Multicellular selection readily acts on these traits, increasing the frequency of multicellular adaptations such as elongate cells, which result in the formation of larger groups by increasing cellular packing density (Jacobeen et al., 2018), and elevated programmed cell death (PCD), which results in the production of smaller, faster-growing propagules that repeatedly displace clusters with lower rates of PCD (Pentz, Taylor, & Ratcliff, 2015; Ratcliff et al., 2012).

Here, we examine the response of snowflake yeast to an environment where the strength of settling selection was such that individual clusters had a very low chance of survival. We predicted two possible responses to this selection: 1) individual snowflake

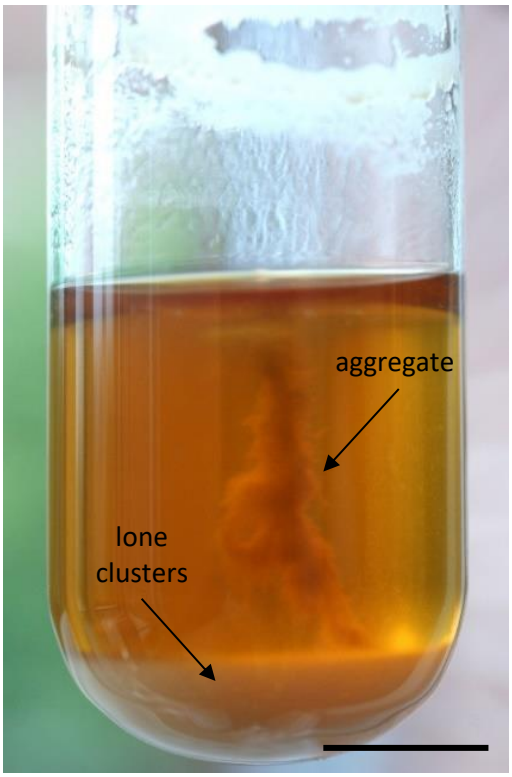

Figure 5. A typical aggregate formed by strain *t227b.15* after 24 h of growth. Scale bar is 10 mm.

yeast clusters could have evolved to be larger, improving their survival, though at a likely cost to growth rate (Ratcliff et al., 2012), or 2) if increased size were either difficult to achieve or too costly, snowflake yeast clusters could have evolved to be small and fast-growing, effectively ignoring settling selection. The latter response would result in the transfer of a random subsample of yeast to the next test tube.

Instead, we found that the repeated response to this selection was social: in two separate experiments, snowflake yeast evolved to form cooperative groups that dramatically improved the survival of the yeast within. These cooperative groups, which we term 'aggregates', have a tangled, ropelike appearance, and contain hundreds of individual snowflake yeast clusters (Figure 5). Proteins hold aggregates together, causing

them to settle seven times faster than solitary clusters, thus increasing survival during settling selection by nine-fold. Aggregate formation is, however, a common good, subject to exploitation by non-aggregating yeast genotypes. The resulting lack of genetic relatedness within a proteinaceous aggregate may have contributed to their inability to persevere within selection experiments; despite their survival benefit, we did not observe aggregates in either experiment more than a few hundred generations after their initial evolution.

2.2 Methods

2.2.1 Yeast culture

Unless otherwise specified, we grew yeast at 30°C in Yeast Peptone Dextrose medium (YPD; per L: 20 g glucose, 20 g peptone, 10 g yeast extract), in 25 x 150 mm tubes shaken at 250 rpm.

2.2.2 Aggregate discovery and creation of t227b.15

We isolated an aggregate forming strain, *t227b.15*, from a lineage that initially began with a diploid, isogenic, unicellular Y55, henceforth referred to as t0 for having undergone 0 days of settling selection. Previously described experiments (Ratcliff et al., 2012) utilized settling speed through liquid media as a proxy for size. Selection for fast-settling, then, gave larger yeast a survival advantage over smaller yeast. Initially, they gave 10 mL of t0 yeast 45 minutes to settle on the bench in a tall (16 x 150 mm) tube before selection (Table 1). They imposed selection by discarding the top 9.9 mL of yeast, which settled more

slowly, and transferring the bottom 100 µL to a tube of fresh media, which they selected the next day (Ratcliff et al., 2012).

After 7 days of daily settling selection, Ratcliff et al. altered this regime, applying settling selection by placing 1.5 mL of yeast and media, randomly sampled from the 10 mL population, in a microcentrifuge tube (9.9 x 39 mm), and then centrifuging at 100 g for 10 seconds. After this centrifugation, they imposed selection by discarding the top 1.4 mL and placing only the fastest settling, bottom 100 µL in fresh media for the next day's selection. This selection was relatively weak, so Ratcliff et al. (2013) increased the strength of selection on day 30 by allowing the 1.5 mL of yeast to settle on the bench in a microcentrifuge tube for 5 minutes (300 seconds), without any centrifugation prior to imposing selection by allowing only the bottom 100 µL to survive. At 65 days of selection, Ratcliff et al. increased the strength of selection again by decreasing the time yeast were given to settle, this time to 75 seconds before selection (Table 1), where it remained until day 227 (William C. Ratcliff et al., 2013).

We isolated a large, fast-settling strain of snowflake yeast derived from day 227 of the experiment described above, dubbed *t227* (Table 1). Our initial experimental goal was to determine if there was a genetic relationship between cluster size and proportion of dead cells. We began this experiment by generating diversity in the *t227* isolate, reasoning that such a relationship might manifest via a bulked segregant analysis. In order to force sexual (as opposed to asexual) reproduction, we sporulated this clone by growing it for four days (30 °C, 250 rpm) in 10 mL sporulation media (per L: 20 g potassium acetate, 2.2 g yeast extract, 865 mg amino acid complete [40mg/L adenine, 20 mg/L arginine, 100 mg/L aspartic acid, 20 mg/L histidine, 30 mg/L isoleucine, 20 mg/L leucine, 20 mg/L lysine, 40

mg/L methionine, 300 mg/L phenylalanine, 20 mg/L tryptophan, 25 mg/L tyrosine, 10 mg/L uracil, 150 mg/L Valine], 0.5 g dextrose). To separate the resultant tetrads, we pelleted and re-suspended 1 mL of spores in 800 μL of Yeast Nitrogen Base (YNB; obtained from VWR, 17g per L) and 200 μL of 200 units/mL of the enzyme zymolyase for thirty minutes at room temperature. To further ensure separation, we added sterile 0.5 mm glass disruption beads and vortexed on high for 60 seconds. In order to isolate single spores, we diluted the resulting mixture 1:10,000 in sterile water and plated on YPD agar. Then, we selected individual colonies (which originated from single spores) at random. To quantify cluster size and cell death, we grew 417 colonies overnight in liquid media, then stained with propidium iodide (PI; 10 μL per mL; stock 1mg/mL) and Cell Tracker Blue (CTB; from ThermoFisher Scientific; 3 μL/mL) and characterized cluster size (see Measuring cluster size) and the frequency of dead cells (see Measuring cell death).

After quantifying cluster size, we found that five out of the 417 post-sex isolates we assayed produced unusually large (>300 μm in diameter) clusters. They were so large that we became curious if there was an upper bound on snowflake yeast cluster size, and selected these very large clusters further for rapid settling through liquid media. We first subjected 1 mL of three replicates of each of these five isolates to strong (30 seconds of settling) daily selection for large size in standard microcentrifuge tubes. Specifically, we randomly sampled 1 mL from each 10 mL population, vortexed on medium-high to ensure uniformity, and then allowed the sample to sit on the bench for 30 seconds, after which we discarded the top 900 μL and transferred the bottom 100 μL to fresh media for selection the following day. Though the ancestor *t227* was capable of proteinaceous aggregate formation, only one out of five of these isolates, *t227b*, could form aggregates by 24 hours.

We isolated an aggregate-producing strain by separating three aggregates from the rest of the population (Figure 5) and plating them on YPD. We chose three individual colonies from each plate and grew each in YPD media to determine which colony produced aggregates most reliably after 24 hours of growth. The isolate that best formed aggregates at 24 hours we termed *t227b.15*, to denote its derivation from auto-diploidized *t227* and the fifteen days of selection it underwent thereafter. Note that while *t227b* formed aggregates more frequently than *t227b.15* (97% vs. 86% at 24 hours), *t227b.15*'s aggregates were much larger. This large aggregate size made *t227b.15* easy to work with experimentally, we used it for future aggregate experiments unless otherwise noted.

2.2.3 Evolving aggregate formation from an ancestral snowflake yeast

We repeated the above selection experiment using an ancestral snowflake yeast, seeking to re-evolve aggregate formation from a very early snowflake yeast. This experimental isolate, which we term *t7*, evolved from unicellular, diploid, isogenic Y55 after just 7 days of settling selection, and was homozygous for a loss of function mutation within the transcription factor ACE2 (Ratcliff, Hawthorne, & Libby, 2015). We chose this isolate since it was early enough in the snowflake yeast lineage that we felt confident it lacked any mutations that could have eventually permitted (or made more likely) proteinaceous aggregate formation. We selfed this isolate via auto-diploidization to limit genetic variation. To give these small snowflake yeast the opportunity to gradually evolve larger size, we increased the strength of settling selection periodically throughout the duration of the experiment. Initially, we gave each of the five experimental replicates 240 seconds to reach the bottom 10% of the tube, reducing the time allowed for settling selection by 15 seconds every 10 days until we reached 60 seconds at day 120. After the allocated time,

we selected upon them as in previous experiments by randomly sampling 1 mL from a 10 mL population, and transferring only the bottom 100 µL to fresh media. We maintained 60 seconds of selection until day 163, when the experiment ended.

2.2.4 Measuring cluster size

We measured the size distribution of clusters by following the protocol of Pentz et al. (2015). Briefly, we fluorescently labelled vacuoles with CTB, then, after a 30-minute incubation in the dark, imaged flattened clusters using wide field microscopy (35 stitched fields of view taken with a 10x objective on a Nikon Ti-E inverted microscope). We analyzed the resulting images in ImageJ using a custom script to count the number of vacuoles, a good proxy for cell number, per cluster. Averaging the results from thousands of clusters allowed us to obtain good strain-level data for the typical number of cells in a cluster.

2.2.5 Measuring cell death

To estimate proportions of dead cells, we re-suspended liquid cultures in water and stained with both PI (10 µL / mL), and CTB (3 µL / mL). We allowed the cultures to sit at room temperature for 30 minutes in the dark, then used wide field microscopy (36 stitched fields of view taken with a 10x objective on a Nikon Ti-E inverted microscope) to image the same clusters for both red and blue fluorescence. Using a custom ImageJ script, we compared the number of total cells present (indicated by CTB) to the number of dead cells present (indicated by PI) on a per-cluster basis.

2.2.6 Aggregate formation, cell death, and cluster size in ancestral strains

In order to determine if there was a relationship between aggregate formation, cell death, and cluster size, we assayed all of the available snowflake yeast isolates in the lineage leading up to *t227* and *t227b.15* for each of these traits. Cell death and cluster size were determined per the protocols Measuring cell death and Measuring cluster size. We assayed proteinaceous aggregate production for all strains by adding 100 μL of stationary phase liquid culture to 10 mL of YPD in a 25 mm borosilicate tube kept at 30°C with 250 rpm shaking, with fifty replicates per strain. Each day for five days, we examined all fifty replicates for aggregate formation. For some strains (t227a-e), we used sixty replicates.

2.2.7 Heritability of aggregate formation

Broad-sense heritability (H2), which is the only estimate of heritability possible for asexual reproduction, was estimated as the proportion of total variance that is among strains (Herron et al., 2018). Using the data in Table 1, we estimated the heritability of aggregate formation at 24 h and at 48 h. We treated aggregate formation as a binary trait and estimated variances within and among strains using an ANOVA.

2.2.8 Aggregate composition

Microscopy indicated that aggregates contain both DNA and proteins (Figure 6B). To determine if either or both play a major structural role within the aggregate, we exposed the aggregates to both a protease and a DNase. We grew thirty replicates of the aggregate-producing strain *t227b.15* in YPD for 24 hours; 28 of these replicates produced aggregates. We put seven of the aggregates in 200 μL buffer (10mM Tris-HCl; 2.5mM MgCl2; 0.5mM CaCl2) only as a control. We put seven more aggregates in 190 μL buffer plus 10 μL DNase I (stock 2042 units/mL), seven in 190 μL buffer with 10 μL Proteinase K (stock 20 mg/mL),

and seven in 180 µL buffer with both 10 µL DNase I and 10 µL Proteinase K. We incubated the aggregates overnight at 30°C and 300 rpm. Afterwards, we centrifuged them at 5,000 rpm for 1 minute and removed 4 µL of the supernatant to measure protein and DNA levels on a Qubit Fluorometer v3.0.

2.2.9 Cell death and aggregate formation

In order to determine if there is a connection between cell death and proteinaceous aggregate formation, we induced apoptosis in *t227b.15*'s ancestor *t65* by exposing it to hydrogen peroxide. We chose this isolate because it has a weak ability to produce aggregates, not forming them until around 36 hours of growth (Table 1). Since strains that produce aggregates earlier also have higher levels of cell death (Figure 7), our rationale was that this strain might be particularly sensitive to changes in cell death, potentially resulting in earlier aggregate formation. Further, we knew that aggregates were capable of formation earlier than 36 hours; had we used *t227b.15* and not seen a strong relationship between cell death and aggregate formation, it could have been because no such relationship exists, or because aggregates are highly unlikely to form before 24 hours for other, unknown reasons.

We grew forty 10 mL populations of *t65*, and used half of them to generate spent media. After 24 hours, we exposed ten tubes to 5 µM of H2O2, which is known to induce apoptosis in yeast (F. Madeo et al., 2002; Ribeiro, Corte-Real, & Johansson, 2006), for one hour. We then pelleted and re-suspended the ten exposed tubes as well as the ten controls in the spent media of the remaining twenty cultures, none of which we exposed to H2O2. We monitored these populations for aggregate formation for 15 hours. In addition, we took

samples before exposure and at 4, 8, and 12 hours after exposure to H2O2 in order to measure the percentage of apoptotic and dead cells in both the exposed and unexposed populations. We measured apoptosis with the fluorescent dye dihydrorhodamine 123 (DHR), which labels cells producing reactive oxygen species, a hallmark of yeast apoptosis (Perrone, Tan, & Dawes, 2008). After washing twice in YNB, we added 10 µL/mL (stock 2.5g DHR/L in ethanol) of DHR to the culture and allowed it to sit for 2 hours in the dark. We then washed the culture twice more in YNB before imaging. We measured cell death by dual-labeling cells with PI and CTB, as described in Measuring cell death. We counted apoptotic and dead cells on flattened clusters using wide-field microscopy (36 stitched fields of view taken with a 10x objective on a Nikon Ti-E inverted microscope). We used the statistical language R to perform a bootstrap test to determine if aggregates formed earlier, or in higher proportion, in the exposed population.

2.2.10 Divergent selection experiment

To determine if aggregates increase the fitness of snowflake yeast under strong selection for rapid settling, we performed a divergent selection experiment. We generated within-population diversity for the trait of proteinaceous aggregate formation by selfing strain *t227*. We chose this strain since it is a moderate aggregate former, producing aggregates in roughly half of tubes at 24 hours. Further, we knew from previously conducted pilot experiments this strain would, upon auto-diploidization, produce descendants with variation for the trait of aggregate formation. We recovered approximately 1,000 isolates (scraping auto-diploidized colonies from 10 plates, each containing about 100 colonies), combining them to form a single population. We grew this overnight and used it to inoculate ten tubes, each containing 10 mL of YPD. For the next 5 days, we selected 5

populations for fast settling, wherein we vortexed 1 mL of culture, and after 60 seconds transferred the bottom 100 μL to a fresh tube of YPD media. We selected the remaining 5 populations for slow settling, wherein we vortexed 1 mL of culture, and after 60 seconds transferred the top 100 μL to a fresh tube of media. After five days of selection, we isolated 10 colonies per population, for a total of 100 colonies. We grew each of these colonies in triplicate and scored the fraction that made an aggregate within 24 hours. Additionally, cell size (see Measuring cluster size) and cell death (see Measuring cell death) were also determined for one of the three triplicates.

2.2.11 Settling speed

We attached a modified 15 mL Falcon tube to a standard slide with epoxy and filled the tube with water, then measured the settling speed of thirty-nine *t227b.15* aggregates. We placed each proteinaceous aggregate in 100 μL of water and vortexed it on medium-high for 3-5 seconds (as during selection), and then transferred it to the top of the settling apparatus. We recorded the time it took each aggregate to reach the bottom of the slide with a timer, since aggregates are visible to the naked eye. In addition, we measured the settling speeds of individual clusters not within aggregates. Since individual clusters are not visible to the naked eye, we placed the apparatus on a Nikon Ti microscope, and set up a video recording with 1 frame per second to measure the time clusters took to settle to the bottom.

2.2.12 Aggregate formation and survival

We directly examined the benefit of aggregate formation by separately examining the survival of aggregates and solitary clusters under strong selection for fast settling (60

seconds). For 10 populations of *t227b.15*, we separated aggregates from solitary clusters. We performed settling selection on each, and then compared the amount of biomass in the top 90%, which we would have discarded, to the amount of biomass in the bottom 10%, which we would have transferred to fresh media, using the stain CTB and the Qubit Fluorometer to measure fluorescence.

2.2.13 Determining if aggregates discriminate against unicellular yeast

To investigate if aggregates primarily benefit snowflake yeast, relative to unicellular yeast, we co-cultured unicellularized *t227b.15* with a snowflake yeast that does not produce aggregates, *t28*, in a 99:1 ratio, giving both strains similar starting biomass. We chose *t28* since it is the largest snowflake yeast strain (in terms of cluster size) that does not produce aggregates, even after 5 days of growth. We engineered *t227b.15* to grow as a unicellular yeast by restoring a functional copy of ACE2 using the LiAc/ssDNA/PEG method of transformation (ace2/ACE2-KANMX4; Gietz & Schiestl, 2007). We separated aggregates from the bulk population in 10 replicate tubes. After we digested the proteinaceous aggregates with Proteinase K (see Aggregate Composition), we analyzed both groups with CTB according to the protocol in Measuring cluster size to determine if the multicellular clusters were present in the aggregates at the same frequency as in the bulk population.

2.2.14 Determining if aggregate formation is a common good

To determine if a non-aggregating strain could incorporate within an aggregate as readily as a producer, we co-cultured *t227b.15* with a non-aggregating snowflake competitor (*t28* URA3/ura3::TEF1-GFP), tagged with green fluorescent protein. We chose *t28* since it is the snowflake yeast strain with the largest clusters that does not produce aggregates (Figure

7). After 24 hours of growth, we combined *t227b.15* and *t28* in varying proportions (10-90% *t227b.15* in 10% increments) in triplicate, and allowed them to grow for a further 48 hours. We also maintained three replicates of the two pure cultures, containing only *t227b.15* or the non-aggregating strain as controls. We separated the aggregates from the bulk population, and then digested the aggregates using Proteinase K as described above. We determined the frequency of *t227b.15* within both the aggregate and bulk population using CTB and wide-field microscopy, as described above, comparing the fraction of GFP to non-GFP cells. Our analysis algorithm was reasonably accurate: we recorded GFP-only controls as being 97% GFP, (standard deviation of 3 replicates = 1.5%), while *t227b.15*-only controls were 99.9% *t227b.15* (standard deviation of 3 replicates = 0.13%).

2.3 Results

2.3.1 Snowflake yeast evolved a novel form of cooperation under strong settling-rate selection

In response to intense selection for fast settling, snowflake yeast evolved a novel form of cooperation. Hundreds of snowflake yeast clusters combined to form aggregative structures up to 3 cm long (Figure 5). We never observed more than one aggregate within a single tube. A composite image (Figure 6B) shows that aggregates are composed of protein (Figure 6C), extracellular DNA (Figure 6D), and snowflake yeast clusters (Figure 6E).

We first observed aggregates forming in snowflake yeast that had been transferred for 227 days, in an experiment in which we gradually increased the strength of size-based selection (Ratcliff et al. 2013b). In previously described experiments, Ratcliff et al. (2012)

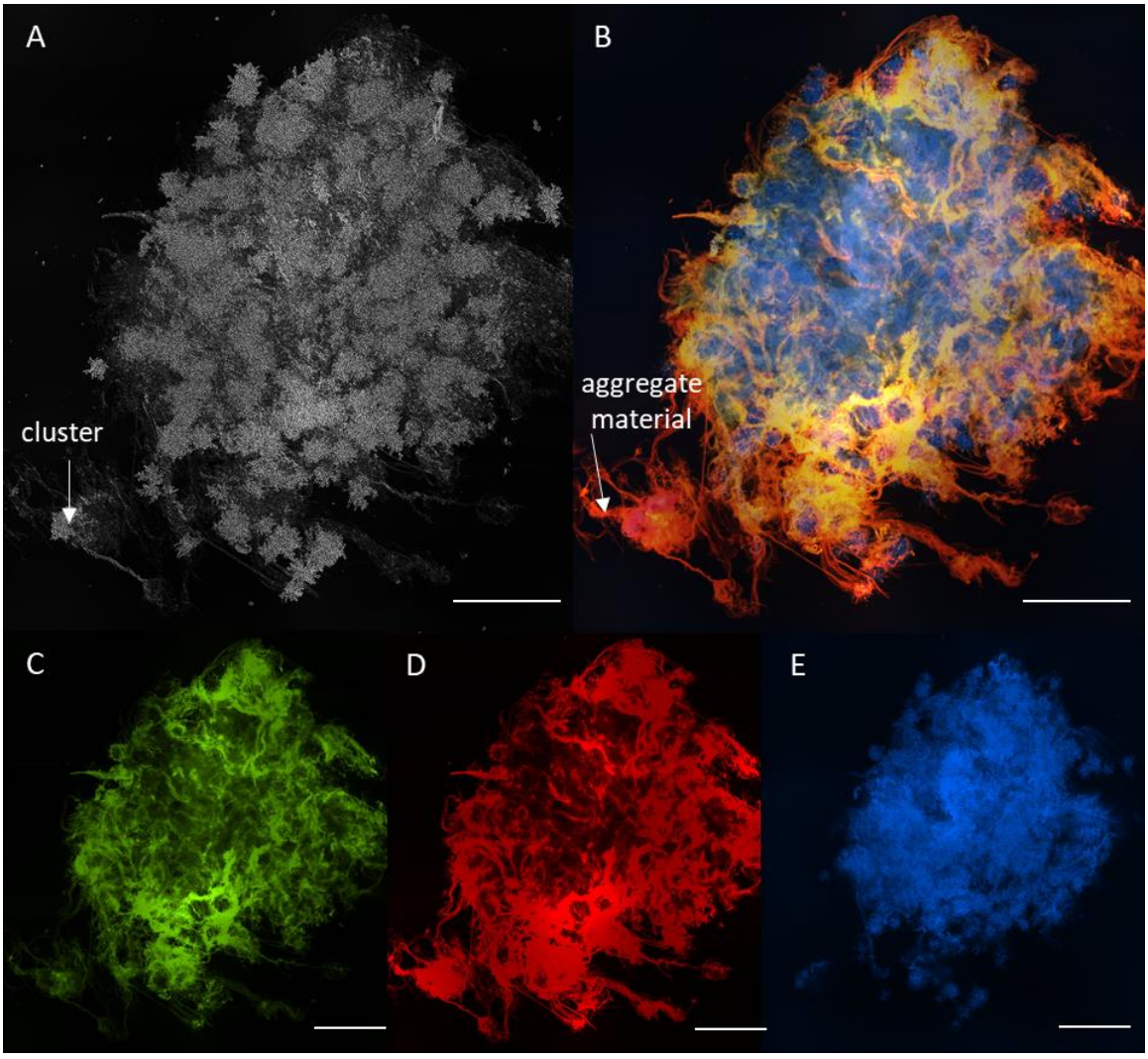

Figure 6. Evolution of proteinaceous aggregates that bind many multicellular clusters. When subjected to strong settling selection, snowflake yeast evolved to form cooperative aggregates composed of hundreds of clusters (A). A composite image (B) reveals the aggregates are composed of both protein (C, green, Qubit fluorescent protein stain;) and DNA (D, red, propidium iodide [PI]). Cells embedded within the aggregate are shown in blue (E, Cell Tracker Blue [CTB]). Scale bars are 500 µm.

initially gave 10 mL of unicellular yeast 45 minutes to settle to the bottom of tall (16 x 150 mm) tubes before discarding the top 9.9 mL of yeast, and transferring the bottom 100 µL to fresh media for the same regime on the following day. This selection favored larger yeast, which were able to settle more rapidly than their smaller counterparts, and quickly

led to the evolution of a cluster-forming phenotype dubbed ‘snowflake yeast’ (Ratcliff et al., 2012).

After 7 days of daily settling selection, Ratcliff et al. altered this regime, applying settling selection by placing 1.5 mL of yeast and media, randomly sampled from the 10 mL population, in a 2 mL microcentrifuge tube (9.9 x 39 mm), and then centrifuging at 100 g for 10 seconds. After this centrifugation, they imposed selection as before, by discarding the top 1.4 mL and placing only the fastest settling, bottom 100 µL in fresh media for the next day’s selection. On day 30, Ratcliff et al. (2013b) increased the strength of selection by allowing the 1.5 mL of yeast to settle on the bench in a microcentrifuge tube for 5 minutes (300 seconds), without any centrifugation, prior to imposing selection by allowing only the bottom 100 µL to survive. At 65 days of selection, they increased the strength of selection again by decreasing the time yeast were given to settle, this time to 75 seconds before selection (Table 1), where it remained until day 227 (Ratcliff et al. 2013b).

We first observed large, macroscopic aggregates forming in the 227-day isolate (which we refer to as strain *t227*) around 24 hours of growth- the time at which daily transfers occurred. We were interested in studying how snowflake yeast would adapt to very strong gravitational selection, and thus chose five isolates of auto-diploidized *t227* that each formed very large, fast-settling clusters (dubbed *t227*a-e) for further selection. At the end of each day for 70 days, we subjected three replicate populations of each isolate to strong gravitational selection, giving a randomly-selected 1 mL subsample of each population only 30 seconds to settle before discarding the top 90% of the volume in the microcentrifuge tube. Only one out of five of the starting isolates formed aggregates within

Table 1. **Selective regime and aggregate production of yeast strains. The strains of yeast used in these experiments (underlined) evolved from a unicellular ancestor in response to increasingly-strong selection for settling speed through liquid media, first in 10 mL glass test tubes and then in 2 mL microcentrifuge (MCF) tubes. We first observed aggregate formation at 48 hours in a 65-day isolate, and we first observed aggregate formation at 24 hours in a 227-day isolate. We auto-diploidized the 227-day isolate, and chose five of the resulting isolates for further selection (*t227a, t227b, t227c, t227d, t227e*). One of these lineages (*t227b)* led to the aggregate forming strain *t227b.15*, which we created by selecting upon *t227b* for 15 days. *t227b.15* reliably produces large aggregates within 24 hours of growth; its ancestor *t227b* produced much smaller aggregates at higher frequency.**

STRAIN	SELECTIVE REGIME	REFERENCE	FIGURE(S)	AGGREGATE PRODUCTION	
				24 h	48 h
T0 (Y55)	45 min, glass test tubes	(Ratcliff et al., 2012)	3, 5F	0/50	0/50
T7	100 g for 10 s, MCF tubes	(Ratcliff et al., 2012)	3	0/50	0/50
T14	100 g for 10 s, MCF tubes	(Ratcliff et al., 2012)	3	0/50	0/50
T21	100 g for 10 s, MCF tubes	(Ratcliff et al., 2012)	3	0/50	0/50
T28	100 g for 10 s, MCF tubes	(Ratcliff et al., 2012)	3, 5E	0/50	0/50
T65	1 g for 300 s, MCF tubes	(William C. Ratcliff et al., 2013)	3, 4	0/50	46/50
T227	1 g for 75 s, MCF tubes	(William C. Ratcliff et al., 2013)	3, 5A, 5B	27/50	47/50
T227B	1 g for 30 s, MCF tubes	this manuscript	-	58/60	56/60
T227B.15	1 g for 30 s, MCF tubes	this manuscript	1, 2, 3, 5B, 5C, 5D, 5E	43/50	46/50

24 hours of growth, though at very high rates (97% of tubes at 24 h). We observed aggregate formation in all 15 replicates sporadically throughout the 70 days of selection, though none formed aggregates by the end of the experiment. From transfer 15, we isolated a strain that reliably forms large aggregates, which we termed *t227b.15* (Table 1) since it had undergone 15 further transfers since auto-diploidization of *t227*, and used this strain to further study the biology of aggregates. Although *t227b* formed aggregates more frequently than *t227b.15* (97% vs. 86% at 24 h), *t227b.15*'s aggregates were much larger and more amenable to study.

2.3.2 De novo evolution of aggregation

To investigate the possibility that aggregates would evolve repeatedly in populations under strong selection for rapid settling, we performed a separate selection experiment starting with a simple snowflake yeast, an isolate that had evolved a complete loss of function at the ACE2 locus after only seven days of selection (*t7*), made homozygous at all loci by selfing from a single haploid cell (auto-diploidization; Ratcliff, Fankhauser, et al., 2015). This isolate did not form aggregates and was unlikely to already contain potentiating mutations for aggregate formation, since we did not observe the earliest aggregates until *t65*, and even then, only at 48 hours of growth.

We selected these five replicate populations for strong and escalating ability to settle rapidly. We initially allowed the populations to settle for 4 minutes (240 seconds) before transfer, decreasing the duration of settling selection (thus increasing the strength of selection) by 15 seconds every 10 days, until we reached 60 seconds on day 120. We continued the selection experiment for a total of 163 days. We first observed aggregates on day 105, and by 135 days, which was when we observed the last aggregate, four out of five replicate populations had evolved them. By day 163, there was still no aggregate formation in any of the populations, as assayed by growth in twenty replicate tubes per population at 24 hours. Aggregates thus evolved and were lost repeatedly across two experiments, starting from a unicellular yeast in the first instance and a small multicellular yeast in the second.

2.3.3 Aggregates form in snowflake yeast with high levels of cell death

We assayed a variety of snowflake yeast strains in the lineage leading up to *t227b.15* for their ability to form aggregates, as well as for cluster size and proportion of dead cells, to determine if there was an association between these traits. In general, this lineage evolved larger size and a higher fraction of dead cells over time (Figure 7). Each day for five days, we examined fifty technical replicates of each strain for aggregate formation. We similarly analyzed the auto-diploidized isolates t227a-e using sixty technical replicates. Of all the strains analyzed, only *t227*, *t227b*, and *t227b.15* were capable of producing aggregates within the first 24 hours of culture, with *t227* producing aggregates 54% of the time (27/50 tubes), *t227b* producing aggregates 97% of the time (58/60 tubes), and *t227b.15* producing aggregates 86% of the time (43/50 tubes). Though *t227b* formed aggregates more often at 24 hours, they were overall much smaller than those produced by *t227b.15*. *t65* made aggregates at in 92% of the tubes after 48 hours of culture (46/50 tubes). More distant ancestors (t0, *t7*, *t14*, *t21*, *t28*) did not produce aggregates even after 72 hours of growth. Interestingly, *t227*, the third-best aggregate-forming strain in our experiment, contained 2.6% dead cells after 24 hours of culture (the ancestor t0, which does not produce aggregates, had only 0.08%), while *t227b* had an astonishing 10.3% dead cells after 24 hours, and *t227b.15* exhibited 8% cellular mortality at 24 hours (Figure 7).

2.3.4 Heritability of aggregate formation

A partitioning of variances approach showed that aggregate formation has high heritability. Using the data in Table 1, we estimated the heritability of aggregate formation at 24 h and at 48 h. Broad-sense heritability (H^2), which is the only estimate of heritability possible for asexual reproduction, was estimated as the proportion of total variance that is among strains (Herron et al., 2018). We treated aggregate formation as a binary trait and estimated

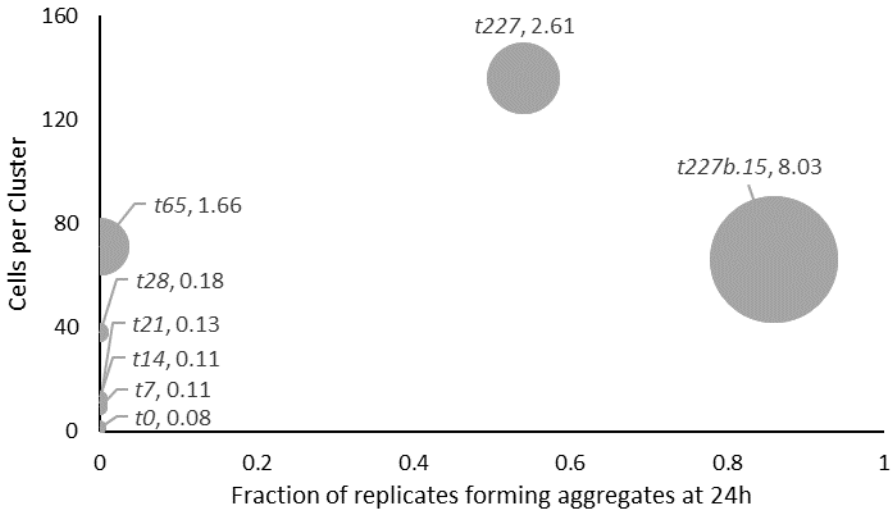

Figure 7. Across-strain relationship between cluster size, cell death and aggregate production. Each strain measured here is on the lineage leading to *t227b.15* (days of evolution for each strain denoted by *t(d)*). The frequency of dead cells at stationary phase (24 h) is indicated by bubble size and is printed next to the strain name as a percent of all cells. Both aggregate-forming strains of yeast in our experiment, *t227* and *t227b.15* have relatively high levels of cellular mortality.

variances within and among strains using an ANOVA. At 24 h, the mean square among strains was 9.00; mean square error was 0.045. Variance among strains was therefore 1.36, within strains 0.045, total variance 1.39, and the proportion of variance explained by strain $H^2 = 0.96$. At 48 h, the mean square among strains was 12.30; mean square error was 0.031. Variance among strains was therefore 0.99, within strains 0.031, total variance 1.04, and the proportion of variance explained by strain $H^2 = 0.98$.

A limitation to this approach is that the ANOVA assumption of homogeneous variance is rather obviously violated, with several strains having zero variance at each time point (strains in which we never observed aggregates). In addition, strains are not, strictly speaking, independent, since some are ancestors of others. However, our purpose in

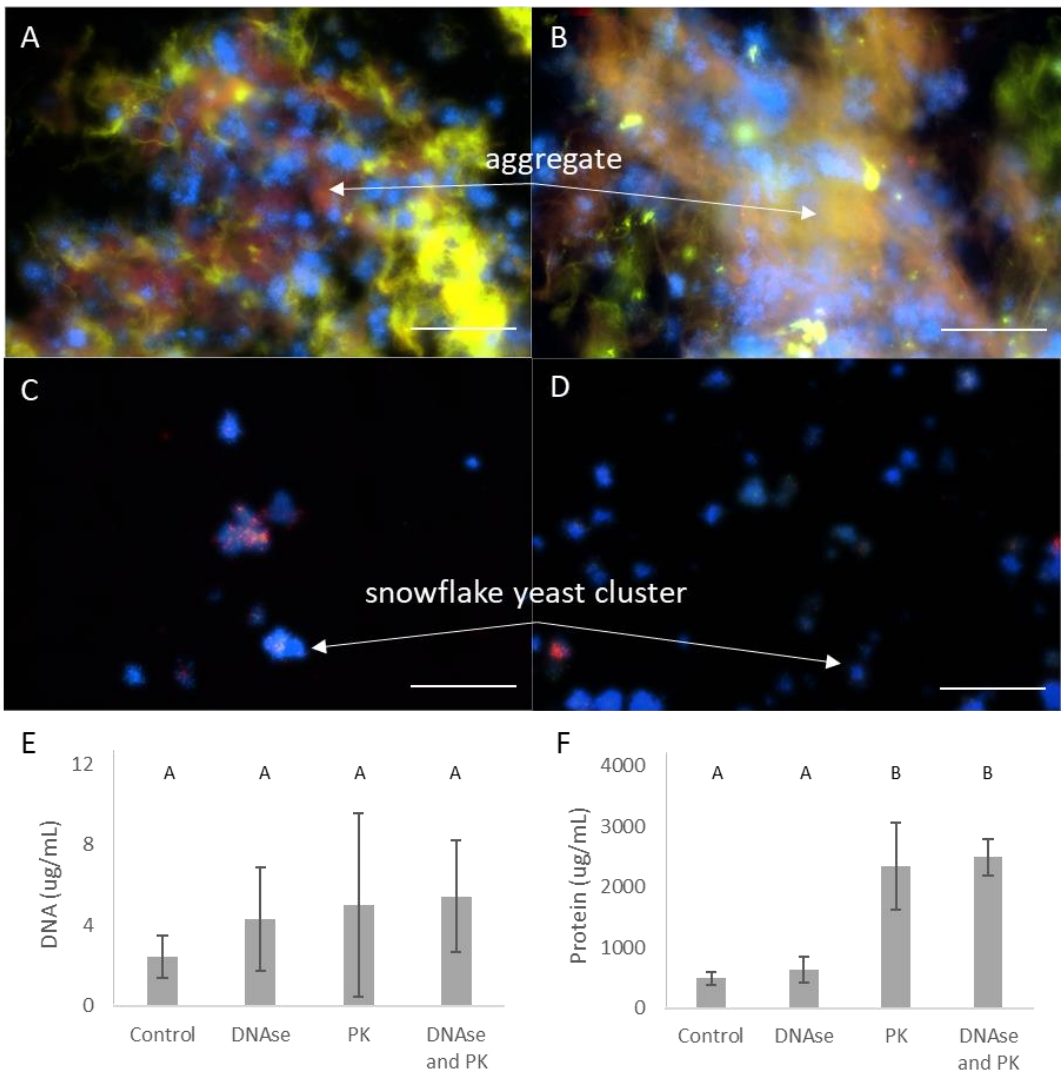

Figure 8. Proteins provide structural integrity to aggregates. We exposed aggregates to a DNase buffer control (A), DNase (B), proteinase K (C; PK), and both enzymes (D) overnight. PK alone was sufficient to fully degrade the aggregate, returning it to whole clusters (C). We analyzed the supernatant from seven replicates of each treatment for DNA and protein levels using a Qubit Fluorometer. The concentration of exogenous DNA was similar in all treatments (E), while only those with PK exhibited higher protein concentrations (F). Letters denote significant differences assessed with ANOVA and Tukey's HSD. Error bars are one standard deviation. Scale bars are 500 µm.

performing this analysis was not to determine the exact heritability of aggregate formation, which would in any case change depending on the mixture of strains. Rather, we wish to show that the majority of variation in aggregate formation is genetic.

2.3.5 Proteins are the main structural component of aggregates

Fluorescent stains showed that both DNA and protein are present in the aggregate material (Figure 6B). To determine if either or both were necessary for the structural integrity of the aggregate, we exposed aggregates to an enzyme-free control (Figure 8A), DNase I (Figure 8B), Proteinase K (PK; Figure 8C), and both enzymes (Figure 8D). After an overnight incubation, we measured the levels of both protein and DNA in the supernatant. We saw no significant difference in the amount of DNA measured in any group, regardless of exposure to DNase (Figure 8E; $F_{3,24} = 1.4$; $p = 0.28$; one-way ANOVA). However, the media containing aggregates exposed to the protease did contain significantly higher levels of protein than the unexposed aggregates (Figure 8F; $F_{3,24} = 49.2$; $p < 0.0001$; one-way ANOVA. Differences between treatments assessed via Tukey's HSD). Specifically, the aggregates not treated with the protease had an average free protein level of 561 µg/mL, whereas the exposed aggregates had an average level of 2,419 µg/mL. Visual inspection confirmed that the protease digested the aggregates (Figure 8C-D), whereas the aggregates exposed to the DNase or buffer control remained intact (Figure 8A-B).

2.3.6 Aggregates result from cell death

Proteinaceous aggregates only formed in strains that have high rates of cell death during the normal growth cycle, suggesting that aggregates are the result of proteins released from lysed cells. This cell death appears to be the result of cellular suicide: 8% of *t227b.15* cells were dead according to the stain propidium iodide (PI) after 24 h of growth in YPD, with 0.54% of cells undergoing apoptosis as labelled by dihydrorhodamine 123 (DHR) at 12 h, and 4.22% at 24 h.

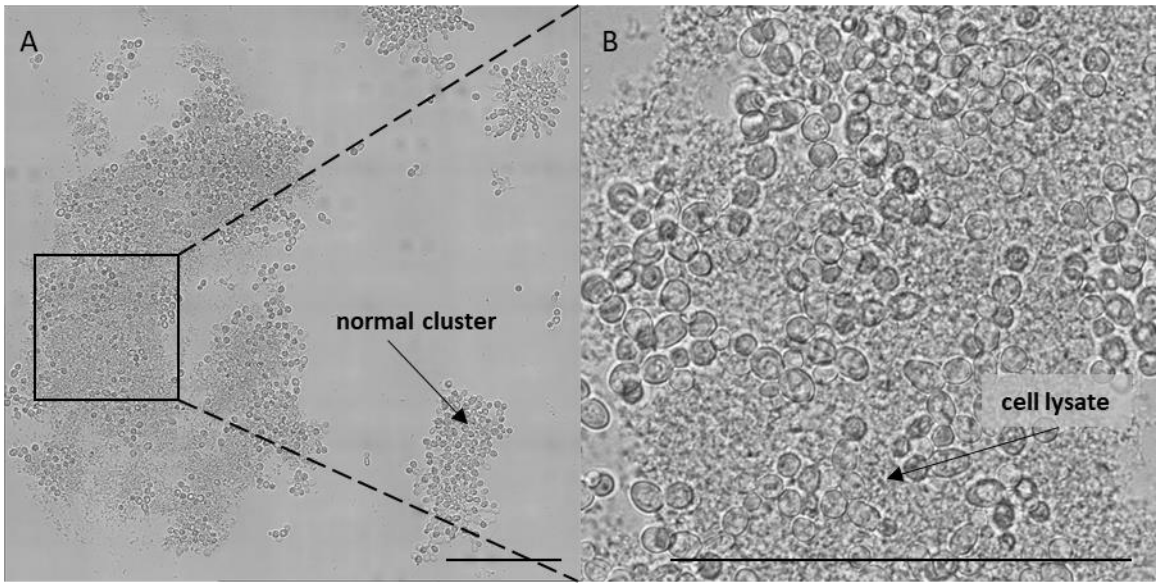

Figure 9. Hydrogen peroxide exposure results in extensive programmed cell death. We experimentally induced apoptosis via a one-hour exposure to 5 µM H_2O_2. 12 h after this treatment, H_2O_2–exposed cells were visually degraded (A&B, photo representative of 10 biological replicates). Scale bars are 500 µm.

We examined this relationship further by inducing apoptosis with hydrogen peroxide (H2O2; Frank Madeo et al., 2002; Ribeiro et al., 2006) in an ancestor of *t227b.15*, *t65*, that does not form aggregates within the first 24 h of growth. We chose this strain because it is capable of aggregate formation, but only after approximately 36 hours. We expected that if a link exists between cell death and aggregate formation, we would see aggregates form at an earlier time and/or in greater frequency in populations exposed to hydrogen peroxide than in control populations. Since other strains (*t227*, *t227b*, *t227b.15*) are capable of aggregate formation by 24 hours, we also knew that there was no inherent barrier to aggregate formation at these earlier times.

We exposed stationary phase populations (grown for 24 h) to 5 µM H2O2 for one hour, then monitored apoptosis and cell death over the next 12 h, and aggregate formation

over 15 h. 12 h after H2O2 exposure, yeast cells were visibly degraded (Figure 9A&B), with higher levels of both dead (Figure 10A&D; $F_{7,72} = 12.2$; $p < 0.0001$; one-way ANOVA; differences between treatments assessed via Tukey's HSD) and apoptotic (Figure 10B&E; $F_{7,72} = 5.4$; $p < 0.0001$; one-way ANOVA; differences between treatments assessed via Tukey's HSD) cells (Figure 10C) than unexposed populations.

Populations exposed to H2O2 formed aggregates earlier (Figure 10F; bootstrap support 99.5%) and more frequently than unexposed populations (Figure 10F; bootstrap support 100%). The H2O2 treatment group first produced an aggregate 10 hours after exposure; by 11 hours, 7 out of 10 tubes contained an aggregate. The control group did not produce an aggregate until 13 hours after exposure, and only 2 out of 10 tubes had an aggregate by 14 hours after exposure. Inducing apoptosis, leading to cellular lysis and the release of cellular proteins, thus promotes proteinaceous aggregate formation.

2.3.7 Aggregate formation is advantageous when fast settling is favoured

We used a divergent selection experiment to examine if aggregates would increase in abundance in response to strong selection for rapid settling. We selfed *t227*, the weak aggregate-forming ancestor to *t227b.15*, to generate a population comprised of ~1,000 F1 recombinants that were homozygous at all loci. We chose this strain because we knew the F1 would feature some offspring capable of proteinaceous aggregate formation, and some offspring incapable of proteinaceous aggregate formation, providing a diverse starting population. After selfing, we subjected five replicate populations to selection for rapid settling (cells taken from the bottom 10% of the tube after 60 seconds of settling) and five replicate populations to selection for slow settling (cells taken from the top 10% of the tube

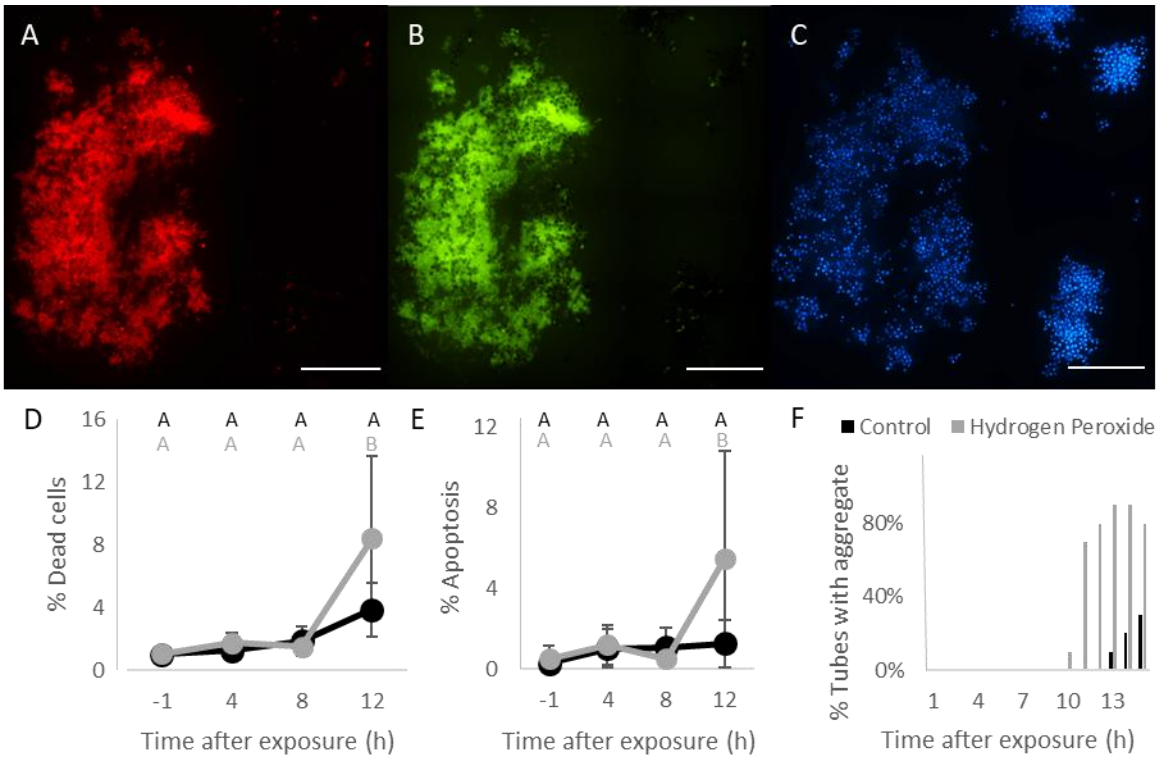

Figure 10. Apoptosis promotes proteinaceous aggregate formation. We experimentally induced apoptosis in stationary phase (24 h) cultures via a one-hour exposure to 5 µM H_2O_2. 12 h after this treatment, H_2O_2–exposed cells had higher levels of cell death (A, D) and reactive oxygen species (ROS) production (B, E), indicating elevated rates of apoptosis. Cell vacuoles labeled in blue (C). Aggregates formed earlier and at a higher frequency in populations exposed to H_2O_2, suggesting that programmed cell death plays a direct role in aggregate formation by releasing proteins from cells into growth media (F). Letters denote significant differences assessed with ANOVA and Tukey's HSD, with black letters representing unexposed populations and gray letters representing exposed populations. Scale bars are 500 µm.

after 60 seconds of settling) for five transfers. We then assayed aggregate formation in 10 technical replicates of each evolved population.

Yeast populations under selection for rapid settling showed a strong tendency to produce aggregates. 44% of technical replicates formed aggregates in 24 hours, in contrast to just 2% of the replicates from the population selected for slow settling (Figure 11A; $X^2 = 19.2$; $p < 0.0001$). Further, isolates that formed aggregates had higher rates of cell death (3.93%

vs. 2.40%; *t14* = 2.2; $p = 0.028$; two-sample t-test) but similar cluster sizes (weighted mean size of 96.79 vs. 97.01 cells, respectively; *t14* = 0.004; $p = 0.99$; two-sample t-test), regardless of whether we selected them for slow or fast settling. This suggests that selection was acting directly on higher rates of cell death, rather than on cluster size per se, and that aggregate formation is either an adaptation to selection for rapid settling or is a pleiotropic consequence of an adaptation.

2.3.8 Aggregates settle faster than individual clusters, increasing survival

We calculated the settling rate of both aggregates and individual clusters in water by measuring the length of time it took for each to travel 10 centimeters. Aggregates settled more than seven times as fast as individual clusters, at average rates of 0.79 cm/s and 0.11 cm/s, respectively (Figure 11B; $t_{22} = 26.32$; $p < 0.0001$; two sample t-test). Since proteinaceous aggregates float within the tube during cell culture (Figure 5), we did not expect that they would provide a settling rate advantage. However, the key step seems to be the partial degradation of the aggregate upon vortexing, which occurs immediately before settling selection. We did not observe aggregates settling without this step. Vortexing may release carbon dioxide gas bubbles, produced during growth, that cause large aggregates to float, thereby allowing aggregate fragments to settle rapidly.

The faster settling rate of aggregates results in a nine-fold survival advantage for clusters within aggregates, relative to individual solitary clusters, in our selective regime (Figure 11C; $t_9 = 3.2$; $p = 0.0053$; two-sample t-test). Specifically, clusters that did not start out in the lower 10% of the tube had an 80.3% chance of making it to the bottom during

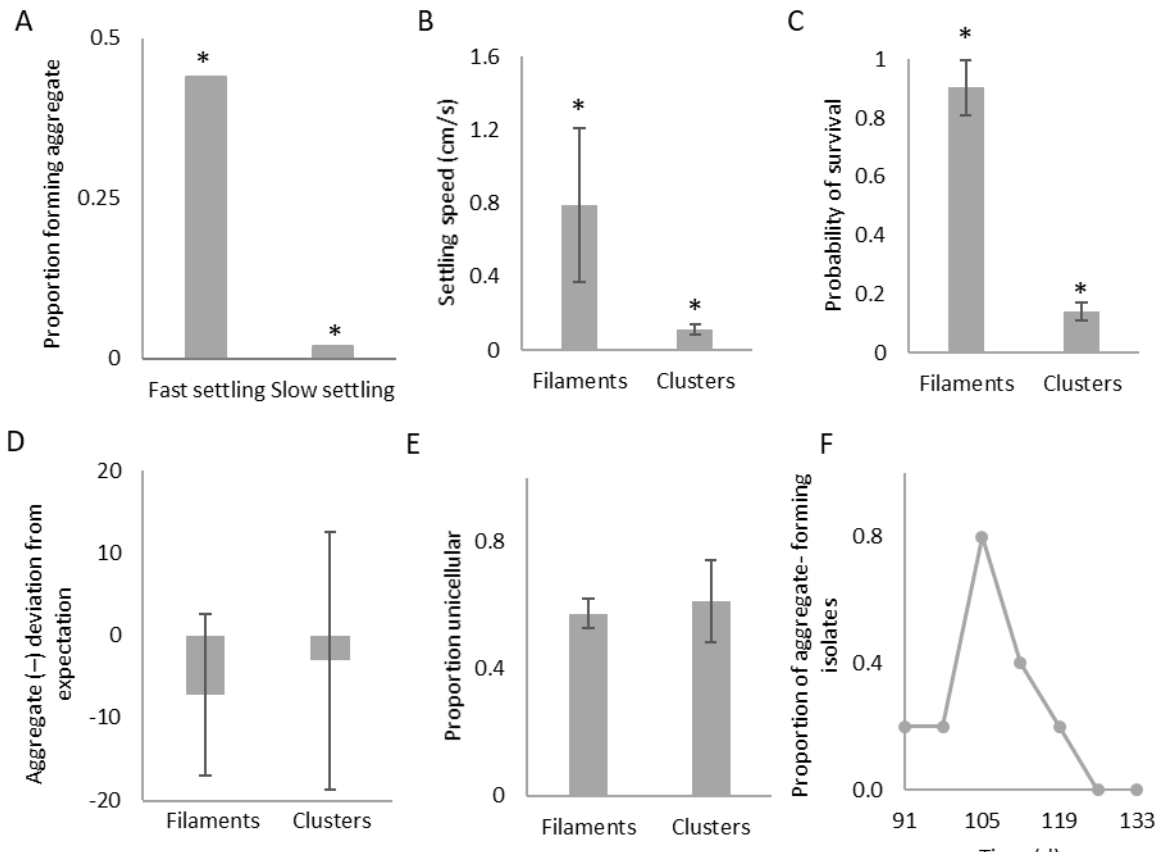

Figure 11. Proteinaceous aggregates are adaptive under strong selection for rapid settling, but are a common good. We performed a divergent selection experiment to determine if aggregate formation is adaptive under strong settling selection. We selfed *t227* (the ancestor of *t227b.15*, which weakly forms aggregates) *en masse*, and then selected for either fast or slow settling in five replicate populations of ~1,000 auto-diploidized lineages. After 5 transfers, far more of the randomly-selected yeast genotypes (n=100) from the rapid settling treatment formed aggregates than from the slow settling treatments (A). Aggregates provide a strong benefit under selection for rapid settling, increasing settling velocity seven-fold (B), and increasing a cluster's odds of surviving settling selection by nine-fold (C). Aggregates, however, appear to be a common good. Snowflake yeast that do not form aggregates are found within aggregates in proportion to their overall population frequency (D), and even unicellular yeast are found within aggregates at comparable rates to snowflake yeast cells (E). Examining a single population over time, we find that aggregate-forming yeast rapidly increased in frequency, becoming the dominant strategy after 105 days, and then rapidly fell below our threshold for detection (F). * indicates a significant difference ($p < 0.05$) as assessed by a two-sample *t*-test.

settling selection if they were in an aggregate, but their chances fell to just 0.14% if they were alone.

2.3.9 Aggregates are a common good

Since aggregates are not necessarily composed of related clusters, we investigated if they act as a common good, entangling yeast regardless of whether or not they contribute to aggregate production. First, we co-cultured *t227b.15* with a GFP-labeled non-aggregate-producing strain (*t28* URA3/ura3::TEF1-GFP) at frequencies ranging from 0-100% in 10% increments. We chose this strain since it has the most cells per cluster of the strains that do not produce aggregates (Figure 7). Overall, we found non-producers within aggregates at rates similar to their overall population frequency in the 70, 80, and 90% *t227b.15* tubes (Figure 11D; $t_9 = 1.3$; $p = 0.22$; pre-planned contrast after analysis via nested ANOVA), which were the only aggregate-producers in the mixed populations. This result demonstrates that the benefits of joining a proteinaceous aggregate are accessible to any snowflake yeast in the population, not just aggregate producers.

Next, we examined whether or not aggregates discriminate between unicellular and snowflake yeast, by co-culturing *t28* with unicellularized *t227b.15* (ace2/ACE2-KANMX4). Surprisingly, we found that unicellular *t227b.15* was not only still able to produce an aggregate, but was also equally well-represented within the aggregates, found at similar frequencies as in the overall population (Figure 5E; $t_9 = 0.63$; $p = 0.070$; two-sample t-test). These results show that snowflake yeast that do not contribute to aggregate production can exploit this common good.

Finally, we examined the dynamics of aggregate formation within a single population. We randomly selected five isolates from a single population (taken from our second experiment, which started from a homozygous *t7* isolate) every week from days 91-

133. This population formed aggregates consistently between days 105 and 118 in our original experiment. We screened each of these isolates for aggregate formation during 24 h of culture by growing each in triplicate (all isolates that formed aggregates did so in at least 2/3 replicates). Interestingly, aggregate-forming strains rapidly increased in frequency within this population, becoming the dominant strategy after 105 days, and then fell below our threshold for detection (Figure 11F). These dynamics are consistent with aggregate formation being a beneficial, cooperative behavior that is susceptible to invasion by non-cooperating cheats.

2.4 Discussion

Microbes often cooperate to survive stressful conditions through collective action, perhaps best exemplified by altruistic behaviors such as fruiting body construction (S. I. Li, Buttery, Thompson, & Purugganan, 2014) or cellular differentiation into spores and defensive cells that produce antibiotics until they lyse (Yague, Lopez-Garcia, Rioseras, Sanchez, & Manteca, 2012). A growing body of experiments shows that both common goods and group formation can evolve quickly in response to environmental challenges. For example, *Pseudomonas fluorescens* bacteria produce a cellulosic polymer, which causes the formation of biofilm-forming groups, in response to mortality caused by catastrophic disturbances (Brockhurst et al., 2010). Similarly, yeast secrete invertase when consuming sucrose (Greig & Travisano, 2004; Maclean & Brandon, 2008), and selection for efficient use of this common good can drive the evolution of group formation (Koschwanez, Foster, & Murray, 2013).

In this paper, we show that intense settling selection can drive the evolution of macroscopic structures in yeast through increased production of a common good. Initially, this appears to be a non-adaptive side-effect of high rates of programmed cell death, which by liberating proteins from lysed cells results in the formation of proteinaceous aggregates. This is clear from the observation that strains isolated after 65 days of selection form proteinaceous aggregates at high rates (92%) within 48 hours of growth, but none within the first 24 hours. Because we transferred yeast to fresh medium every 24 hours, this phenotype could not have been a target of direct selection since it was not yet expressed in the experimental populations.

As these yeasts evolved higher rates of cell death, though, aggregates eventually began to appear during the first 24 hours. It appears that yeast entanglement within a fast-settling aggregate provides a strong benefit under conditions of very strong selection for rapid sedimentation (60 s settling on the bench), increasing the odds that yeast starting outside the 'survival zone' (bottom 10% of the tube during settling selection) would survive to 80%, relative to just 0.14% for individual snowflake yeast. Similarly, in a divergent selection experiment, aggregate formation did not decline when selection favored rapid settling, but was rapidly lost when selection favored slow settling (Figure 5A), likely due to the considerable fitness cost of the high PCD rate required to express this trait under both selection regimes. However, in both selection experiments aggregate formation ultimately proved to be evolutionarily unstable, failing to persist despite the high survival benefit aggregate membership confers.

Aggregate formation appears to be a common good, highly heritable though exploitable by non-producers (Figure 11D&E). We use the term 'common good', rather

than the traditional ‘public good’, because it is more accurate in this case. The number of clusters producing extracellular proteins and DNA constrains aggregate size. Since space within an aggregate is limited, access to the good is rivalrous (Dupré, 2009; T. W. Smith, 1999)— its use by one cluster can prevent it from being used by another.

Proteinaceous aggregate formation is costly, requiring at least 2% of cells to commit suicide to create an aggregate within 24 hours (just 0.08% of cells are undergoing PCD at 24 h in the unicellular ancestor; Figure 8). Because aggregate-producing strains do not preferentially occupy the aggregates they produce, this behavior is altruistic at both the cell and strain levels under our experimental conditions. Specifically, individual cells that contribute to aggregate formation by dying cannot benefit from the aggregate, and strains that exhibit a high rate of cell death will, all else equal, grow less quickly and thus have lower fitness during the growth phase of the culture cycle. This altruism may have led to the evolutionary instability of aggregate formation over long periods of time (Figure 11F).

Under selective conditions, we would expect that a non-producing cheat would gain the same benefits of aggregate formation (an increase from 0.14% to 80% survival) as aggregate-producers, without paying the high associated cost in cellular suicide. Specifically, our experiments demonstrated that a non-producer (*t28*, which only has 0.18% cell death at 24 h) was able to incorporate within an aggregate at equal proportion to a producer (*t227b.15*, which has 8.03% cell death, Figure 11D). However, under non-selective conditions we would not expect a non-producing cheat to benefit from incorporation within an aggregate, as there is no advantage to forming large groups without settling selection. Indeed, growth rates within an aggregate may be lower than in the

unincorporated clusters if the dense cellular packing reduces access to nutrients and oxygen.

Aggregates are a somewhat unusual form of group. They are temporary structures-regularly forming, dissolving, and re-forming, analogous in some ways to a herd or school, but they also impose a high cost of formation, more similar in some ways to a biofilm produced by the lysis of individual cells (Turnbull et al., 2016). Aggregate formation may represent a step towards the creation of a new level of selection. Defining a level of selection is not without controversy (Istvan Jr, 2013), but in general a unit of selection is accepted as a biological level of organization upon which natural selection acts (Hull, 2001; Okasha, 2006; Wade et al., 2010). Aggregates meet this definition, since after vortexing large fragments of the aggregate either survive or perish as a unit. However, conflicts between levels of selection may preclude aggregate-level adaptation. The cells within aggregates are not clonal; indeed, non-aggregating strains can become readily incorporated within the aggregate. Since high relatedness (O. M. Gilbert, Foster, Mehdiabadi, Strassmann, & Queller, 2007), or another mechanism aligning the fitness of cooperators (i.e., vertical transmission or reciprocity; Herre, Knowlton, Mueller, & Rehner, 1999; Trivers, 1971; Vautrin & Vavre, 2009) is needed to maintain costly cooperation (such as the programmed cell death necessary to produce aggregates), it is unclear whether aggregate-level selection is strong enough to overcome lower-level (i.e., cluster- or cell-level) selection.

Indeed, yeast aggregate production was evolutionarily unstable. Despite the benefits of cooperation, aggregate formation was lost from all populations within a few hundred generations of evolving this novel behavior, highlighting the importance of positive

assortment between cooperators during the formation of a new level of selection. Nonetheless, it is striking how readily simple multicellular proto-organisms evolve a collective response when selection is so strong that individuals have little chance of survival.

CHAPTER 3. DIVERSE CONDITIONS SUPPORT NEAR-ZERO GROWTH IN YEAST: IMPLICATIONS FOR THE STUDY OF CELL LIFESPAN

Baker's yeast has a finite lifespan and ages in two ways: a mother cell can only divide so many times (its replicative lifespan), and a non-dividing cell can only live so long (its chronological lifespan). Wild and laboratory yeast strains exhibit natural variation for each type of lifespan, and the genetic basis for this variation has been generalized to other eukaryotes, including metazoans. To date, yeast chronological lifespan has chiefly been studied in relation to the rate and mode of functional decline among non-dividing cells in nutrient-depleted batch culture. However, this culture method does not accurately capture two major classes of long-lived metazoan cells: cells that are terminally differentiated and metabolically active for periods that approximate animal lifespan (e.g. cardiac myocytes), and cells that are pluripotent and metabolically quiescent (e.g. stem cells). Here, we consider alternative ways of cultivating *Saccharomyces cerevisiae* so that these different metabolic states can be explored in non-dividing cells: (i) yeast cultured as giant colonies on semi-solid agar, (ii) yeast cultured in retentostats and provided sufficient nutrients to meet minimal energy requirements, and (iii) yeast encapsulated in a semisolid matrix and fed ad libitum in bioreactors. We review the physiology of yeast cultured under each of these conditions, and explore their potential to provide unique insights into determinants of chronological lifespan in the cells of higher eukaryotes.

3.1 Introduction

Aging, or the progressive loss of function over time, is a hallmark feature of all living cells, including 'simple' organisms such as baker's yeast (Flatt). More than half a century ago,

Mortimer and Johnson (Mortimer & Johnston, 1959) reported that individual yeast cells are mortal and have a limited capacity for cell division. Subsequent demographic analyses showed that mortality increased exponentially as yeast populations underwent successive rounds of replication in batch culture. Replicatively aging yeast undergo characteristic morphological and biochemical changes that include increasing cell size, accumulation of bud scars, slowing of the cell cycle, and accumulation of extrachromosomal rDNA circles (Arlia-Ciommo, Piano, Leonov, Svistkova, & Titorenko; Jo, Liu, Gu, Dang, & Qin; Wasko & Kaeberlein, 2014). Genetic variation is associated with strain-specific differences in the rate of functional decline, manifest as strikingly different mean replicative lifespans (RLS) among wild and laboratory yeasts (Denoth Lippuner, Julou, & Barral, 2014; Stumpferl et al., 2012).

Yeast also age chronologically, as evidenced by the decline and eventual death of a non-dividing cell over its chronological lifespan (CLS). Because microbes cannot divide in the absence of essential nutrients, yeast CLS has most frequently been studied in relation to the survival of free-floating (planktonic) cells in nutrient-depleted liquid culture (C. R. Burtner, C. J. Murakami, B. Olsen, B. K. Kennedy, & M. Kaeberlein; E. Garay et al.; Powers, Kaeberlein, Caldwell, Kennedy, & Fields). Such cells enter G_0 arrest and initially undergo metabolic and structural changes that include accumulation of storage carbohydrate, cell wall thickening, an overall decline in protein synthesis, an increase in stress tolerance, and a shift to respiratory metabolism (Christopher R. Burtner, Christopher J. Murakami, Brian K. Kennedy, & Matt Kaeberlein, 2009; Powers et al., 2006). Viability among starving planktonic yeast cells diminishes over time, as does their replicative capacity, suggesting that RLS and CLS may be linked mechanistically (Christopher R.

Burtner et al., 2009). Caloric restriction (CR) during the time non-dividing yeast age delays the progressive reduction in replicative lifespan (L. G. Boender, M. J. Almering, et al., 2011; S.-J. Lin et al., 2002; D. L. Smith, Jr., McClure, Matecic, & Smith, 2007). Indeed, among chronologically old cells, those that have the lowest mitochondrial membrane potential (reducing ATP production) (Zorova et al., 2018) also have the longest subsequent replicative lifespan; thus, mitochondrial function may constitute a causal link between CLS and RLS (J. R. Delaney et al.). Further evidence for this link is provided by rho(0) cells, which experience both lower mitochondrial membrane potential and longer RLS than do rho(+) cells (Miceli, Jiang, Tiwari, Rodriguez-Quinones, & Jazwinski, 2011). Strain-specific variation in CLS exists among wild yeast isolates, assayed as survivorship of starving planktonic cells (Qin & Lu, 2006), and the genetics underlying this variation has been generalized to other eukaryotes, including animals (Kwan, Foss, Kruglyak, & Bedalov, 2011).

3.2 Chronological aging in starved planktonic cultures

Screens for CLS mutants in starved yeast cultures have uncovered genes involved in stress-resistance and nutrient-signaling pathways (Christopher R. Burtner, Christopher J. Murakami, Brady Olsen, Brian K. Kennedy, & Matt Kaeberlein, 2011; Joe R. Delaney et al., 2013; Erika Garay et al., 2014; Wei, Madia, & Longo, 2011). Some of these pathways, like the target-of-rapamycin (TOR)-pathway, are highly conserved among eukaryotes and have been implicated in aging processes in worms, flies and mammals (Fontana, Partridge, & Longo, 2010; C. He, Zhou, & Kennedy, 2018; Valter D. Longo & Fabrizio, 2012; Swinnen, Ghillebert, Wilms, & Winderickx, 2014). However, starvation poorly mimics the physiology of major classes of metazoan cells. Terminally differentiated cells such as

cardiac myocytes and neurons consume a large proportion of the organism's energy and are typically well nourished (Bourre, 2006). Although growth-arrested, such cells remain metabolically active and perform large amounts of work with minimal functional decline, often for decades in higher animals (Bergmann et al., 2015). Starvation also poorly mimics the physiology of mitotically quiescent cells, such as hematopoietic stem cells and myosatellite cells that, respectively, can quickly be recruited to form blood cells or to regenerate injured skeletal muscle. Satellite cells are "lying low but ready for action," being not only mitotically but also metabolically quiescent, having few mitochondria, and deriving most of their maintenance energy requirements from anaerobic (i.e., fermentative) metabolism (Montarras, L'Honore, & Buckingham, 2013). Hematopoietic stem cells also appear to derive most of their maintenance energy requirements from fermentative metabolism, and indeed, the switch to mitochondrial respiration appears to be necessary for stem cell differentiation (Kocabas et al., 2015; Takubo et al., 2013).

The starving yeast aging paradigm, where lifespan is measured in nutrient-depleted planktonic cells, therefore falls short as a model to study the physiology of cells that are either growth-arrested but metabolically active, or growth-arrested but metabolically quiescent, i.e., those cells that are on the front lines and those that are held in reserve. To make up for this shortfall, alternative yeast culture conditions are needed in which mitotically-arrested cells can be studied under conditions that range from caloric excess to caloric restriction. Here, we consider alternatives to the starving yeast paradigm (Figure 12A), where near-zero growth rates can be achieved by other means. These include aging yeast cultured on solid medium (Figure 12B), in retentostats (Figure 12C), or as encapsulated cells in continuously-fed bioreactors (Figure 12D). With these culture methods

at their disposal, yeast researchers can investigate factors governing chronological lifespan in different contexts: closed systems (Figure 12A, B), and open systems (Figure 12C, D), matrix-free (Figure 12 A, C), and matrix-associated (Figure 12B, D), nutrient-limited (Figure 12A, B, C), and nutrient-replete (Figure 12D). Below we consider how these different contexts lead to physiological states that better approximate metabolism in non-dividing animal cells than do starving planktonic yeast.

3.3 Chronological aging in yeast colonies

Yeast chronological lifespan has been studied in the context of aging colonies on the surface of nutrient agar (J. Hu, Wei, Mirisola, & Longo, 2013; Mináriková, Kuthan, Řičicová, Forstová, & Palková, 2001), typically under aerobic conditions on complex media (Palkova, Vachova, Gaskova, & Kucerova, 2009; Váchová, Čáp, & Palková, 2012) for periods ranging from 20-130+ days. Unlike cells cultured in ideally-mixed liquid media, cells cultured on solid media are in a spatially-structured environment, where they experience gradients of nutrients, waste products, signaling molecules, and gases (M. Cap, Stepanek, Harant, Vachova, & Palkova, 2012). These gradients, in turn, influence how cells stratify in colonies and age within those strata, much like a morphogenetic field in early embryological development (Alberts B, 2002). By ten days post-inoculation, colonies have differentiated vertically into two cell types, only one of which divides (Vachova & Palkova, 2011). In this respect, the colony resembles a multicellular organism, in that it is largely clonal and consists of a mixed population of dividing and non-dividing cells.

3.3.1 Cells in a colony display slower growth, and higher viability than aging planktonic cells

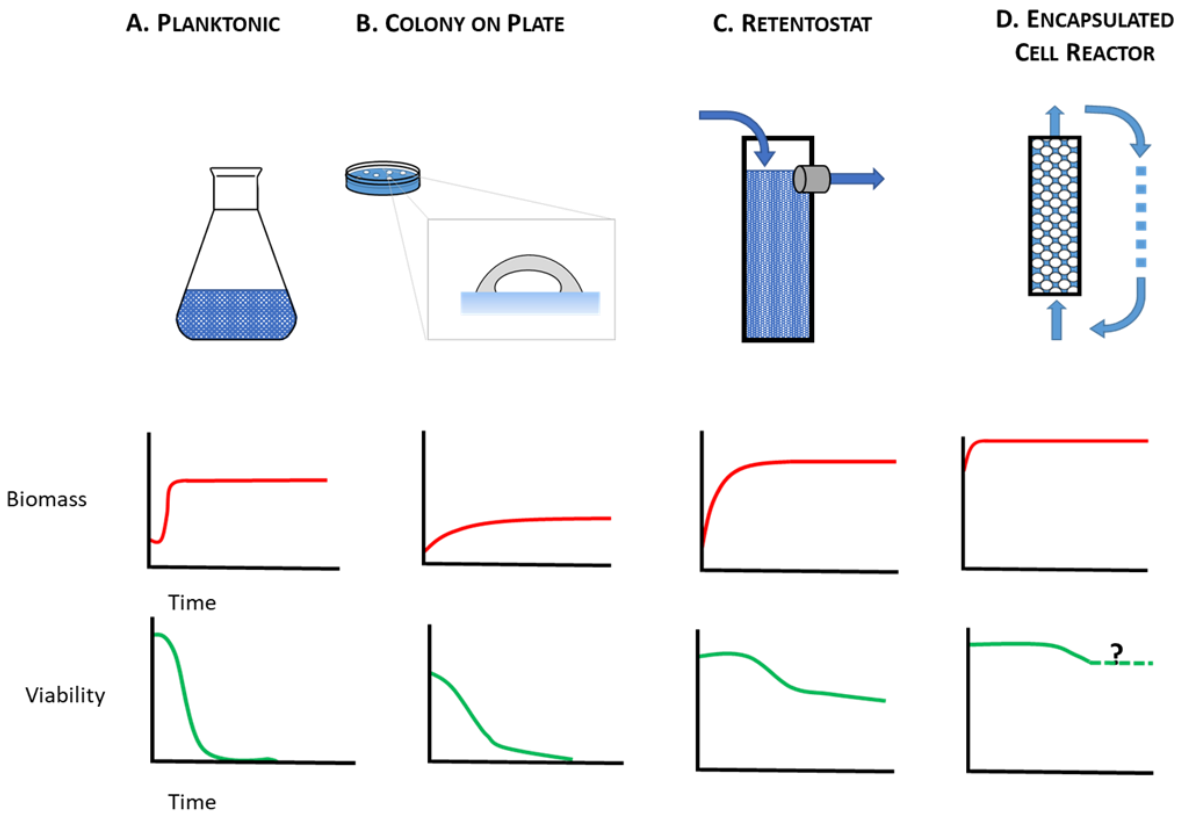

Figure 12. Chronological lifespan of non-dividing yeast has been studied using multiple culture methods: (A) planktonic cultures, (B) colonies on plates, (C) retentostats, and (D) encapsulated cell reactors, each of which presents a different time-dependent profile of biomass accumulation and cell viability.

The various gradients experienced by cells in colonies create selective pressures not experienced by planktonic cells in liquid culture. Cells on agar and cells in liquid culture behave similarly immediately after inoculation (Váchová et al., 2012). But soon thereafter colonies undergo a longer period of slow growth than do planktonic cells (>8 days on solid medium vs. 40 hours in liquid) (Meunier & Choder, 1999). Diffusion provides cells growing on solid agar with a slow, steady nutrient supply (Vachova & Palkova, 2011), making it possible for the population to gradually expand for up to 32 days (Palkova et al., 2009). However, not every cell in a colony can divide: the number of colony-forming units (CFUs) recovered after dilution and plating on fresh agar asymptotes after 18 days. And by 90 days

as much as 25% of a colony consists of cells that are alive but unable to reproduce on rich medium, a likely result of chronic nutrient deprivation, similar to how oligotrophic environments in nature generate large numbers of viable but nonculturable microbes (Oliver, 2005).

Patterns of reproduction and survivorship in giant colonies contrast sharply with those patterns in planktonic culture, where biomass accumulation typically ceases 3 days post-inoculation (P. Fabrizio et al., 2004). After 10 days in synthetic dextrose complete (SDC; 2% dextrose) medium, starving planktonic yeast may exhibit ~5% viability (Paola Fabrizio et al., 2004); by contrast, after 10 days on solid GM medium (1% yeast extract, 3% glycerol), yeast in giant colonies (created by transferring a cell suspension onto GM agar (Vachova, Hatakova, Cap, Pokorna, & Palkova, 2013)) are 90% viable and do not fall to 5% until after 135 days. In both instances, viability was estimated as the proportion of total direct counts recovered as CFUs (Palkova et al., 2009). At all time-points measured, yeast in colonies exhibit greater viability than their isogenic counterparts in planktonic culture, even among strains that differ in CLS (Palkova et al., 2009; Piper, Harris, & MacLean, 2006; Vachova & Palkova, 2005). This observation has led Palkova and colleagues to speculate that prolonged slow growth of yeast cells in colonies is analogous in some ways to caloric restriction (Palkova et al., 2009), a factor shown to increase lifespan in all species examined to date (L. G. Boender, M. J. Almering, et al., 2011; Kaeberlein et al., 2005; C. Lee & Longo, 2016; D. L. Smith, Jr. et al., 2007).

3.3.2 Yeast in aging colonies become physiologically-differentiated

In an aging colony, subpopulations of cells differentiate in both vertical (Figure 13A; upper vs. lower) and horizontal (Figure 13B; center vs. margin) dimensions, with subpopulations aging in different ways and at different rates (Vachova, Cap, & Palkova, 2012; Váchová & Palková, 2018). Following 10 days of incubation, spatially-segregated cell types can be distinguished from one another and from their progenitors with respect to morphology, nutrient utilization, and stress resistance. Cellular differentiation within giant colonies has been linked to production of volatile ammonia, which is believed to contribute to, or even drive, formation of stratified layers within a colony. The process has been described in detail (Palkova et al., 2002; Palkova & Vachova, 2006; Palková & Váchová, 2003; Vachova, Kucerova, Devaux, Ulehlova, & Palkova, 2009), and recently reviewed by Vachova and Palkova (Vachova et al., 2012; Váchová & Palková, 2018).

Vertical stratification of U and L cells in aging yeast colonies

Along the vertical axis, cells in giant aging colonies stratify into upper (U) cells and lower (L) cells. U cells typically exhibit multiple small vacuoles and swollen mitochondria having few cristae (M. Cap et al., 2012). Further characteristics of U cells include glycogen accumulation, formation of large lipid droplets, and poor mitochondrial transmembrane potential, as indicated by $DiOC_6$, a lipophilic mitochondrial dye. In contrast with U cells, L cells contain numerous mitochondria with well-developed cristae, and exhibit a high transmembrane potential by $DiOC_6$ staining, (Čáp, Štěpánek, Harant, Váchová, & Palková, 2012; Váchová et al., 2012). Accordingly, L cells produce 3-fold more reactive oxygen species than U cells, and have higher respiratory capacity (Čáp et al., 2012).

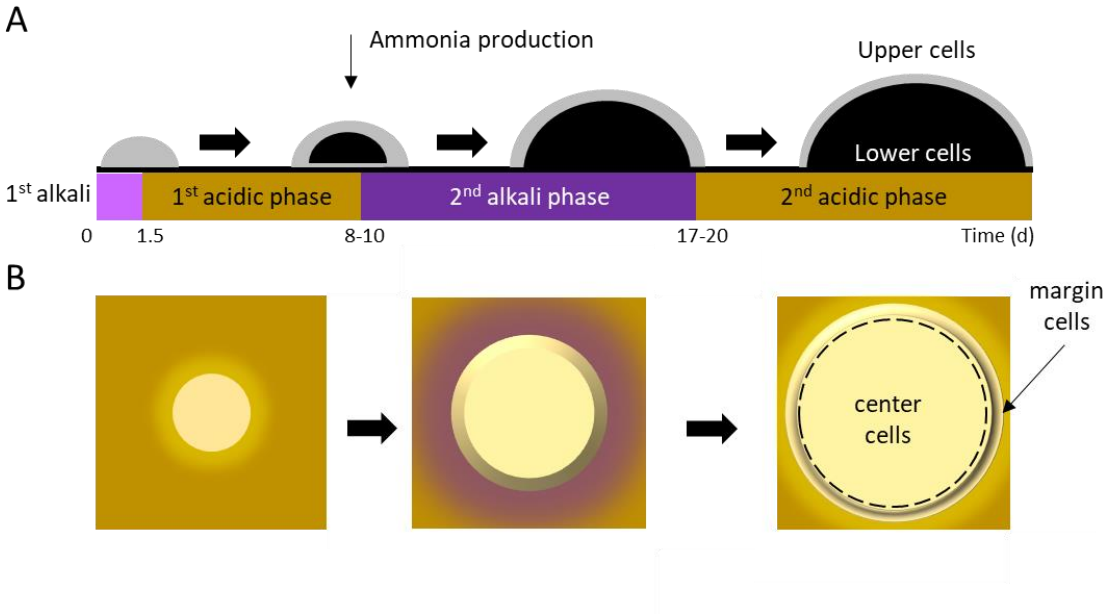

Figure 13. Yeast colonies transition through alkali (pH ~6.8) and acidic (pH ~5.2) phases, causing the area around a colony to change in color from yellow to purple and back again on agar containing Bromocresol purple. The pH changes contribute to cellular differentiation in both the vertical (A) and horizontal (B) dimensions. Gray indicates healthy, dividing cells and black indicates non-dividing cells.

Paradoxically, L cells display attributes reminiscent of both starved and exponentially-growing planktonic cells. Similar to starved planktonic cells, L cells possess an active sucrose non-fermentable (SNF) pathway; glucose-repressible genes are de-repressed, and cells are respiring. Instead, genes are upregulated in mitochondrial biogenesis, oxidative phosphorylation, and nonfermentable carbon source utilization (e.g., *HAP5*, *USV1*, *RTG1*). Like exponential-phase planktonic cells, L cells are sensitive to heat shock, cell wall dissolution by zymolyase, and exhibit no TOR activity. Further, recent studies on finely-dissected giant colonies indicate that among L-cells, upper and lower L subpopulations can be discriminated on the basis of their distinct patterns of gene expression (Wilkinson et al., 2018).

Physiological differences between U and L cells lead to differences in stress resistance and CLS within an ageing colony. For example, at day 50 only 10% of L cells are still viable, compared to 50% of U cells (Vachova et al., 2012). Higher viability among U cells is correlated with activation of regulatory pathways like TOR, typical of cells growing under nutrient-rich conditions (Hinnebusch, 2005). But U cells also exhibit features typical of yeast under nutrient limitation, such as activation of the general amino acid control pathway (Vachova et al., 2012). This unusual physiology suggests active consumption of some nutrients, but limitation by others, and contrasts with the physiology of L cells, which upregulate genes involved in nonfermentable carbon source utilization rather than TOR.

3.3.3 Cell stratification benefits some cell types at the expense of others, contributing to colony longevity

Autophagy is important for survival in U, but not L, cells. Colonies derived from strains having defects in autophagy (*atg1Δ, atg12Δ, atg5Δ, atg8Δ*) exhibit reduced U cell viability, particularly in older colonies, but have no effect on L cell viability. This observation raises the possibility that L cells may provide an energy source for U cells. Not only do L cells activate degradative mechanisms, such as proteasomal and vacuolar functions, and upregulate expression of genes involved in glucose export (Vachova et al., 2012), but defects in these genes diminish U cell viability, indicating that U cells depend on L cell degradation and L cell glucose export for their survival. Ninhydrin staining indicates that L cells also release amino acids, with their total intracellular amino acid content decreasing by 23% between days 15 and 20. L cells are also sensitive to zymolyase and upregulate cell wall glucanases (Scw11p, Dse4p, Egt2p), suggesting they may release cell wall

constituents that serve as carbon sources for U cells. The consumption of L cells by U cells may benefit the colony as a whole, assuring not only its survival, but also its dispersal. Cells on a colony's exterior are more likely to be dispersed than those on the interior, either by water or by insects; but such cells are further from nutrients on the colony substratum. L cells may therefore engage in a form of altruism that benefits their kin, as U and L cells are essentially clones of one another (Palkova, Wilkinson, & Vachova, 2014).

Horizontally-stratified cells may also engage in autophagy. Cells in the colony center begin to differ from those on its margins around the same time U and L cells differentiate (Figure 13). Superoxide concentrations increase in center cells, even as they simultaneously decrease in margin cells (Michal Cap, Vachova, & Palkova, 2009; Vachova et al., 2009). As a result, center cells undergo accelerated programmed cell death (PCD) relative to margin cells. In contrast with either accidental or regulated cell lysis, PCD does result in the release of lytic enzymes that damage or destroy healthy neighboring cells (Vachova et al., 2012; Váchová & Palková, 2018). Thus, similar to U cells receiving nourishment from L cells, center cells' PCD may contribute to overall colony survival by providing nutrients that nourish margin cells. This idea is supported by the removal of center cells from a differentiated colony, which leads to diminished growth at the colony margin (Vachova & Palkova, 2005). Though cells in a giant yeast colony undergo apoptosis similar to cells undergoing PCD in a multicellular organism, the process does not recruit Mca1p or Aif1p, and must therefore be regulated differently than in metazoans (Váchová et al., 2012). Unlike starving planktonic cells in a homogeneous environment, both horizontal and vertical stratification appear to prolong the lifespan of certain cells in aging yeast colonies.

3.3.4 Giant colonies as a model to study aging and cancer

Cells in a colony age differently than starving, planktonic cells. For example, the latter increasingly express stress-defense genes as they age (*SOD1, SOD2, CTT1*) (Čáp, Váchová, & Palková, 2010; Kourtis & Tavernarakis, 2011). However, in colonies, the expression of stress-related genes, including those which encode oxidative stress defense enzymes, decreases with age (Palkova et al., 2002). Also, while Sod1 is known to be essential for yeast longevity in liquid cultures (Gralla & Valentine, 1991; V. D. Longo, Gralla, & Valentine, 1996), Sod1 appears not to be essential for colony survival and longevity (Michal Cap et al., 2009; Čáp et al., 2010). Cells in colonies are exposed to gradients of nutrients, waste products and gases whose complex spatial and temporal dynamics result in a mosaic of physiologically differentiated cell types and a host of cell-cell interactions. Consequently, yeast growing as colonies on agar are more similar to the tissues of multicellular organisms than are planktonic yeast in liquid culture (Čáp et al., 2010). Yeast growing in colonies can also be used to model mammalian cancer cells, which have high glycolytic flux and resemble yeast cells grown in colonies more than they do starving planktonic cells, which may better serve as a model for tumor necrosis (Čáp et al., 2012; Leontieva & Blagosklonny, 2011).

Because U and L cells can be easily isolated (Váchová et al., 2012), the differences between each subpopulation could be exploited to model different types of metazoan cells. U cells have certain attributes of tumor cells, inasmuch as both exhibit progressive changes in mitochondrial morphology such as swelling and loss of cristae (Arismendi-Morillo & Castellano-Ramirez, 2008), autophagy induced by ammonia (Eng, Yu, Lucas, White, & Abraham, 2010), a lowered respiratory capacity (Čáp, Váchová, & Palková, 2015), and the activation of TOR and amino acid metabolism (Čáp et al., 2012; DeBerardinis & Cheng,

2010). Further, both U and tumor cells may switch to potentially conserved metabolic programs designed to exploit other cells within their environment (Čáp et al., 2012; Váchová & Palková, 2018). Cells grown in colonies, then, could more accurately model eukaryotic cell-cell communication as well as specific types of metazoan cells, like tumor cells, than cells grown in liquid culture. However, like starving planktonic cells in nutrient-depleted liquid media, a yeast colony on agar constitutes a closed system that excludes all material transfer with the environment, save for gases or volatiles such as alcohols. In this respect, both techniques imperfectly model metazoan cells, which exist as open systems.

3.4 Chronological aging in continuous culture: the retentostat

In yeast, cell reproduction is usually coupled with metabolism (Burnetti, Aydin, Buchler, & Solomon, 2015). Thus, regardless of whether cultured as planktonic cells in liquid medium batches, or as colonies on agar, yeast eventually cease to divide because they lack essential nutrients. By contrast, many animal cell types undergo G_0 arrest in the presence of excess nutrients (Westman, Bonander, Taherzadeh, & Franzen, 2014), and then begin to age chronologically. Another way to better model mammalian CLS with yeast is to culture it in a retentostat (Figure 12C), a continuous-flow system whose operational principles were first described by Herbert (Herbert, 1961). This apparatus is a variant of the more familiar chemostat (Edmunds, 1972; Kubitschek, 1954; Monod, 1950; Novick & Szilard, 1950a, 1950b) where balanced growth of planktonic cells is achieved by continuous flow of a growth limiting-nutrient through a bioreactor. At steady state, microbial specific growth rate, μ, is equal to the dilution rate, D, defined as the outflow flow rate of spent medium (F_{out} in L/h) over the liquid volume of culture (VL) in the bioreactor. Depending on species, strain and type of limiting nutrient, chemostats are typically run at $0.4\ h^{-1} > D > 0.03\ h^{-1}$. Similar

to chemostat, in a retentostat all nutrients save one, an energy source, are present in non-limiting concentrations. However, unlike a chemostat, cells in a retentostat are prevented from leaving the reactor in the spent medium stream. Thus, cells can be cultured to high cell densities (Figure 12C; ~15 g biomass per L) (Boender, de Hulster, van Maris, Daran-Lapujade, & Pronk, 2009) at near-zero growth rates ($D < 0.001\ h^{-1}$). Continuous retentostat cultures maintain homeostasis between cells' rate of substrate consumption and their maintenance energy requirements. Like a chemostat, and indeed like a metazoan with a circulatory system, the retentostat is an open system, which continuously exchanges nutrients and wastes with the external environment.

3.4.1 Retentostat growth and viability

Boender et al. 2009 were among the first to study *S. cerevisiae* in retentostats. Under anaerobic conditions, in a chemostat running at $D = 0.025\ h^{-1}$, cells satisfy their maintenance energy requirements, estimated to be 0.50 mmol of glucose per gram of biomass per hour. Starting at $D = 0.025\ h^{-1}$, cell outflow was blocked by filtration, transforming the chemostat into a retentostat. After 7 days, growth rate decreased to $< 0.004\ h^{-1}$, and after 22 days growth rate fell to $< 0.001\ h^{-1}$, which corresponded to a doubling time of 27 days. Over 22 days of retentostat cultivation, cell viability fell from 91 ± 8% to 79 ± 6%. Glycogen content more than doubled over this interval, from 4.3 ± 0.8% in chemostat cultures at $D = 0.025\ h^{-1}$ to 9.1 ± 0.6% in retentostat cultures at 22 d ($D < 0.001\ h^{-1}$), whereas trehalose content did not change (1 ± 0.4%). Retentostats thus open up possibilities for studying cell physiology under conditions of severe CR and very low growth rate.

3.4.2 Transcriptomics

Later studies (L. G. Boender, A. J. van Maris, et al., 2011) examined the genome-wide transcriptional response to low growth rates relative to expression patterns in both faster growing (D = 0.025 h^{-1}) and stationary phase (SP) cultures. Beginning with a culture growth rate of 0.025 h^{-1} at day 0, growth rate in the retentostat decreased after 2 days to 0.0084 h^{-1}, then leveled off at 0.00063 h^{-1} after 22 days (L. G. Boender, A. J. van Maris, et al., 2011). 15% of cells were budded in 22-day cultures, typical for non-growing *S. cerevisiae* (Lewis, Northcott, Learmonth, Attfield, & Watson, 1993), and viability was estimated to be ~80% (L. G. Boender, A. J. van Maris, et al., 2011). Relative to chemostat-grown cells (D = 0.025 h^{-1}), transcript levels in retentostat-grown cells (D = 0.00063 h^{-1}) were increased for 615 genes, and decreased for 241 genes (q-value < 0.000188 by *K*-means clustering). Transcript levels of many house-keeping genes (e.g. *ACT1, PDA1, ALG9, TAF10, TFC1, UBC6)* did not differ between these two cultivation regimes (L. G. Boender, A. J. van Maris, et al., 2011), possibly indicating sustained metabolic activity. Among genes whose transcript levels increased, those related to mitochondrial function were strikingly over-represented, including 32 out of 76 genes that encode mitochondrial ribosomal proteins, as well as genes that encode respiratory chain sub-units (e.g. *ATP4, ATP7, ATP15, COX5B, COX8, COX9, COX11, COQ5, COQ9, SOC1, SCO2),* protein processing (*IMP1, IMP2, SOM1),* and mitochondrial membrane transport (*TIM17, TOM6*) (L. G. Boender, A. J. van Maris, et al., 2011). This finding was surprising given that under anaerobic conditions, yeast mitochondria are thought to play a biosynthetic rather than an energetic role in cell metabolism (Visser, Scheffers, Batenburg-van der Vegte, & van Dijken, 1990). Upregulation of mitochondrial functions may therefore represent specific cellular adaptations to near-zero growth that are not related to either oxygen or glucose concentration

(L. G. Boender, A. J. van Maris, et al., 2011). Of genes whose transcript levels decreased, those in lipid and sterol metabolism were over-represented, though this could be an artifact of amending anaerobic cultures with ergosterol and the oleate ester Tween-80.

Transcript levels were elevated for multiple genes involved in the repair of damage to protein or DNA (*SIR2, RAD10, RAD24, RAD27*). Upregulation of SIR2 and its homologs may enhance genetic stability of retentostat-grown cells. Under-expression of *SIR2* homologs has been shown to diminish longevity (Bellizzi et al., 2005), and deletion of *SIR2* increases genome instability (Foss et al., 2017). The behavior of these genes is thus especially relevant to the study of human aging; in addition, a RAD homolog has been linked to human colon carcinoma (Bao et al., 1999). In conclusion, retentostat cells under CR at near-zero growth rates are metabolically active, and their gene expression program suggests they may be protected against DNA and/or protein damage, even after 22 days (L. G. M. Boender et al., 2011).

3.4.3 Proteomics

Given the transcriptomic data, it is unsurprising that the yeast proteome also changes upon induction of near-zero growth under CR (N. A. Binai et al., 2014). Of 3813 proteins detected in a comparison of retentostat cells versus exponentially-growing cells, the levels of 252 proteins increased and 252 proteins decreased, about 13% of the proteome. By comparison, 31% of the proteome is expressed differently between exponential phase and SP batch cultures (Webb, Xu, Park, & Yates, 2013). Among proteins whose expression increased were those in the oxidative branch of the TCA and glyoxylate cycles, and 5 of 6 proteins in the succinate dehydrogenase complex (Sdh1p, Sdh2p, Sdh3p, Sdh1bp, and

Shh3p) (Nadine A. Binai et al., 2014), the last long thought to be inactive under anaerobic conditions (Camarasa, Grivet, & Dequin, 2003). Though there were no enriched categories among the 252 proteins whose levels were decreased in retentostats relative to exponential planktonic culture, this group did include 4/17 proteins involved in ergosterol biosynthesis, and 8/14 proteins forming the Like-Sm ribonucleoprotein core (N. A. Binai et al., 2014), thought to be involved in activating mRNA decapping (W. He & Parker, 2000).

Interestingly, the transcriptome and proteome datasets correlated poorly, with only 146 of 504 proteins changing with the same sign and magnitude as their associated transcripts (N. A. Binai et al., 2014). Of the 146 proteins whose changes were consistent with changes in their transcript levels, two-thirds were higher in retentostats, notably 28 of 110 of mitochondrial proteins and 11 of 53 proteins in oxidative phosphorylation. Poor correlation between regulation of transcript and protein levels has been previously observed in SP cultures in *S. cerevisiae* and in *Schizosaccharomyces pombe* (Fuge, Braun, & Werner-Washburne, 1994; Marguerat et al., 2012). This observation may stem from half-life differences between proteins (0.5 h < $t_{½}$ < 20 h) (Helbig et al., 2011) and mRNAs (3 min < $t_{½}$ < 8 h) (Y. Wang et al., 2002); these differences may be exaggerated in cells under nutrient limitation as more energy is required to synthesize proteins (1957 mmol ATP/100 g formed biomass) than mRNAs (201 mmol ATP/100 g formed biomass) (Verduyn, Postma, Scheffers, & van Dijken, 1990). Transcriptomic and as well as proteomic datasets do indicate increased activity of and tight regulation over proteins and transcripts related to O_2 consumption, suggesting that this is of special importance to calorically restricted cells.

3.4.4 Starvation vs. caloric restriction

A key distinction between cells in retentostats and cells in nutrient-depleted planktonic cultures is that the former are not starving. Unrelieved, starvation inexorably leads to cellular deterioration (Albers, Larsson, Andlid, Walsh, & Gustafsson, 2007; Beck, Schmidt, & Hall, 1999; C. B. Jones et al., 2012; Suzuki, Onodera, & Ohsumi, 2011). By contrast, retentostat cells are calorically restricted, a condition operationally defined as cells being fed one third to one half that of cells fed ad libitum, without inducing malnutrition or starvation (N. A. Binai et al., 2014; Kaeberlein et al., 2005; S.-J. Lin et al., 2002; Wei et al., 2008). In a retentostat cells are supplied with enough carbon and energy for cell maintenance and survival, but not enough for reproduction. But while they exhibit some features of starving cells, like increased heat shock resistance and expression of certain quiescence-related genes (L. G. Boender, A. J. van Maris, et al., 2011), calorically-restricted retentostat yeast are more metabolically active and have higher viability (L. G. Boender, M. J. Almering, et al., 2011).

Starvation and caloric restriction are physiologically different states; this can be illustrated by inducing starvation in a retentostat with the elimination of glucose from the medium. Calorically restricted yeast in a retentostat turn over ATP at a rate of 1 mmol per gram of biomass per hour (L. G. Boender, M. J. Almering, et al., 2011). By contrast, within hours of starvation induction, ATP turnover rate drops to 0.013 mmol per gram of biomass per hour. Twenty-one days after starvation induction, turnover rate drops further to 0.0002 mmol per gram of biomass per hour. Retentostat yeast show little evidence of protein damage, even after 22 days in culture (N. A. Binai et al., 2014; L. G. Boender, A. J. van Maris, et al., 2011), indicating ongoing protein synthesis and recycling despite the energetic cost (Stouthamer, 1973) of these processes. Compared to cells in low-dilution-

rate chemostats ($D \cong 0.025\ h^{-1}$), retentostat yeast do show decreased expression of genes required for protein synthesis. But starvation results in the immediate downregulation of one-quarter of these genes (L. G. Boender, M. J. Almering, et al., 2011). Active protein synthesis and recycling in retentostat yeast helps to explain their high levels of metabolic activity (>70%) and viability (60%), even in 22-day old cultures (N. A. Binai et al., 2014). Nevertheless, such cells are highly susceptible to further dietary restriction. Within just 26 hours of starvation induction, 22-day old retentostat cells exhibit high levels of PCD (43%) and greatly diminished viability (15%).

To compare the transcriptome of CR cells, whose maintenance energy requirements were being met, to the transcriptome of starving cells, Boender et al. cultured yeast in retentostats with and without glucose. 549 genes were differentially expressed (L. G. Boender, M. J. Almering, et al., 2011); 140 were upregulated in carbon starved cells, including genes encoding dehydrogenases (e.g. *MDH3, DLD1, BDH1, BDH2, SDH1*) as well as genes whose products are required for growth on non-fermentable carbon sources (e.g. *HBT1, FMP45, SPG4, SPG1*). Transcript levels for the remainder were downregulated in starved cells, including 109 genes involved in protein synthesis, as well as 30 genes involved in amino acid biosynthesis. Starvation and CR are therefore distinct physiological states that can be expected to have very different impacts on cell lifespan.

3.4.5 Yeast retentostats as a model for the study of chronological aging

Calorically restricted cells in retentostats can be used to refine our study of cellular lifespan in non-dividing metazoan cells. Unlike starving planktonic cells, retentostat CR cells do not differentiate into quiescent and non-quiescent cell types (Allen et al., 2006); instead,

cells remain in an extended G_1 phase (Bisschops et al., 2017). The ability of yeast to achieve near-zero growth in a retentostat makes it possible to use this model to study novel aspects of aging and disease (Zimmermann et al., 2018). For example, retentostat analysis of a *rim15Δ* mutant strain uncovered similarities in its phenotype to cancer cells, including decreased resistance to heat shock (M. M. M. Bisschops, P. Zwartjens, S. G. F. Keuter, J. T. Pronk, & P. Daran-Lapujade, 2014), and a lack of response to anti-growth signals (Hanahan & Weinberg, 2000). With its active metabolism and near-zero growth rate, retentostat yeast is well-suited to model non-proliferating metazoan cells that have exited the replicative cycle but remain metabolically active. However, retentostat cells are still nutrient-limited, whereas somatic metazoan cells are not; further, even retentostat advocates attest to the fact that they are technically demanding to set-up and maintain (Boender et al., 2009; O. Ercan et al., 2015; Sauer & Mattanovich, 2016; Vos et al., 2016).

3.5 Chronological aging in continuously-fed immobilized cell reactors

Microbial, plant and metazoan cells can be immobilized in a variety of matrices, ranging from naturally-derived hydrogels such as agarose, alginate, chitosan, collagen, fibrin, gelatin, and hyaluronic acid (Drury & Mooney, 2003) to synthetic hydrated polymers and inorganic substrates, such as silica gels, sintered glass, and ceramic beads (A. Nussinovitch, 2010). In naturally-derived hydrogels, microbial encapsulation (a type of immobilization) typically results in spherical beads whose diameter can be fixed in the range of micro- to millimeters. These beads, and the cells they contain (Figure 14), can then be placed into immobilized cell reactors (ICRs; Figure 12D) and operated either as closed, batch-culture systems or as open, continuously-fed systems. The latter, which include stirred tank, packed and fixed-bed reactors (Nedović et al., 2015), allows for continuous exchange of

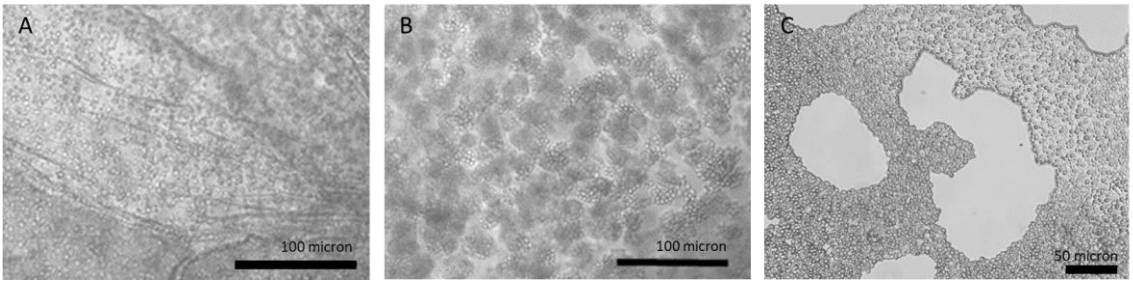

Figure 14. Yeast microcolonies form in alginate-encapsulated beads packed in immobilized cell reactors. Immediately after gelation (A), the interior of bead consists of primarily single, unbudded cells evenly dispersed throughout alginate matrix, but by 3 days in ICR (B), cells have evenly dispersed in clonal clusters of 4 or more cells. After 14 days in ICR (C), cells are tightly packed, occupying majority of matrix material. Hollow chambers are dispersed throughout beads, presumably formed by CO_2 generation.

nutrients and waste between cells in their extracellular matrix and the liquid medium flowing through the reactor.

3.5.1 Industrial applications

ICRs have chiefly been studied with an eye towards their use in biotechnology. There, they offer three advantages over conventional planktonic batch culture: (i) high productivity in terms of yield per cell, (ii) increased stability during the production cycle, and (iii) prolonged dry storage times. These advantages, reported by many (Behera, Mohanty, & Ray, 2011; G.-Y. Li, Huang, Jiang, & Ding, 2007; Sylvain Norton & D'Amore, 1994; Plessas et al., 2007a; Farid Talebnia & Taherzadeh, 2007; Verrills, 2006), arise from the fact that gel-encapsulated cells reproduce slowly, if at all, and therefore divert little substrate to new biomass, which allows for more efficient substrate utilization (Verbelen, De Schutter, Delvaux, Verstrepen, & Delvaux, 2006). Longer production cycles can be attributed to encapsulated cells' greater resistance to acids (Krisch & Szajani, 1997; Taipa, Cabral, & Santos, 1993), organic solvents (Desimone, Degrossi, D'Aquino, & Diaz, 2003;

Qun, Shanjing, & Lehe, 2002), ethanol (Zaldivar, Nielsen, & Olsson, 2001), osmotic stress, and thermal stress (Z.-J. Sun et al., 2007; Ylitervo, Franzen, & Taherzadeh, 2011). Greater stress resistance can also be associated with altered composition and organization of both the cell wall and plasma membrane (Galazzo & Bailey, 1990), as well as with mechanical protection against shear provided by the encapsulating matrix (Amos Nussinovitch, 2010). In yeast, increased dry storage time without substantial loss in viability is consistent with the immobilized cells' higher content of storage and structural polysaccharides (Doran & Bailey, 1986; Nagarajan et al., 2014; Sylvain Norton & D'Amore, 1994).

3.5.2 Potential for social interactions among encapsulated yeast

Yeast cells immobilized in alginate 'beads' cease to divide after reaching a certain density, which accounts for their high fermentative capacity, and likely also their exceptional longevity and resistance to stress. It is tempting to speculate that the physical proximity of such cells in a semi-solid matrix (Figure 14), coupled with their entry into a G_0-like state, confers upon them certain features of tissue level-organization, including cooperativity. Strains isolated from the wild exhibit a variety of behaviors that have the potential to facilitate social interactions; these include floc (K. V. Goossens et al., 2015) and flor formation (Alexandre, 2013), adhesion (Bruckner & Mosch, 2012; K. Goossens & Willaert, 2010; Honigberg, 2011), as well as a kind of primitive multicellularity (Holmes, Lancaster, Lindquist, & Halfmann, 2013; Koschwanez et al., 2013; Oud et al., 2013; Ratcliff et al., 2012). Yeast can also form biofilms (Honigberg, 2011), which in effect causes cells to become immobilized. Many of these behaviors are correlated with increased resistance to ethanol stress (Jeffries & Jin, 2000; Lei, Zhao, Ge, & Bai, 2007) enhanced thermotolerance and osmotolerance (Claro, Rijsbrack, & Soares, 2007), and improved

survivorship in the presence of inhibitory compounds (Westman, Mapelli, Taherzadeh, & Franzén, 2014). Similarly, encapsulated yeast become stress tolerant, though particular resistance profiles are specific to the type of encapsulating matrix (Z.-J. Sun et al., 2007; Westman, Taherzadeh, & Franzen, 2012).

Social behavior in immobilized yeast appears to rely on intercellular signaling or quorum sensing (QS), which can be mediated by peptide pheromones (Y. Wang & Dohlman, 2004) or by various organic compounds (alcohols, aldehydes and volatiles) (Avbelj, Zupan, & Raspor, 2016). An important criterion for a QS mediator is that it needs to reach a certain concentration before eliciting a concerted response, which goes beyond the cellular response needed to metabolize or detoxify the compound (Albuquerque & Casadevall, 2012). One example of collective behavior of yeast cells is the appearance of cooperative glycolytic oscillations that rely on autocatalytic regulation of phosphofructokinase (Richard, 2003). Glycolytic oscillations with a period of 25-32 s become synchronized in yeast cells depending on cell concentration in alginate (Amemiya et al., 2015) and chitosan (Shibata et al., 2018) beads, and are probably induced by locally high concentrations of acetaldehyde. Encapsulated yeast may behave cooperatively and signal to each other in ways reminiscent of metazoan somatic cells (Chien-Chi Lin & Anseth, 2011). Whether the G_0-like state observed in such yeast is induced by QS, by mechanical forces like "self-jamming" (Delarue et al., 2016), or is maintained by combination of chemical and mechanical factors remains to be explored.

3.5.3 Physiology and transcriptomics

Nagarajan *et al.* 2014 validated that reproduction is uncoupled from metabolism in continuously-fed, alginate encapsulated yeast, described one of its genetic determinants, and provided evidence that such cells are exceptionally long-lived (Nagarajan et al., 2014). The authors also showed that continuously-fed immobilized yeast exhibit a stable pattern of gene expression that is distinct from both growing and starving planktonic cells, consisting of an increased expression of genes in cell wall remodeling, glycolysis, and stress resistance, and an decreased expression of genes in the TCA cycle and cell cycle regulation (Figure 15 and discussion below) (Nagarajan et al., 2014). These highly metabolically active cells achieved near-zero growth rates within 72 h post-encapsulation, and maintained this state for nearly 3 weeks, during which time upwards of 80% of cells remained virgin daughters. Together, these attributes open up the possibility for developing a model to study cellular senescence and chronological lifespan in non-dividing eukaryotic cells, both in the absence and in the presence of caloric restriction.

Kruckeberg *et al.* developed methods to perform, for the first time, global analysis of gene expression in immobilized microbial cells (Kruckeberg, Nagarajan, McInnerney, & Rosenzweig, 2009). Affymetrix GeneChips were used to profile the transcriptome of encapsulated yeast cells, compared to that of planktonic yeast grown either in glucose-limited chemostats or in glucose batch culture (mid-log and early SP). Data from immobilized cultures revealed a pattern of gene expression that differed from planktonic cells, and remained stable over >2 weeks of continuous culture. Fewer than 100 genes changed by more than two-fold and none changed in sign. Transcript abundance conspicuously increased for multiple glycolytic genes (e.g., *HXK2*, *PFK2* and *PGK1*) and decreased for genes in the TCA cycle (e.g., *CIT2,3* and *ACO1,2*) and in the cell cycle (e.g.,

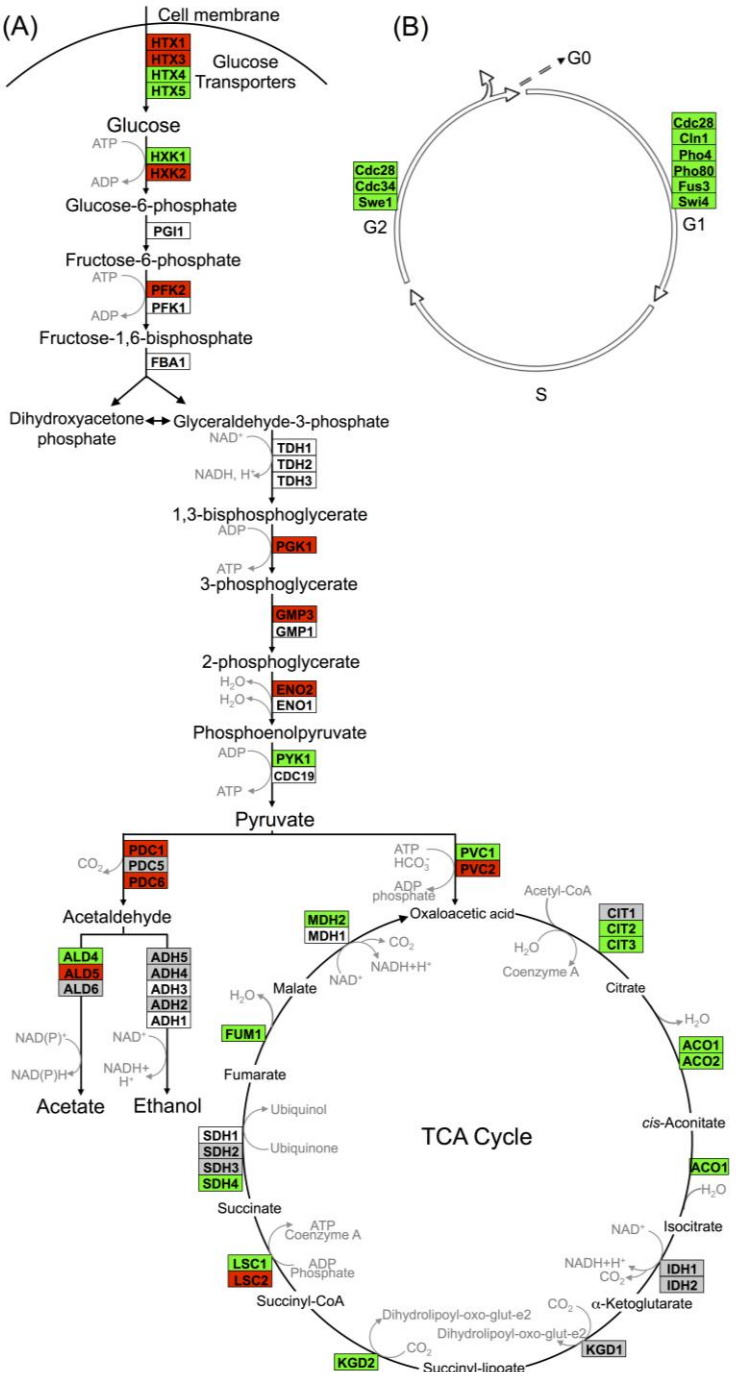

Figure 15. Alginate-encapsulated yeast cultured in continuously-fed bioreactors exhibit a stable pattern of gene expression in A) intermediary metabolism, and B) cell cycle where transcript abundance of glycolytic genes is increased, and that of TCA cycle and cell cycle genes is decreased. Red indicates genes where expression was at least two-fold greater in encapsulated cells than in planktonic cells over the course of 2 weeks culture. Green indicates instances where those values were at least two-fold less. Gray indicates no significant difference in sign or magnitude between planktonic and encapsulated cells (image adopted from Nagarajan et al. 2014)

CLN1 and *CDC28*) (Maršíková et al., 2017). These data provide yet another line of evidence that ICR yeast is metabolically active, but growth-arrested.

Additional features of this dataset included increased transcription of genes that act in cell wall remodeling. *RPI1* up-regulation in encapsulated cells is especially noteworthy. Rpi1 acts as an antagonist to the RAS–cAMP pathway, and prepares yeast for entry into SP by inducing transcription of genes whose products fortify the cell wall (Sobering, Jung, Lee, & Levin, 2002). Like non-reproductive quiescent cells and spores, and like cells in the retentostat, immobilized yeast is highly heat-shock and zymolyase-resistant. However, unlike such cells, immobilized yeast fed ad libitum sustains a high rate of metabolism. In experiments described by Nagarajan et al. (2014), medium was continuously circulated within the bioreactor, exchanging the void volume once per minute. Every 48 h the feed reservoir was replaced with fresh SDC medium containing a five-fold excess of all micronutrients amended with 10% glucose as sole carbon source. Over 9 such cycles glucose was continuously fermented at near-theoretical yield with an undiminished rate of conversion.

Transcript levels of stress response regulators *MSN4* and *RIM15* were significantly increased in immobilized, but not in planktonic, cells. *RIM15* plays a role in cell cycle arrest, as multiple nutrient-sensing pathways converge on Rim15p (Tsang & Lin, 2015). *RIM15* has also been reported to promote chronological longevity in both starving planktonic yeast (Fabrizio, Pozza, Pletcher, Gendron, & Longo, 2001; Wei et al., 2008) and yeast in retentostats (M. M. Bisschops, P. Zwartjens, S. G. Keuter, J. T. Pronk, & P. Daran-Lapujade, 2014). Based on these converging lines of evidence, Nagarajan et al. hypothesized that this master regulator played a central role in uncoupling metabolism

from reproduction in immobilized yeast. Flow cytometry of DNA content revealed that unlike wild type cells, *rim15Δ* cells exhibit a pronounced G_2 peak at later time points in ICR culture, indicating that they continue to divide. After 5 days of continuous culture viability of immobilized *rim15Δ* yeast fell to 25%, compared to >90% in immobilized wild-type cells. *RIM15* thus helps to mediate cell cycle arrest and stress resistance in the ICR model, and may contribute to ICR cells' extraordinary chronological longevity. The discovery that this remarkable physiological state is under genetic control opens the door to screening large numbers of barcoded knock-outs, a procedure likely to reveal new classes of longevity genes that alter lifespan in the absence of severe caloric restriction.

Of particular interest, but as yet not studied, is *XBP1*, which encodes a global regulator of entry into quiescent (Q) phase (Mai & Breeden, 1997). In this context, Xbp1 represses hundreds of genes following exhaustion of glucose, including G_1 cyclins such as *CLN3* (Miles, Li, Davison, & Breeden, 2013). The Rad9/Rad53 checkpoint may act in the same pathway, protecting cells from replicative stress in cultures lacking glucose (Zegerman & Diffley, 2009). Similar to Q cells, recent data show that encapsulated cells are exceptionally resistant to starvation. Indeed, survivorship of starved encapsulated cells is several-fold higher than starved planktonic cells (E. Cook and E. Kroll, unpublished data). The XBP1/G_1 cyclin pathway, in conjunction with starvation/stress signal transduction and replicative checkpoints, needs to be studied in encapsulated cells that cease to divide, similar to Q cells, but do so in the presence of nutrients, unlike Q cells. This may further connect well-fed encapsulated yeast cells to somatic cells in metazoans that also adjust their cell cycle machinery so that cell division ceases even when nutrients are non-limiting (Neganova & Lako, 2008).

3.5.4 Proteomics and metabolomics

Consistent with conclusions drawn from transcriptomics, a proteomic study of alginate-chitosan-encapsulated yeast in comparison with isogenic planktonic cells uncovered widespread changes in gene expression (J. O. Westman, M. J. Taherzadeh, et al., 2012). Encapsulated and planktonic cells were grown for 25 h in synthetic medium amended with 5% glucose, and the relative levels of 842 proteins were analyzed by mass spectrometry and 2D gel electrophoresis. A significant increase in central metabolic proteins was observed among immobilized cells, especially glutamine metabolism and fermentation, including proteins normally under glucose inhibition, such as high-affinity hexose transporters (Hxt6, Hxt7) and hexose kinases (Hxk, Glk1). This study also noted marked decreases in the level of proteins involved in protein synthesis and RNA transport. Interestingly, some stress response proteins were upregulated (Ssb2, Hsp12, Hsp26, Hsp78 and Hsp104), while others were downregulated (Ras2, Sod1, and many others) (J. O. Westman, M. J. Taherzadeh, et al., 2012).

Metabolite levels also differ between encapsulated and planktonic culture conditions. When encapsulated cells are fed ad libitum, as in Nagarajan et al. (Nagarajan et al., 2014), levels of succinate, citramalate, and citrate increase by several-fold relative to planktonic cells as determined by liquid chromatography mass-spectrometry (Figure 16). By contrast, while levels of fumarate and malate are similar across all conditions, alpha-ketoglutarate levels decrease many-fold in encapsulated cells. Some of these metabolomic changes could not easily have been predicted from the transcriptomic data. For example, expression data reveal no significant differences between planktonic and encapsulated cells in the transcript levels of *IDH1/2* or *KGD1*, yet their respective substrate

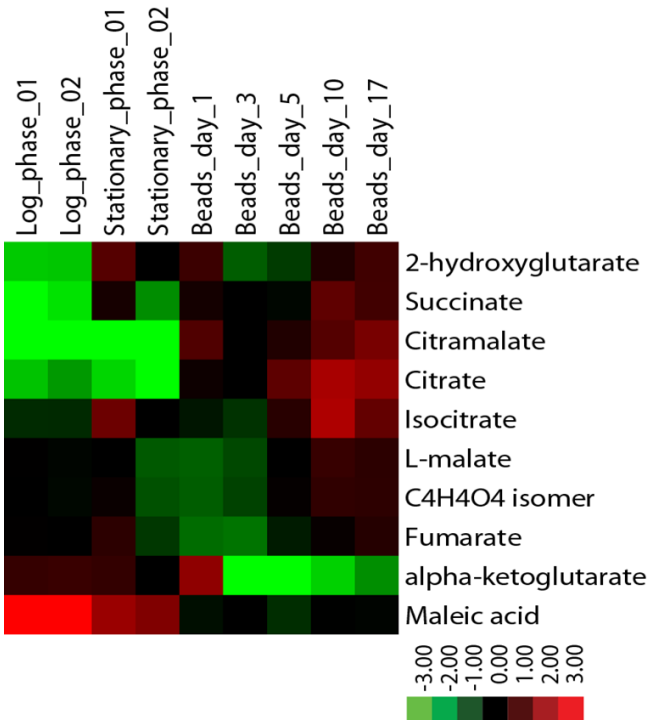

Figure 16. Levels of citric acid cycle metabolites in continuously-fed encapsulated yeast differ from planktonic yeast in exponential and stationary phases. Metabolites were extracted from flash-frozen cell pellets grown in batch or in continuous culture as indicated (Rosebrock & Caudy, 2017) and analyzed by LC-MS using a reversed phase method. Metabolite levels were normalized to the quantity of input cells, and displayed as a log2 fold change centered around the median value for each metabolite.

and product, alpha-ketoglutarate, is at very low levels in ICR. It is possible that such discrepancies can be explained, for example, by diminished expression of key enzymes upstream of a metabolite pool. In the case of alpha-ketoglutarate, expression of both citrate synthase (*CIT2/CIT3*) and aconitase (*ACO1/ACO2*) isoenzymes is significantly decreased in encapsulated cells relative to planktonic. Going forward, comparison of transcriptomic and metabolomic data obtained under identical conditions is sure to provide insight into biochemical changes that ensue following encapsulation, and further elucidate mechanism(s) by which encapsulated cells uncouple metabolism from cell division.

3.5.5 ICRs for the identification of anti-aging compounds

Yeast microcolonies originating from a single cell are often used in high-throughput drug screens. As the measurement of colony size can be automated, this approach allows for large numbers of anti-aging compounds to be rapidly screened (Teng & Hardwick, 2013). An obvious disadvantage of this approach is that it relies on cell division; hence, microcolony assays may fail to identify compounds that also extend CLS (Zimmermann et al., 2018). Because ICRs are populated with non-dividing, nutrient-replete cells, they offer the drug discovery process the advantage of directly assaying CLS. Though ICR-based assays are unlikely to be as easily multiplexed as those based on microcolony growth, or growth in liquid media, they could provide a valuable tool for testing whether anti-aging compounds uncovered by high-throughput assays also extend CLS.

3.5.6 Encapsulated, continuously-fed yeast as a model for studying chronological lifespan

In metazoans, the great majority of cells exist in a non-dividing state, G_0 (Coller, 2007; Pardee, 1974; S. L. Spencer et al., 2013). While most are terminally-differentiated and will never divide, the lifespan of some G_0 cells approximates the lifespan of the whole organism (Magrassi, Leto, & Rossi, 2013; Petralia, Mattson, & Yao, 2014), during which time they operate at full metabolic capacity (Lemons et al., 2010). Encapsulated yeast confined in ICR and fed ad libitum provides a reasonable approximation to post-mitotic metazoan cells like cardiac myocytes and neurons that are amply nourished but do not divide. Indeed, of all the zero-growth yeast models reviewed here, only the ICR model provides a way to study CLS in a simple eukaryote in the *absence* of caloric restriction, or starvation. This model could also be adapted for the study of CLS in the *presence* of caloric restriction simply by limiting carbon to levels that are one-third to one-half that of cells fed ad libitum,

without inducing malnutrition or starvation (N. A. Binai et al., 2014; Kaeberlein et al., 2005; S.-J. Lin et al., 2002; Wei et al., 2008). Systematic improvements that would enhance the utility of this model include: (1) multiplexing mini-ICRs so that individual columns could be sacrificially sampled over the course of weeks to months of continuous culture, (2) introducing mechanisms to sparge mini-ICRs so that CLS can be modeled under oxic and anoxic conditions, and (3) devising techniques to ensure even dispersal of diverse genotypes in a given bead, so that representatives of the barcoded yeast knock-out and overexpression collections could be studied under conditions of long-term growth arrest, either in the presence or absence of caloric restriction.

3.6 Conclusions and Future Directions

Genetic screens using the starving yeast model have provided insight into the behavior of eukaryotic cells under prolonged stress, showing how pathways such as TOR and genes like SIR are integrated and together contribute to cell survival. Because starving yeast are not dividing, this model has been used to measure chronological lifespan. However, because such cells are, by definition, nutrient-deprived, experimental results have been interpreted in the light of how chronological lifespan is affected by caloric restriction, a factor shown to extend longevity in virtually every species where it has been studied. But having few calories (caloric restriction) is not the same as having no calories (starvation). Thus, starving yeast does not mimic the physiology and lifespan of major classes of metazoan cells. Cardiac myocytes and neurons are terminally differentiated in a state of G_0 arrest, but remain metabolically active and well-fed for the life of the organism. Muscle stem cells are also in G_0-arrest and remain metabolically quiescent until recruited to enter G_1 and produce cells that differentiate into, for example, myoblasts.

Alternative culture methods exist that enable yeast researchers to circumvent this fundamental problem. Yeast in giant colonies receive low levels of nutrients by diffusion, allowing them to divide over longer periods (~18 d vs. ~30 h) than starving planktonic cells. This longer period of slow growth contributes to the higher viability of aging cells in colonies relative to aging planktonic cells. Unlike starving planktonic cells, whose populations are not spatially structured, cells grown in colonies exhibit a primitive type of context-dependent cellular differentiation as they age, with some cell classes alive, but growing at near-zero rates. Ultimately though, yeast grown in giant colonies, like starving planktonic yeast, live in a closed, nutrient-depleted culture system that scarcely resembles a metazoan body.

Retentostats, an open system where nutrients and waste products are exchanged with the environment, overcome multiple limitations associated with studying cell lifespan in starving planktonic cells. Retentostat yeast is cultured at near-zero growth rates and provided with maintenance energy requirements. Retentostat yeast is under caloric restriction, a physiological state distinct from starvation. Cell viability remains high (80% after 22 days) with little evidence of protein and DNA damage. Aging retentostat yeast may therefore serve as a surrogate for classes of metazoan cells that have exited the replicative cycle and become quiescent, like pluripotent stem cells.

A third alternative to starving planktonic yeast is encapsulated yeast, which can be cultured in ICRs at near-zero growth rates. This matrix-associated, open culture system offers flexibility in nutrient supply. Yeast can be fed ad libitum so that non-dividing cells remain viable for weeks on end, conditions that mimic metabolism and longevity in terminally-differentiated metazoan cells. ICR yeast could also be cultured under nutrient-

limiting conditions, making it possible to study cells in a tissue-like matrix under caloric restriction. Nutrient levels could even be reduced to where only maintenance energy requirements are met, creating an ICR model for the study of stem cells.

Caution should be exercised in the use of starving, planktonic microbial cells to evaluate determinants of chronological lifespan in metazoan stem cells and metazoans cells that are terminally differentiated. Since these cell types have their energy requirements met, alternative systems are needed that better mimic their physiologies. Yeast growing in colonies, in retentostats, and in immobilized cell reactors all provide a higher degree of biological realism.

CHAPTER 4. MATRICES (RE)LOADED: DURABILITY, VIABILITY AND FERMENTATIVE CAPACITY OF YEAST ENCAPSULATED IN BEADS OF DIFFERENT COMPOSITION DURING LONG-TERM FED-BATCH CULTURE

Encapsulated microbes have been used for decades to produce commodities ranging from methyl ketone to beer. Encapsulated cells undergo limited replication, which enables them to more efficiently convert substrate to product than planktonic cells and which contributes to their stress-resistance. To determine how encapsulated yeast support long-term, repeated fed-batch ethanologenic fermentation, and whether different matrices influence that process, fermentation and indicators of matrix durability and cell viability were monitored in high-dextrose, fed-batch culture over 7 weeks. At most timepoints, ethanol yield (g/g) in encapsulated cultures exceeded that in planktonic cultures. And frequently, ethanol yield differed among the four matrices tested: sodium alginate crosslinked with Ca^{2+}, sodium alginate crosslinked with Ca^{2+} and chitosan, Protanal alginate crosslinked with Ca^{2+} and chitosan, Protanal alginate crosslinked with Ca^{2+}, with the last of these consistently demonstrating the highest values. Young's modulus and viscosity were higher for matrices cross-linked with chitosan over the first week; thereafter values for both parameters declined and were indistinguishable among treatments. Encapsulated cells exhibited greater heat shock tolerance at 50°C than planktonic cells in either stationary or exponential phase, with similar thermotolerance observed across all four matrix types. Altogether, these data demonstrate the feasibility of re-using encapsulated yeast to convert dextrose to ethanol over at least seven weeks.

4.1 Introduction

Cellular encapsulation was first achieved by Vincenzo Bisceglie in 1933, who showed that tumor cells embedded in a heterochthonous matrix maintained high viability (Bisceglie, 1934). Since then, microbial, plant, and metazoan cells have been encapsulated within various structures (Galvez-Martin, Martin, Ruiz, & Clares, 2017), including a variety of natural gels like agarose, alginate, chitosan, collagen, fibrin, gelatin, and hyaluronic acid (Drury & Mooney, 2003; Hussain, Kangwa, & Fernandez-Lahore, 2017), as well as in synthetic hydrated polymers and inorganic substrates, such as silica gels, sintered glass, and ceramic 'beads' (Amos Nussinovitch, 2010). In these matrices, encapsulated cells have been used to produce a variety of commercial products, including amino acids (Chibata & Tosa, 1977; Chibata, Tosa, & Sato, 1976; Y. Hu, Tang, Yang, & Zhou, 2009), lactic acid (Abelyan & Abelyan, 1996; Roukas & Kotzekidou, 1996), beer and cider (White & Portno, 1978; Willaert & Nedovic, 2006; Williams & Munnecke, 1981), wine (Hong et al., 2010; Naouri et al., 2007), sparkling wine (Miličević B., 2017; Tataridis, Ntagas, Voulgaris, & Nerantzis, 2005), sake (Hirotsune, 1987; Nunokawa, 1993), soy sauce (Hamada, Sugishita, Fukushima, Fukase, & Motai, 1991; Mizunuma, 1986), probiotics for yogurt (Burgain et al., 2011), orange juice debittering (Iborra, Manjón, Cánovas, Lozano, & Martínez, 1994), vanillin (Ramachandra Rao & Ravishankar, 2000) and methyl ketone (Larroche, Cruely, & Gros, 1995), among others.

In the realm of biomanufacturing, encapsulated cells offer two important advantages over free-floating, or planktonic cells: higher service life and higher product yield per cell (Behera et al., 2011; G.-Y. Li et al., 2007; Sylvain Norton & D'Amore, 1994; Plessas et al., 2007b; F. Talebnia & Taherzadeh, 2006; Verrills, 2006). Extended service life has been attributed to encapsulated cells' resistance to acids (Krisch & Szajani, 1997; Taipa et al.,

1993), organic solvents (Desimone et al., 2003; Qun et al., 2002), ethanol (Zaldivar et al., 2001), and osmotic and thermal stress (Z.-J. Sun et al., 2007; Ylitervo et al., 2011). These features are likely consequences of altered cell wall and plasma membrane composition following encapsulation (Galazzo & Bailey, 1990), and possibly also protection from shear forces afforded by the encapsulating matrix (Amos Nussinovitch, 2010). Encapsulated cells typically achieve higher product yield than planktonic cells as they divert less substrate to the formation of new biomass (Moreno-Garcia, Garcia-Martinez, Mauricio, & Moreno, 2018; Verbelen et al., 2006), enabling them to more efficiently process feedstock.

Nagarajan *et al.* 2014 encapsulated the yeast *Saccharomyces cerevisiae* in Ca^{2+}-alginate, which uncoupled reproduction from metabolism and allowed for the study of chronological lifespan in non-dividing cells. This study provides evidence that, when continuously fed *ad libitum*, encapsulated cells are much longer-lived than planktonic cells (Nagarajan et al., 2014), all the while exhibiting a stable pattern of gene expression that is distinct from either growing or starving planktonic cells. Relative to planktonic yeast grown in chemostats, or planktonic yeast in exponential or stationary phase, continuously-fed encapsulated yeast exhibits increased transcript levels of genes involved in cell wall remodeling, glycolysis, and stress resistance, and diminished transcript levels of tricarboxylic acid cycle genes and those regulating the cell cycle. Encapsulated cells are thus physiologically distinct from planktonic cells and age differently (Nagarajan et al., 2014).

Encapsulated cells have been studied in both continuous and repeated fed-batch culture systems. At present, because continuous culture systems do not easily scale up, repeated fed-batch culture is the favored means by which yeast is used to produce

bioethanol (Ariyanti & Hadiyanto, 2013; Mohd Azhar et al., 2017; O'Brien & Craig, 1996) and other valuable commodities (Rymowicz, Fatykhova, Kamzolova, Rywińska, & Morgunov, 2010; Sirianuntapiboon, Jeeyachok, & Larplai, 2005). In repeated fed-batch systems using encapsulated yeast, high (85-90% g/g) yields of ethanol have been demonstrated after 5 (Y. Ercan, Irfan, & Mustafa, 2013), 24 (El-Dalatony et al., 2016), and 28 days (Youssef, Ghareib, & Khalil, 1989). This is higher efficiency than has been demonstrated using planktonic yeast in repeated fed batch systems, which achieve up to 75% yield over 30 days (Lu, Li, Duan, Shi, & Mao, 2003). Continuous culture systems offer more precise control over growth conditions, and this can translate into higher yields (Chen et al., 2013; Vancanneyt, De Vos, Maras, & De Ley, 1990). Indeed, prior studies have shown that continuously-fed encapsulated yeast produce ethanol at 88-100% efficiency for one week (J. E. McGhee, G. St. Julian, R. W. Detroy, & R. J. Bothast, 1982b), for 3 weeks (Taherzadeh, Millati, & Niklasson, 2001), and for up to 3 months (McGhee, St Julian, & Detroy, 1982). Thus, while multiple studies suggest that encapsulated cells could be re-used over several weeks, few (Cha et al., 2012; Gilson & Thomas, 1995) have explored whether and how different encapsulation matrices impact fermentation capacity and related parameters over longer time periods (Moreno-Garcia et al., 2018).

To fill these knowledge gaps, glucose consumption and ethanol production by *Saccharomyces cerevisiae* was monitored over the course of 7 weeks, comparing the performance of cells in planktonic culture with cells encapsulated as ~4 mm ‘beads’ composed of four different matrices. To simulate industrial fermentation, a fed-batch system was used instead of a continuously-fed system like that described by Nagarajan et al. (2014). We evaluated parameters related to bead resilience (Young’s modulus,

viscosity, size, and mass) and biological parameters related to fermentation capacity (ethanol yield, cell number/viability, and thermotolerance). Encapsulation matrices varied most in terms of viscosity and bead swelling over time, with the presence or absence of chitosan impacting results more than the type of alginate used. As a whole, encapsulated cells generated higher ethanol yield (g/g from dextrose) than planktonic cells, and had greater heat shock resistance. These results demonstrate the potential for re-using encapsulated yeast in successive fed-batch cultures lasting at least 7 weeks, and allow for comparisons to be made about long-term behavior of different encapsulation matrices.

4.2 Materials and Methods

4.2.1 Strains and culture conditions

All experiments were performed using the same strain, *Saccharomyces cerevisiae* Ethanol Red (ER), an ethanol-tolerant (up to 18% (Fermentations, 2019)) industrial strain obtained from Leaf Lessafre (Marcq-en-Barœul, France). Yeast were cultured at 30°C in 250 mL screw-cap Erlenmeyer flasks placed on a gyrorotary platform shaking at 50 rpm. To mimic the high sugar content typically used in biorefinery feedstock (Kajiwara, Aritomi, Suga, Ohtaguchi, & Kobayashi, 2000; Krishnan, Nghiem, & Davison, 1999) YEP medium (1% yeast extract, 2% peptone) was employed, amended with 15% dextrose (fermentation medium).

Often, industrial-scale bioreactors are fed-batch, with new substrate supplied and product removed on 2- to 5-day cycles (Qazizada, 2016), each cycle being re-pitched with fresh yeast. To mimic conditions encapsulated cells would encounter through multiple cycles of re-use, all cultures were provided fresh medium twice weekly, with spent medium

discarded and fresh fermentation medium added. In both planktonic and encapsulated cell fermentations, the same cells were retained throughout the experiment. Spent medium was removed from encapsulated cultures by sieving it through a sterile brass sieve of 3-inch diameter and mesh size 10 (2 mm, McMaster Carr, Elmhurst, IL, Catalog #34735K216). Fresh sterile fermentation medium (250 mL final volume) was then placed into the same flask, containing the same beads, without cleaning/sterilization of the flask or beads. Spent medium was removed from planktonic cultures by decanting the entire 250 mL culture volume into 50 mL Falcon tubes, centrifuging these at 2000 *x g* for 2-3 minutes, then discarding spent medium. Pelleted cells were resuspended in fresh fermentation medium to a final culture volume of 250 mL, also without any cleaning or sterilization of the flask. Following addition of fresh medium, encapsulated and planktonic cultures were routinely checked for contamination by plating a sample of dilute cells on solid YPD (containing 1.5% agar).

4.2.2 Preparation of encapsulation matrices and cell encapsulation

Four encapsulation matrices were tested: sodium alginate, sodium alginate and chitosan, Protanal LF 10/60, and Protanal LF 10/60 and chitosan (Table 2). Sodium alginate was sterilized by combining 60 g of alginic acid sodium salt (sodium alginate; Sigma Aldrich Catalog #180947) with approximately 300 mL of 95% ethanol; this mixture was left overnight. This approach was utilized as other sterilization methods can alter the viscosity of alginate (Leo, McLoughlin, & Malone, 1990). This same procedure was repeated with the Protanal LF 10/60 (Protanal; gift from FMC Biopolymer). After mixtures sat overnight, ethanol was separated from the alginate by use of a 0.2 micron bottle top vacuum filter unit and the alginate was allowed to dry overnight at room temperature on the top of the filter.

Table 2. Types of matrices utilized in this manuscript. Five replicates of four types of alginate matrix, as well as five planktonic controls, were tested. All beads were approximately 4 mm in diameter.

Alginate	Cross-linker	Abbreviation
Sodium alginate	0.2 M $CaCl_2$	NaAlg
Sodium alginate	1% acetic acid + 0.2 M $CaCl_2$ + 0.25% chitosan	NaAlgCh
Protanal LF 10/60	0.2 M $CaCl_2$	Pr
Protanal LF 10/60	1% acetic acid + 0.2 M $CaCl_2$ + 0.25% chitosan	PrCh
None (planktonic)	N/A	-

To avoid pseudo-replication, twenty separate batches of encapsulation matrices were made in two rounds, the first round consisting of ten batches using sodium alginate and the second consisting of ten batches using Protanal. 110 mL of sterile distilled water and 6 g of dry, sterile sodium alginate were added to each of ten sterile plastic 1 L beakers. Alginate was mixed into water using a Jiffy Mixing Blades Power Tool Attachment (purchased from Home Depot, Catalog #DC408) and a standard power drill. Next, 80 mL of stationary phase (24 h) yeast were centrifuged at 2000 *x g* for 5 minutes, after which the supernatant was discarded and cells re-suspended in 40 mL of fresh fermentation medium. The suspension of yeast and medium was gently mixed into the alginate-water mixture, creating a 4% alginate-and-yeast suspension.

Ten 60 mL plastic syringes were each filled with alginate and yeast solution. Five of the syringes dripped into a 500 mL beaker containing 350 mL of the cross-linking solution 0.2 M $CaCl_2$, and the other five dripped into a 500 mL beaker containing 350 mL of the cross-linking solution 0.16 M acetic acid with 0.2 M $CaCl_2$ and 0.25% (w/v) chitosan (Sigma Aldrich, Catalog #448869). After the entire volume of alginate and yeast had

dripped into the cross-linking solution, all equipment was sterilized and the procedure repeated, producing 10 batches of Protanal beads that each contained 4.5 g (3%) Protanal. Both the sodium alginate and Protanal beads were hardened in the cross-linking solutions overnight at 4°C before being transferred to 250 mL screw-cap Erlenmeyer flasks that contained fermentation medium up to 250 mL. This process produced approximately 1,750 beads per replicate, each of which initially contained ~1.1 x 10^6 cells. All 1,750 beads were placed in a 250 mL flask, resulting in approximately 2 x 10^9 total cells per flask at the start of the experiment. Planktonic control cultures were treated similarly, with each replicate receiving 80 mL of stationary phase yeast re-suspended in 40 mL fermentation (the same starting amount of yeast as encapsulated cultures). So as to be comparable to encapsulated yeast, planktonic yeast suspensions also sat at 4°C overnight before being placed in fresh fermentation medium in 250 mL screw-cap Erlenmeyer flasks.

4.2.3 Estimation of Young's modulus, viscosity, and bead size via Universal Testing Machine

A Zwick Roell Z010 Universal Testing Machine (UTM; Zwick Roell, Ulm, Germany) was used to measure bead Young's modulus, viscosity, and bead size. Specifically, three replicate beads from each of the 20 encapsulated populations were tested over the course of 7 weeks by programming a probe (5 N maximum) to push down against the beads until the probe recorded 0.3 N of resistance. The probe then maintained that position for 50 seconds as it measured how the bead relaxed against constant force. A linear trendline was then applied to a graph of standard force (N) vs. strain (mm), with the slope of this line, multiplied by $\frac{2}{\Pi r}$, where r is the radius of each bead, reading out the Young's modulus

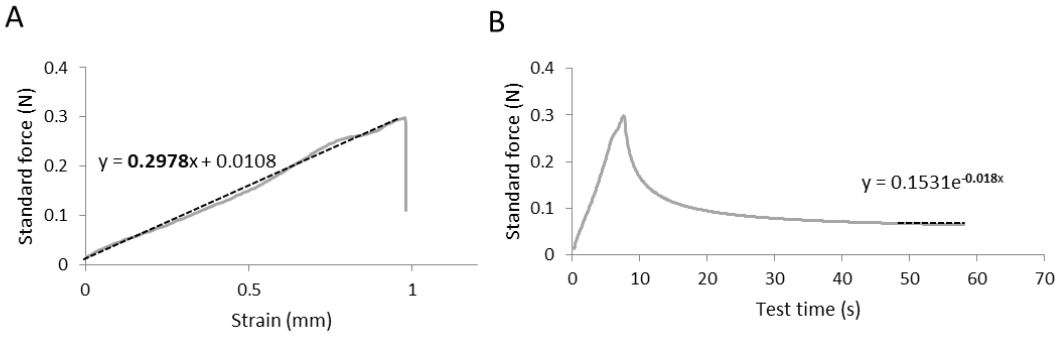

Figure 17. Calculating Young's modulus and viscosity. Young's modulus was calculated by fitting a linear trendline (dashed black line) to a graph of force vs. strain (A; gray line), and then multiplying the slope of that line (bolded) by $\frac{2}{\Pi r}$. Next, an exponential trendline (dashed black line) was fit to the last ten seconds of a graph of force vs. time (gray line) to find the decay constant (B; number bolded). Viscosity was calculated by dividing the Young's modulus by the absolute value of the decay constant.

(Figure 17A). An exponential fit of the last ten seconds of a graph plotting standard force (N) vs. time (s) was used to measure the decay constant. The Young's modulus was divided by the absolute value of the decay constant to calculate viscosity (Figure 17B). The UTM was also used to estimate bead diameter, by recording the tool separation distance when the 5 N probe first felt resistance.

4.2.4 Estimation of wet weight bead mass

At each time point, and for each of the twenty replicates containing encapsulated cells, the mass of 10 beads was measured as a group using a Mettler Toledo MS104TS analytical balance.

4.2.5 Fermentative capacity

Over the course of seven weeks, the fermentative capacity of planktonic and immobilized cells was monitored 12 h after media exchange, in other words, 12 h after each culture was

resuspended in fresh fermentation medium containing 15% dextrose. 12 h was chosen because we determined empirically that glucose was not exhausted until >24 h. Thus, the 12 h time-point was well before cells underwent the diauxic shift and began to consume ethanol. Glucose consumed and ethanol produced were assayed using the EnzyChrom™ Glucose Assay Kit (BioAssay Systems, Hayward, CA, Catalog #EBGL-100) and the Ethanol Test Kit (Fisher Scientific, Waltham, MA, Catalog #NC9508587), in both cases using methods provided by the manufacturer.

4.2.6 Cell enumeration and cell viability

To estimate cell number, yeast encapsulation matrices were dissolved by placing 5 beads into 10 mL of 10% (w/v) sodium metaphosphate solution (Fisher Scientific, Hampton, NH, Catalog #10124-56-8), a calcium chelating agent. Beads were agitated overnight at room temperature in a tissue drum rotator (New Brunswick Scientific, Edison, NJ, Item #TC-6). The following day, any remaining bead particles were mechanically disrupted by manual pipetting. Following dissolution, optical density (OD) of cell suspensions was determined at OD = 600 nm using a Synergy HTX multi-mode UV/VIS spectrophotometer (BioTek Instruments, Winooski, VT, Catalog #16022315). OD values were converted to cells mL-1 using a standard curve plotting OD600 against Ethanol Red cell number estimated using a Multisizer 4e Coulter Counter (Beckman, Indianapolis, IN, Catalog #B43905; Figure 18). Planktonic cells, including those that had escaped encapsulation within encapsulated cultures (‘escaped cells’), were enumerated in the same manner, though without overnight incubation in 10% sodium metaphosphate.

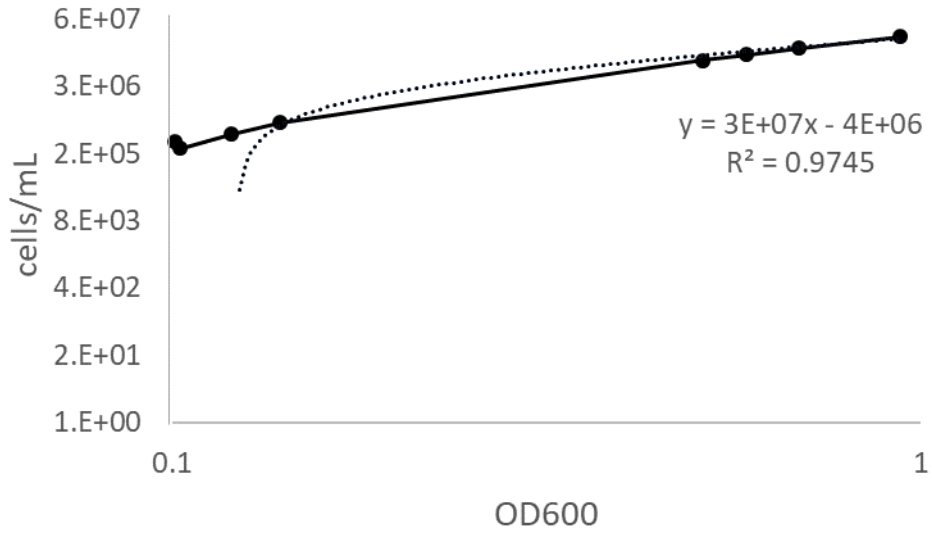

Figure 18. Relation of cell number to optical density. A standard curve for the strain Ethanol Red was determined using a Coulter Counter and spectrophotometer (solid black line). A trendline was fit to this data (dotted line) to allow us to interpolate cells/mL based on OD600.

Cell viability was estimated by measuring plasma membrane permeability to propidium iodide (PI), a fluorogenic compound that binds stoichiometrically to nucleic acids, producing a fluorescence emission that is proportional to cellular DNA content (Riccardi & Nicoletti, 2006). Membrane permeability to PI is indicative of cells that are dead or dying (Crowley et al., 2016; Newbold, Martin, Cullinane, & Bots, 2014). 2 mL of cell suspensions were diluted 1:200 in sterile water, then stained with 5 µg mL^{-1} PI (ThermoScientific, Waltham, MA Catalog #P1304MP; stock 10 mg/mL). At least 10,000 cells per sample were counted using a Sysmex CyFlow Space flow cytometer (Sysmex, Kobe, Japan, Catalog #1604063918). Controls containing heat-killed dead cells, live cells, and a mix of both were used to establish proper gating between live and dead cells, with a typical range for live cells consisting of 0.1 to 1 FL2(590-50) at 488 nm with a log4 gain of 450.

4.2.7 Heat shock tolerance

Heat shock tolerance was assayed for yeast encapsulated in each of four matrices, as well as for two planktonic controls: one consisting of yeast in exponential phase and the other consisting of cells that had reached stationary phase (24 h). Freshly encapsulated beads were prepared according to the procedure outlined above in Section 2.2, after which cells were provided with fresh YPD medium (2% dextrose, 2% peptone, 1% yeast extract) daily for 3 days to allow cells to recover from encapsulation. The planktonic control was exposed to exactly the same conditions (including overnight at 4°C to improve bead durability for encapsulated cultures) followed by three consecutive days of feeding.

Exponentially growing cells were obtained by diluting a stationary phase yeast culture 1:100 into fresh YPD medium, then culturing the population for ~3.5 h to an OD of 0.3 - 0.5 at OD = 600 nm. Three replicates for all four bead types were assayed, as well as three replicates for the two planktonic controls. Prior to heat shock, a baseline CFU mL^{-1} was calculated for each culture by making eight 1:10 serial dilutions into sterile water, and then plating six 5 µL spots of each dilution (undiluted to 10^{-7}) on a YPD agar plate.

Heat stress was applied by immersing each bead (or an equivalent number of planktonic cells) in 1 mL of pre-warmed medium then placing them in a 50°C incubator. Following high temperature incubation at 5, 15, 30, 90, and 180 minutes, cells were cooled on ice for 1 minute. Then, both planktonic and encapsulated cells were resuspended in 1 mL of 10% sodium metaphosphate for 15 minutes, to dissolve beads; beads were further disrupted by pipetting up and down using a 1000 µL pipet. The resulting cell suspensions were successively diluted 1:10 seven times, and from each of these dilutions six 5 µL spots were

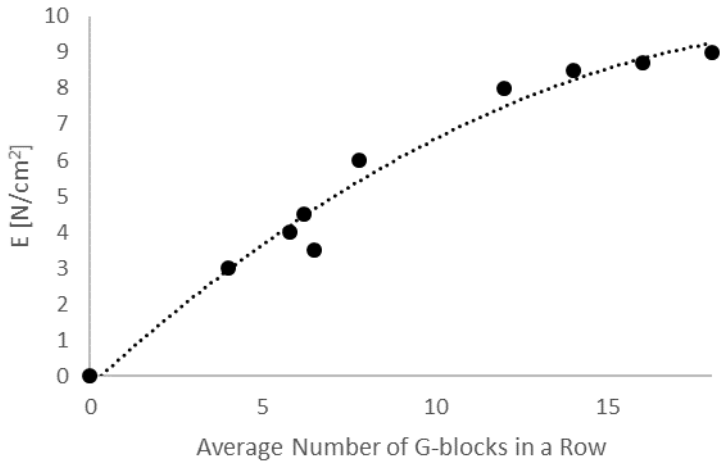

Figure 19. The modulus of rigidity as a function of the average length of G-Blocks. The modulus serves as a good illustration of how the gel-strength of alginate gels depends on the raw material the polymer is extracted from. Figure adapted from FMC Biopolymer.

plated on a YPD agar plate (Thomas, Sekhar, Upreti, Mujawar, & Pasha, 2015). Plates were incubated overnight at 30°C before scoring for cell growth.

4.2.8 Statistical analyses

Bead viscosity, bead mass, bead diameter, ethanol yield, cell number, and cell viability were compared using ANOVA tests with Tukey's post-hoc tests. An alpha value of 0.05 was used as a cut-off for significance in all cases. In some cases, a Pearson's coefficient was calculated to determine if a correlation existed between two parameters.

4.3 Results and Discussion

4.3.1 Young's modulus and viscosity of alginate beads declined over time

The Young's modulus and viscosity of different types of alginate-containing beads were

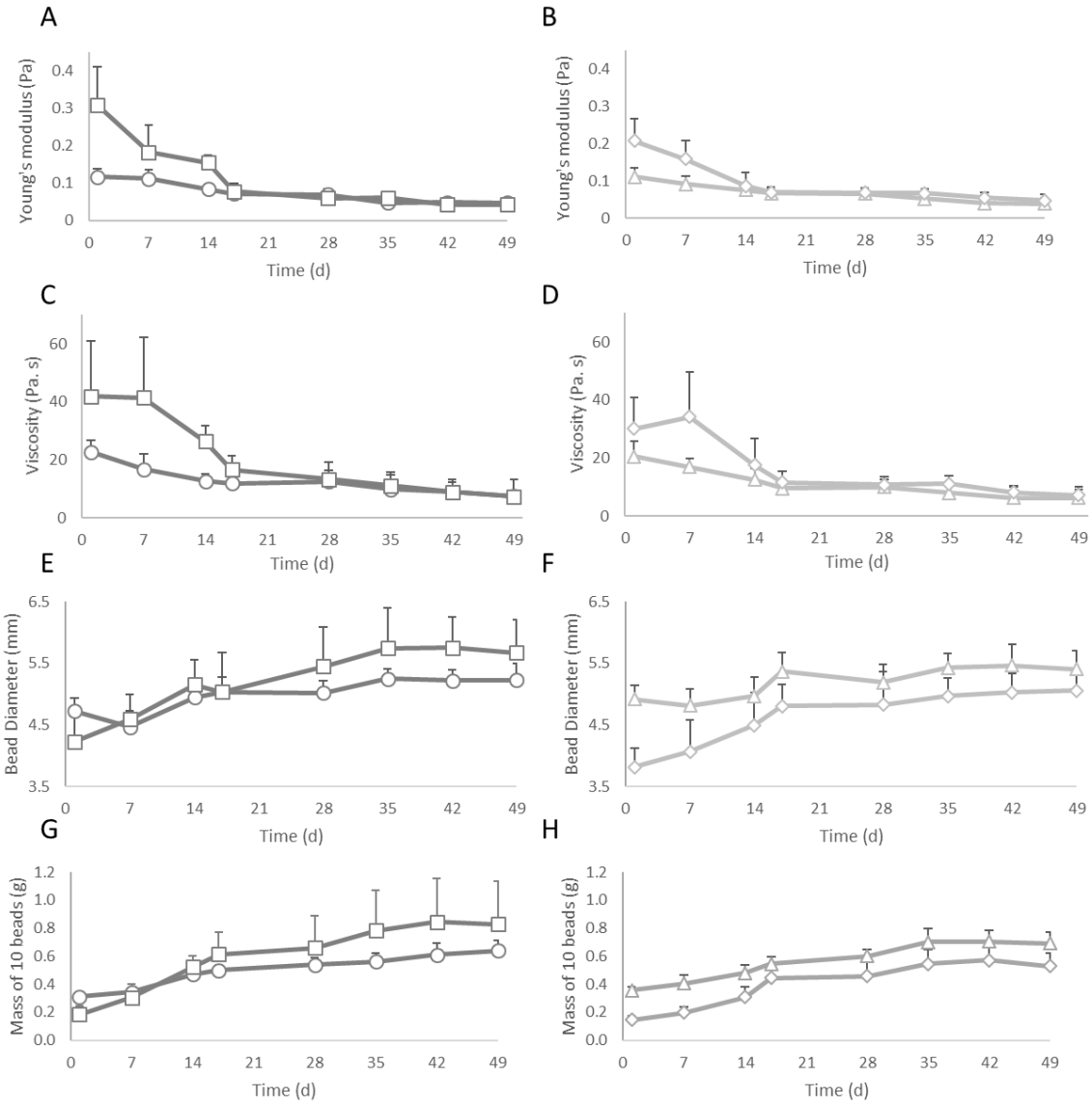

Figure 20. Bead durability and swelling. The Young's modulus and viscosity of 3 beads from each of 20 replicates was measured using a Universal Testing Machine. Over time, both Young's modulus (A&B) and viscosity (C&D) decreased. Beads increased in both diameter (E&F) and mass (G&H), becoming visibly larger as time progressed. Dark gray circles represent NaAlg beads, dark gray squares represent NaAlgCh beads, light gray triangles represent Pr beads, and light gray diamonds represent PrCh beads. Error bars represent one standard deviation.

Table 3. Differences in Young's modulus over time. An ANOVA with Tukey's post-hoc test was utilized to compare the Young's modulus of different bead types at each time point. Bead types that do not share a letter in common are significantly different, with alphabetical ordering representing a higher Young's modulus. Shading allows for easier visualization of letter differences, with darker shading shown for lower letters. F ratios and p-values are also listed for reference.

Time (d)	1	7	14	17	28	35	42	49
NaAlg	C	B	A	A	A	B	A	A
NaAlgCh	A	A	A	A	A	AB	A	A
Pr	C	B	A	A	A	AB	A	A
PrCh	B	A	A	A	A	A	A	A
F ratio	35.5	12.0	0.6	1.3	0.9	4.1	2.5	1.4
p-value	<0.0001	<0.0001	0.58	0.28	0.44	0.01	0.07	0.25

measured to determine how they structurally weakened over time. Cell encapsulation matrices differed in chemical composition in ways that could be expected to affect their durability in prolonged culture. Specifically, different types of alginates exhibit differences in viscosity and rigidity, both of which have been shown to impact the physical stress that beads can endure (Figure 19). Chitosan was added to two of four matrices as it has been previously shown to improve bead durability, perhaps by reducing calcium chelation (Segale, Giovannelli, Mannina, & Pattarino, 2016; Takka & Gürel, 2010).

To estimate the mechanical and structural decline experienced by different matrices as they aged, we calculated both the Young's modulus, a measure of the ability of a material to withstand changes in length when under lengthwise tension or compression, and viscosity, a parameter that integrates resistance to force and relaxation under a constant

Table 4. Differences in viscosity over time. An ANOVA with Tukey's post-hoc test was utilized to compare the viscosity of different bead types at each time point. Bead types that do not share a letter in common are significantly different, with alphabetical ordering representing a higher viscosity. Shading allows for easier visualization of letter differences, with darker shading shown for lower letters. F ratios and p-values are also listed for reference.

Time (d)	1	7	14	17	28	35	42	49
NaAlg	B	B	A	B	A	A	A	A
NaAlgCh	A	A	A	A	A	A	A	A
Pr	B	B	A	B	A	A	A	A
PrCh	B	A	A	B	A	A	A	A
F ratio	10.5	12.9	2.9	8.4	2.1	1.9	1.8	0.39
p-value	<0.0001	<0.0001	0.04	<0.0001	0.11	0.13	0.14	0.78

force (Olderoy et al., 2012; Webber & Shull, 2004). Specifically, for each bead type, the Young's modulus and viscosity were measured at eight time-points by applying 0.3 N of force, then maintaining that position for 50 seconds. The Young's modulus and viscosity were calculated from the resulting data (Figure 17A-D), and these data were compared across bead types.

Overall, similar trends were observed in both parameters. Both Young's modulus and viscosity revealed significant differences based on an ANOVA with Tukey's post-hoc test on 3 out of 8 timepoints (Tables S1&S2). Over the initial phase of our experiments, both matrices that incorporated chitosan exhibited significantly higher Young's modulus and viscosity than matrices that did not (Table 3 and Table 4, ANOVA with Tukey's post-hoc). However, by day 14 those chitosan-related differences had largely disappeared, with differences in Young's modulus on day 35 and viscosity on day 17 unrelated to the

Table 5. Chemical composition of different alginates. A variety of brown algae species are used to produce alginates, each varying in the average length of guluronic acid (G)-blocks. Protanal is sourced from the stem of *Laminaria hyperborea*, whereas sodium alginate is sourced from *Macrocystis pyrifeira*. Table modified from FMC Biopolymer.

Brown algae	Avg. # G-blocks
Laminaria hyperborea (stem)	17
Laminaria hyperborea (leaf)	9
Lessonia nigrescens	7
Macrocystis pyrifeira	6
Laminaria japonica	6
Laminaria digitala	6
Asophyllum nodosum	4

presence or absence of chitosan. Both Young's modulus and viscosity declined by roughly half over 49 days (Figure 20A-D), with much of this change occurring between days 1-17, and comparatively less between days 17-49 (Figure 20A-D). One explanation for this observation relates to the behavior of alginate gels under different magnitudes of stress; under smaller stresses (<5 mN), they behave elastically, but under larger stresses, they behave viscoelastically, settling into a new steady state (Webber & Shull, 2004). The gradual chelation of Ca^{2+} ions, which are essential to the structural integrity of alginate gels, likely also contributed to the observed decrease in mechanical stability over time (Tong et al., 2017).

Alginates are extracted from brown algae, and are composed of alternating 1-4 α-L-guluronic (G-block) and β-D-mannuronic (M-block) acid residues (George & Abraham,

Table 6. Differences in bead size (mm) over time. An ANOVA with Tukey's post-hoc test was utilized to compare the diameter of different bead types at each time point. Bead types that do not share a letter in common are significantly different, with alphabetical ordering representing a larger bead size. Shading allows for easier visualization of letter differences, with darker shading shown for lower letters. F ratios and p-values are also listed for reference.

Time (d)	1	7	14	17	28	35	42	49
NaAlg	A	B	A	AB	B	BC	BC	B
NaAlgCh	B	AB	A	A	A	A	A	A
Pr	A	A	A	A	AB	AB	AB	AB
PrCh	C	C	B	B	B	C	C	B
F ratio	37.9	16.4	8.3	6.9	6.2	10.8	11.4	6.9
p-value	<0.0001	<0.0001	<0.0001	0.0005	0.0011	<0.0001	<0.0001	0.0005

2006). Alginates form hydrogels in the presence of divalent cations, including Ca^{2+} (used in this study), Ba^{2+}, Sr^{2+}, and Zn^{2+} (S. Bajpai & S. Sharma, 2004; C. Ouwerx, N. Velings, M. Mestdagh, & M. Axelos, 1998). Specifically, Pr is derived from the stem of the algae *Laminaria hyperborea*, whereas NaAlg is derived from *Macrocystis pyrifeira*. These algae differ in the average length of G-block acids (Table 5), which affects bead rigidity (Figure 19). Based on these data, we expected that Pr beads would exhibit higher Young's modulus than NaAlg beads. Contrary to expectations, Pr beads displayed similar Young's modulus to NaAlg beads (Figure 20A-D). Earlier reports suggested that certain types of sodium alginate can have higher viscosity than Protanal LF 10/60 beads (C. Ouwerx, N. Velings, M. M. Mestdagh, & M. A. V. Axelos, 1998); the higher alginate concentration used in sodium alginate preparation may also have contributed to higher viscosity of this bead type (Table 2).

Our data support the notion that cross-linking with chitosan improves bead viscosity in both NaAlg and Pr beads for up to a week. Chitosan is commonly derived from crustacean shells, and is a linear polysaccharide composed of D-glucosamine and N-acetyl-D-glucosamine units linked by β-(1-4) glycosidic linkages (Roberts, 1992). Chitosan, a polycation, strengthens beads by forming a complex with alginate, which may protect crosslinking Ca^{2+} from metal chelators (Segale et al., 2016; Takka & Gürel, 2010). Figure 20A-D indicate that the presence of chitosan significantly improved Young's modulus and viscosity for 7 days (Table 3 and Table 4), consistent with previous studies noting increased durability with chitosan (Berger et al., 2004; Takka & Gürel, 2010).

4.3.2 Bead size and mass increased over time

Bead swelling has been linked to structural instability, and is thus undesirable (Chaenyung, Rin, Yong-Su, & Hyunjoon, 2012). To investigate whether some bead types were more prone to swelling than others, bead diameter and mass were measured as a function of time. The UTM was employed as a caliper to measure bead diameter (Figure 20E&F), and a scale was utilized to measure the wet mass of 10 beads (Figure 20G&H). Significant differences among treatments were observed for bead diameter at each time point (**Error! Reference source not found.**; ANOVA with Tukey's post-hoc). Alginate b eads cross-linked with chitosan swelled more than twice as rapidly as beads lacking chitosan; NaAlgCh beads increased by approximately 1.4 mm in diameter over 49 days, PrCh beads by ~1.2 mm, and NaAlg and Pr beads both increased by ~0.5 mm. Similar patterns were observed for bead mass. NaAlgCh beads increased by approximately 0.65 g over 49 days, whereas PrCh beads increased by ~0.39 g, and NaAlg and Pr beads both increased by ~0.33 g. In general, fewer differences were observed among treatments based

Table 7. Differences in bead mass (g) over time. An ANOVA with Tukey's post-hoc test was utilized to compare the wet mass of 10 beads of different bead types at each time point. Bead types that do not share a letter in common are significantly different, with alphabetical ordering representing a larger bead mass. Shading allows for easier visualization of letter differences, with darker shading shown for lower letters. F ratios and p-values are also listed for reference.

Time (d)	1	7	14	17	28	35	42	49
NaAlg	A	A	A	AB	A	A	A	A
NaAlgCh	B	AB	A	A	A	A	A	A
Pr	A	A	A	AB	A	A	A	A
PrCh	B	B	B	B	A	A	A	A
F ratio	25.6	10.9	10.8	3.0	2.3	2.6	2.5	2.8
p-value	<0.0001	0.0005	0.0005	0.045	0.1	0.09	0.09	0.07

on bead mass than were observed based on bead diameter, with significant differences observed among matrices through day 17 (Table 7; ANOVA with Tukey's post-hoc).

Bead swelling and shrinking has been previously linked to changes in a variety of conditions, including pH (S. K. Bajpai & S. Sharma, 2004), temperature (Polona Smrdel, Bogataj, & Mrhar, 2008; Woo et al., 2007), and cross-linking solution (P Smrdel et al., 2006). Regular changes in pH, from 5.8 to 4.6 over each 3.5 day feeding episode, were observed in this experiment, and likely contributed to bead swelling. Swelling could also have been caused by gradual loss of calcium cations over time (Chaenyung et al., 2012), allowing for an increase in bead size and the development of seams (Figure 20) in most beads after 28 days. This swelling may have also contributed to time-dependent changes in Young's modulus and viscosity (Figure 20A-D). A Pearson's correlation coefficient of -0.45 revealed a strong association between larger beads and lower viscosity across all bead

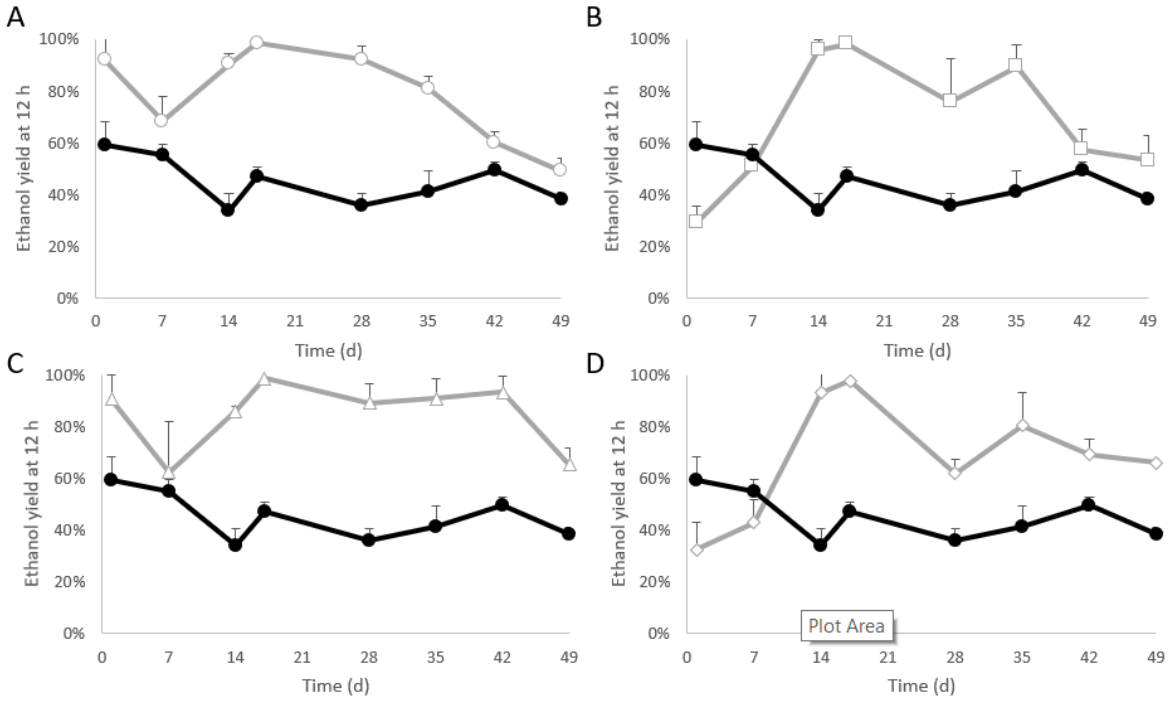

Figure 21. Ethanol yield over time in planktonic and encapsulated cultures. Encapsulated and planktonic cells were grown in 250 mL Erlenmeyer flasks with gentle (50 rpm) shaking at 30 °C in a 250 mL culture volume of fermentation medium containing 150 g/L dextrose. The ethanol yield was calculated as a percentage of the theoretical maximum yield for the grams of ethanol produced from the grams of dextrose consumed after 12 h. Yield was measured in five replicate cultures from each combination of alginate and cross linker: A) NaAlg beads (gray circles), B) NaAlgCh beads (gray squares), C) Pr beads (gray triangles), and D) PrCh beads (gray diamonds). The ethanol yield in five planktonic only controls is indicated by the black circles. Error bars represent one standard deviation.

types. Interestingly, although chitosan improved Young's modulus and viscosity in the short term, it also increased the rate of bead swelling relative to beads not cross-linked with chitosan, potentially contributing to lower Young's modulus and viscosity in the long-term. This is in agreement with studies indicating that chitosan contributes to bead swelling at low pH (~5) values (Takka & Gürel, 2010), conditions our beads experienced for 48 h in each cycle after glucose was depleted and before fresh medium was added.

4.3.3 Ethanol yield (g/g) from dextrose varied among treatments

Table 8. Differences in ethanol yield (g/g) from dextrose over time. An ANOVA with Tukey's post-hoc test was utilized to compare the ethanol yield (g/g) from dextrose of different bead types at each time point. Bead types that do not share a letter in common are significantly different, with alphabetical ordering representing a higher yield. Shading allows for easier visualization of letter differences, with darker shading shown for lower letters. F ratios and p-values are also listed for reference.

Time (d)	1	7	14	17	28	35	42	49
Planktonic	B	A	B	B	C	B	B	B
NaAlg	A	A	A	A	A	A	B	AB
NaAlgCh	B	A	A	A	AB	A	B	AB
Pr	A	A	A	A	A	A	A	A
PrCh	B	A	A	A	B	A	B	A
F ratio	13.2	0.94	28.2	47.0	9.3	7.0	11.5	5.9
p-value	<0.0001	0.46	<0.0001	<0.0001	0.0002	0.0012	<0.0001	0.0028

To determine which treatment consistently resulted in the highest ethanol yield over successive fermentation cycles, glucose consumed and ethanol produced was measured 12 h after adding fresh substrate. The 12 h timepoint was chosen because it was prior to glucose exhaustion (and potential ethanol consumption), which did not occur until >24 h.

Ethanol yield was generally higher in encapsulated than in planktonic cultures (Figure 21). While both NaAlg and Pr beads exhibited significantly higher ethanol yields than planktonic cultures on day 1, cells in NaAlgCh and PrCh beads did not attain comparable levels until 14 days (; ANOVA with Tukey's post-hoc). Since chitosan does not fully dissolve in water, 0.16 M acetic acid was used as a solvent; the matrices cross-linked with chitosan were therefore exposed to the acetic acid overnight, whereas the other matrices and the planktonic control were not. Acetic acid is known to negatively impact

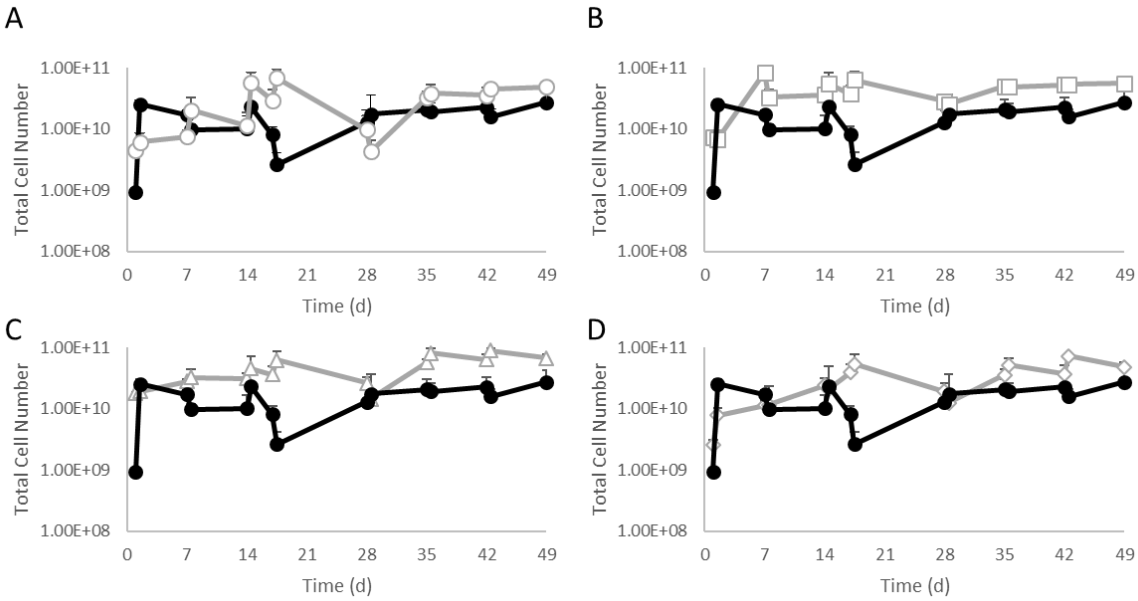

Figure 22. Encapsulated populations have similar cell numbers to planktonic populations. The number of encapsulated and planktonic cells before and 12 h after the addition of fresh medium across 49 days was measured. The number of cells in encapsulated cultures is indicated by the gray lines. Black lines indicate the average number of cells in five planktonic replicates. Five replicates of each of two types of alginates were tested using two cross-linking solutions: A) NaAlg (circles), B) NaAlgCh (squares), C) Pr (triangles), and D) PrCh (diamonds). Error bars represent one standard deviation.

cell viability, and could account for lower yields observed at early time points (Christopher R. Burtner et al., 2009; Orlandi, Ronzulli, Casatta, & Vai, 2013). NaAlgCh and PrCh beads also exhibited a decline in ethanol yield on day 28 (following a missed feeding on day 24) that was absent in NaAlg and Pr beads. This observation could be attributed to a subsequent decline in cell viability that also occurred on day 28 (**Error! Reference source not found.**). Yield in all four encapsulation matrices approached 100% (though with somewhat differing frequencies), and was generally high (>90%) between 14 and 35-42 days (depending on matrix type), whereas yield for the planktonic control never exceeded 60%. The high yields observed for encapsulated cells here accord with previous findings using

encapsulated *S. cerevisiae.* High (>80%) fermentation efficiencies have been demonstrated on starch (Jamai, Ettayebi, El Yamani, & Ettayebi, 2007) and 10% dextrose (McGhee, Julian, et al., 1982a) for single batches, as well as high (>85%) yields from re-used beads over 5 days (Watanabe et al., 2012), 10 days (K. H. Lee, Choi, Kim, Yang, & Bae, 2011), 12.5 days (Kondo et al., 2002), and 15 days (Chen et al., 2013). Others have noted no differences in ethanol production based upon the presence or absence of chitosan (X. Li, 1996).

Overall, our results indicate that encapsulated systems have higher ethanol yields than planktonically grown cells, in some cases for at least 49 days. Among encapsulated systems, significant differences were observed according to an ANOVA with Tukey's post hoc-test on four out of eight timepoints, with Pr beads displaying the highest yields; indeed, Pr beads had significantly higher ethanol yields than planktonic cells even after 49 days of culture. Further, our results indicate that the culture system is robust to missed feedings; even after low yields were recorded following the missed feeding, the system was able to recover and again achieve yields and viabilities comparable to those observed before the missed feeding (**Error! Reference source not found.**).

4.3.4 Following outgrowth, total cell number was similar across encapsulated and planktonic cultures

A culture with more cells should, all else being equal, produce ethanol more rapidly than a culture with fewer cells. In order to assess ethanol production based on culture method (rather than on cell number), experiments were initiated at similar cell population sizes across encapsulated and planktonic treatments. Specifically, approximately 2×10^9 cells

Table 9. A comparison of total cell number across different bead types over time. Cell number was measured immediately before and 12 h after the addition of fresh medium across 49 days. An ANOVA with Tukey's post-hoc was run for each timepoint, with the connecting letters report listed for each day and time. Groups that do not share a letter in common are significantly different, with alphabetical ordering representing a higher cell number. Shading allows for easier visualization of letter differences, with darker shading shown for lower letters. F ratios and p-values are also listed for reference.

Time (d)	**1**		**7**		**14**		**17**		**28**		**35**		**42**		**49**	
	0h	12h	0h	12h	0h	12h	0h	12h	0h	12h	0h	12h	0h	12h	0h	12h
Planktonic	B	A	B	A	A	A	A	B	A	A	B	C	B	B	B	B
NaAlg	B	B	B	A	A	A	A	A	A	A	AB	BC	AB	AB	AB	B
NaAlgCh	B	B	A	A	A	A	A	A	A	A	A	B	AB	AB	AB	AB
Pr	A	A	B	A	A	A	A	A	A	A	A	A	A	A	A	A
PrCh	B	B	B	A	A	A	A	A	A	A	AB	B	AB	A	AB	AB
F ratio	23.9	32.7	31.9	2.8	2.6	3.0	1.9	7.0	1.3	1.7	4.9	15.6	2.9	5.6	3.3	4.7
p-value	<0.0001	<0.0001	<0.0001	0.054	0.067	0.043	0.14	0.0012	0.29	0.19	0.0067	<0.0001	0.048	0.0038	0.036	0.0083

were added to 250 mL cultures of four bead types (Table 2; NaAlg, NaAlgCh, Pr, PrCh) as well as to the planktonic control. Total cell number in each flask was estimated immediately following (0 h) and 12 h after the addition of fresh medium at all eight timepoints across 49 days (Figure 22). Cell number was estimated indirectly by optical density of cell suspensions by regressing direct cell counts obtained by a Coulter Counter Multisizer 4e against OD600 (y = 3E+07x - 4E+06, Figure 18).

Across all treatments, no appreciable changes in cell number were observed after the initial week-long outgrowth period (Figure 22). Analysis of absolute OD values by 1-way ANOVA (Table 9) suggested that while cell number remained constant from days 7-28, cell number in the planktonic control did not increase as rapidly as it did in certain encapsulated cultures (Table 9; ANOVA with Tukey's post-hoc), particularly the Pr matrix.

The carrying capacity of encapsulated treatments was comparable to values previously reported for fed-batch cultures *of S. cerevisiae* (Roukas, 1994). However, it should be noted that optical density measurements, which rely on light scattering, can be less accurate than direct enumeration by microscopy or Coulter count (Myers, Curtis, & Curtis, 2013). Variance in cell number was higher than observed for alginate-encapsulated yeast that were fed *ad libitum* in immobilized cell reactors, with some treatments varying by as much as an order of magnitude even following outgrowth (Nagarajan et al., 2014). The latter observation could be attributed to the feast-and-famine nature of repeated fed-batch culture, which introduces variability in culture conditions not experienced by continuously-fed cells (Suarez-Mendez, Sousa, Heijnen, & Wahl, 2014).

Among different matrix types, Pr beads contained more total cells than at least one other matrix type at 8 out of 16 timepoints (one-way ANOVA, $p < 0.05$), and fewer cells than any another matrix type at only one (Table 9). This higher cell number may have contributed to the higher ethanol yields observed for Pr beads, but does not explain this difference in and of itself. There is overlap at three timepoints where Pr beads showed higher yield and more cells than other bead types, but there was also one timepoint wherein Pr beads had higher ethanol yield but not more cells (day 28), and another point where they had more cells but not a higher yield (day 35). Differences in rates of cell escape and in cell viability would also be expected to impact yield.

4.3.5 Cell escape increased over time, except in Pr beads

Cell escape, where encapsulated cells exit the bead and become planktonic, is known to occur in alginate gels, where it can result in less efficient substrate utilization as well as

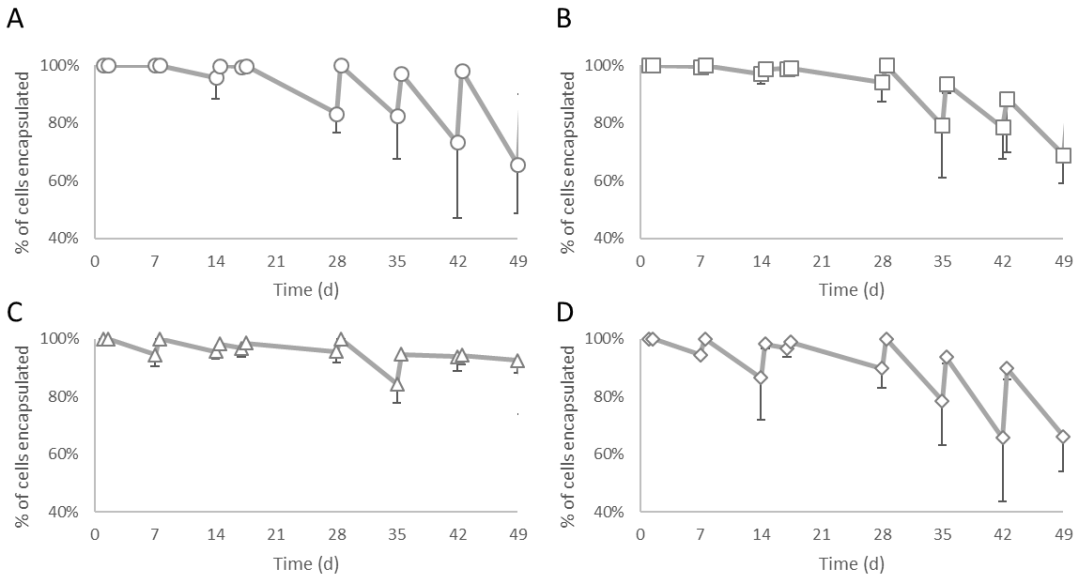

Figure 23. Cell escape over time. The number of encapsulated and planktonic cells before and 12 h after the addition of fresh medium across 49 days was measured. The number of cells that escaped encapsulation to become planktonic was compared to the number of all cells (escaped and encapsulated) to find the percent of cells encapsulated at various timepoints. An average of five replicates from A) NaAlg, B) NaAlgCh, C) Pr, and D) PrCh matrices was utilized. Error bars represent one standard deviation.

competition with encapsulated cells for nutrients (King, Daugulis, Goosen, Faulkner, & Bayly, 1989; Laca, García, & Díaz, 2000). Total cell number reported for encapsulated treatment groups includes both encapsulated and escaped cells; "percent cell escape" represents the fraction of that total that was formerly encapsulated, but escaped the bead and became planktonic. Percent cell escape increased as beads aged (Figure 23; **Error! R eference source not found.**), with a strong correlation (Pearson's coefficient of 0.55) between declining viscosity and increased incidence of cell escape. The number of cells escaping was low in all matrices up until day 28, after which Pr beads generally had fewer escapees (Figure 23); significant differences assessed by one-way ANOVA were detected

only on days 28 and 49 (**Error! Reference source not found.**) due to high variance among r eplicates. Although they did not have more cells than the other matrix types on day 28, Pr beads had a significantly higher fraction of encapsulated cells, which may help account for higher ethanol yields observed in Pr beads on day 28. This result is surprising as neither Pr Young's modulus, viscosity, bead diameter, nor mass could be distinguished statistically from that of other matrix types on those days, suggesting that some other factor not measured here, perhaps pore size, also contributes to cell escape, or lack thereof (Machado et al., 2013).

4.3.6 Cell viability declined over time in both encapsulated and planktonic cell cultures

As cells age, their viability declines (Mortimer & Johnston, 1986). To compare time-dependent changes in this parameter between encapsulated and planktonic cells, cell viability was assessed 12 h after each addition of fresh medium by staining cells with propidium iodide (PI) and counting >10,000 individual cells via flow cytometry (**Error! R eference source not found.**). Viability assessed by PI staining was compared to viability assessed by colony forming units (CFUs) in both encapsulated and planktonic cultures at day 1, after which PI alone was used. For both encapsulated and planktonic cells, viability assessed by PI staining was twice that estimated by CFUs, likely because the former method scores cells that are alive

but unable to form colonies. Across all treatments, decline in viability was biphasic; viability declined rapidly during the first week of fed-batch culture, then slowly over the ensuing six weeks. A missed feeding on day 24 helps to account for lower viability

Table 10. Differences in viability over time. An ANOVA with Tukey's post-hoc test was utilized to compare the viabilities of different groups at each time point. Bead types that do not share a letter in common are significantly different, with alphabetical ordering representing a higher viability. Shading allows for easier visualization of letter differences, with darker shading shown for lower letters. F ratios and p-values are also listed for reference.

Time (d)	1	7	14	17	28	35	42	49
Planktonic	A	A	B	A	A	A	A	A
NaAlg	B	A	A	A	B	A	A	B
NaAlgCh	C	A	A	A	B	A	A	B
Pr	AB	A	A	A	B	A	A	AB
PrCh	C	A	A	A	B	A	A	AB
F ratio	29.2	0.58	7.8	3.0	9.2	2.3	1.2	5.2
p-value	<0.0001	0.67	0.0007	0.044	0.0003	0.092	0.33	0.0052

measured on day 28; thereafter viability quickly recovered to pre-starvation levels, indicating a robust culture system. When experiments were terminated at 7 weeks, cell viability in most treatments was ~20%, with planktonic yeast exhibiting only marginally greater viability than yeast that had been encapsulated (**Error! Reference source not found.**; Table 10).

Overall, few viability differences were observed among treatments. NaAlgCh and PrCh beads had lower viability than both other matrix types and planktonic cells on day 1, likely due to their recent overnight exposure to 0.16 M acetic acid (necessary to dissolve chitosan) (C. R. Burtner, C. J. Murakami, B. K. Kennedy, & M. Kaeberlein, 2009; Orlandi et al., 2013). Following the initially low viability of some cultures, which was likely due to encapsulation itself, (and disregarding day 28 as an artifact of a missed feeding), there were only two days in which significant differences were observed (1-way ANOVA with

Tukey's post-hoc, $p < 0.05$): day 49, when some encapsulated populations had lower viability than the planktonic control, and day 14, when all encapsulated treatments had higher viability than the planktonic control (**Error! Reference source not found.**; A NOVA with Tukey's post-hoc). Significant differences among encapsulated treatments were noted only on Day 1, during the initial recovery period, indicating that the encapsulation matrices tested here do not significantly affect cell viability over time. As viability differences were largely absent, as has been reported under some conditions by others (Baruch & Machluf, 2006), it is unlikely that this parameter contributed to differences in ethanol yields observed among different matrix types.

Other culture systems support higher yeast viability over prolonged incubations, even considering that viability here is based on PI staining, rather than on number of CFU. Cells in giant colonies grown on GM (1% yeast extract, 3% glycerol) agar retain 90% viability after 10 days, then slowly decline to 5% viability after 135 days (Palkova et al., 2009). Planktonic *Saccharomyces cerevisiae* cultured in nutrient-limited retentostats retain 80% viability after 22 days (Boender et al., 2009), and alginate-encapsulated yeast continuously fed ad libitum exhibited >90% viability after almost three weeks continuous culture (Nagarajan et al., 2014). The lower viability reported here may stem from cells being subjected to repeated cycles of feast and famine, each of which is attended by pronounced changes in pH, glucose, ethanol and acetate concentrations. pH was found to change from 5.8 to 4.6 over 3.5 days, glucose from 15% to 0%, ethanol from 0% to 4-7.5%, and acetate from 0 to 15 mM. Prolonged exposure to 15 mM of acetate at pH of ~4.5 has been shown to negatively impact planktonic yeast cell viability, and likely affected viability of encapsulated cells as well (C. R. Burtner et al., 2009; Orlandi et al., 2013). Since the *S.*

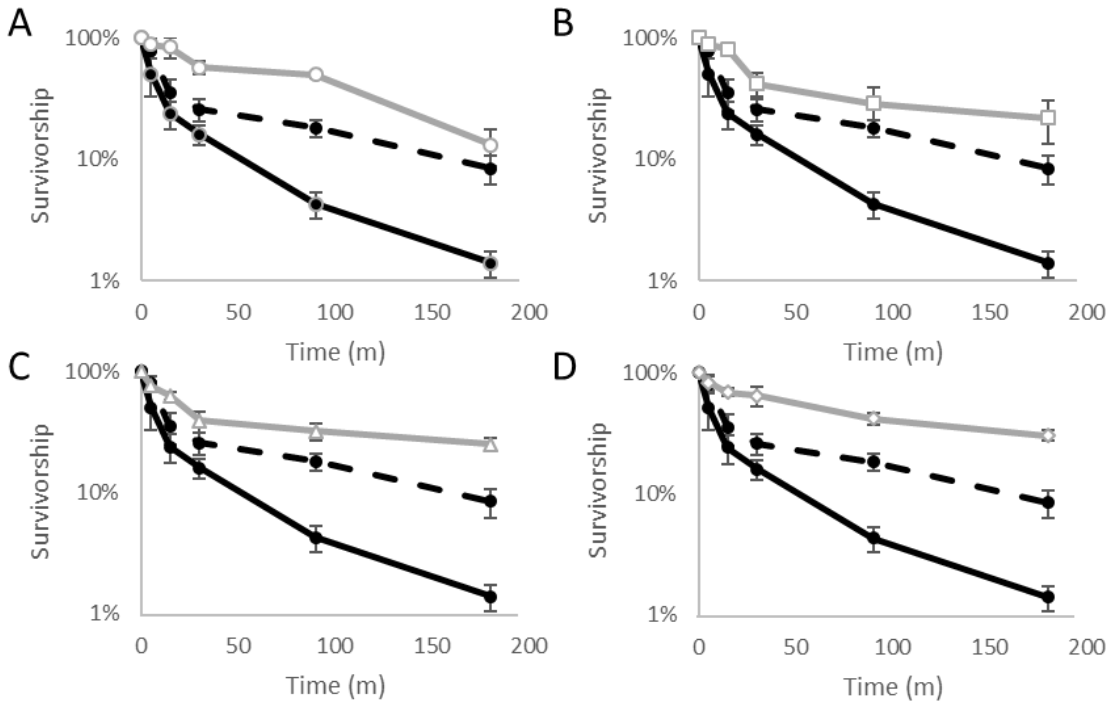

Figure 24. Survivorship of encapsulated and planktonic cells at 50°C. Three replicates of A) NaAlg beads (gray circles), B) NaAlgCh beads (gray squares), C) Pr beads (gray triangles), and D) PrCh beads (gray diamonds) as well as planktonic cells in the exponential (solid black line) and stationary (dashed black line) growth phases were exposed to 50°C for three hours. Survivorship was tracked by calculating CFUs/mL using the spot plate technique. Error bars represent one standard deviation.

cerevisiae strain used here is purported to be tolerant of ethanol up to 17% (Fermentations, 2019), it is unlikely that a maximum theoretical concentration of 7.5% caused a significant decline in viability, making acetate and pH changes more plausible explanations. These fluctuating conditions stand in marked contrast with conditions experienced by colonies on agar, cells in retentostats, and cells in continuously fed immobilized cell reactors, all of which are relatively constant environments, albeit having different levels of substrate input. A Pearson's correlation coefficient relating viability to ethanol yield was only 0.168, indicating a weak association between viability and ethanol yield. Neither encapsulated nor planktonic cultures exhibited lower ethanol yield between days 14 and 35, when PI-staining

cells constituted ~80% of populations, than they did when viability was much higher. Our results are in line with other studies reporting a decrease in cell viability from 80% to 30% over 5 fed-batch cycles, even as yields remained constant at ~80% (Pereira, Gomes, Guimarães, Teixeira, & Domingues, 2012), as well as an association between lower viability and pH changes (Branska, Pechacova, Kolek, Vasylkivska, & Patakova, 2018).

4.3.7 Encapsulated cells are more heat-shock resistant than planktonic cells, but no one matrix confers greater heat-shock resistance than another

Simultaneous saccharification (enzymatic degradation of starch to sugars) and fermentation (conversion of sugars to ethanol) has been widely implemented in the bioethanol industry due to its higher efficiency (Terán Hilares et al., 2017; Won, Kim, & Oh, 2012), even though most enzymes operate optimally well above yeasts' preferred growing temperatures (S. Y. Huang & Chen, 1988; Mutturi & Lidén, 2013). Thus, a more thermotolerant yeast could improve the efficiency of this step (Talukder, Easmin, Mahmud, & Yamada, 2016; Techaparin, Thanonkeo, & Klanrit, 2017). Moreover, cooling costs for fermentation tanks can be costly in the summer, especially in warmer regions (McAloon, Taylor, Yee, Ibsen, & Wooley, 2000); a more thermotolerant yeast could also help reduce cooling costs, and is thus doubly favored. Indeed, recent analyses suggest that for every 5°C increase in the fermentation temperature, in today's market approximately $30,000 per year could be saved for a 30,000 kL scale ethanol plant, not including reductions in initial investment costs (Abdel-Banat, Hoshida, Ano, Nonklang, & Akada, 2010).

To discover whether certain encapsulation matrices offer more protection against thermal stress than others, yeast were subjected to heat shock at 50°C for 180 minutes.

Table 11. Differences in heat shock resistance over time. An ANOVA with Tukey's post-hoc test was utilized to compare the thermotolerance of different groups at each time point. Bead types that do not share a letter in common are significantly different, with alphabetical ordering representing a higher thermotolerance. Shading allows for easier visualization of letter differences, with darker shading shown for lower letters. F ratios and p-values are also listed for reference.

Time (m)	5	15	30	90	180
Planktonic exponential	B	B	D	D	C
Planktonic stationary	AB	B	CD	CD	C
NaAlg	A	A	AB	A	BC
NaAlgCh	A	A	BC	BC	AB
Pr	AB	A	BC	BC	A
PrCh	AB	A	A	AB	A
F ratio	4.3	20.3	16.2	28.1	18.7
p-value	0.018	<0.0001	<0.0001	<0.0001	<0.0001

Planktonic cells, in either exponential or stationary phase, as well as cells encapsulated in each of four matrices, were exposed to 50°C for 5, 15, 30, 90, and 180 minutes (Figure 24), after which viability was assessed as CFUs following dilution and plating on rich agar. Consistent with prior studies, viability of planktonic exponential-phase cells declined more rapidly than that of stationary-phase cells (Kreft & Bonhoeffer). Viability of encapsulated yeast consistently declined less rapidly than either planktonic treatment. However, few differences could be discerned among encapsulation matrices. Although significant differences were seen at the 30, 90, and 180 m time points (Table 11; ANOVA with Tukey's post-hoc), no clear trend emerged to suggest one type of matrix conferred more thermal protection than another.

This result is perhaps to be expected given the known heat stability of alginates, which are stable at far higher temperatures than the yeast inside them could withstand (Draget, 2009; Naydenova et al., 2014). Overall, heat-shock resistance in these matrices was similar to that previously reported for alginate-encapsulated *S. cerevisiae* (Nagarajan et al., 2014). Increased heat resistance displayed by encapsulated cells was once attributed to nutrient deficiency in cells close to the core of the bead, triggering a stress-response similar to that observed for cells entering stationary phase (F. Talebnia, Niklasson, & Taherzadeh, 2005; F. Talebnia & Taherzadeh, 2006; J. O. Westman et al., 2014). Upon encapsulation and upon entry into stationary phase, yeast ceases to divide, which is accompanied by thickening of their cell wall and accumulation of reserve carbohydrates, both of which help to protect cells from stress (Werner-Washburne, Braun, Johnston, & Singer, 1993). Encapsulated cells are demonstrably heat-shock tolerant (Figure 24) (Nagarajan et al., 2014; Westman, Taherzadeh, & Franzén, 2012); others have shown that as much as 25% of this phenotype can be attributed to protection by the matrix itself (Nagarajan et al., 2014). However, we now know that it is physiological change brought on by encapsulation that provides much of the stress tolerance exhibited by such cells (Ylitervo et al., 2011). This physiological change is evident in the yeast transcriptome, where stress-related genes such as YAP1, ATR1 and FLR1 are induced soon after encapsulation (Westman, Manikondu, Franzen, & Taherzadeh, 2012).

4.3.8 Encapsulation matrices vary in cost

Potential advantages to using encapsulated cells in biorefineries include higher service life and superior yields (Behera et al., 2011; S. Norton, Watson, & D'Amore, 1995; Verrills, 2006). Cost of matrix components would contribute to the selection of one matrix over

others for commercial applications. Matrices that do not contain chitosan are more economical than those that do. Currently, chitosan costs 83.6 cents per gram, and an additional estimated 0.22 cents per bead (with beads formed according to *Preparation of encapsulation matrices and cell encapsulation*), which translates to an additional $3.85 for the 250 mL volume used here (pricing from VWR; Item# 9012-76-4; 250 g quantity). Among alginates, sodium alginate currently costs 25.4 cents per gram (pricing from Sigma Aldrich, Product #180947, 500 g quantity). Protanal is no longer available, but a comparable product also derived from *Laminaria hyperborea* costs 36.8 cents/gram (pricing from Sigma Aldrich; Product #A1112; 500 g quantity), 45% more than sodium alginate. Purchases at larger scales would significantly reduce the cost per gram of both the alginates and chitosan, but are unlikely to reduce the cost of Pr below that of NaAlg.

Chitosan is a costly addition, and while it improved Young's modulus and viscosity for 7 days (Figure 17A-D), chitosan was also associated with increased bead swelling (Figure 17C-F), and decreased cell number (Figure 22) and viability (**Error! Reference s ource not found.**), which may have negatively impacted ethanol yields (Figure 21). Therefore, our data do not support addition of chitosan to matrices for bioethanol production under repeated fed-batch conditions. Between Pr and NaAlg beads, Pr beads exhibited higher ethanol yields (Figure 21), possibly due to higher cell numbers therein (Figure 22) and lower percentages of cell escape (Figure 23). Critically, Pr beads demonstrated higher ethanol yields than NaAlg beads and planktonic cultures at days 42 and 49, indicating that they could be re-used for longer than NaAlg beads, and potentially for longer than 49 days. Cell viability and thermotolerance between the two alginate types was also comparable. Therefore, even though Pr beads are more costly, our finding that

they can be reliably used for at least 2 weeks longer than NaAlg beads recommends them as the best matrix for commercial applications calling for repeated, fed-batch culture.

4.4 Conclusions

Our findings demonstrate that in extended fed-batch culture, encapsulated yeast have higher thermotolerance and ethanol yield than planktonic yeast, exhibit similar viability, and that they can be re-used for at least seven weeks. PrCh beads were lightest and smallest throughout our experiment, making them suitable for situations where small bead size is desirable. NaAlgCh beads demonstrated the highest Young's modulus and viscosity early on, but also the poorest product yield of any bead type; experiments that are short in duration but require a highly durable bead should utilize this matrix. NaAlg beads were the most economical to produce, and displayed average performance for many of the metrics examined here; they should be used for extremely price-sensitive applications. For the purposes of ethanol production from encapsulated cells, our data recommend Pr beads, which consistently demonstrate highest ethanol yields over repeated fed-batch culture.

CHAPTER 5. ENCAPSULATION INCREASES GENOME STABILITY OF YEAST DIKARYONS PRODUCED VIA PROTOPLAST FUSION

A major barrier to cost-effective biofuel production from cellulosic hydrolysates is the need to ferment both 5-carbon and 6-carbon sugars. One possible strategy for overcoming this barrier is the creation of protoplast fusants (dikaryons) from fungal species that have complementary metabolic capabilities. To date, however, this strategy has proved impractical as dikaryons quickly revert to their parental genotypes by segregational loss of one or the other nucleus during cell division. Here, we tested cell encapsulation in Ca^{2+}-alginate as a means to restrict cell division and thereby preserve the dikaryon genome with its expanded metabolic capability. We monitored glucose and xylose consumption and ethanol production of both Ca^{2+}-alginate encapsulated and planktonic protoplast fusants of *Saccharomyces cerevisiae* (which can ferment 6-carbon sugars) and *Pichia stipitis* (which can ferment 5- and 6-carbon sugars) in fed-batch culture over 19 days. We further compared their fermentative kinetics to both encapsulated and planktonic mixed non-fusant cultures, as well as to encapsulated and planktonic pure cultures of only *S. cerevisiae* or *P. stipitis*. Though we did not observe simultaneous co-fermentation of 5- and 6-carbon sugars, we do show for the first time that encapsulated cultures retain significantly more fusants than planktonic cultures, reducing the instability associated with segregation. Relative to planktonic cultures encapsulated cultures also retained antifungal-resistance plasmids, and maintain a fixed ratio of *S. cerevisiae* to *P. stipitis* cells.

5.1 Introduction

Fossil fuels' negative environmental impacts have created a demand for alternative sources of fuel in the transportation industry (Meng et al., 2019). One widely used renewable biofuel is ethanol, which can be produced from a variety of source materials (Gerbrandt et al., 2016). In the United States, conventional ethanol production relies almost exclusively on corn kernels, whereas cellulosic ethanol production uses inedible biomass like corn stover, tree branches, and *Miscanthus* grass (S. T. Lee et al., 2009; W. C. Lee & Kuan, 2015; Qureshi, Zhang, & Bao, 2015). Since cellulosic ethanol uses biomass that may otherwise have been discarded, it reduces greenhouse gas (GHG) emissions by 57-156% as compared to gasoline production, depending on the source material used and production facility (Dwivedi et al., 2015). Conventional ethanol, though chemically indistinguishable from cellulosic ethanol, only reduces GHG emissions by 21-46% as compared to gasoline, also depending on the source material and production facility (Chavez-Rodriguez & Nebra, 2010). Further, since cellulosic ethanol is derived from waste biomass, it does not compete with food production like conventional ethanol, which is derived primarily from corn kernels (Goettemoeller & Goettemoeller, 2007; Lee R. Lynd et al., 2017; Mohd Azhar et al., 2017). Despite the environmental advantages of cellulosic ethanol, only 10 million gallons of cellulosic ethanol were made in the United States in 2017 (Erickson, 2018), as compared to 15.9 billion gallons of conventional ethanol produced during the same time period (Association, 2019).

One reason for this discrepancy is the higher production cost of cellulosic ethanol. Not only are cellulosic feedstocks more difficult to degrade than conventional feedstocks (requiring more expensive enzymes), but cellulosic feedstocks contain significant (20-60%) percentages of pentose, or 5-carbon, sugars (Kuhad, Gupta, Khasa, Singh, & Zhang,

2011). In contrast, corn kernels consist almost entirely of 6-carbon sugars that can be readily converted to ethanol by naturally-existing yeast like *Saccharomyces* spp. (Favaro, Jansen, & van Zyl, 2019). No naturally-occurring organisms can co-ferment 5- and 6-carbon sugars although some, like *P. stipitis*, will first ferment 6-carbon sugars and then 5-carbon sugars. To reduce production costs of cellulosic ethanol, many have attempted to address the 5C/6C co-fermentation difficulty using genetically modified bacteria (Dien et al., 2000; C. G. Liu et al., 2019; Mohagheghi, Evans, Chou, & Zhang, 2002; Ohta, Beall, Mejia, Shanmugam, & Ingram, 1991; Yomano, York, & Ingram, 1998) or yeast (Fujita et al., 2002; Lawford & Rousseau, 2003; E. Liu & Hu, 2010; Sreenath & Jeffries, 2000; Tantirungkij, Izuishi, Seki, & Yoshida, 1994), co-culture of two organisms that respectively digest 5- and 6-carbon sugars (I. De Bari et al., 2013; Fang, 2010; Zhu et al., 2016), or protoplast fusion of the same (Heluane, Spencer, Spencer, De Figueroa, & Callieri, 1993; Cheng-Chang Lin, Hsieh, Mau, & Teng, 2005). Combinations of these methods including the co-culture of immobilized cells (Isabella de Bari, Cuna, Nanna, & Braccio, 2004; N. Fu, Peiris, Markham, & Bavor, 2009; Grootjen, Meijlink, van der Lans, & Luyben, 1990; Lebeau, Jouenne, & Junter, 2007), immobilization of recombinants (Zhao & Xia, 2010), fusion of recombinants (Pasha, Kuhad, & Rao, 2007), and co-culture of recombinants (Chen et al., 2018; C. R. Lee et al., 2017; F. Liu et al., 2017; Y. Zhang et al., 2017) have also been investigated.

Here, we examined glucose and xylose consumption in relation to ethanol production by four different treatments: 1) hygromycin-resistant *Saccharomyces cerevisiae*, 2) geneticin (G418)-resistant *Pichia stipitis*, 3) a 1:1 mixed culture of *hyg*^{r} *S. cerevisiae* and *G418*^{r} *P. stipitis*, and 4) protoplast fusants of *hyg*^{r} *S. cerevisiae* and *G418*^{r} *P. stipitis*. Each

was cultured in triplicate for 19 days under two different culture conditions, planktonic and encapsulated in a Ca^{2+}-alginate matrix (Figure 25). Under each condition, cultures were provided with fresh YPDX (2% dextrose, 2% xylose, 2% peptone, 1% yeast extract) medium every five days. Initial seed populations were grown under antifungal drug selection for 24 h. Drugs were omitted thereafter for the duration of each experiment, enabling us to compare, in encapsulated and in planktonic cultures, the relative stability of drug resistance plasmids (Treatments #1 and #2), the ratio of different species in mixed culture (Treatment #3), and the dikaryons formed by protoplast fusion (Treatment #4).

We did not observe simultaneous co-fermentation of glucose and xylose in any treatment containing both *P. stipitis* and *S. cerevisiae*, either as bona fide species or as dikaryons harboring both genomes. Instead, we observed preferential uptake of glucose followed by xylose fermentation. Fusant dikaryons and mixed cultures of *P. stipitis* and *S. cerevisiae* produced similar amounts of ethanol with encapsulated cultures producing much more ethanol on a per cell basis than their planktonic counterparts. In the absence of drug selection, encapsulation stabilized plasmids bearing antifungal drug resistance genes (Treatments #1 and #2), maintained a fixed ratio of the two species in mixed populations (Treatment #3) and stabilized dikaryons (Treatment #4). To our knowledge, we are the first to demonstrate the long-term (19 d) stability of dikaryons in an encapsulated system, potentially enabling their use in biomanufacturing.

5.2 Materials and Methods

5.2.1 Strains and culture conditions

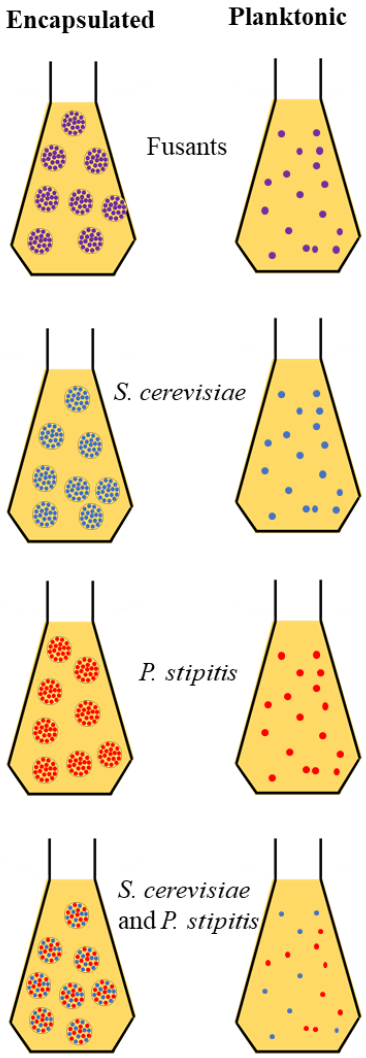

Figure 25. **Yeast species and growth methods assayed in this experiment. Fusants were created via protoplast fusion (Jassim Shalsh et al., 2016) of *S. cerevisiae* and *P. stipitis*, and were analyzed for parameters related to ethanol production and fusant stability for 20 days, with fresh medium provided every 5 days, in both encapsulated and planktonic cultures. Pure cultures of *S. cerevisiae* and *P. stipitis* were also monitored for ethanol production and antifungal plasmid stability, as both encapsulated and planktonic cells. Lastly, we examined a 1:1 mix of *S. cerevisiae* and *P. stipitis*, also as either encapsulated or planktonic cells.**

Experiments were conducted with *Saccharomyces cerevisiae* Ethanol Red, an ethanol-tolerant (up to 18% (Fermentations, 2019)) industrial strain obtained from Leaf Lessafre (Marcq-en-Barœul, France), and *Pichia stipitis* (strain unknown) obtained from Designer Energy (Rehovot, Israel). To confer resistance to the antifungal drug hygromycin, we

Table 12. Strains of yeast used in this chapter.

Strain	*Source*	*Abx Resistance*	*Genomic content*
Saccharomyces cerevisiae	Leaf Lesaffre	hygromycin	pCORE-hp53
Pichia stipitis	Designer Energy	geneticin	pCORE-kp53
S. cerevisiae/P. stipitis dikaryon	this manuscript	hygromycin and geneticin	pCORE-hp53 and pCORE-kp53

transformed *S. cerevisiae* with the 6,319 base pair plasmid p-CORE-Hp53, using the LiAc/ssDNA/PEG method of transformation (Gietz & Schiestl, 2007). To confer resistance to the antifungal drug geneticin, we transformed *P. stipitis* with the 6,073 base pair plasmid p-CORE-Kp53, also using the LiAc/ssDNA/PEG method of transformation (Table 12). Antifungal drug-resistant mutants were created in preparation for protoplast fusion, as a method for selecting fusants consisting of both yeast species.

We cultured yeast in 250 mL of YPDX medium (2% dextrose, 2% xylose, 2% peptone, 1% yeast extract) in 250 mL screw-cap Erlenmeyer flasks, at 30°C shaking on a gyro-rotary platform at 50 rpm. Many industrial-scale bioreactors are fed-batch, with new substrate supplied and product removed on 2- to 5-day cycles (Qazizada, 2016), each cycle being re-pitched with fresh yeast. Since encapsulated yeast is inherently more expensive to produce than unencapsulated yeast, for the former to be commercially viable they would need to be re-used for multiple cycles. To mimic conditions cells would encounter through multiple cycles of re-use, all cultures were provided fresh medium every five days, 24 hours after xylose exhaustion, with spent medium discarded and fresh YPDX medium added. Briefly, in both planktonic and encapsulated cell fermentations, the same cells were retained throughout the experiment. Spent medium was removed from encapsulated

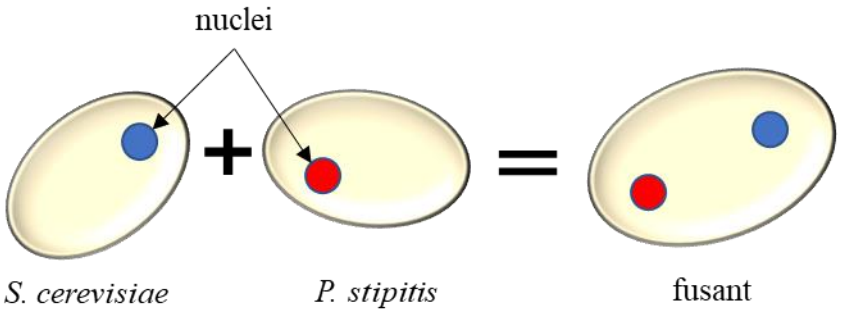

Figure 26. A schematic of protoplast fusion. Fusants were created via protoplast fusion (Jassim Shalsh, Ibrahim, Mohammed, & Shobirin Meor Hussi, 2016) of hygromycin-resistant *S. cerevisiae* and geneticin-resistant *P. stipitis.* Fusants were selected for by plating upon double antifungal plates, and further confirmed with flow cytometry and DAPI staining.

cultures by sieving it through a sterile brass sieve of 3-inch diameter and mesh size 10 (2 mm, McMaster Carr, Elmhurst, IL, Catalog #34735K216). Fresh sterile YPDX medium (250 mL final volume) was then placed into the same flask, containing the same beads, without cleaning/sterilization of the flask or beads. Spent medium was removed from planktonic cultures by decanting the entire 250 mL culture volume into 50 mL Falcon tubes, centrifuging these at 2000 *x g* for 2-3 minutes, then discarding spent medium. Pelleted cells were resuspended in fresh YPDX medium to a final culture volume of 250 mL, also without any cleaning or sterilization of the flask.

5.2.2 Protoplast formation and fusion

Protoplasts were created by modifying the protocol described in (Shalsh, Ibrahim, Mohammed, & Meor Hussin, 2016) (Figure 26). Both hyg^r *S. cerevisiae* and $G418^r$ *P. stipitis* were grown to stationary phase in the presence of 200 µg/mL hygromycin and 200 µg/mL geneticin, respectively. Then, 5 mL of each culture was placed into 15 mL Falcon tubes and centrifuged at 4,000 *x* g for 2 minutes, after which the supernatant was removed

and 0.1 M phosphate buffer (pH 7.5) added. This step was repeated, after which cells were re-suspended in 10 mL protoplast solution (1.2 M sorbitol, 0.1 M Tris, 0.02 M ethylenediamine tetraacetic [EDTA] acid and pH 9.8) with 50 µL β-mercapto-ethanol (Sigma Aldrich; catalog #60-24-2), and allowed to incubate at RT for 15 minutes. Next, cells were washed with 1.2 M sorbitol, and then transferred to 1.2 M sorbitol amended with 0.075 mg/mL 20T zymolyase (VWR; catalog #IC320921), where they incubated at 30°C for 30 (*P. stipitis*) and 45 (*S. cerevisiae*) minutes.

To collect protoplasts, 15 mL Falcon tubes were centrifuged at 100 *x* g for 10 minutes, then cells were washed three times in 10 mL buffer solution (0.1 M phosphate buffer and 1.2 M sorbitol), using a centrifugation speed of 100 *x* g for 10 minutes each time and for all future centrifugations. After washing, the two strains of protoplasts in buffer solution were mixed at a 1:1 ratio, then re-suspended in fusion buffer solution (0.6 M sorbitol; 10 mM Tris-HCl, 35% PEG and 10 mM $CaCl_2$) and incubated at 30°C at 100 rpm for 30 minutes. Following this incubation, yeast was plated on YPD (2% dextrose, 2% peptone, 1% yeast extract) agar plates containing 200 µg/mL hygromycin, 200 µg/mL geneticin, and 0.2, 0.4, 0.6, 0.8, 1.0 or 1.2 M sorbitol. After 4 days of incubation at 30°C, resultant colonies from each sorbitol level were grown in liquid YPD with 200 µg/mL hygromycin and 200 µg/mL geneticin then stained with propidium iodide (PI) and 4,6-diamidino-2-phenylindole (DAPI) to assess via flow cytometry and via light microscopy, respectively, whether they were fusants harboring both parental nuclei.

5.2.3 Verification of dikaryons using PI staining

PI dye (ThermoScientific, Waltham, MA Catalog #P1304MP; stock 10 mg/mL) was used to verify fusants. 21 colonies were randomly chosen and fixed in stationary phase by re-suspending cells in 70% ethanol. Controls consisting of hyg^r *S. cerevisiae*, G418^r *P. stipitis*, haploid *S. cerevisiae* strain BY4741, a diploid *S. cerevisiae* YE658, and a tetraploid strain *S. cerevisiae* YE643 were also fixed. 300 µL of fixed cells were washed in 1 mL of 50 mM sodium citrate, and then the washed cells were re-suspended in 500 µL of 50 mM sodium citrate containing 0.1 mg/mL RNase A, and allowed to incubate at 37°C for 2 hours. Then, 500 µL of 50 mM sodium citrate with 8 µg/mL PI was added to the cells before analyzing the samples using a Sysmex CyFlow Space flow cytometer (Sysmex, Kobe, Japan, Catalog #1604063918). Controls containing diploid (2N) or tetraploid (4N) *S. cerevisiae* , or a mix of such cells were used to establish proper gating to discriminate ploidy. A typical range for 2N cells was 1.1 to 1.4 FL2(590-50), and a typical range for 4N cells was 1.5 to 10, in both cases at 488 nm with a log4 gain of 450.

5.2.4 Verification of dikaryons using DAPI staining

DAPI staining (Sigma Aldrich, Catalog # D9542) was performed as described in (Oberto et al., 2009). Briefly, exponential phase cells were fixed with 70% ethanol for 30 minutes, and then washed twice with PBS buffer. Then, DAPI was added to a final concentration of 1 mg/mL and cells were left in the dark for 5-10 minutes, before washing cells again with PBS buffer prior to imaging using a Zeiss Axioskop epifluorescence microscope using 100x magnification and a UV light filter.

5.2.5 Preparation of encapsulation matrices and cell encapsulation

Protanal LF 10/60 alginate (gift from FMC Biopolymer) was sterilized by combining 60 g of alginic acid sodium salt (sodium alginate; Sigma Aldrich Catalog #180947) with approximately 300 mL of 95% ethanol and left overnight. This approach was utilized as other sterilization methods can alter alginate viscosity (Leo et al., 1990). After the mixture sat overnight, ethanol was separated from the alginate using a 0.2-micron bottle top vacuum filter unit, and the alginate was allowed to dry overnight at room temperature on the top of the filter.

To avoid pseudo-replication, 24 separate batches of encapsulation matrix were made in two batches of 12 (Figure 25). 70 mL of sterile distilled water and 4.5 g of dry, sterile Protanal alginate were added to each of twelve sterile plastic 1 L beakers. Alginate was mixed into water using a Jiffy Mixing Blades Power Tool Attachment (purchased from Home Depot, Catalog #DC408) and a standard power drill. Next, 80 mL of stationary phase (24 h) yeast that had been grown to high density in YPDX medium amended with either 200 µg/mL geneticin ($G418^r$ *P. stipitis)* or 200 µg/mL hygromycin (hyg^r *S. cerevisiae*) or both antifungal drugs (fusants of $G418^r$ *P. stipitis* and hyg^r *S. cerevisiae*) were gently mixed into the alginate-water mixture, creating a 3% alginate-and-yeast suspension.

Twelve 60 mL plastic syringes were each filled with alginate and yeast solution. The syringes dripped into a 500 mL beaker containing 350 mL of the cross-linking solution 0.2 M $CaCl_2$. All equipment was sterilized before repeating this procedure for the creation of an additional twelve batches. The Protanal beads were hardened in the cross-linking solution overnight at 4°C before being transferred to 250 mL screw-cap Erlenmeyer flasks that contained 250 mL YPDX medium without any antifungals. This process produced approximately 1,750 beads per replicate, each of which initially contained approximately

3 x 10^6 cells. All 1,750 beads were placed in a 250 mL flask, resulting in approximately 5 x 10^9 total cells per flask at the start of the experiment.

Planktonic control cultures were treated similarly, with each replicate receiving 80 mL of stationary phase yeast (the same starting amount of yeast as encapsulated cultures) grown to high density in the presence of antifungals. So as to be comparable to encapsulated yeast, planktonic yeast suspensions also were also incubated overnight at 4°C before being placed in fresh YPDX medium without antifungal drugs in 250 mL screw-cap Erlenmeyer flasks.

5.2.6 Cell enumeration, viability, and population dynamics

To estimate cell number in encapsulated yeast, the alginate matrix was dissolved by placing 5 beads into 5 mL of 10% (w/v) sodium metaphosphate solution (Fisher Scientific, Hampton, NH, Catalog #10124-56-8), a calcium chelating agent. Beads were agitated for 2-3 h at room temperature in a tissue drum rotator (New Brunswick Scientific, Edison, NJ, Item #TC-6), after which any remaining bead particles were mechanically disrupted by manual pipetting. Following disruption, cells were diluted 1-50x in YPDX medium and enumerated using a modified Neubauer hemocytometer. Planktonic cultures were also diluted in YPDX medium and enumerated using a modified Neubauer hemocytometer (Sigma Aldrich, St. Louis, USA, Catalog#BR717810).

Cell viability was estimated by counting colony forming units (CFUs) as well as by PI staining. Using the cell counts obtained from the hemocytometer, cells were diluted in YPDX medium before scoring the number of colonies formed on YPDA (2% dextrose, 2% peptone, 1% yeast extract, 1.5% agar). Moreover, this same dilution was plated on an

additional plate type for each treatment. To assess the percentage of fusants remaining at various time-points, the fusants were also plated on YPDA containing both 200 µg/mL hygromycin and 200 µg/mL geneticin. It is expected that all colonies, even non-fusants, would grow on the YPD plates, but only fusants would be able to grow on plates with both antifungal drugs present. Though antifungal drugs were present in the seeded cell populations, they were not provided during the course of the experiment in order to determine whether encapsulation affected fusant stability. Similarly, to assess the percentage of cells with antifungal-resistance plasmids remaining, *S. cerevisiae* and *P. stipitis* pure cultures were also plated on both YPDA and YPDA containing either 200 µg/mL hygromycin or 200 µg/mL geneticin, respectively. Finally, to estimate the percentage of the mixed population that consisted of *P. stipitis*, mixed cultures were plated on both YPDA and YPXA (2% xylose, 2% peptone, 1.5% agar, 1% yeast extract) plates, with all cells expected to grow on the YPD plates, but only *P. stipitis* expected to grow on the xylose plates. All mixed cultures initially consisted of *P. stipitis* and *S. cerevisiae* at a 1:1 ratio.

Fusant stability was also assessed immediately after the addition of fresh medium using the PI staining protocol described above. Beginning on day 5, cell viability as also assessed using PI staining of live cells. Specifically, 2 mL of cell suspensions were diluted 1:200 in sterile water, then stained with 5 µg mL^{-1} PI (ThermoScientific, Waltham, MA Catalog #P1304MP; stock 10 mg/mL). At least 10,000 cells per sample were counted using a Sysmex CyFlow Space flow cytometer (Sysmex, Kobe, Japan, Catalog #1604063918). Controls containing heat-killed dead cells, live cells, and a mix of both were used to

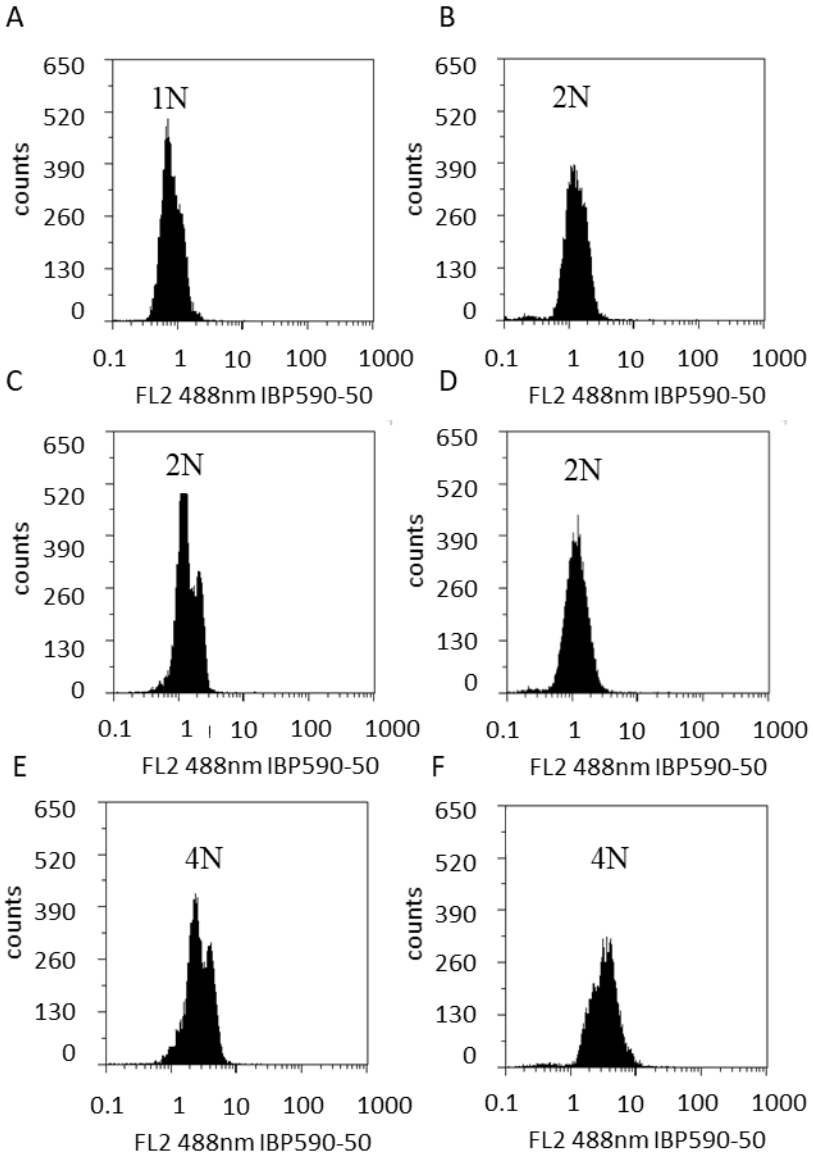

Figure 27. Verification of protoplast fusion via flow cytometry. The dye propidum iodide, which binds to DNA, was used to verify protoplast fusion. A haploid control (A) is left-shifted on a logarithmic axis as compared to diploid *S. cerevisiae* (B), a diploid control (C), and diploid *Pichia stipitis* (D). These diploids are in turn left-shifted with respect to both a tetraploid control (E) and the *S. cerevisiae P. stipitis* fusants (F).

establish proper gating between live and dead cells, with a typical range for live cells consisting of 0.1 to 1 FL2(590-50) at 488 nm with a log4 gain of 450.

5.2.7 Fermentation parameters

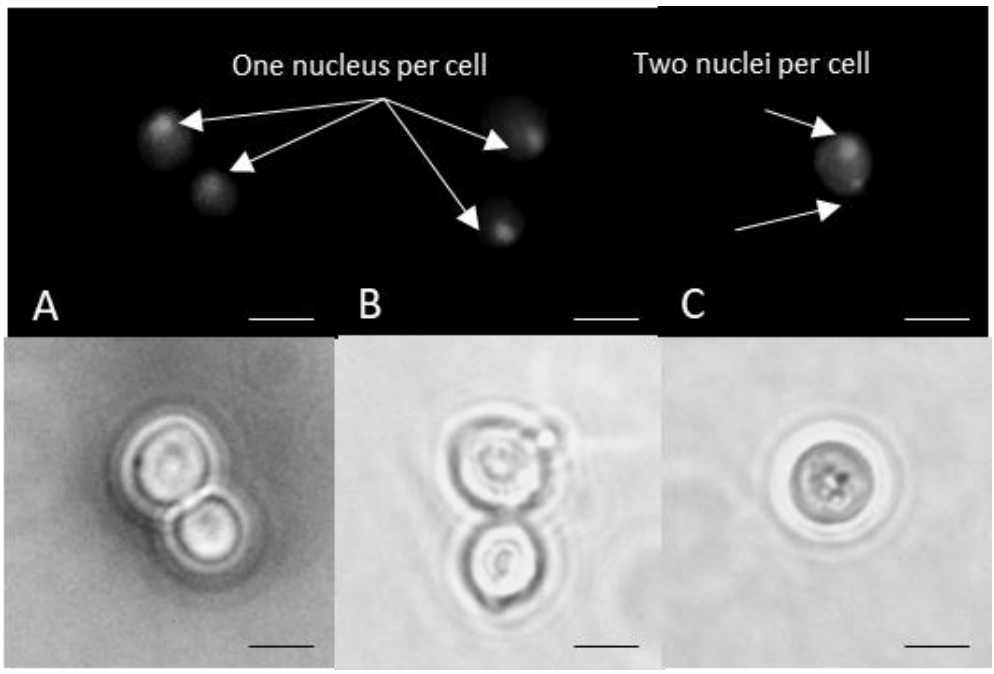

Figure 28. Verification of protoplast fusion via DAPI. The dye 4,6-diamidino2-phenylindole (DAPI) which binds to AT regions of dsDNA, was also used to verify protoplast fusion. Only one nucleus is detected in *S. cerevisiae* (A) and *P. stipitis* (B), whereas two nuclei are visible in fusants (C). Scale bar is 5 µm.

Glucose consumed, xylose consumed, and ethanol produced were assayed using the EnzyChrom™ Glucose Assay Kit (BioAssay Systems, Hayward, CA, Catalog #EBGL-100), the D-Xylose Assay Kit (Megazyme, Bray, Ireland), and the Ethanol Test Kit (Fisher Scientific, Waltham, MA, Catalog #NC9508587), in all cases using methods provided by the manufacturer.

5.2.8 Statistical analyses

Two-way ANOVA tests with Tukey's post-hoc were used to compare treatments, using time and treatment as main effects. An alpha value of 0.05 was used as a cut-off for significance in all cases.

5.3 Results and Discussion

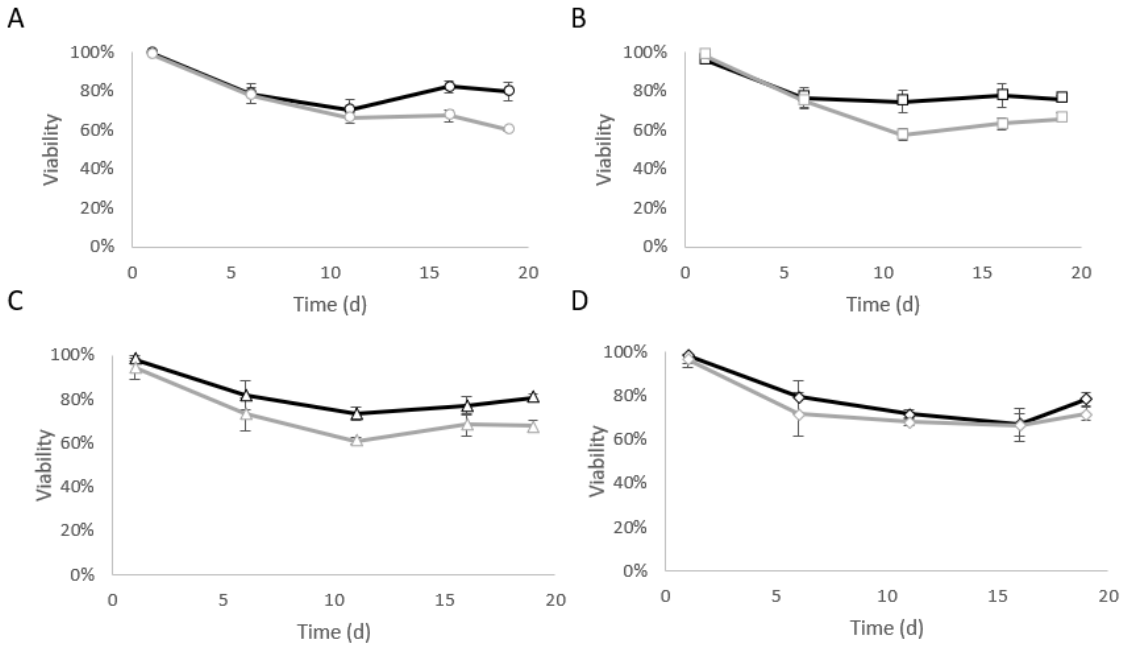

Figure 29. Viability was similar among all cultures over time. Viability was assessed by counting CFUs; cultures were supplied with fresh medium every five days. Black **lines indicate encapsulated cultures,** gray **lines indicate planktonic cultures. Circles represent fusants (A), squares represent *S. cerevisiae* (B), triangles represent *P. stipitis* (C), and diamonds represent mixed cultures of *S.cerevisiae* and *P. stipitis* (D). Error bars represent one standard deviation. No significant differences were found by a two-way ANOVA with Tukey's post-hoc ($F_{8,86}$= 0.68, p > 0.05).**

5.3.1 Verification of dikaryons

Dikaryons of G418^r *P. stipitis* and hyg^r *S. cerevisiae* were created as described in *Protoplast formation and fusion* (Figure 25). PI staining (Figure 27) verified dikaryon formation by showing more DNA in 4N than in 2N cultures. Dikaryon verification was further verified by DAPI staining, which revealed the presence of just one nuclei per cell in the parental strains (Figure 28A&B), but two nuclei per cell in dikaryons (Figure 28C).

5.3.2 Encapsulation impacts cell viability over repeated fed-batch culture

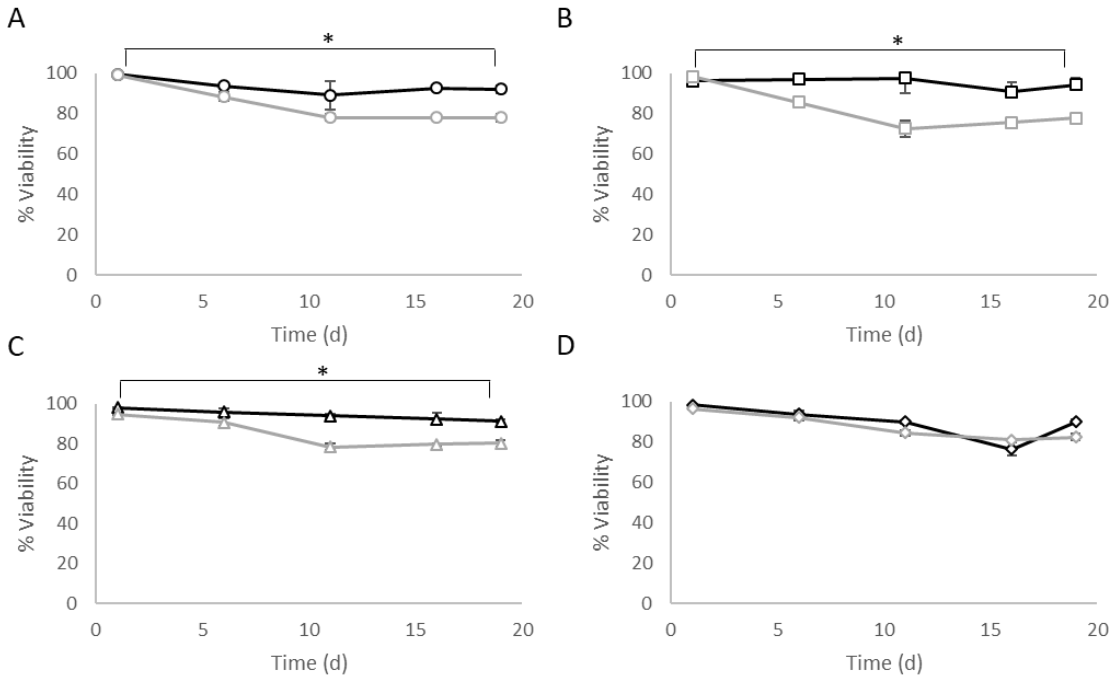

Figure 30. Viability by PI staining was higher in encapsulated cultures over time. Viability as assessed by PI staining; cultures were supplied with fresh medium every five days. Black **lines indicate encapsulated cultures,** gray **lines indicate planktonic cultures. Circles represent fusants (A), squares represent *S. cerevisiae* (B), triangles represent *P. stipitis* (C), and diamonds represent mixed cultures of *S.cerevisiae* and *P. stipitis* (D). Error bars represent one standard deviation. * indicates a significant difference as assessed by a two-way ANOVA with Tukey's post-hoc ($F_{8,86}$= 26.5, p < 0.0001).**

At the onset of our experiments viability, as assessed by CFUs, was >95% for all yeast strains (Figure 29), after which it declined steadily over the course of 19 days. When viability was assessed in terms of CFUs, encapsulated cells were still 75-80% viable after 19 days, compared to planktonic cells, which were 60-70% viable at that time-point. However, these differences were not statistically significant (p > 0.05). By contrast, when propidium iodide (PI) staining was to assess viability we found that encapsulated strains were 90-95% viable after 19 days as compared to planktonic cells, which were 77-83%. These differences were significant ($F_{8,86}$= 5.0, p < 0.001, two-way ANOVA with Tukey's

post-hoc; Figure 30). The discrepancy between viability estimates can be attributed to the different methodologies used to make those estimates: PI staining records cells that are alive, but not necessarily cultivable, whereas CFUs count cultivable cells only.

Encapsulation has been previously shown to confer tolerance to a variety of stressors including acids (Krisch & Szajani, 1997; Taipa et al., 1993), organic solvents (Desimone et al., 2003; Qun et al., 2002), ethanol (Zaldivar et al., 2001), and osmotic and thermal shock (Z.-J. Sun et al., 2007; Ylitervo et al., 2011). This increased tolerance relative to planktonic cells may result from altered cell wall and plasma membrane composition following encapsulation (Galazzo & Bailey, 1990), and possibly also protection from shear forces afforded by the encapsulating matrix (Amos Nussinovitch, 2010). Previously (Gulli, Yunker, & Rosenzweig, 2019), using PI staining we noted that encapsulated yeast grown in high-sugar (15% dextrose) medium sometimes exhibited lower viability than their planktonic counterparts, with both treatment groups being ~30-40% viable after 19 days. However, in the more moderate sugar levels used here (2% dextrose, 2% xylose), viability was high even after 19 days, an observation that we attribute to the small fluctuations in pH (~0.1) and acetate levels ($\leq$4 mM) during each feeding cycle.

5.3.3 Encapsulation reduces the accumulation of biomass

Cells were enumerated via an improved Neubauer hemocytometer. In all cases, encapsulated cultures accumulated significantly less biomass, measured as cell number and assessed via two-way ANOVA with Tukey's post-hoc ($F_{8,86}$= 28.9, $p < 0.001$) than did planktonic cultures. Specifically, although all treatments were initiated with approximately

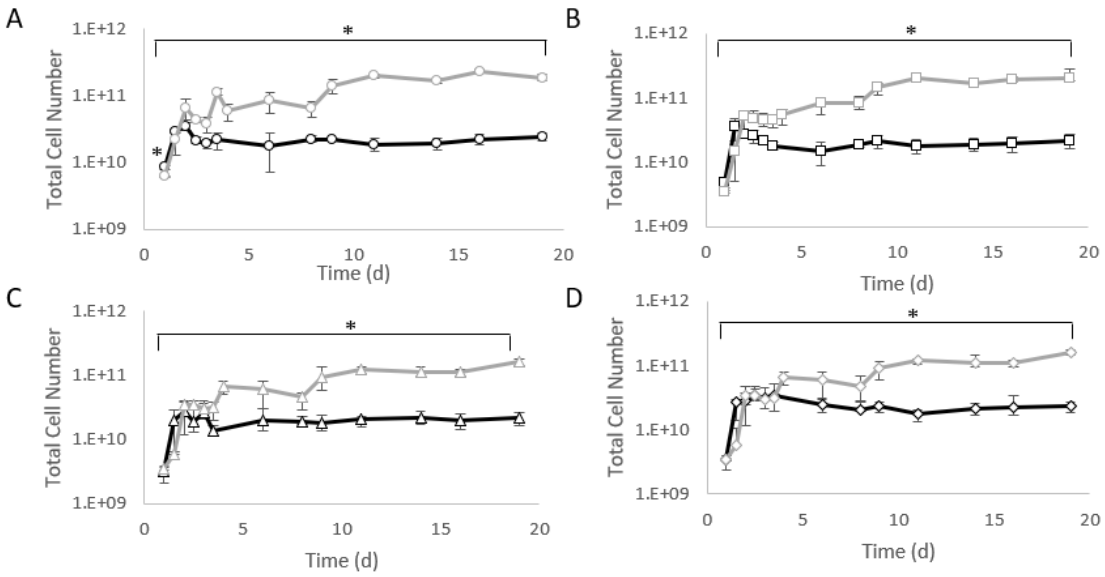

Figure 31. Encapsulation reduces biomass accumulation. Despite being seeded with equal cell numbers, planktonic cultures had more total cells (as assayed by a Neubauer hemocytometer) than encapsulated cultures at most points measured, increasing by roughly an order of magnitude more than encapsulated cells over 19 days. Black **lines indicate encapsulated cultures,** gray **lines indicate planktonic cultures. Circles represent fusants (A), squares represent *S. cerevisiae* (B), triangles represent *P. stipitis* (C), and diamonds represent mixed cultures of *S.cerevisiae* and *P. stipitis* (D). Error bars represent one standard deviation. * indicates a significant difference as assessed by a two-way ANOVA with Tukey's post-hoc ($F_{8,86}$= 64.7, $p < 0.0001$).**

5 x 10^9 cells in the entire culture volume, planktonic cultures had 1.6 to 2 x 10^{11} cells after 19 days, roughly five cell doublings. In contrast, encapsulated cultures had 2.2 to 2.4 x 10^{10} cells after 19 days, only two cell doublings; in both treatments most of the increase occurred during the first two days (Figure 31).

Encapsulation has previously been shown to impede cell division, even under conditions of nutrient excess (Nagarajan et al., 2014). Nagarajan *et. al* showed that after an initial outgrowth period lasting ~ 3 days, most cells in populations of immobilized *S. cerevisiae* were virgin daughters over the course of nearly 3 weeks. They further discovered that cell cycle arrest in encapsulated yeast was marked by a stable pattern of

gene expression that differed from starving or growing planktonic yeast, and that this state could be abolished by disruption of serine/threonine protein kinase, RIM15. The carrying capacity of encapsulated treatments observed here was comparable to that previously reported for fed-batch cultures *of S. cerevisiae* (Roukas, 1994).

5.3.4 Encapsulation enhances genetic stability

Fungal protoplast fusion is known to be unstable, with cell division frequently resulting in the segregation of a dikaryon's two nuclei (Gupthar, 1992; Yoon, Lee, Kim, Seo, & Ryu, 1996). Indeed, even though fusants of *S. cerevisiae* and *P. stipitis* can show superior xylose utilization (Yoon et al., 1996) relative to the parental species, their genomic instability led Jeffries and colleagues to conclude that fusants were unsuitable for industrial applications like cellulosic ethanol production (Jeffries & Jin, 2004). To test whether encapsulation could help overcome this problem protoplast fusants were first grown to high density under dual antifungal drug selection, which ensured that non-fusants would perish. Then, half of this culture was encapsulated, and the other half was allowed to remain planktonic; both treatments were provided with fresh YPDX medium every 5 days for 19 days. Immediately after the addition of fresh medium, the percentage of cells that remained fusants was measured both by plating on antifungal drug medium and by PI staining.

Our results clearly show that cell cycle arrest brought on by encapsulation (Figure 31) can be exploited to stabilize dikaryons created by protoplast fusion (Figure 32A). In the first 5 days of outgrowth in the absence of drug selection, the percentage of encapsulated fusants declined likely due to segregational loss during cell division. Thereafter, cell number remained remarkably constant, increasing only slightly between

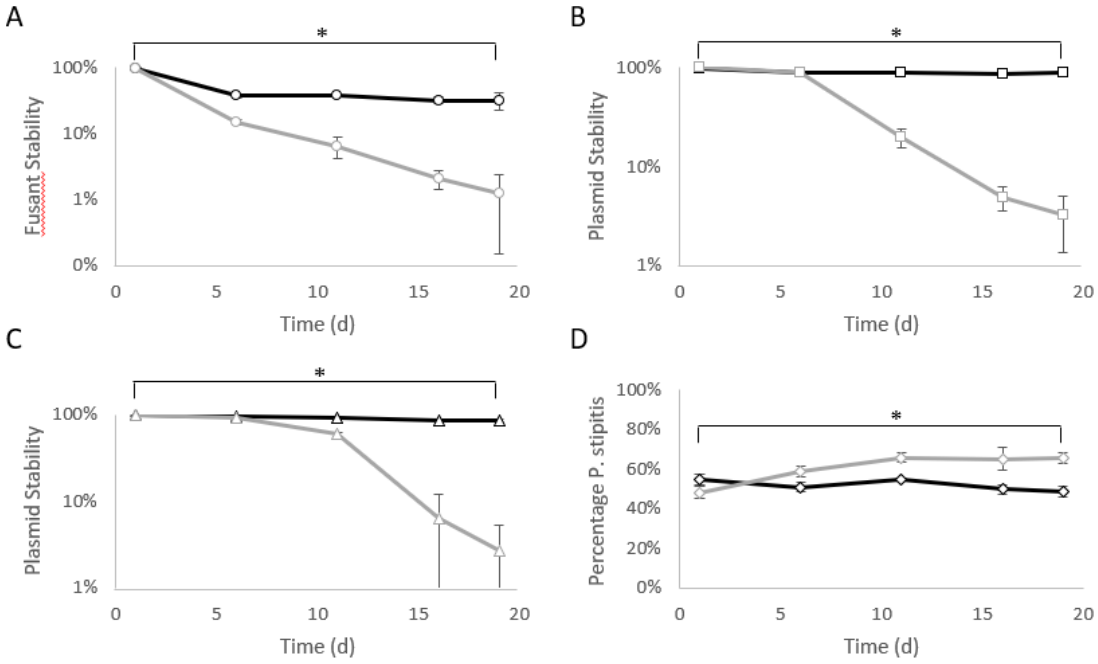

Figure 32. Encapsulation stabilizes fusants, plasmids, and strain ratio in mixed cultures. Over the course of 20 days in medium not containing antifungals, fusant stability (A) and antifungal plasmids' (p-CORE-Hp53, B; p-CORE-Kp53, C) stability were determined by comparing the number of colonies that could grow on YPD medium to the number of colonies that could grow on YPD medium plus antifungal(s). Antifungals were absent from the regular growth medium, causing both fusants and plasmids to decline more over time in planktonic than encapsulated cultures. Encapsulation also preserved a 1:1 mix of *S. cerevisiae* and *P. stipitis* (D), which drifted up to 65% *P. stipitis* in planktonic cultures. Black **lines indicate encapsulated cultures,** gray **lines indicate planktonic cultures. Circles represent fusants, squares represent *S. cerevisiae*, triangles represent *P. stipitis*, and diamonds represent mixed cultures of *S.cerevisiae* and *P. stipitis.* Error bars represent one standard deviation. * indicates a significant difference as assessed by a two-way ANOVA with Tukey's post-hoc ($F_{8,86}$= 26.6, p < 0.0001).**

days 5 and 19, during which time the proportion of fusants decreased only slightly. By contrast, cell number in the planktonic fusant treatment continued to increase throughout the experiment, resulting in just 1% of the population retaining resistance to both antifungal drugs by day 19. These results accord with fusant stability assessed by PI staining (Figure 33), which show after nineteen days, 32% of cells in encapsulated cultures were fusants

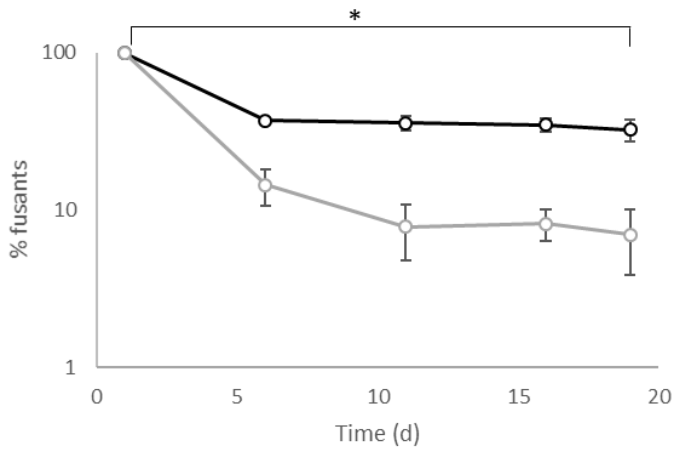

Figure 33. Fusant stability as determined by PI staining. The percent of the culture that remained a fusant was assessed by PI staining. Black **lines indicate encapsulated cultures,** gray **lines indicate planktonic cultures. Error bars represent one standard deviation. * indicates a significant difference as assessed by a two-way ANOVA with Tukey's post-hoc ($F_{2,27}$= 21.9, p < 0.0001).**

compared to 7% of cells in planktonic culture. Thus, whether assessed by plating or PI staining, encapsulation significantly ($F_{8,86}$= 124.8, p < 0.001, two-way ANOVA with Tukey's post-hoc) enhanced the stability of fusant genome content (Figure 7A&S2). We speculate that this difference would be further magnified by maintaining antifungal drug selection during the initial 5-day outgrowth period.

Although several others (HANSEN, RÖCKEN, & EMEIS, 1990; J. F. Spencer, Spencer, & Reynolds, 1988; Vidoli, Yamazaki, Nasim, & Veliky, 1982) have encapsulated fusants in alginate beads to assist in their recovery from protoplast fusion, we are the first, to the best of our knowledge, to investigate this system as a means of long-term stabilization for dikaryons created via protoplast fusion.

Encapsulation also significantly improved the stability of extranuclear genetic elements. 80-85% of encapsulated *S. cerevisiae* and *P. stipitis* transformants remained

plasmid-bearing after 19 days, as assessed by plating on YPDA and YPDA amended with 200 µg/mL of either hygromycin or geneticin. By comparison, planktonic transformant cultures were only 34-38% plasmid-bearing after the same period of time (Figure 32B&C). As with dikaryons, the most likely explanation for enhanced plasmid stability is less cell division – and reduced segregational loss – in encapsulated as compared to planktonic cells (Figure 31). Even though non-plasmid bearers would be expected to out-compete plasmid bearers in the absence of antifungal drug selection, the low incidence of replication in encapsulated cultures (Nagarajan et al., 2014) offsets this advantage.

The use of encapsulation to stabilize plasmids was already well-established by 1994 (BARBOTIN, 1994; Berry, Sayadi, Nasri, Barbotin, & Thomas, 1988; M. Nasri, Sayadi, Barbotin, Dhulster, & Thomas, 1987; Moncef Nasri, Sayadi, Barbotin, & Thomas, 1987), with Sayadi *et al.* demonstrating that 88% of cells retained plasmids after 120 generations in encapsulated cultures, whereas planktonic cultures only had ~40% of cells with retained plasmids (Sayadi, Nasri, Berry, Barbotin, & Thomas, 1987). Our data (Figure 32B&C) confirm these previous results, as well as newer findings (Lú Chau, Guillán, Roca, Núñez, & Lema, 2000; Park & Chang, 2000) demonstrating that encapsulation improves the stability of a wide variety of plasmids in both bacteria and yeast.

Our results further indicate that cell cycle arrest stemming from encapsulation can be used to maintain desired species ratios in mixed populations (Figure 32D). We seeded mixed cultures with *P. stipitis* and S. *cerevisiae* at a 1:1 ratio. Over the course of 19 days, encapsulated cultures remained ~50% *P. stipitis*, while planktonic cultures saw an increase of P. stipitis to ~65% (Figure 32D). Under certain conditions, a 1:1 ratio of these two species can be optimal for mixed sugar fermentation (Chen, 2011). Indeed, modeling

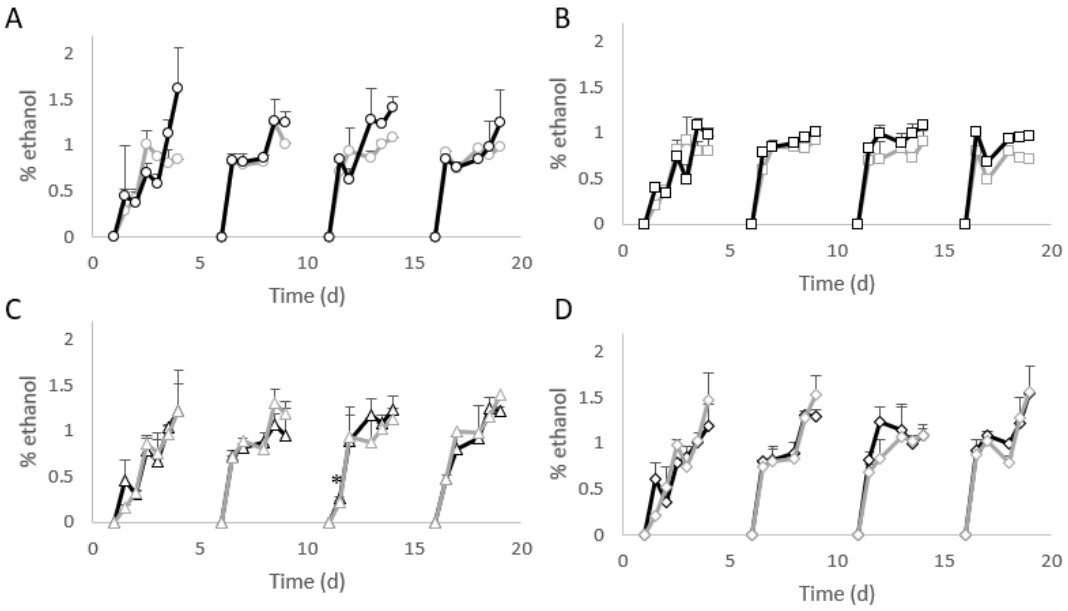

Figure 34. Encapsulation did not affect overall ethanol production. Encapsulated cultures produced significantly more ethanol than their planktonic counterparts on only a handful of time points. All cultures were provided with fresh medium every five days. Black **lines indicate encapsulated cultures,** gray **lines indicate planktonic cultures. Circles represent fusants (A), squares represent *S. cerevisiae* (B), triangles represent *P. stipitis* (C), and diamonds represent mixed cultures of *S.cerevisiae* and *P. stipitis* (D). Error bars represent one standard deviation. No significant differences were found by a two-way ANOVA ($F_{8,86}$= 0.19, p > 0.05).**

suggests that the ideal ratio of *S. cerevisiae: P. stipitis* is 1:1 when the glucose:xylose ratio is 3:1 (Unrean & Khajeeram, 2015). Since our glucose: xylose ratio was 1:1, a higher relative amount of *P. stipitis* could have allowed for more rapid conversion of xylose to ethanol.

5.3.5 Encapsulation increases ethanol production on a per-cell basis

Ethanol production was examined regularly after the addition of fresh YPDX medium, which was added every five days for 19 days. Encapsulation was expected to increase ethanol yield, since the lack of cell division leads to higher substrate conversion to ethanol

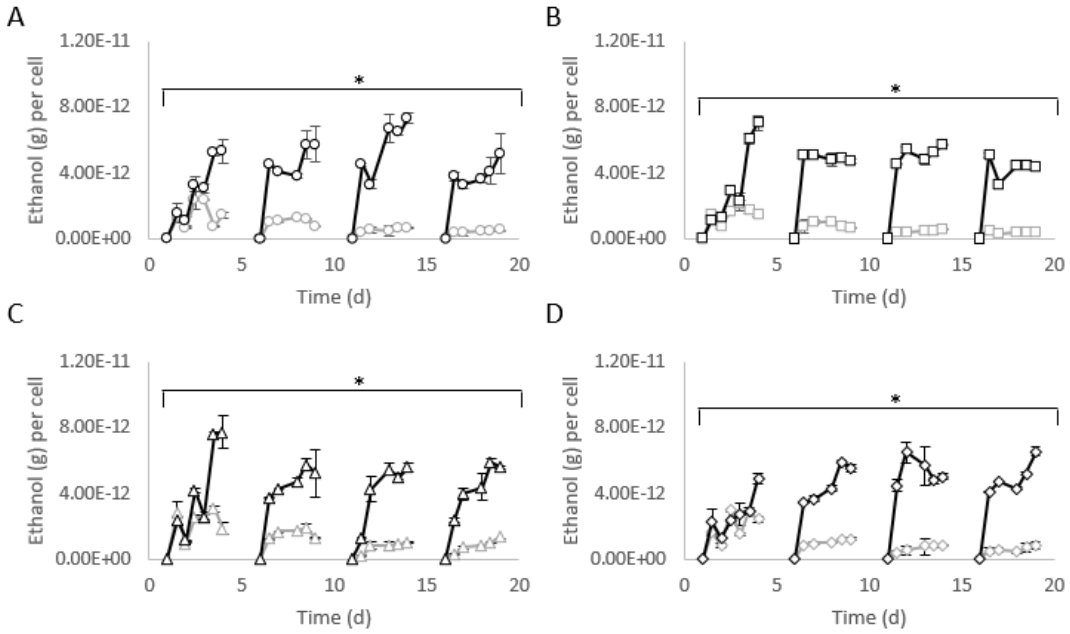

Figure 35. Encapsulation increases ethanol production on a per cell basis. Encapsulated cultures produced significantly more ethanol than their planktonic counterparts on a per-cell basis most of the time. All cultures were provided with fresh medium every five days. Black **lines indicate encapsulated cultures,** gray **lines indicate planktonic cultures. Circles represent dikaryons (A), squares represent *S. cerevisiae* (B), triangles represent *P. stipitis* (C), and diamonds represent mixed cultures of *S.cerevisiae* and *P. stipitis* (D). Error bars represent one standard deviation. * indicates a significant difference as assessed by a two-way ANOVA with Tukey's post-hoc ($F_{8,86}$= 5.3, p = 0.0065).**

– an observation experimentally confirmed by many (Chen et al., 2013; Jamai et al., 2007; Kondo et al., 2002; K. H. Lee et al., 2011; McGhee, Julian, et al., 1982a; Watanabe et al., 2012). When considering overall ethanol production (in contrast to per-cell production), we observe statistically significant differences between treatments only when comparing fusant, mixed, or pure *P. stipitis* to pure *S. cerevisiae*, which produced less ethanol than the other treatments since it cannot utilize xylose (Figure 34). We did not observe any difference in ethanol production based on encapsulation, potentially due to differences in cell number between the two treatments; that is, even if the planktonic cells are generally less efficient, their greater numbers might compensate for lower per capita conversion of

fermentable substrate to product. This is confirmed by analysis of ethanol production on a per-cell basis (Figure 35), which shows that encapsulated cells make significantly more ethanol than planktonic cells ($F_{8,86}$= 6.4, $p < 0.0001$, two-way ANOVA with Tukey's post-hoc).

An examination of fermentation kinetics between treatments revealed no major difference in glucose consumption between treatments ($F_{8,86}$= 0.11, $p > 0.05$, two-way ANOVA with Tukey's post-hoc); xylose consumption differed only between pure *S. cerevisiae*, which cannot utilize xylose, an d all other treatments ($F_{8,86}$= 15.3, $p < 0.0001$, two-way ANOVA with Tukey's post-hoc). Encapsulated cells, considered as an entire group, did not differ significantly in per-cell ethanol production, nor did planktonic cells if considered as a group; however, significant differences were observed when comparing per-cell ethanol production of encapsulated and planktonic cells ($F_{8,86}$= 6.4, $p < 0.0001$, two-way ANOVA with Tukey's post-hoc). Predictably, both planktonic and encapsulated *S. cerevisiae* produced less ethanol per cell than the other treatments (as well as less ethanol overall), since these pure cultures were incapable of utilizing xylose. However, the encapsulated treatment did convert glucose at near-theoretical levels to ethanol (**Error! R eference source not found.**C), similar to previous findings (Gulli et al., 2019).

Mixed populations, consisting of one microbial species capable of fermenting 5-carbon sugars and another capable of fermenting 6-carbon sugars, have been previously examined by many (Chen, 2011; Taniguchi, Tohma, Itaya, & Fujii, 1997). Indeed, though some have found deleterious effects from co-culture (Grootjen, Jansen, van der Lans, & Luyben, 1991), others have observed simultaneous co-fermentation of xylose and glucose (Gutiérrez-Rivera, Waliszewski-Kubiak, Carvajal-Zarrabal, & Aguilar-Uscanga, 2012;

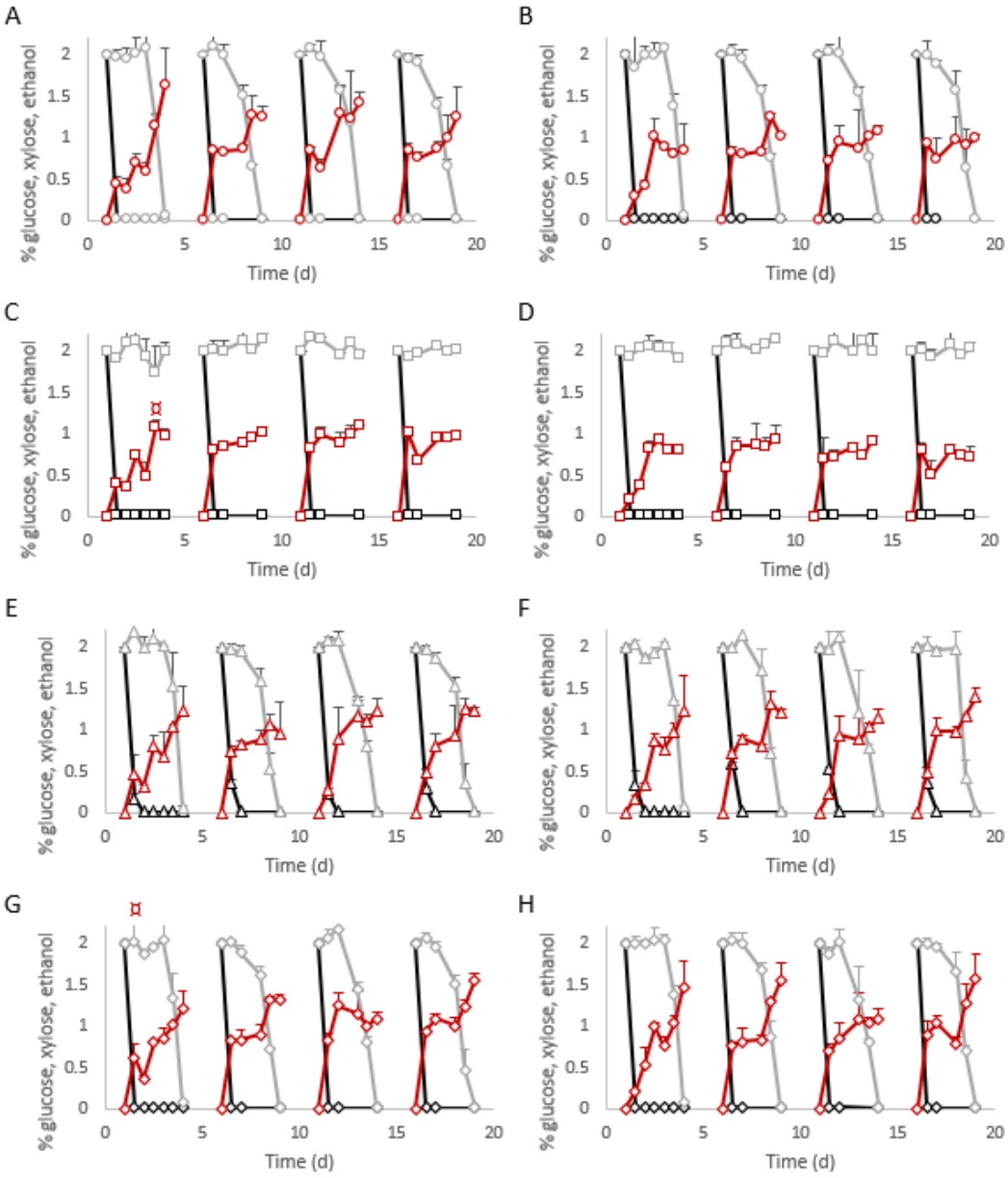

Figure 36. Fermentation kinetics. A comparison of glucose (black **lines) and xylose (**gray **lines) consumption and ethanol (**red **lines) production across all cultures revealed that encapsulated mixed cultures produced the most ethanol more frequently than any other cell and culture type. Circles represent encapsulated (A) and planktonic (B) fusants, squares represent encapsulated (C) and planktonic (D) *S. cerevisiae,* triangles represent encapsulated (E) and planktonic (F) *P. stipitis*, and diamonds represent mixed encapsulated (G) and planktonic (H) cultures of *S.cerevisiae* and *P. stipitis* (D). Error bars represent one standard deviation.**

Unrean & Khajeeram, 2015). We did not observe simultaneous co-fermentation from either

dikaryons or mixed cultures; instead we noted rather in all experiments a lag phase following glucose consumption before xylose began to be metabolized (**Error! Reference s ource not found.**). Previous work has shown (Slininger, Thompson, Weber, Liu, & Moon, 2011) that this lag phase varies according to the strain of *P. stipitis* employed, as well as the initial glucose concentration.

Xylose fermentation in *P. stipitis* is highly dependent on culture conditions, and is repressed or inefficient if ambient ethanol exceeds 3% (Frank K. Agbogbo & Guillermo Coward-Kelly, 2008; Chen, 2011), or if excessive oxygen (Delgenes et al., 1988; du Preez, van Driessel, & Prior, 1989; Klinner, Fluthgraf, Freese, & Passoth, 2005; Taniguchi et al., 1997), glucose (Grootjen et al., 1991; Panchal, Bast, Russell, & Stewart, 1988), or xylitol (Frank K. Agbogbo & Guillermo Coward-Kelly, 2008) is present. Since only moderate (2% glucose, 2% xylose) sugar concentrations were used here and cultures were regularly provided fresh medium, cells were not exposed to inhibitory levels of ethanol and acetate for prolonged periods, which is reflected in their high viability over 19 day culture (Figure 29). Oxygen levels were not measured, but were assumed to be low based on the minimal head space in the cultures (250 mL volume in a 250 mL flask), the screw-cap tops employed, and the slow rate of agitation (50 rpm); xylitol production is usually minimal under low oxygen conditions, as well (Frank K. Agbogbo & Guillermo Coward-Kelly, 2008). It is unlikely, then, that this long lag time between glucose and xylose fermentation is due to repressive culture conditions, and may instead be a feature of the strain of *P. stipitis* used.

5.4 Conclusions

Our results demonstrate that encapsulation can be used to stabilize *P. stipitis*-*S. cerevisiae* dikaryons created by protoplast fusion (Figure 7, S2). Dikaryons retained the metabolic capacity encoded by both parental genomes in extended glucose+xylose fed-batch cultures. We did not observe simultaneous co-fermentation of 5- and 6-carbon sugars. Instead, like immobilized mixed cultures of *P. stipitis* and *S. cerevisiae* as well as like planktonic mixed cultures of these same species, we observed ethanologenic fermentation of glucose succeeded by that of xylose, with no difference among treatments in the kinetics of substrate-to-product conversion.

Overall, our results recommend mixed cultures for use in larger-scale cellulosic ethanol production. Mixed cultures, either encapsulated or planktonic, produced similar amounts of ethanol to encapsulated and planktonic dikaryons, but do not require the costly and technically-demanding step of protoplast fusion.

Enhanced genomic stability in encapsulated relative to planktonic cultures was driven by limits on cell division. Fusants are currently used in an array of fields, such as the production of amylase enzymes (Pandey et al., 2000), oil recovery (S. Sun et al., 2013), and even microbial weed control (TeBeest, 2012). The ability to stabilize fusants over long periods of time could render these applications more economical. Encapsulated dikaryons and transformants, with their high viability, low biomass production and stable genomes may be better suited for high-value, small-batch production systems than for large-scale commercial cellulosic ethanol production.

CHAPTER 6. DISCUSSION

6.1 Overview

In general, this body of work shows that densely packed yeast behave differently than their unicellular or planktonic counterparts. We began in Chapter 2 by examining dense assemblages of snowflake yeast clusters that formed a new type of group, with a focus on looking at producers and non-producers of aggregate material. We demonstrated that even for a highly beneficial trait (aggregate formation) non-producers could cause phenotypic instability. In Chapter 4, we examined the niche of densely packed yeast specifically without the complications associated with aggregate formation by encapsulating cells within a calcium-alginate matrix. We demonstrated that encapsulated yeast produce more ethanol than their planktonic counterparts, and that these matrices age differently over time, affecting their potential for re-use in large ethanol plants. In Chapter 5, we further examined yeast at experimentally-imposed high densities to determine if encapsulation could benefit cellulosic ethanol production. We found that dikaryons, plasmids, and mixed populations could be stabilized via encapsulation, and that encapsulated cells made more ethanol on a per cell basis than planktonic cells.

In this chapter, we will first begin by further discussing aggregates. Specifically, we will note that aggregates inconsistent formation and lack of genetic relatedness make them unlikely to represent a new level of selection, and recommend that future work focus on both the mechanical and genetic basis of aggregate formation. Secondly, we will discuss the economic feasibility of applying encapsulated yeast to the current system of ethanol production, with a recommendation that future work address a variety of industry-specific

questions surrounding the scale-up of this technology. Lastly, we discuss the problem of genomic instability and how encapsulation could be applied to improve biomanufacturing. Though we do not recommend dikaryons for cellulosic ethanol production, we do suggest several experiments to verify their stability at higher levels and for even longer periods of time.

6.2 Aggregate formation is temporary

Curiously, despite their macroscopic size, aggregates were ephemeral, and could be observed to form, dissolve, and re-form within ~4 hours. This suggests a much more casual association than snowflake yeast clusters, which typically only increase in size when cells divide, and only decrease in size as propagules split off (William C. Ratcliff et al., 2013). At no point, however, does a snowflake yeast cluster revert to individual yeast cells; indeed, they are quite resistant to shear forces induced by vortexing. Aggregates, on the other hand, do dissolve and re-form. Their most likely mechanism of formation is adhesion based on sticky proteins holding clusters together. This hypothesis is based on evidence that proteinases, but not DNases, will dissolve an aggregate into individual clusters (Figure 8). Coupled with the observation that aggregates were never observed before 22 hours of growth, this suggests that older yeast clusters start undergoing higher levels of apoptosis around this time, leading to large quantities of cellular debris in the media. This cellular debris causes nearby clusters to stick together, thereby forming an aggregate.

This hypothesis of aggregate formation does not explain the dissolution and re-formation of aggregates. Culture conditions include continual shaking at 250 rpm, so this is unlikely to be a factor in filament dissolution. Higher levels of apoptosis are expected in

older cultures, so it also seems unlikely that there would be less cellular debris present at, for example, 24 hours after inoculation than there was at 22 hours after inoculation. Further, if adhesive proteins were solely responsible for aggregate formation, then we might expect to see multiple aggregates within a single tube, which was never observed. Although cell death certainly seems correlated with aggregate formation (Figure 10), a build-up of sticky proteins may not be the only factor causing aggregates to form. The presence of an additional substance, or some other mechanism of cluster group formation, therefore cannot be ruled out.

6.3 Aggregates are unlikely to represent a new level of selection

In Chapter 2, we established that group formation can readily evolve as a response to low individual survival. Previously, (Ratcliff et al., 2012) unicellular yeast developed a mutation in the *ACE2* region of the genome (Ratcliff, Fankhauser, et al., 2015), which controls mother-daughter cell separation. Cells with this mutation did not fully separate from their daughters, forming clonal clusters; this can be contrasted with groups of unrelated yeast that form due to flocculation (K. Goossens & Willaert, 2010). As a clonal cluster (barring any *de novo* mutations), the fitness of members is highly aligned, and therefore more likely to form a stable group (Krupp, 2016). Indeed, 'snowflake' yeast clusters meet the definition of a new level of selection. Though the exact definition of a new level of selection is not agreed upon by all (Istvan Jr, 2013), a unit of selection is generally accepted as a biological level of organization upon which natural selection acts (Hull, 2001; Okasha, 2006; Wade et al., 2010). Snowflake yeast clusters meet this definition, since the entire cluster either settles to the bottom of the tube quickly enough to survive, or fails to do so and perishes.

It is less clear if yeast aggregates meet the definition of a new level of selection. The benefits of inclusion in an aggregate are clear: clusters in an aggregate are nearly 80% more likely to settle rapidly enough to survive to the next day's selection than lone clusters. However, this type of group formation, like eusociality or adhesion (as discussed in the Introduction), requires a high cost. We did not observe aggregate formation in any strains that had less than 2% apoptosis, and the strains that formed large aggregates regularly had 7-15% apoptosis. When physically handled (usually with pipette tips), most aggregates were quite sturdy and even somewhat elastic.

During selection, cultures are routinely vortexed to homogenize them before settling selection commences. Aggregates, which float to the top of the tube (Figure 5), typically break apart into smaller fragments upon vortexing. However, this break-up is not consistent. Some aggregates remain whole upon vortexing, and continue to float near the top of the tube rather than turn into 3-4 fast-settling aggregate particles; others break up too much upon vortexing, becoming scarcely larger than individual clusters. This leads to a wide variability in aggregate settling rates (Figure 11), and suggests that the most successful aggregates are the ones with a narrow range of resistance to vortexing.

The break-up of aggregates upon vortexing means that the aggregate as an entire unit is not a consistent level of selection. If the entire aggregate fails to break apart upon vortexing and continues to float, then the aggregate has been selected upon as a unit and perishes as a unit. If, however, the aggregate does break apart upon vortexing and settle rapidly, then those individual aggregate particles become the level of selection, since they will survive or perish as a group. On the other hand, if the aggregate breaks apart too

thoroughly due to vortexing, the level of selection is reduced back to that of the individual cluster. An aggregate, then, does not meet the definition of a new level of selection.

6.4 Aggregates lack a mechanism of fitness alignment

Snowflake yeast clusters are composed of clonal (barring *de novo* mutation) cells, and are thus strongly aligned in terms of fitness (Kinnersley et al., 2014). This strong alignment helped clusters to evolve new responses to an environment that required continually faster settling through liquid media, including larger cell size, more cells per cluster, a higher rate of apoptosis, and a rounder profile (William C. Ratcliff et al., 2013). Aggregates, however, are composed of potentially unrelated clusters, and thus lack a similar mechanism of fitness alignment. This lack of relatedness among aggregates, coupled with the high cost of their formation, almost certainly contributed to their evolutionary instability (Figure 11F) over longer periods of time.

Since aggregates often form in strains with 7% apoptosis or higher, they are vulnerable to 'cheaters,' which may not have high enough levels of apoptosis to make an aggregate themselves, but benefit from aggregate inclusion equally to a 'producer,' which did have a high enough apoptosis level to form an aggregate. These cheaters eventually rose to a high enough frequency in the population (Figure 11F) so as to preclude aggregate formation altogether. Our results demonstrated that aggregates would incorporate non-producers at a rate roughly equal to their representation in the overall population (Figure 11), and thus had no mechanism of kin selection. Kin selection, however, does exist in other organisms (Gadagkar, 2016; J. E. Strassmann, Gilbert, & Queller, 2011; Wade et al., 2010), and has been shown to reduce the effects of cheating (Queller, Ponte, Bozzaro, &

Strassmann, 2003; Travisano & Velicer, 2004). If aggregates did have some mechanism of preferentially including other producers, they may have been able to persist over evolutionary lengths of time, and indeed to evolve as a unit of selection (or potentially aggregate particles). Our results, then, demonstrate the importance of some mechanism aligning the fitness of group members for long-term, stable group formation.

6.5 Suggestions for future work with aggregates

Identifying more precisely the mechanism of aggregate formation would shed more light on their mysterious dissolution and re-formation, and might also provide insight as to why some aggregates break apart so differently upon vortexing. We have evidence that proteins play a strong structural role in the aggregate (Figure 8), but we do not know what proteins. Use of an SDS-PAGE gel could help us to determine which proteins are present and their relative abundances, which could provide more information on aggregate formation. If, for example, the proteins found in the aggregate material are similar to those found in the proteome at large, then that provides evidence for the hypothesis that aggregates form as the result of large quantities of lysed cell debris adhering nearby clusters. If, on the other hand, the proteins found in the aggregate material are disproportionate to their representation in the proteome at large, this may provide evidence that aggregate-forming strains are secreting a special sticky protein to aid in aggregate formation.

Our work in Chapter 2 demonstrated the importance of a mechanism aligning in-group fitness to long-term group stability. An interesting follow-up experiment to test this theory would be to attempt to study the stability of aggregate formation in a divergent selection experiment. Previously, aggregates were evolved from both a unicellular ancestor

and a small, genetically homogenous snowflake yeast. It took 105 days, or ~500 generations, before aggregate formation evolved in this population, presumably generating considerable genetic diversity during this time. If, instead, an experiment was conducted starting with a clonal aggregate former, it would allow us to further investigate the role of cheaters in the long-term stability (or lack thereof) of aggregate formation.

Specifically, a single colony that forms aggregates could be used to inoculate several replicates of a starting population. This population could be selected upon for rapid settling each day to maintain pressure for aggregate formation, and the number of aggregates formed each day could be scored, as could other features of interest, for example apoptosis rate. Simultaneously, a diverse population of aggregate formers could be created via sexual reproduction and selected upon similarly. If the diverse population loses aggregate formation as a trait more rapidly than the homogenous population, then this would provide further evidence that cheaters within the population were the main cause of aggregate instability. If, however, the diverse and homogenous populations stop forming aggregates around a similar time, then that may suggest that the presence of cheaters was not the most important factor in the instability of aggregate formation, but that aggregate formation was perhaps inherently unstable for some other reason.

Lastly, the genetic basis of aggregate formation, if known, might permit the genetic manipulation of existing strains to ask additional questions about aggregates. The genetic cause of aggregate formation could be determined fairly easily since aggregate formation has already been evolved in a homogenous background. One way to determine the genetic basis of this trait would be to conduct a bulked segregant analysis. Specifically, we could start by pooling the appropriate strains into two groups- those that form filaments and those

that do not- and extracting DNA from each for sequencing. Plotting the differences between the two pools as the proportional difference in genetic composition at each locus for each chromosome would indicate regions statistically associated with filamentation, which could then be ranked based on the location of these mutations to generate candidate genes. These candidate genes could be validated by both removing the candidate gene(s) from an aggregate former to ensure that it has lost this phenotype, and adding the candidate gene(s) to a strain incapable of aggregate formation to see if the phenotype is gained.

6.6 Feasibility of using encapsulated yeast at industry scales

We demonstrated in Chapter 4 that encapsulation can be used to improve ethanol yields (g/g) from dextrose. However, the feasibility of this method at larger scales remains to be determined. Our results demonstrated that Protanal beads were the most suitable candidates for scale up. Even though they declined considerably in viscoelasticity over 49 days, they had the lowest rates of cell escape of any bead type, and had higher yields of ethanol as compared to planktonic cells even at day 49.

The longevity of alginate beads is critical to their potential implementation. Currently, yeast is one of the cheapest components of ethanol production, generally around 0.5 cents per gallon of tank volume (Jacques, 2003); substrate acquisition is typically the largest cost (Technology, 2011). Indeed, an average-size plant with four 250,000 gallon fermenters (total volume 1 million gallons) would only need to pay $260,000 a year for yeast, assuming the tanks are re-filled each week (Qazizada, 2016). This hypothetical plant could expect to produce roughly 11.6 million gallons of 99.5% pure ethanol from these

tanks, which would translate to $16.5 million in revenue assuming with the current rack price of ethanol at $1.44 per gallon as of July 2019.

Encapsulated yeast would cost significantly more than 0.5 cents per gallon of fermenter volume. Based on the currently utilized ratio of beads to flask volume (around 26,000 per gallon), encapsulated yeasts would cost an additional 28 cents per gallon of fermenter volume, or 56 times more than current yeast costs. These cost increases can be somewhat alleviated by the higher ethanol yields demonstrated by encapsulated cultures. Our results (Figure 21) indicate that ethanol yields are consistently 35% higher for encapsulated cultures, allowing the same hypothetical plant to now make ~15.6 million gallons of ethanol per year from the same amount of substrate. If the yeast were re-pitched weekly, this would still result in an unreasonable expenditure of $14.8 million/year spent on yeast alone. Therefore, even though the yields associated with encapsulated yeast are higher than those for planktonic yeast, encapsulated yeast are not economically feasible unless they can be re-pitched for multiple fermentations.

Currently, yeast are not re-pitched for multiple cycles due to the risk of contamination. Industrial yeast fermentation tanks are much larger than benchtop flasks, and consequently more difficult to keep sterile as well. Encapsulated yeast, which are cultured at high densities in the population and shielded by the encapsulation matrix, may be less susceptible to contamination, but this has not yet been studied (see discussion in section 6.6). Potential contamination in encapsulated cultures could therefore represent a major barrier to the re-use of encapsulated cultures for longer periods of time.

If this barrier can be overcome, we demonstrated that encapsulated yeast can be re-used for at least 49 days (Figure 21). Assuming that this could not be extended further, this would result in fresh yeast being pitched approximately 7.5 times per year, instead of 52 times per year as with planktonic yeast. For the hypothetical plant with a 1 million gallon tank capacity, this means that instead of making 11.6 million gallons of ethanol with a $260,000 yearly yeast expenditure, they could now make 15.6 million gallons of ethanol with a ~$2.1 million dollar yearly yeast expenditure, with the same substrate costs. The additional 4.5 million gallons of ethanol produced by the encapsulated yeast would earn an additional $6.48 million in revenue, or an extra ~$4.4 million in potential annual profit (once the cost of the encapsulated yeast is subtracted) as compared to the planktonic yeast system. Re-using encapsulated yeast for long periods of time, then, is critical to their economic potential.

Encapsulated yeast could affect other costs associated with ethanol production, as well. As a product, encapsulated yeast would not require any equipment modifications beyond a metal filter over the outflow pipe, to keep the beads from escaping along with the ethanol; the cost of this would likely be negligible. Changes to labor costs as a result of adopting this product would likely also be negligible. Encapsulation could potentially alter the typical temperature of the fermentation reaction. We (Figure 24) and others (Nagarajan et al., 2014; Johan O. Westman et al., 2012) have demonstrated that encapsulated yeast are significantly more thermotolerant than planktonic yeast. This could potentially allow fermenters to run at higher temperatures, (Terán Hilares et al., 2017; Won et al., 2012) which would allow for more optimal enzyme performance (S. Y. Huang & Chen, 1988; Mutturi & Lidén, 2013). Further, a higher continual temperature could reduce cooling

costs, which are especially significant in warmer regions (McAloon et al., 2000). A recent analyses suggested that for every 5°C increase in the fermentation temperature, $30,000 per year could be saved for a 30,000 kL scale ethanol plant, not including reductions in initial investment costs (Abdel-Banat et al., 2010). While the thermotolerance conferred by encapsulation would have to be confirmed over longer experiments, it seems likely that encapsulation could generate cost savings by permitting a higher temperature reaction.

Encapsulation may, however, be much costlier than planktonic yeast in another area of production. DDGs are a type of animal feed produced at ethanol plants in roughly equal quantities as the ethanol itself, and they are largely dependent on the protein content of the post-fermentation material (Jacques, 2003). If encapsulation were to reduce the protein content of the post-fermentation material, this could result in substantial alterations to the composition of the DDGs, potentially jeopardizing its use as animal feed.

The adoption of encapsulated yeast, then, is hindered by a lack of research. Four important questions must be answered before encapsulated yeast could be adopted by the ethanol industry: 1) Will encapsulated yeast retain the same performance advantages at large scales as they did at benchtop scales? 2) Does encapsulation reduce the risk of 'fouling' due to contamination?, 3) What is the highest temperature that encapsulated yeast can be exposed to for long periods of time without reducing ethanol yields?, and 4) Does encapsulation affect the protein content of post-fermentation waste? These will be discussed further in section 6.6.

6.7 Suggestions for future experiments on the use of encapsulated yeast for conventional ethanol production

Scale up of new technologies can be costly, difficult, and unpredictable (Pate, Klise, & Wu, 2011). Therefore, this process is typically done gradually, over the course of several years. Our experiments used a 250 mL volume; moving next into a 5-10 L volume would be appropriate, before then transitioning into a ~30 L reactor, then ~100 L, followed by pilot and commercial scale experiments. At each size increase, glucose consumption and ethanol production must be monitored to ensure that similar or higher yield increases are observed. If they are not, a wide variety of further experiments must be conducted to determine if the yield can be raised; for example, more vigorous stirring, a different bead to tank volume ratio, and the presence of additional micro-nutrients in the media might all be expected to change ethanol yields. Methods for matrix production, currently performed mostly by hand, would also have to be significantly scaled up, and would likely require the purchase and/or design of highly specialized equipment. Further, several long-term experiments may need to be conducted at each scale to test the maximum thermotolerance of encapsulated yeast, since this could be influenced by tank volume (Tang et al., 2010). The post-fermentation waste material should also be analyzed for protein content and composition at each of these scales, to determine if and how it differs from the post-fermentation waste of planktonic yeast.

A preliminary experiment could be to determine if encapsulation is more resistant to tank fouling (contamination by undesired species) than planktonic yeast. Both planktonic and encapsulated yeast could be seeded with low numbers of bacteria, and the number of bacteria in the populations could be measured over long periods of time, alongside ethanol yields, which would be compared to the yields of populations not seeded with bacteria. This critical experiment could help determine the feasibility of using encapsulated yeast at

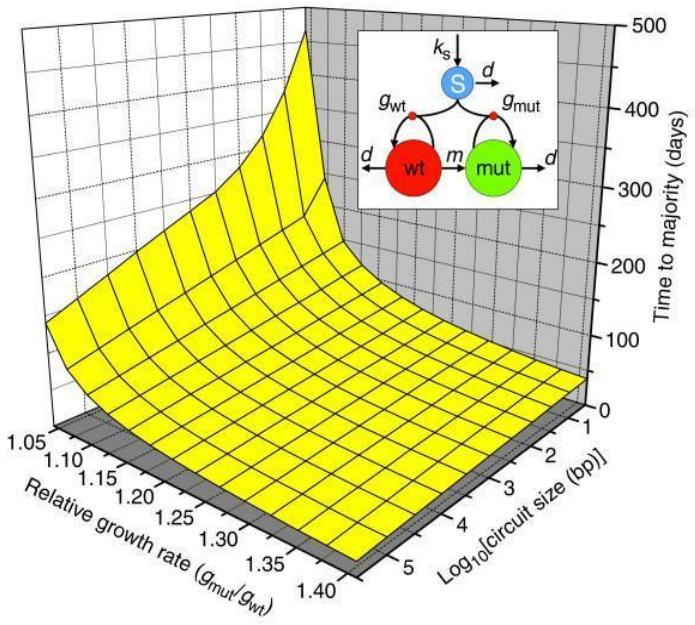

Figure 37. Factors influencing function loss in synthetic circuits. As the relative growth rate of the mutant to the wild-type increases, and circuit size increases, the time to loss of function decreases. Adapted from Arkin and Fletcher 2006.

larger scales. Unless they are highly resistant to tank fouling, they cannot be re-used for extended periods of time, and if they cannot be re-used for extended periods of time, then they are no longer cost-effective.

6.8 Genome instability: the problem

In Chapter 5 we demonstrated that encapsulation could be utilized to stabilize dikaryons. Genome stability is a significant obstacle to a wide variety of applications, both industrial and academic. For thousands of years, humans have utilized selective breeding to enhance everything from our foods to our pets (Marsden et al., 2016; Muller et al., 2016). The relatively new field of synthetic biology utilizes recombinant DNA research to create novel useful behaviors much more rapidly than could be achieved using selective breeding (Arkin & Fletcher, 2006; Capell & Christou, 2004; Vaughn S. Cooper & Lenski, 2000; Itakura et

al., 1977). This field has enormous untapped potential- since the first functional synthetic protein was expressed in *Escherichia coli* in 1977 (Itakura et al., 1977), synthetic biology has been used to produce antimalarial drugs (Tsuruta et al., 2009) biofuels (Bayer et al., 2009; Steen et al., 2010) treatment for bladder cancer (Kassouf & Kamat, 2004), and to improve crops (Amin et al., 2016) among many other applications. The ability to cheaply create large quantities of useful substances has attracted much interest in recent years. Yet the field of synthetic biology remains limited in its scope due to the difficulties involved in both creating the circuit (often plasmid addition to *E. coli*) and sustainably producing metabolites of interest (Arkin & Fletcher, 2006; Endy, 2005; Sprinzak & Elowitz, 2005).

Sleight *et al.* 2010 comments that "general design principles are needed for engineering evolutionary robust circuits that permit the long-term study or applied use of synthetic circuits". Yet evolutionary stability in synthetic circuits is notoriously difficult to achieve (Arkin & Fletcher, 2006; You, Cox, Weiss, & Arnold, 2004; Zarrinpar, Park, & Lim, 2003). To create synthetic constructs, or circuits, extra DNA is added to a wild-type cell, often in the form of a plasmid, in order to induce expression of the compound of interest, such as a biofuel. The burden of this extra plasmid is two-fold: energy must be spent producing the biofuel, and it takes longer to replicate the additional DNA.

The design of the circuit, its size, copy number, and metabolic state all affect how large of a burden the extra plasmid adds. To encourage maximum production, synthetic constructs are typically grown in bioreactors that continually provide optimal nutrients while siphoning off waste products. In this environment, cells are dividing and growing very rapidly. Any mutation they acquire that allows them to grow more quickly will be heavily favored, and rapidly sweep to fixation within the population. Synthetic circuits are

unstable, then, because they put a burden on cell growth in conditions where rapid growth is favored. A cell that does not produce the biofuel will grow more quickly than a cell that does. Even though the population begins with entirely biofuel-producing cells, mutation ensures that non-producers will eventually arise; once they exist, these non-producers grow more quickly than producers, and rapidly out-reproduce them until no producers remain (Sleight, Bartley, Lieviant, & Sauro, 2010). This instability is only magnified for dikaryons. With two nuclei in a single cell, they have a strong tendency to segregate to their original parental genotypes unless strong selection is maintained (Gupthar, 1992).

The difficulties associated with genome stability are well illustrated by the experiments carried out by You *et al.* 2004, whose 4,000 base pair (bp) insertion into *E. coli* was destabilized within 3-6 days. Sleight *et al*. 2010 looked into this problem further with the aim of determining principles for better circuit design. They created two independent circuits, both in *E. coli*. The first lost function in less than 20 generations (~1 day) due to a deletion event that occurred between homologous transcriptional terminators, and the second circuit lost function in less than 50 generations (~ 2 days) due to a deletion between repeated operator sequences in the promoter. Through altering circuit design, they were able to improve this 2- and 17-fold, respectively (Sleight et al., 2010).

The lack of circuit stability has been predicted via modelling by Arkin and Fletcher 2006, who found that even with small circuits that result in relatively minor growth differences, function loss still occurs within a matter of days (Figure 37. Factors influencing function loss in synthetic circuits. As the relative growth rate of the mutant to the wild-type increases, and circuit size increases, the time to loss of function decreases. Adapted from Arkin and Fletcher 2006). The use of antibiotic markers, a traditional method

for retaining plasmids, was found to be ineffective by both Arkin and Fletcher 2006 and Sleight *et al.* 2010. This circuit stability problem can be ameliorated, in part, by better circuit design. Indeed, this has been the focus of several studies who advocate low circuit expression, avoiding repeated sequences, the use of inducible promoters, and moving circuits into the chromosome as methods to delay function loss (Vaughn S. Cooper & Lenski, 2000; V. S. Cooper, Schneider, Blot, & Lenski, 2001; Sleight et al., 2010).

6.9 **Encapsulation as a means of improving genome stability**

We demonstrated that through the reasonably cheap and easy (when compared to circuit design) process of encapsulation, two antibiotic resistance plasmids (pCORE-hp53 and pCORE-kp53) could be maintained at high proportion for at least 19 days in the absence of selection (**Error! Reference source not found.**). Encapsulation is preferable for most a pplications to achieving plasmid stability through antibiotic selection. Not only are antibiotics expensive, but their over-usage hastens the development of antibiotic resistance, a global health threat, and much-discussed topic (Ventola, 2015). However, encapsulation may not be a suitable method for stabilizing some plasmids. For large molecules excreted from the cell, the matrix itself could possibly prevent, for example, the proper folding of large, complex proteins, or even prevent a large molecule from exiting the matrix altogether; the likelihood of this depends on the molecule, but large proteins like insulin have been successfully produced from encapsulated cells (N. Wang, Adams, Buttery, Falcone, & Stolnik, 2009).

6.10 Encapsulated dikaryons for cellulosic ethanol production

Dikaryons are seldom grown on large, commercial scales like plasmid-bearing microbes are, due in part to their greater instability (Gupthar, 1992). Dikaryons have, however, attracted quite a lot of interest for their potential usage in the production of cellulosic ethanol (Erickson, 2018; Hahn-Hägerdal, Karhumaa, Fonseca, Spencer-Martins, & Gorwa-Grauslund, 2007). The dikaryons we examined in Chapter 5 were unlikely candidates for usage in large-scale cellulosic ethanol production. Protoplast fusion, the process used to create dikaryon, is time-consuming, difficult to scale-up, and expensive (Jassim Shalsh et al., 2016). Ethanol, as a commodity product, needs to be produced cheaply and in large quantities. Even if the cost of producing encapsulated dikaryons could be reduced enough so as to make their production economical, perhaps by using cheaper substitute reagents or re-using for periods of 6 months or more, scale-up of protoplast fusion would remain a large technical hurdle.

Though the dikaryons used here did not produce more ethanol than the mixed populations (making them further unlikely candidates for scale-up), others have found higher ethanol yields from dikaryons than their parental strains (Ge, Zhao, Zhang, Zhang, & Ping, 2014; M. Zhang, Xiao, Zhu, Zhang, & Wang, 2012). While encapsulated dikaryons need to overcome challenges related to cost and scale-up for ethanol production, these findings indicate that protoplast fusion can sometimes produce dikaryons with superior yields or tolerance than their parental strains. Encapsulated dikaryons, then, could be better suited for high-cost, small-batch products, such as specialty whiskey.

6.11 Suggestions for future experiments utilizing encapsulated dikaryons

Though our work demonstrated that dikaryons could be stably maintained for at least 19 days, initial cell outgrowth during the first 2-3 days (**Error! Reference source not found.**) c aused the percentage of dikaryons in the overall population to drop down to approximately 36% (**Error! Reference source not found.)**. For industrial production, this would cause a n unacceptably low drop in product formation, if not outright product fouling. To verify that encapsulation can maintain dikaryons at high numbers (rather than just at 1/3 of the population), an experiment should be conducted that either 1) maintains antibiotic selection for the first two days, until cell number stabilizes, or 2) seeds more starting cells in the initial population. Of these choices, the first is preferable, since the variables associated with cell density are numerous, and additional division after inoculation may still occur, even if a higher starting number of cells is used (Fleet, 1990).

Secondly, determining how long dikaryons can be reasonably stabilized in encapsulation could be investigated. Our studies using encapsulated dikaryons lasted 19 days, but previous studies using encapsulated Ethanol Red yeast (Chapter 4) extended for 49 days, and demonstrated that around 30 days cell escape begins to result (Figure 23) from a weakened bead (Figure 17). Though Pr beads, also used to encapsulate dikaryons, still had low (>15%) rates of cell escape through day 49, even these rates of cell escape could still be too high for some applications. In our experiments looking at ethanol production, cell escape merely led to slightly lower ethanol yields, but if encapsulated dikaryons were to be used for a small-batch process like specialty whiskey, then escaped cells would likely segregate rapidly and could produce unwanted flavors or other byproducts that negatively affect the final product.

6.12 General Conclusions

In this body of work, we investigated yeast grown in high densities. In Chapter 2, yeast was locked into high densities due to failed mother-daughter cell separation that formed snowflake yeast clusters encompassing hundreds of cells. In response to selection for rapid settling through liquid media, these clusters evolved high levels of apoptosis that allowed them to form even larger (macroscopic), denser aggregates consisting of hundreds of clusters. Though these aggregates had high much higher rates of survival (80% vs. 1%) than lone clusters, they were ultimately evolutionarily unstable, likely due to the presence of cheaters (Figure 11).

In Chapter 4, unicellular yeast were encapsulated in a Ca^{2+}-alginate matrix and forced to remain at high density. Encapsulated yeast made significantly more ethanol from the same amount of substrate than their planktonic counterparts, in some cases for at least 49 days. Though a number of questions remain about the suitability of encapsulated yeast for industrial use (see section 6.7), our work demonstrates the promise of this method for large-scale ethanol production. In Chapter 5, we demonstrated for the first time that encapsulation could also be used to stabilize dikaryons, for at least 19 days. The dikaryons remained at much higher (32% vs. 1%) percentages in encapsulated cultures than planktonic cultures, two antibiotic resistance plasmids were also stabilized by encapsulation. Though encapsulated dikaryons are not likely candidates for improving cellulosic ethanol production, the ability to stabilize dikaryons using encapsulations has further implications for such diverse fields as enzyme production and oil recovery.

Taken together, these results demonstrate the tremendous utility and research potential of *S. cerevisiae*, an organism that has been used for thousands of years to brew

beer and bake bread, and can now be used to study topics like the stability of group formation and the improvement of biofuel production.

REFERENCES

Abdel-Banat, B. M. A., Hoshida, H., Ano, A., Nonklang, S., & Akada, R. (2010). High-temperature fermentation: how can processes for ethanol production at high temperatures become superior to the traditional process using mesophilic yeast? *Applied Microbiology and Biotechnology, 85*(4), 861-867. doi:10.1007/s00253-009-2248-5

Abelyan, V. A., & Abelyan, L. A. (1996). *Production of lactic acid by immobilized cells in stirred reactors* (Vol. 32).

Administration, U. E. I. (2017).

Agbogbo, F. K., & Coward-Kelly, G. (2008). Cellulosic ethanol production using the naturally occurring xylose-fermenting yeast, Pichia stipitis. *Biotechnol Lett, 30*(9), 1515-1524. doi:10.1007/s10529-008-9728-z

Agbogbo, F. K., & Coward-Kelly, G. (2008). Cellulosic ethanol production using the naturally occurring xylose-fermenting yeast, Pichia stipitis. *Biotechnol Lett, 30*(9), 1515-1524. doi:10.1007/s10529-008-9728-z

Agency, E. P. (2017). Greenhouse Gas Emissions. Retrieved from https://www.epa.gov/ghgemissions/sources-greenhouse-gas-emissions

Albers, E., Larsson, C., Andlid, T., Walsh, M. C., & Gustafsson, L. (2007). Effect of Nutrient Starvation on the Cellular Composition and Metabolic Capacity of Saccharomyces cerevisiae. *Appl Environ Microbiol, 73*(15), 4839-4848. doi:10.1128/aem.00425-07

Alberts B, J. A., Lewis J, et al. (2002). *Molecular Biology of the Cell.* (Vol. 4th edition). New York: Garland Sciences.

Alberts, J. R. (1978). Huddling by rat pups: Group behavioral mechanisms of temperature regulation and energy conservation. *Journal of Comparative and Physiological Psychology, 92*(2), 231-245. doi:10.1037/h0077459

Albuquerque, P., & Casadevall, A. (2012). Quorum sensing in fungi--a review. *Med Mycol, 50*(4), 337-345. doi:10.3109/13693786.2011.652201

Alexandre, H. (2013). Flor yeasts of Saccharomyces cerevisiae--their ecology, genetics and metabolism. *Int J Food Microbiol, 167*(2), 269-275. doi:10.1016/j.ijfoodmicro.2013.08.021

Allen, C., Büttner, S., Aragon, A. D., Thomas, J. A., Meirelles, O., Jaetao, J. E., . . . Werner-Washburne, M. (2006). Isolation of quiescent and nonquiescent cells from yeast stationary-phase cultures. *J Cell Biol, 174*(1), 89-100. doi:10.1083/jcb.200604072

Amemiya, T., Obase, K., Hiramatsu, N., Itoh, K., Shibata, K., Takinoue, M., . . . Yamaguchi, T. (2015). Collective and individual glycolytic oscillations in yeast cells encapsulated in alginate microparticles. *Chaos, 25*(6), 064606. doi:10.1063/1.4921692

Amin, U. S., Biswas, S., Elias, S. M., Razzaque, S., Haque, T., Malo, R., & Seraj, Z. I. (2016). Enhanced Salt Tolerance Conferred by the Complete 2.3 kb cDNA of the Rice Vacuolar Na(+)/H(+) Antiporter Gene Compared to 1.9 kb Coding Region with 5' UTR in Transgenic Lines of Rice. *Front Plant Sci, 7*, 14. doi:10.3389/fpls.2016.00014

Arismendi-Morillo, G. J., & Castellano-Ramirez, A. V. (2008). Ultrastructural mitochondrial pathology in human astrocytic tumors: potentials implications pro-therapeutics strategies. *J Electron Microsc (Tokyo), 57*(1), 33-39. doi:10.1093/jmicro/dfm038

Ariyanti, D., & Hadiyanto, H. (2013). Ethanol production from whey by kluyveromyces marxianus in batch fermentation system: Kinetics parameters estimation. *Bulletin of Chemical Reaction Engineering and Catalysis, 7*(3), 179-184. doi:10.9767/bcrec.7.3.4044.179-184

Arkin, A. P., & Fletcher, D. A. (2006). Fast, cheap and somewhat in control. *Genome Biology, 7*(8), 1-6. doi:10.1186/gb-2006-7-8-114

Arlia-Ciommo, A., Piano, A., Leonov, A., Svistkova, V., & Titorenko, V. I. (2014). Quasi-programmed aging of budding yeast: a trade-off between programmed processes of cell proliferation, differentiation, stress response, survival and death defines yeast lifespan. *Cell Cycle, 13*(21), 3336-3349. doi:10.4161/15384101.2014.965063

Association, R. F. (2019). *Ethanol Industry Outlook*. Retrieved from https://ethanolrfa.org/wp-content/uploads/2019/02/RFA2019Outlook.pdf

Avbelj, M., Zupan, J., & Raspor, P. (2016). Quorum-sensing in yeast and its potential in wine making. *Appl Microbiol Biotechnol, 100*(18), 7841-7852. doi:10.1007/s00253-016-7758-3

Bajpai, S., & Sharma, S. (2004). Investigation of swelling/degradation behaviour of alginate beads crosslinked with Ca2+ and Ba2+ ions. *Reactive and Functional Polymers, 59*(2), 129-140.

Bajpai, S. K., & Sharma, S. (2004). Investigation of swelling/degradation behaviour of alginate beads crosslinked with Ca2+ and Ba2+ ions. *Reactive and Functional Polymers, 59*(2), 129-140. doi:https://doi.org/10.1016/j.reactfunctpolym.2004.01.002

Bao, S., Chang, M.-S., Auclair, D., Sun, Y., Wang, Y., Wong, W.-K., . . . Chen, L. (1999). HRad17, a Human Homologue of the Schizosaccharomyces

pombe Checkpoint Gene rad17, Is Overexpressed in Colon Carcinoma. *Cancer Research, 59*(9), 2023-2028.

BARBOTIN, J.-N. (1994). Immobilization of Recombinant Bacteria: A Strategy to Improve Plasmid Stability. *Annals of the New York Academy of Sciences, 721*(1), 303-309. doi:10.1111/j.1749-6632.1994.tb47403.x

Baruch, L., & Machluf, M. (2006). Alginate–chitosan complex coacervation for cell encapsulation: Effect on mechanical properties and on long-term viability. *Biopolymers, 82*(6), 570-579. doi:10.1002/bip.20509

Bayer, T. S., Widmaier, D. M., Temme, K., Mirsky, E. A., Santi, D. V., & Voigt, C. A. (2009). Synthesis of Methyl Halides from Biomass Using Engineered Microbes. *Journal of the American Chemical Society, 131*(18), 6508-6515. doi:10.1021/ja809461u

Bechara, R., Gomez, A., Saint-Antonin, V., Schweitzer, J. M., & Marechal, F. (2016). Methodology for the optimal design of an integrated first and second generation ethanol production plant combined with power cogeneration. *Bioresour Technol, 214*, 441-449. doi:10.1016/j.biortech.2016.04.130

Beck, T., Schmidt, A., & Hall, M. N. (1999). Starvation Induces Vacuolar Targeting and Degradation of the Tryptophan Permease in Yeast. *J Cell Biol, 146*(6), 1227-1238. doi:10.1083/jcb.146.6.1227

Becks, L., Ellner, S. P., Jones, L. E., & Hairston, N. G., Jr. (2012). The functional genomics of an eco-evolutionary feedback loop: Linking gene expression, trait evolution, and community dynamics. *Ecol Lett, 15*(5), 492-501. doi:10.1111/j.1461-0248.2012.01763.x

Behera, S., Mohanty, R. C., & Ray, R. C. (2011). Ethanol production from mahula (Madhuca latifolia L.) flowers with immobilized cells of Saccharomyces cerevisiae in Luffa cylindrica L. sponge discs. *Applied Energy, 88*(1), 212-215. doi:https://doi.org/10.1016/j.apenergy.2010.07.035

Bellizzi, D., Rose, G., Cavalcante, P., Covello, G., Dato, S., De Rango, F., . . . De Benedictis, G. (2005). A novel VNTR enhancer within the SIRT3 gene, a human homologue of SIR2, is associated with survival at oldest ages. *Genomics, 85*(2), 258-263. doi:https://doi.org/10.1016/j.ygeno.2004.11.003

Berger, J., Reist, M., Mayer, J. M., Felt, O., Peppas, N. A., & Gurny, R. (2004). Structure and interactions in covalently and ionically crosslinked chitosan hydrogels for biomedical applications. *European Journal of Pharmaceutics and Biopharmaceutics, 57*(1), 19-34. doi:https://doi.org/10.1016/S0939-6411(03)00161-9

Bergmann, O., Zdunek, S., Felker, A., Salehpour, M., Alkass, K., Bernard, S., . . . Frisén, J. (2015). *Dynamics of Cell Generation and Turnover in the Human Heart* (Vol. 161).

Berleman, J. E., Chumley, T., Cheung, P., & Kirby, J. R. (2006). Rippling is a predatory behavior in Myxococcus xanthus. *J Bacteriol, 188*(16), 5888-5895. doi:10.1128/jb.00559-06

Berry, F., Sayadi, S., Nasri, M., Barbotin, J. N., & Thomas, D. (1988). Effect of growing conditions of recombinantE.coli in carrageenan gel beads upon biomasse production and plasmid stability. *Biotechnol Lett, 10*(9), 619-624. doi:10.1007/bf01024712

Bikadi, Z. (1995). The Oil Weapons.

Bike, C. a. (2016). Retrieved from https://auto.ndtv.com/news/indias-passenger-car-ownership-to-grow-775-per-cent-by-2040-study-1425954

Binai, N. A., Bisschops, M. M., van Breukelen, B., Mohammed, S., Loeff, L., Pronk, J. T., . . . Slijper, M. (2014). Proteome adaptation of Saccharomyces cerevisiae to severe calorie restriction in Retentostat cultures. *J Proteome Res, 13*(8), 3542-3553. doi:10.1021/pr5003388

Binai, N. A., Bisschops, M. M. M., van Breukelen, B., Mohammed, S., Loeff, L., Pronk, J. T., . . . Slijper, M. (2014). Proteome Adaptation of Saccharomyces cerevisiae to Severe Calorie Restriction in Retentostat Cultures. *J Proteome Res, 13*(8), 3542-3553. doi:10.1021/pr5003388

Bisceglie, V. (1934). Über die antineoplastische Immunität. *Zeitschrift für Krebsforschung, 40*(1), 122-140. doi:10.1007/BF01636399

Bisschops, M. M., Zwartjens, P., Keuter, S. G., Pronk, J. T., & Daran-Lapujade, P. (2014). To divide or not to divide: a key role of Rim15 in calorie-restricted yeast cultures. *Biochim Biophys Acta, 1843*(5), 1020-1030. doi:10.1016/j.bbamcr.2014.01.026

Bisschops, M. M. M., Luttik, M. A. H., Doerr, A., Verheijen, P. J. T., Bruggeman, F., Pronk, J. T., & Daran-Lapujade, P. (2017). Extreme calorie restriction in yeast retentostats induces uniform non-quiescent growth arrest. *Biochimica et Biophysica Acta (BBA) - Molecular Cell Research, 1864*(1), 231-242. doi:https://doi.org/10.1016/j.bbamcr.2016.11.002

Bisschops, M. M. M., Zwartjens, P., Keuter, S. G. F., Pronk, J. T., & Daran-Lapujade, P. (2014). To divide or not to divide: A key role of Rim15 in calorie-restricted yeast cultures. *Biochimica et Biophysica Acta (BBA) - Molecular Cell Research, 1843*(5), 1020-1030. doi:https://doi.org/10.1016/j.bbamcr.2014.01.026

Blacher, P., Huggins, T. J., & Bourke, A. F. G. (2017). Evolution of ageing, costs of reproduction and the fecundity-longevity trade-off in eusocial insects. *Proc Biol Sci, 284*(1858). doi:10.1098/rspb.2017.0380

Boender, L. G., Almering, M. J., Dijk, M., van Maris, A. J., de Winde, J. H., Pronk, J. T., & Daran-Lapujade, P. (2011). Extreme calorie restriction and energy source starvation in Saccharomyces cerevisiae represent distinct physiological states. *Biochim Biophys Acta, 1813*(12), 2133-2144. doi:10.1016/j.bbamcr.2011.07.008

Boender, L. G., de Hulster, E. A., van Maris, A. J., Daran-Lapujade, P. A., & Pronk, J. T. (2009). Quantitative physiology of Saccharomyces cerevisiae at near-zero specific growth rates. *Appl Environ Microbiol, 75*(17), 5607-5614. doi:10.1128/aem.00429-09

Boender, L. G., van Maris, A. J., de Hulster, E. A., Almering, M. J., van der Klei, I. J., Veenhuis, M., . . . Daran-Lapujade, P. (2011). Cellular responses of Saccharomyces cerevisiae at near-zero growth rates: transcriptome analysis of anaerobic retentostat cultures. *FEMS Yeast Res, 11*(8), 603-620. doi:10.1111/j.1567-1364.2011.00750.x

Boender, L. G. M., Almering, M. J. H., Dijk, M., van Maris, A. J. A., de Winde, J. H., Pronk, J. T., & Daran-Lapujade, P. (2011). Extreme calorie restriction and energy source starvation in Saccharomyces cerevisiae represent distinct physiological states. *Biochimica et Biophysica Acta (BBA) - Molecular Cell Research, 1813*(12), 2133-2144. doi:https://doi.org/10.1016/j.bbamcr.2011.07.008

Boraas, M., Seale, D., & Boxhorn, J. (1998). Phagotrophy by a flagellate selects for colonial prey: A possible origin of multicellularity. *Evolutionary Ecology, 12*(2), 153-164. doi:10.1023/A:1006527528063

Bourre, J. M. (2006). Effects of nutrients (in food) on the structure and function of the nervous system: update on dietary requirements for brain. Part 2 : macronutrients. *J Nutr Health Aging, 10*(5), 386-399.

Branska, B., Pechacova, Z., Kolek, J., Vasylkivska, M., & Patakova, P. (2018). Flow cytometry analysis of Clostridium beijerinckii NRRL B-598 populations exhibiting different phenotypes induced by changes in cultivation conditions. *Biotechnol Biofuels, 11*, 99. doi:10.1186/s13068-018-1096-x

Brock, V. E., & Riffenburgh, R. H. (1960). Fish schooling: A possible factor in reducing predation. *ICES Journal of Marine Science, 25*(3), 307-317. doi:10.1093/icesjms/25.3.307

Brockhurst, M. A., Habets, M. G., Libberton, B., Buckling, A., & Gardner, A. (2010). Ecological drivers of the evolution of public-goods cooperation in bacteria. *Ecology, 91*(2), 334-340. doi:doi:10.1890/09-0293.1

Bruckner, S., & Mosch, H. U. (2012). Choosing the right lifestyle: adhesion and development in Saccharomyces cerevisiae. *FEMS Microbiol Rev, 36*(1), 25-58. doi:10.1111/j.1574-6976.2011.00275.x

Bull, L. (1999). On the evolution of multicellularity and eusociality. *Artificial Life, 5*(1), 1-15. doi:10.1162/106454699568656

Burgain, J., Gaiani, C., Linder, M., & Scher, J. (2011). Encapsulation of probiotic living cells: From laboratory scale to industrial applications. *Journal of Food Engineering, 104*(4), 467-483. doi:https://doi.org/10.1016/j.jfoodeng.2010.12.031

Burnetti, A. J., Aydin, M., Buchler, N. E., & Solomon, M. J. (2015). Cell cycle Start is coupled to entry into the yeast metabolic cycle across diverse strains and growth rates. *Mol Biol Cell, 27*(1), 64-74. doi:10.1091/mbc.e15-07-0454

Burtner, C. R., Murakami, C. J., Kennedy, B. K., & Kaeberlein, M. (2009). A molecular mechanism of chronological aging in yeast. *Cell Cycle, 8*(8), 1256-1270. doi:10.4161/cc.8.8.8287

Burtner, C. R., Murakami, C. J., Kennedy, B. K., & Kaeberlein, M. (2009). A molecular mechanism of chronological aging in yeast. *Cell Cycle, 8*(8), 1256-1270. doi:10.4161/cc.8.8.8287

Burtner, C. R., Murakami, C. J., Olsen, B., Kennedy, B. K., & Kaeberlein, M. (2011). A genomic analysis of chronological longevity factors in budding yeast. *Cell Cycle, 10*(9), 1385-1396. doi:10.4161/cc.10.9.15464

Burtner, C. R., Murakami, C. J., Olsen, B., Kennedy, B. K., & Kaeberlein, M. (2011). A genomic analysis of chronological longevity factors in budding yeast. *Cell Cycle, 10*(9), 1385-1396. doi:10.4161/cc.10.9.15464

Cafazzo, S., Lazzaroni, M., & Marshall-Pescini, S. (2016). Dominance relationships in a family pack of captive arctic wolves (Canis lupus arctos): the influence of competition for food, age and sex. *PeerJ, 4*, e2707. doi:10.7717/peerj.2707

Camarasa, C., Grivet, J.-P., & Dequin, S. (2003). Investigation by 13C-NMR and tricarboxylic acid (TCA) deletion mutant analysis of pathways for succinate formation in Saccharomyces cerevisiae during anaerobic fermentation. *Microbiology, 149*(9), 2669-2678. doi:doi:10.1099/mic.0.26007-0

Cap, M., Stepanek, L., Harant, K., Vachova, L., & Palkova, Z. (2012). Cell differentiation within a yeast colony: metabolic and regulatory parallels with a tumor-affected organism. *Mol Cell, 46*(4), 436-448. doi:10.1016/j.molcel.2012.04.001

Čáp, M., Štěpánek, L., Harant, K., Váchová, L., & Palková, Z. (2012). Cell Differentiation within a Yeast Colony: Metabolic and Regulatory Parallels with a Tumor-Affected Organism. *Mol Cell, 46*(4), 436-448. doi:10.1016/j.molcel.2012.04.001

Cap, M., Vachova, L., & Palkova, Z. (2009). Yeast colony survival depends on metabolic adaptation and cell differentiation rather than on stress defense. *Journal of Biological Chemistry*. doi:10.1074/jbc.M109.022871

Čáp, M., Váchová, L., & Palková, Z. (2010). How to survive within a yeast colony. *Commun Integr Biol, 3*(2), 198-200. doi:10.4161/cib.3.2.11026

Čáp, M., Váchová, L., & Palková, Z. (2015). Longevity of U cells of differentiated yeast colonies grown on respiratory medium depends on active glycolysis. *Cell Cycle, 14*(21), 3488-3497. doi:10.1080/15384101.2015.1093706

Capell, T., & Christou, P. (2004). Progress in plant metabolic engineering. *Current Opinion in Biotechnology, 15*(2), 148-154. doi:http://dx.doi.org/10.1016/j.copbio.2004.01.009

Carolan, M. S. (2009). A Sociological Look at Biofuels: Ethanol in the Early Decades of the Twentieth Century and Lessons for Today. *Rural Sociology, 74*(1), 86-112. doi:10.1526/003601109787524034

Cassidy, K. A., Mech, L. D., MacNulty, D. R., Stahler, D. R., & Smith, D. W. (2017). Sexually dimorphic aggression indicates male gray wolves specialize in pack defense against conspecific groups. *Behav Processes, 136*, 64-72. doi:10.1016/j.beproc.2017.01.011

Center, A. F. D. (2017).

Cha, C., Kim, S. R., Jin, Y. S., & Kong, H. (2012). Tuning structural durability of yeast-encapsulating alginate gel beads with interpenetrating networks for sustained bioethanol production. *Biotechnol Bioeng, 109*(1), 63-73. doi:10.1002/bit.23258

Chaenyung, C., Rin, K. S., Yong-Su, J., & Hyunjoon, K. (2012). Tuning structural durability of yeast-encapsulating alginate gel beads with interpenetrating networks for sustained bioethanol production. *Biotechnology and Bioengineering, 109*(1), 63-73. doi:doi:10.1002/bit.23258

Chavez-Rodriguez, M. F., & Nebra, S. A. (2010). Assessing GHG Emissions, Ecological Footprint, and Water Linkage for Different Fuels. *Environ Sci Technol, 44*(24), 9252-9257. doi:10.1021/es101187h

Chen, Y. (2011). Development and application of co-culture for ethanol production by co-fermentation of glucose and xylose: a systematic review. *J Ind Microbiol Biotechnol, 38*(5), 581-597. doi:10.1007/s10295-010-0894-3

Chen, Y., Liu, Q., Zhou, T., Li, B., Yao, S., Li, A., . . . Ying, H. (2013). Ethanol production by repeated batch and continuous fermentations by Saccharomyces cerevisiae immobilized in a fibrous bed bioreactor. *J Microbiol Biotechnol, 23*(4), 511-517.

Chen, Y., Wu, Y., Zhu, B., Zhang, G., & Wei, N. (2018). Co-fermentation of cellobiose and xylose by mixed culture of recombinant Saccharomyces cerevisiae and kinetic modeling. *PLoS One, 13*(6), e0199104. doi:10.1371/journal.pone.0199104

Chibata, I., & Tosa, T. (1977). Transformations of organic compounds by immobilized microbial cells. *Adv Appl Microbiol, 22*, 1-27.

Chibata, I., Tosa, T., & Sato, T. (1976). Production of L-aspartic acid by microbial cells entrapped in polyacrylamide gels. *Methods Enzymol, 44*, 739-746.

Claro, F. B., Rijsbrack, K., & Soares, E. V. (2007). Flocculation onset in Saccharomyces cerevisiae: effect of ethanol, heat and osmotic stress. *J Appl Microbiol, 102*(3), 693-700. doi:10.1111/j.1365-2672.2006.03130.x

Coller, H. A. (2007). What's taking so long? S-phase entry from quiescence versus proliferation. *Nat Rev Mol Cell Biol, 8*(8), 667-670. doi:10.1038/nrm2223

Cooper, V. S., & Lenski, R. E. (2000). The population genetics of ecological specialization in evolving Escherichia coli populations. *Nature, 407*(6805), 736-739.

Cooper, V. S., Schneider, D., Blot, M., & Lenski, R. E. (2001). Mechanisms causing rapid and parallel losses of ribose catabolism in evolving populations of Escherichia coli B. *J Bacteriol, 183*(9), 2834-2841. doi:10.1128/jb.183.9.2834-2841.2001

Cox, R. T., & Carlton, C. E. (1991). Evidence of Genetic Dominance of the 13-year Life Cycle in Periodical Cicadas (Homoptera: Cicadidae: Magicicada spp.). *The American Midland Naturalist, 125*(1), 63-74. doi:10.2307/2426370

Crowley, L. C., Scott, A. P., Marfell, B. J., Boughaba, J. A., Chojnowski, G., & Waterhouse, N. J. (2016). Measuring Cell Death by Propidium Iodide Uptake and Flow Cytometry. *Cold Spring Harb Protoc, 2016*(7). doi:10.1101/pdb.prot087163

Damage Assessment, R. a. R. P. (2010).

de Bari, I., Cuna, D., Nanna, F., & Braccio, G. (2004). *Ethanol Production in Immobilized-Cell Bioreactors from Mixed Sugar Syrups and Enzymatic Hydrolysates of Steam-Exploded Biomass*, Totowa, NJ.

De Bari, I., De Canio, P., Cuna, D., Liuzzi, F., Capece, A., & Romano, P. (2013). Bioethanol production from mixed sugars by Scheffersomyces stipitis free and immobilized cells, and co-cultures with Saccharomyces cerevisiae. *N Biotechnol, 30*(6), 591-597. doi:10.1016/j.nbt.2013.02.003

DeBerardinis, R. J., & Cheng, T. (2010). Q's next: the diverse functions of glutamine in metabolism, cell biology and cancer. *Oncogene, 29*(3), 313-324. doi:10.1038/onc.2009.358

Delaney, J. R., Murakami, C., Chou, A., Carr, D., Schleit, J., Sutphin, G. L., . . . Kaeberlein, M. (2013). Dietary restriction and mitochondrial function link replicative and chronological aging in Saccharomyces cerevisiae. *Exp Gerontol, 48*(10), 1006-1013. doi:10.1016/j.exger.2012.12.001

Delaney, J. R., Murakami, C., Chou, A., Carr, D., Schleit, J., Sutphin, G. L., . . . Kaeberlein, M. (2013). Dietary restriction and mitochondrial function link replicative and chronological aging in Saccharomyces cerevisiae. *Exp Gerontol, 48*(10), 1006-1013. doi:10.1016/j.exger.2012.12.001

Delarue, M., Hartung, J., Schreck, C., Gniewek, P., Hu, L., Herminghaus, S., & Hallatschek, O. (2016). Self-Driven Jamming in Growing Microbial Populations. *Nature Physics, 12*(8), 762-766. doi:10.1038/nphys3741

Delgenes, J. P., Moletta, R., & Navarro, J. M. (1988). Fermentation ofd-xylose,d-glucose andl-arabinose mixture byPichia stipitis Y 7124: sugar tolerance. *Applied Microbiology and Biotechnology, 29*(2), 155-161. doi:10.1007/bf01982895

Denchak, M. (2015). Retrieved from https://www.nrdc.org/stories/dirty-fight-over-canadian-tar-sands-oil

Denoth Lippuner, A., Julou, T., & Barral, Y. (2014). Budding yeast as a model organism to study the effects of age. *FEMS Microbiol Rev, 38*(2), 300-325. doi:doi:10.1111/1574-6976.12060

Desai, J. V., & Mitchell, A. P. (2015). Candida albicans Biofilm Development and Its Genetic Control. *Microbiol Spectr, 3*(3). doi:10.1128/microbiolspec.MB-0005-2014

Desimone, M. F., Degrossi, J., D'Aquino, M., & Diaz, L. E. (2003). Sol-gel immobilisation of Saccharomyces cerevisiae enhances viability in organic media. *Biotechnol Lett, 25*(9), 671-674. doi:10.1023/a:1023481304479

Dien, B. S., Nichols, N. N., O'bryan, P. J., & Bothast, R. J. (2000). Development of new ethanologenic Escherichia coli strains for fermentation of lignocellulosic biomass. *Applied Biochemistry and Biotechnology, 84*(1-9), 181-196.

Domenici, P., Steffensen, J. F., & Marras, S. (2017). The effect of hypoxia on fish schooling. *Philos Trans R Soc Lond B Biol Sci, 372*(1727). doi:10.1098/rstb.2016.0236

Doran, P. M., & Bailey, J. E. (1986). Effects of immobilization on growth, fermentation properties, and macromolecular composition of Saccharomyces cerevisiae attached to gelatin. *Biotechnology and Bioengineering, 28*(1), 73-87. doi:doi:10.1002/bit.260280111

Draget, K. I. (2009). 29 - Alginates. In G. O. Phillips & P. A. Williams (Eds.), *Handbook of Hydrocolloids (Second Edition)* (pp. 807-828): Woodhead Publishing.

Drury, J. L., & Mooney, D. J. (2003). Hydrogels for tissue engineering: scaffold design variables and applications. *Biomaterials, 24*(24), 4337-4351.

du Preez, J. C., van Driessel, B., & Prior, B. A. (1989). D-xylose fermentation by Candida shehatae and pichia stipitis at low dissolved oxygen levels in fed-batch cultures. *Biotechnol Lett, 11*(2), 131-136. doi:10.1007/bf01192189

Dupré, L. (2009). The common good and the open society. *The Review of Politics, 55*(4), 687-712. doi:10.1017/S0034670500018052

Dwivedi, P., Wang, W., Hudiburg, T., Jaiswal, D., Parton, W., Long, S., . . . Khanna, M. (2015). Cost of abating greenhouse gas emissions with cellulosic ethanol. *Environ Sci Technol, 49*(4), 2512-2522. doi:10.1021/es5052588

Edmunds, L. N. (1972). Introduction to Research with Continuous Cultures. H. E. Kubitschek. *Q Rev Biol, 47*(1), 88-88. doi:10.1086/407133

El-Dalatony, M. M., Kurade, M. B., Abou-Shanab, R. A. I., Kim, H., Salama, E.-S., & Jeon, B.-H. (2016). Long-term production of bioethanol in repeated-batch fermentation of microalgal biomass using immobilized Saccharomyces cerevisiae. *Bioresour Technol, 219*, 98-105. doi:https://doi.org/10.1016/j.biortech.2016.07.113

Eller, D. (2018). Trump moves to allow more ethanol in gas with E15 available year-round.

Endy, D. (2005). Foundations for engineering biology. *Nature, 438*(7067), 449-453.

Eng, C. H., Yu, K., Lucas, J., White, E., & Abraham, R. T. (2010). Ammonia derived from glutaminolysis is a diffusible regulator of autophagy. *Sci. Signal., 3*(119), ra31-ra31.

Ercan, O., Bisschops, M. M., Overkamp, W., Jorgensen, T. R., Ram, A. F., Smid, E. J., . . . Kleerebezem, M. (2015). Physiological and Transcriptional Responses of Different Industrial Microbes at Near-Zero Specific Growth Rates. *Appl Environ Microbiol, 81*(17), 5662-5670. doi:10.1128/aem.00944-15

Ercan, Y., Irfan, T., & Mustafa, K. (2013). Optimization of ethanol production from carob pod extract using immobilized Saccharomyces cerevisiae cells in a stirred tank bioreactor. *Bioresour Technol, 135*, 365-371. doi:https://doi.org/10.1016/j.biortech.2012.09.006

Erickson, B. (2018). A Rising Tide of Cellulosic Ethanol Production. *Industrial Biotechnology, 14*(2), 77-78. doi:10.1089/ind.2018.29124.ber

Fabrizio, P., Battistella, L., Vardavas, R., Gattazzo, C., Liou, L.-L., Diaspro, A., . . . Longo, V. D. (2004). Superoxide is a mediator of an altruistic aging program in Saccharomyces cerevisiae. *J Cell Biol, 166*(7), 1055-1067. doi:10.1083/jcb.200404002

Fabrizio, P., Battistella, L., Vardavas, R., Gattazzo, C., Liou, L. L., Diaspro, A., . . . Longo, V. D. (2004). Superoxide is a mediator of an altruistic aging program in Saccharomyces cerevisiae. *J Cell Biol, 166*(7), 1055-1067. doi:10.1083/jcb.200404002

Fabrizio, P., Pozza, F., Pletcher, S. D., Gendron, C. M., & Longo, V. D. (2001). Regulation of longevity and stress resistance by Sch9 in yeast. *Science, 292*(5515), 288-290. doi:10.1126/science.1059497

Fang, Z. G. (2010). [Enhanced role of the co-culture of thermophilic anaerobic bacteria on cellulosic ethanol]. *Huan Jing Ke Xue, 31*(4), 1059-1065.

Faucon, B. (2013).

Favaro, L., Jansen, T., & van Zyl, W. H. (2019). Exploring industrial and natural Saccharomyces cerevisiae strains for the bio-based economy from biomass: the case of bioethanol. *Crit Rev Biotechnol*, 1-17. doi:10.1080/07388551.2019.1619157

Fermentations, L. A. (2019). Ethanol Red. Retrieved from https://lesaffreadvancedfermentations.com/ethanol_yeast/

Fisher, R. M., Cornwallis, C. K., & West, S. A. (2013). Group formation, relatedness, and the evolution of multicellularity. *Curr Biol, 23*(12), 1120-1125. doi:10.1016/j.cub.2013.05.004

Flatt, T. (2012). A New Definition of Aging? *Front Genet, 3*, 148. doi:10.3389/fgene.2012.00148

Fleet, G. H. (1990). Growth of yeasts during wine fermentations. *Journal of Wine Research, 1*(3), 211-223. doi:10.1080/09571269008717877

Folse, H. J., 3rd, & Roughgarden, J. (2010). What is an individual organism? A multilevel selection perspective. *Q Rev Biol, 85*(4), 447-472.

Fontana, L., Partridge, L., & Longo, V. D. (2010). Extending healthy life span--from yeast to humans. *Science, 328*(5976), 321-326. doi:10.1126/science.1172539

Foss, E. J., Lao, U., Dalrymple, E., Adrianse, R. L., Loe, T., & Bedalov, A. (2017). SIR2 suppresses replication gaps and genome instability by balancing replication between repetitive and unique sequences. *Proceedings of the National Academy of Sciences, 114*(3), 552-557. doi:10.1073/pnas.1614781114

Fu, F., Kocher, S. D., & Nowak, M. A. (2015). The risk-return trade-off between solitary and eusocial reproduction. *Ecol Lett, 18*(1), 74-84. doi:10.1111/ele.12392

Fu, N., Peiris, P., Markham, J., & Bavor, J. (2009). A novel co-culture process with Zymomonas mobilis and Pichia stipitis for efficient ethanol production on

glucose/xylose mixtures. *Enzyme and Microbial Technology, 45*(3), 210-217. doi:https://doi.org/10.1016/j.enzmictec.2009.04.006

Fuge, E. K., Braun, E. L., & Werner-Washburne, M. (1994). Protein synthesis in long-term stationary-phase cultures of Saccharomyces cerevisiae. *J Bacteriol, 176*(18), 5802-5813.

Fujita, Y., Katahira, S., Ueda, M., Tanaka, A., Okada, H., Morikawa, Y., . . . Kondo, A. (2002). Construction of whole-cell biocatalyst for xylan degradation through cell-surface xylanase display in Saccharomyces cerevisiae. *Journal of Molecular Catalysis B: Enzymatic, 17*(3), 189-195. doi:https://doi.org/10.1016/S1381-1177(02)00027-9

Gadagkar, R. (2016). Evolution of social behaviour in the primitively eusocial wasp Ropalidia marginata: do we need to look beyond kin selection? *Philos Trans R Soc Lond B Biol Sci, 371*(1687), 20150094. doi:10.1098/rstb.2015.0094

Galazzo, J. L., & Bailey, J. E. (1990). Growing Saccharomyces cerevisiae in calcium-alginate beads induces cell alterations which accelerate glucose conversion to ethanol. *Biotechnology and Bioengineering, 36*(4), 417-426. doi:doi:10.1002/bit.260360413

Galvez-Martin, P., Martin, J. M., Ruiz, A. M., & Clares, B. (2017). Encapsulation in Cell Therapy: Methodologies, Materials, and Clinical Applications. *Curr Pharm Biotechnol, 18*(5), 365-377. doi:10.2174/1389201018666170502113252

Garay, E., Campos, S. E., Gonzalez de la Cruz, J., Gaspar, A. P., Jinich, A., & Deluna, A. (2014). High-resolution profiling of stationary-phase survival reveals yeast longevity factors and their genetic interactions. *PLoS Genet, 10*(2), e1004168. doi:10.1371/journal.pgen.1004168

Garay, E., Campos, S. E., González de la Cruz, J., Gaspar, A. P., Jinich, A., & DeLuna, A. (2014). High-Resolution Profiling of Stationary-Phase Survival Reveals Yeast Longevity Factors and Their Genetic Interactions. *PLoS Genetics, 10*(2), e1004168. doi:10.1371/journal.pgen.1004168

Garcia, T., Doulcier, G., & De Monte, S. (2015). The evolution of adhesiveness as a social adaptation. *Elife, 4*. doi:10.7554/eLife.08595

Ge, J., Zhao, J., Zhang, L., Zhang, M., & Ping, W. (2014). Construction and Analysis of High-Ethanol-Producing Fusants with Co-Fermentation Ability through Protoplast Fusion and Double Labeling Technology. *PLoS One, 9*(9), e108311. doi:10.1371/journal.pone.0108311

George, M., & Abraham, T. E. (2006). Polyionic hydrocolloids for the intestinal delivery of protein drugs: alginate and chitosan—a review. *Journal of controlled release, 114*(1), 1-14.

Gerbrandt, K., Chu, P. L., Simmonds, A., Mullins, K. A., MacLean, H. L., Griffin, W. M., & Saville, B. A. (2016). Life cycle assessment of lignocellulosic ethanol: a review of key factors and methods affecting calculated GHG emissions and energy use. *Curr Opin Biotechnol, 38*, 63-70. doi:10.1016/j.copbio.2015.12.021

Gietz, R. D., & Schiestl, R. H. (2007). High-efficiency yeast transformation using the LiAc/SS carrier DNA/PEG method. *Nat Protoc, 2*(1), 31-34. doi:10.1038/nprot.2007.13

Gilbert, C., Robertson, G., Le Maho, Y., Naito, Y., & Ancel, A. (2006). Huddling behavior in emperor penguins: Dynamics of huddling. *Physiol Behav, 88*(4-5), 479-488. doi:10.1016/j.physbeh.2006.04.024

Gilbert, O. M., Foster, K. R., Mehdiabadi, N. J., Strassmann, J. E., & Queller, D. C. (2007). High relatedness maintains multicellular cooperation in a social amoeba by controlling cheater mutants. *Proceedings of the National Academy of Sciences, 104*(21), 8913-8917. doi:10.1073/pnas.0702723104

Gilson, C. D., & Thomas, A. (1995). Ethanol production by alginate immobilised yeast in a fluidised bed bioreactor. *Journal of Chemical Technology & Biotechnology, 62*(1), 38-45. doi:10.1002/jctb.280620106

Goettemoeller, J., & Goettemoeller, A. (2007). *Sustainable Ethanol: Biofuels, Biorefineries, Cellulosic Biomass, Flex-fuel Vehicles, and Sustainable Farming for Energy Independence*: Prairie Oak Pub.

Goossens, K., & Willaert, R. (2010). Flocculation protein structure and cell-cell adhesion mechanism in Saccharomyces cerevisiae. *Biotechnol Lett, 32*(11), 1571-1585. doi:10.1007/s10529-010-0352-3

Goossens, K. V., Ielasi, F. S., Nookaew, I., Stals, I., Alonso-Sarduy, L., Daenen, L., . . . Willaert, R. G. (2015). Molecular mechanism of flocculation self-recognition in yeast and its role in mating and survival. *MBio, 6*(2). doi:10.1128/mBio.00427-15

Gralla, E. B., & Valentine, J. S. (1991). Null mutants of Saccharomyces cerevisiae Cu,Zn superoxide dismutase: characterization and spontaneous mutation rates. *J Bacteriol, 173*(18), 5918-5920.

Greig, D., & Travisano, M. (2004). The Prisoner's Dilemma and polymorphism in yeast SUC genes. *Proceedings of the Royal Society B: Biological Sciences, 271*(Suppl 3), S25-S26.

Gresham, D. (2013). A sticky solution. *Elife, 2*, e00655. doi:10.7554/eLife.00655

Grootjen, D. R. J., Jansen, M. L., van der Lans, R. G. J. M., & Luyben, K. C. A. M. (1991). Reactors in series for the complete conversion of glucose/xylose mixtures by Pichia stipitis and Saccharomyces cerevisiae. *Enzyme and Microbial Technology, 13*(10), 828-833. doi:https://doi.org/10.1016/0141-0229(91)90067-K

Grootjen, D. R. J., Meijlink, L. H. H. M., van der Lans, R. G. J. M., & Luyben, K. C. A. M. (1990). Cofermentation of glucose and xylose with immobilized Pichia stipitis and Saccharomyces cerevisiae. *Enzyme and Microbial Technology, 12*(11), 860-864. doi:https://doi.org/10.1016/0141-0229(90)90023-J

Gulli, J. G., Yunker, P. J., & Rosenzweig, F. (2019). Matrices (re)loaded: Durability, viability and fermentative capacity of yeast encapsulated in beads of different composition during long-term fed-batch culture *Engineering Reports*.

Gupthar, A. S. (1992). Segregation of altered parental properties in fusions between Saccharomyces cerevisiae and the D-xylose fermenting yeasts Candida shehatae and Pichia stipitis. *Can J Microbiol, 38*(12), 1233-1237.

Gutiérrez-Rivera, B., Waliszewski-Kubiak, K., Carvajal-Zarrabal, O., & Aguilar-Uscanga, M. (2012). *Conversion efficiency of glucose/xylose mixtures for ethanol production using Saccharomyces cerevisiae ITV01 and Pichia stipitis NRRL Y-7124* (Vol. 87).

Hahn-Hägerdal, B., Karhumaa, K., Fonseca, C., Spencer-Martins, I., & Gorwa-Grauslund, M. F. (2007). Towards industrial pentose-fermenting yeast strains. *Applied Microbiology and Biotechnology, 74*(5), 937-953. doi:10.1007/s00253-006-0827-2

Hamada, T., Sugishita, M., Fukushima, Y., Fukase, T., & Motai, H. (1991). *Continuous production of soy sauce by a bioreactor system* (Vol. 26).

Hanahan, D., & Weinberg, R. A. (2000). The hallmarks of cancer. *Cell, 100*(1), 57-70.

HANSEN, M., RÖCKEN, W., & EMEIS, C.-C. (1990). CONSTRUCTION OF YEAST STRAINS FOR THE PRODUCTION OF LOW-CARBOHYDRATE BEER. *Journal of the Institute of Brewing, 96*(3), 125-129. doi:10.1002/j.2050-0416.1990.tb01022.x

He, C., Zhou, C., & Kennedy, B. K. (2018). The yeast replicative aging model. *Biochimica et Biophysica Acta (BBA) - Molecular Basis of Disease, 1864*(9, Part A), 2690-2696. doi:https://doi.org/10.1016/j.bbadis.2018.02.023

He, W., & Parker, R. (2000). Functions of Lsm proteins in mRNA degradation and splicing. *Curr Opin Cell Biol, 12*(3), 346-350.

Helbig, A. O., Daran-Lapujade, P., van Maris, A. J., de Hulster, E. A., de Ridder, D., Pronk, J. T., . . . Slijper, M. (2011). The diversity of protein turnover and abundance under nitrogen-limited steady-state conditions in Saccharomyces cerevisiae. *Mol Biosyst, 7*(12), 3316-3326. doi:10.1039/c1mb05250k

Heluane, H., Spencer, J., Spencer, D., De Figueroa, L., & Callieri, D. (1993). Characterization of hybrids obtained by protoplast fusion, between Pachysolen tannophilus and Saccharomyces cerevisiae. *Applied Microbiology and Biotechnology, 40*(1), 98-100.

Herbert-Read, J. E., Rosen, E., Szorkovszky, A., Ioannou, C. C., Rogell, B., Perna, A., . . . Sumpter, D. J. T. (2017). How predation shapes the social interaction rules of shoaling fish. *Proc Biol Sci, 284*(1861). doi:10.1098/rspb.2017.1126

Herbert, D. (1961). A theoretical analysis of continuous culture systems. In D. W. Hastings (Ed.), *Continuous culture of micro-organisms* (pp. 21-53). London, United Kingdon: Society of Chemical Industry.

Herre, E. A., Knowlton, N., Mueller, U. G., & Rehner, S. A. (1999). The evolution of mutualisms: exploring the paths between conflict and cooperation. *Trends in Ecology & Evolution, 14*(2), 49-53. doi:https://doi.org/10.1016/S0169-5347(98)01529-8

Herron, M. D., Zamani-Dahaj, S. A., & Ratcliff, W. C. (2018). Trait Heritability in Major Transitions. *bioRxiv*, 041830. doi:10.1101/041830

Hertel, T. W., Golub, A. A., Jones, A. D., O'Hare, M., Plevin, R. J., & Kammen, D. M. (2010). Effects of US Maize Ethanol on Global Land Use and Greenhouse Gas Emissions: Estimating Market-mediated Responses. *BioScience, 60*(3), 223-231. doi:10.1525/bio.2010.60.3.8

Hinnebusch, A. G. (2005). Translational regulation of GCN4 and the general amino acid control of yeast. *Annu Rev Microbiol, 59*, 407-450. doi:10.1146/annurev.micro.59.031805.133833

Hirotsune, M., Nakada, F., Hamachi, M., and Honma, T. (1987). Continuous fermentation of saccharified rice solution using immobilized yeast. *J. Brew Society Jpn, 82*, 582.

Holmes, D. L., Lancaster, A. K., Lindquist, S., & Halfmann, R. (2013). Heritable remodeling of yeast multicellularity by an environmentally responsive prion. *Cell, 153*(1), 153-165. doi:10.1016/j.cell.2013.02.026

Hong, S. K., Lee, H. J., Park, H. J., Hong, Y. A., Rhee, I. K., Lee, W. H., . . . Park, H. D. (2010). Degradation of malic acid in wine by immobilized Issatchenkia orientalis cells with oriental oak charcoal and alginate. *Letters in Applied Microbiology, 50*(5), 522-529. doi:doi:10.1111/j.1472-765X.2010.02833.x

Honigberg, S. M. (2011). Cell Signals, Cell Contacts, and the Organization of Yeast Communities. *Eukaryot Cell, 10*(4), 466-473. doi:10.1128/EC.00313-10

Hu, J., Wei, M., Mirisola, M. G., & Longo, V. D. (2013). Assessing chronological Aging in Saccharomyces cerevisiae. *Methods Mol Biol, 965*, 463-472. doi:10.1007/978-1-62703-239-1_30

Hu, Y., Tang, T., Yang, W., & Zhou, H. (2009). *Bioconversion of phenylpyruvic acid to L-phenylalanine by mixed-gel immobilization of Escherichia coli EP8-10* (Vol. 44).

Huang, S. Y., & Chen, J. C. (1988). Ethanol production in simultaneous saccharification and fermentation of cellulose with temperature profiling. *Journal of Fermentation Technology, 66*(5), 509-516. doi:https://doi.org/10.1016/0385-6380(88)90083-0

Huang, X., Zhang, K., Deng, M., Exterkate, R. A. M., Liu, C., Zhou, X., . . . Ten Cate, J. M. (2017). Effect of arginine on the growth and biofilm formation of oral bacteria. *Arch Oral Biol, 82*, 256-262. doi:10.1016/j.archoralbio.2017.06.026

Hull, D. L. (2001). *Science and selection: Essays on biological evolution and the philosophy of science*: Cambridge University Press.

Hussain, A., Kangwa, M., & Fernandez-Lahore, M. (2017). Comparative analysis of stirred catalytic basket bio-reactor for the production of bio-ethanol using free and immobilized Saccharomyces cerevisiae cells. *AMB Express, 7*(1), 158-158. doi:10.1186/s13568-017-0460-8

Iborra, J. L., Manjón, A., Cánovas, M., Lozano, P., & Martínez, C. (1994). Continuous limonin degradation by immobilizedRhodococcus fascians cells in K-carrageenan. *Applied Microbiology and Biotechnology, 41*(4), 487-493. doi:10.1007/bf00939041

IndexMundi. (2017). Crude Oil Consumption by Country. Retrieved from https://www.indexmundi.com/energy/?product=oil&graph=consumption&display=rank

Intergovernmental Panel on Climate Change. (2013).

Istvan Jr, M. A. (2013). Gould talking past Dawkins on the unit of selection issue. *Studies in History and Philosophy of Science Part C: Studies in History and Philosophy of Biological and Biomedical Sciences, 44*(3), 327-335. doi:http://dx.doi.org/10.1016/j.shpsc.2013.05.020

Itakura, K., Hirose, T., Crea, R., Riggs, A., Heyneker, H., Bolivar, F., & Boyer, H. (1977). Expression in Escherichia coli of a chemically synthesized gene for the hormone somatostatin. *Science, 198*(4321), 1056-1063. doi:10.1126/science.412251

Jacobeen, S., Pentz, J. T., Graba, E. C., Brandys, C. G., Ratcliff, W. C., & Yunker, P. J. (2017). Cellular packing, mechanical stress and the evolution of multicellularity. *Nature Physics*. doi:10.1038/s41567-017-0002-y

Jacobeen, S., Pentz, J. T., Graba, E. C., Brandys, C. G., Ratcliff, W. C., & Yunker, P. J. (2018). Cellular packing, mechanical stress and the evolution of multicellularity. *Nature Physics, 14*(3), 286-290. doi:10.1038/s41567-017-0002-y

Jacques, K. A. (2003). *The Alcohol Textbook*. Nottingham, UK: Nottingham University Press.

Jamai, L., Ettayebi, K., El Yamani, J., & Ettayebi, M. (2007). Production of ethanol from starch by free and immobilized Candida tropicalis in the presence of alpha-amylase. *Bioresour Technol, 98*(14), 2765-2770. doi:10.1016/j.biortech.2006.09.057

Jarvis, J. U. M., O'Riain, M. J., Bennett, N. C., & Sherman, P. W. (1994). Mammalian eusociality: A family affair. *Trends in Ecology & Evolution, 9*(2), 47-51. doi:http://dx.doi.org/10.1016/0169-5347(94)90267-4

Jassim Shalsh, F., Ibrahim, A., Mohammed, A., & Shobirin Meor Hussi, A. (2016). *Optimization of the Protoplast Fusion Conditions of Saccharomyces cerevisiae and Pichia stipitis for Improvement of Bioethanol Production from Biomass* (Vol. 9).

Jeffries, T. W., & Jin, Y. S. (2000). Ethanol and thermotolerance in the bioconversion of xylose by yeasts. *Adv Appl Microbiol, 47*, 221-268.

Jeffries, T. W., & Jin, Y. S. (2004). Metabolic engineering for improved fermentation of pentoses by yeasts. *Appl Microbiol Biotechnol, 63*(5), 495-509. doi:10.1007/s00253-003-1450-0

Jiang, Y., Levine, H., & Glazier, J. (1998). Possible cooperation of differential adhesion and chemotaxis in mound formation of Dictyostelium. *Biophys J, 75*(6), 2615-2625. doi:10.1016/s0006-3495(98)77707-0

Jo, M. C., Liu, W., Gu, L., Dang, W., & Qin, L. (2015). High-throughput analysis of yeast replicative aging using a microfluidic system. *Proc Natl Acad Sci U S A, 112*(30), 9364-9369. doi:10.1073/pnas.1510328112

Jones, B. M., Kingwell, C. J., Wcislo, W. T., & Robinson, G. E. (2017). Caste-biased gene expression in a facultatively eusocial bee suggests a role for genetic accommodation in the evolution of eusociality. *Proc Biol Sci, 284*(1846). doi:10.1098/rspb.2016.2228

Jones, C. B., Ott, E. M., Keener, J. M., Curtiss, M., Sandrin, V., & Babst, M. (2012). Regulation of membrane protein degradation by starvation-response pathways. *Traffic (Copenhagen, Denmark), 13*(3), 468-482. doi:10.1111/j.1600-0854.2011.01314.x

Kaeberlein, M., Hu, D., Kerr, E. O., Tsuchiya, M., Westman, E. A., Dang, N., . . . Kennedy, B. K. (2005). Increased life span due to calorie restriction in respiratory-deficient yeast. *PLoS Genet, 1*(5), e69. doi:10.1371/journal.pgen.0010069

Kajiwara, S., Aritomi, T., Suga, K., Ohtaguchi, K., & Kobayashi, O. (2000). Overexpression of the OLE1 gene enhances ethanol fermentation by Saccharomyces cerevisiae. *Applied Microbiology and Biotechnology, 53*(5), 568-574. doi:10.1007/s002530051658

Kapheim, K. M., Nonacs, P., Smith, A. R., Wayne, R. K., & Wcislo, W. T. (2015). Kinship, parental manipulation and evolutionary origins of eusociality. *Proc Biol Sci, 282*(1803), 20142886. doi:10.1098/rspb.2014.2886

Kassouf, W., & Kamat, A. M. (2004). Current state of immunotherapy for bladder cancer. *Expert Review of Anticancer Therapy, 4*(6), 1037-1046. doi:10.1586/14737140.4.6.1037

King, G. A., Daugulis, A. J., Goosen, M. F. A., Faulkner, P., & Bayly, D. (1989). Alginate concentration: A key factor in growth of temperature-sensitive baculovirus-infected insect cells in microcapsules. *Biotechnology and Bioengineering, 34*(8), 1085-1091. doi:10.1002/bit.260340809

Kinnersley, M., Wenger, J., Kroll, E., Adams, J., Sherlock, G., & Rosenzweig, F. (2014). Ex uno plures: clonal reinforcement drives evolution of a simple microbial community. *PLoS Genet, 10*(6), e1004430. doi:10.1371/journal.pgen.1004430

Klinner, U., Fluthgraf, S., Freese, S., & Passoth, V. (2005). Aerobic induction of respiro-fermentative growth by decreasing oxygen tensions in the respiratory yeast Pichia stipitis. *Appl Microbiol Biotechnol, 67*(2), 247-253. doi:10.1007/s00253-004-1746-8

Kocabas, F., Xie, L., Xie, J., Yu, Z., DeBerardinis, R. J., Kimura, W., . . . Zheng, J. (2015). Hypoxic metabolism in human hematopoietic stem cells. *Cell & Bioscience, 5*, 39. doi:10.1186/s13578-015-0020-3

Kondo, A., Shigechi, H., Abe, M., Uyama, K., Matsumoto, T., Takahashi, S., . . . Fukuda, H. (2002). High-level ethanol production from starch by a flocculent Saccharomyces cerevisiae strain displaying cell-surface glucoamylase. *Appl Microbiol Biotechnol, 58*(3), 291-296. doi:10.1007/s00253-001-0900-9

Koschwanez, J. H., Foster, K. R., & Murray, A. W. (2013). Improved use of a public good selects for the evolution of undifferentiated multicellularity. *Elife, 2*, e00367. doi:10.7554/eLife.00367

Kourtis, N., & Tavernarakis, N. (2011). Cellular stress response pathways and ageing: intricate molecular relationships. *The EMBO Journal, 30*(13), 2520-2531. doi:10.1038/emboj.2011.162

Kreft, J.-U., & Bonhoeffer, S. (2005). The evolution of groups of cooperating bacteria and the growth rate versus yield trade-off. *Microbiology, 151*(3), 637-641. doi:doi:10.1099/mic.0.27415-0

Krisch, J., & Szajani, B. (1997). Ethanol and acetic acid tolerance in free and immobilized cells of Saccharomyces cerevisiae and Acetobacter aceti. *Biotechnol Lett, 19*(6), 525-528. doi:10.1023/a:1018329118396

Krishnan, M. S., Nghiem, N. P., & Davison, B. H. (1999). Ethanol Production from Corn Starch in a Fluidized-Bed Bioreactor. In B. H. Davison & M. Finkelstein (Eds.), *Twentieth Symposium on Biotechnology for Fuels and Chemicals: Presented as Volumes 77–79 of Applied Biochemistry and Biotechnology Proceedings of the Twentieth Symposium on Biotechnology for Fuels and Chemicals Held May 3–7, 1998, Gatlinburg, Tennessee* (pp. 359-372). Totowa, NJ: Humana Press.

Kruckeberg, A. L., Nagarajan, S., McInnerney, K., & Rosenzweig, F. (2009). Extraction of RNA from Ca-Alginate Encapsulated Yeast for Transcriptional Profiling. *Anal Biochem, 391*(2), 160-162. doi:10.1016/j.ab.2009.04.032

Krupp, D. B. (2016). Causality and the Levels of Selection. *Trends Ecol Evol, 31*(4), 255-257. doi:10.1016/j.tree.2016.01.008

Kubitschek, H. E. (1954). Modifications of the chemostat. *J Bacteriol, 67*(2), 254-255.

Kuhad, R. C., Gupta, R., Khasa, Y. P., Singh, A., & Zhang, Y. H. P. (2011). Bioethanol production from pentose sugars: Current status and future prospects. *Renewable and Sustainable Energy Reviews, 15*(9), 4950-4962. doi:https://doi.org/10.1016/j.rser.2011.07.058

Kwan, E. X., Foss, E., Kruglyak, L., & Bedalov, A. (2011). Natural polymorphism in BUL2 links cellular amino acid availability with chronological aging and telomere maintenance in yeast. *PLoS Genet, 7*(8), e1002250. doi:10.1371/journal.pgen.1002250

Laca, A., García, L. A., & Díaz, M. (2000). Analysis and description of the evolution of alginate immobilised cells systems. *J Biotechnol, 80*(3), 203-215. doi:https://doi.org/10.1016/S0168-1656(00)00252-2

Larroche, C., Cruely, C., & Gros, J.-B. (1995). Fed-batch biotransformation of β-ionone by Aspergillus niger. *Applied Microbiology and Biotechnology, 43*(2), 222-227. doi:10.1007/bf00172816

Lawford, H. G., & Rousseau, J. D. (2003). Cellulosic Fuel Ethanol. In B. H. Davison, J. W. Lee, M. Finkelstein, & J. D. McMillan (Eds.), *Biotechnology for Fuels and Chemicals: The Twenty-Fourth Symposium* (pp. 457-469). Totowa, NJ: Humana Press.

Lebeau, T., Jouenne, T., & Junter, G. A. (2007). Long-term incomplete xylose fermentation, after glucose exhaustion, with Candida shehatae co-immobilized with Saccharomyces cerevisiae. *Microbiological Research, 162*(3), 211-218. doi:https://doi.org/10.1016/j.micres.2006.07.005

Lee, C., & Longo, V. (2016). Dietary restriction with and without caloric restriction for healthy aging. *F1000Res, 5*. doi:10.12688/f1000research.7136.1

Lee, C. R., Sung, B. H., Lim, K. M., Kim, M. J., Sohn, M. J., Bae, J. H., & Sohn, J. H. (2017). Co-fermentation using Recombinant Saccharomyces cerevisiae Yeast Strains Hyper-secreting Different Cellulases for the Production of Cellulosic Bioethanol. *Sci Rep, 7*(1), 4428. doi:10.1038/s41598-017-04815-1

Lee, J. (1997). Biological conversion of lignocellulosic biomass to ethanol. *J Biotechnol, 56*(1), 1-24.

Lee, K. H., Choi, I. S., Kim, Y. G., Yang, D. J., & Bae, H. J. (2011). Enhanced production of bioethanol and ultrastructural characteristics of reused Saccharomyces cerevisiae immobilized calcium alginate beads. *Bioresour Technol, 102*(17), 8191-8198. doi:10.1016/j.biortech.2011.06.063

Lee, S. T., Mitchell, R. B., Wang, Z., Heiss, C., Gardner, D. R., & Azadi, P. (2009). Isolation, characterization, and quantification of steroidal saponins in switchgrass (Panicum virgatum L.). *J Agric Food Chem, 57*(6), 2599-2604. doi:10.1021/jf803907y

Lee, W. C., & Kuan, W. C. (2015). Miscanthus as cellulosic biomass for bioethanol production. *Biotechnol J, 10*(6), 840-854. doi:10.1002/biot.201400704

Lei, J., Zhao, X., Ge, X., & Bai, F. (2007). Ethanol tolerance and the variation of plasma membrane composition of yeast floc populations with different size distribution. *J Biotechnol, 131*(3), 270-275. doi:10.1016/j.jbiotec.2007.07.937

Lemons, J. M., Feng, X. J., Bennett, B. D., Legesse-Miller, A., Johnson, E. L., Raitman, I., . . . Coller, H. A. (2010). Quiescent fibroblasts exhibit high metabolic activity. *PLoS Biol, 8*(10), e1000514. doi:10.1371/journal.pbio.1000514

Leo, W. J., McLoughlin, A. J., & Malone, D. M. (1990). Effects of sterilization treatments on some properties of alginate solutions and gels. *Biotechnol Prog, 6*(1), 51-53. doi:10.1021/bp00001a008

Leontieva, O. V., & Blagosklonny, M. V. (2011). Yeast-like chronological senescence in mammalian cells: phenomenon, mechanism and pharmacological suppression. *Aging (Albany NY), 3*(11), 1078-1091.

Lewis, J. G., Northcott, C. J., Learmonth, R. P., Attfield, P. V., & Watson, K. (1993). The need for consistent nomenclature and assessment of growth phases in diauxic cultures of Saccharomyces cerevisiae. *Microbiology, 139*(4), 835-839. doi:doi:10.1099/00221287-139-4-835

Li, G.-Y., Huang, K.-L., Jiang, Y.-R., & Ding, P. (2007). Production of (R)-mandelic acid by immobilized cells of Saccharomyces cerevisiae on chitosan carrier. *Process Biochemistry, 42*(10), 1465-1469. doi:https://doi.org/10.1016/j.procbio.2007.06.015

Li, S. I., Buttery, N. J., Thompson, C. R., & Purugganan, M. D. (2014). Sociogenomics of self vs. non-self cooperation during development of Dictyostelium discoideum. *BMC Genomics, 15*, 616. doi:10.1186/1471-2164-15-616

Li, X. (1996). The use of chitosan to increase the stability of calcium alginate beads with entrapped yeast cells. *Biotechnol Appl Biochem, 23*(3), 269-272.

Libby, E., Conlin, P. L., Kerr, B., & Ratcliff, W. C. (2016). Stabilizing multicellularity through ratcheting. *Philos Trans R Soc Lond B Biol Sci, 371*(1701). doi:10.1098/rstb.2015.0444

Libby, E., Ratcliff, W., Travisano, M., & Kerr, B. (2014). Geometry Shapes Evolution of Early Multicellularity. *PLoS Comput Biol, 10*(9), e1003803. doi:10.1371/journal.pcbi.1003803

Libby, E., & Ratcliff, W. C. (2014). Ratcheting the evolution of multicellularity. *Science, 346*(6208), 426-427. doi:10.1126/science.1262053

Lin, C.-C., & Anseth, K. S. (2011). Cell–cell communication mimicry with poly(ethylene glycol) hydrogels for enhancing β-cell function. *Proceedings of the National Academy of Sciences, 108*(16), 6380-6385. doi:10.1073/pnas.1014026108

Lin, C.-C., Hsieh, P.-C., Mau, J.-L., & Teng, D.-F. (2005). Construction of an intergeneric fusion from Schizosaccharomyces pombe and Lentinula edodes for xylan degradation and polyol production. *Enzyme and Microbial Technology, 36*(1), 107-117.

Lin, S.-J., Kaeberlein, M., Andalis, A. A., Sturtz, L. A., Defossez, P.-A., Culotta, V. C., . . . Guarente, L. (2002). Calorie restriction extends Saccharomyces cerevisiae lifespan by increasing respiration. *Nature, 418*, 344. doi:10.1038/nature00829

https://www.nature.com/articles/nature00829#supplementary-information

Liska, A. J., Yang, H. S., Bremer, V. R., Klopfenstein, T. J., Walters, D. T., Erickson, G. E., & Cassman, K. G. (2009). Improvements in Life Cycle Energy Efficiency and Greenhouse Gas Emissions of Corn-Ethanol. *Journal of Industrial Ecology, 13*(1), 58-74. doi:10.1111/j.1530-9290.2008.00105.x

Liu, C. G., Xiao, Y., Xia, X. X., Zhao, X. Q., Peng, L., Srinophakun, P., & Bai, F. W. (2019). Cellulosic ethanol production: Progress, challenges and strategies for solutions. *Biotechnol Adv, 37*(3), 491-504. doi:10.1016/j.biotechadv.2019.03.002

Liu, E., & Hu, Y. (2010). Construction of a xylose-fermenting Saccharomyces cerevisiae strain by combined approaches of genetic engineering, chemical mutagenesis and evolutionary adaptation. *Biochemical Engineering Journal, 48*(2), 204-210.

Liu, F., Wu, W., Tran-Gyamfi, M. B., Jaryenneh, J. D., Zhuang, X., & Davis, R. W. (2017). Bioconversion of distillers' grains hydrolysates to advanced biofuels by an

Escherichia coli co-culture. *Microb Cell Fact, 16*(1), 192. doi:10.1186/s12934-017-0804-8

Longo, V. D., & Fabrizio, P. (2012). Chronological Aging in Saccharomyces cerevisiae. *Subcell Biochem, 57*, 101-121. doi:10.1007/978-94-007-2561-4_5

Longo, V. D., Gralla, E. B., & Valentine, J. S. (1996). Superoxide dismutase activity is essential for stationary phase survival in Saccharomyces cerevisiae. Mitochondrial production of toxic oxygen species in vivo. *J Biol Chem, 271*(21), 12275-12280.

Lú Chau, T., Guillán, A., Roca, E., Núñez, M. J., & Lema, J. M. (2000). Enhancement of plasmid stability and enzymatic expression by immobilising recombinant Saccharomyces cerevisiae. *Biotechnol Lett, 22*(15), 1247-1250. doi:10.1023/a:1005669618337

Lu, X., Li, Y., Duan, Z., Shi, Z., & Mao, Z. (2003). A novel, repeated fed-batch, ethanol production system with extremely long term stability achieved by fully recycling fermented supernatants. *Biotechnol Lett, 25*(21), 1819-1826. doi:10.1023/a:1026265513392

Lutermann, H., Bennett, N. C., Speakman, J. R., & Scantlebury, M. (2013). Energetic benefits of sociality offset the costs of parasitism in a cooperative mammal. *PLoS One, 8*(2), e57969. doi:10.1371/journal.pone.0057969

Lynd, L. R., Liang, X., Biddy, M. J., Allee, A., Cai, H., Foust, T., . . . Wyman, C. E. (2017). Cellulosic ethanol: status and innovation. *Curr Opin Biotechnol, 45*, 202-211. doi:10.1016/j.copbio.2017.03.008

Lynd, L. R., Liang, X., Biddy, M. J., Allee, A., Cai, H., Foust, T., . . . Wyman, C. E. (2017). Cellulosic ethanol: status and innovation. *Current Opinion in Biotechnology, 45*, 202-211. doi:https://doi.org/10.1016/j.copbio.2017.03.008

Machado, A. H. E., Lundberg, D., Ribeiro, A. J., Veiga, F. J., Miguel, M. G., Lindman, B., & Olsson, U. (2013). Encapsulation of DNA in Macroscopic and Nanosized Calcium Alginate Gel Particles. *Langmuir, 29*(51), 15926-15935. doi:10.1021/la4032927

Maclean, R., & Brandon, C. (2008). Stable public goods cooperation and dynamic social interactions in yeast. *J Evol Biol, 21*(6), 1836-1843.

Madeo, F., Engelhardt, S., Herker, E., Lehmann, N., Maldener, C., Proksch, A., . . . Frohlich, K. U. (2002). Apoptosis in yeast: A new model system with applications in cell biology and medicine. *Curr Genet, 41*(4), 208-216. doi:10.1007/s00294-002-0310-2

Madeo, F., Herker, E., Maldener, C., Wissing, S., Lächelt, S., Herlan, M., . . . Fröhlich, K.-U. (2002). A caspase-related protease regulates apoptosis in yeast. *Mol Cell, 9*(4), 911-917. doi:https://doi.org/10.1016/S1097-2765(02)00501-4

Magrassi, L., Leto, K., & Rossi, F. (2013). Lifespan of neurons is uncoupled from organismal lifespan. *Proc Natl Acad Sci U S A, 110*(11), 4374-4379. doi:10.1073/pnas.1217505110

Mai, B., & Breeden, L. (1997). Xbp1, a stress-induced transcriptional repressor of the Saccharomyces cerevisiae Swi4/Mbp1 family. *Mol Cell Biol, 17*(11), 6491-6501.

Marguerat, S., Schmidt, A., Codlin, S., Chen, W., Aebersold, R., & Bahler, J. (2012). Quantitative analysis of fission yeast transcriptomes and proteomes in proliferating and quiescent cells. *Cell, 151*(3), 671-683. doi:10.1016/j.cell.2012.09.019

Marsden, C. D., Ortega-Del Vecchyo, D., O'Brien, D. P., Taylor, J. F., Ramirez, O., Vila, C., . . . Lohmueller, K. E. (2016). Bottlenecks and selective sweeps during domestication have increased deleterious genetic variation in dogs. *Proc Natl Acad Sci U S A, 113*(1), 152-157. doi:10.1073/pnas.1512501113

Maršíková, J., Wilkinson, D., Hlaváček, O., Gilfillan, G. D., Mizeranschi, A., Hughes, T., . . . Palková, Z. (2017). Metabolic differentiation of surface and invasive cells of yeast colony biofilms revealed by gene expression profiling. *BMC Genomics, 18*, 814. doi:10.1186/s12864-017-4214-4

McAloon, A., Taylor, F., Yee, W., Ibsen, K., & Wooley, R. (2000). *Determining the Cost of Producing Ethanol from Corn Starch and Lignocellulosic Feedstocks* (NREL/TP-580-28893; TRN: AH200037%%393 United States 10.2172/766198 TRN: AH200037%%393 NREL English). Retrieved from https://www.osti.gov/servlets/purl/766198

McGhee, J. E., Julian, G. S., Detroy, R. W., & Bothast, R. J. (1982a). Ethanol production by immobilized Saccharomyces cerevisiae, Saccharomyces uvarum, and Zymomonas mobilis. *Biotechnol Bioeng, 24*(5), 1155-1163. doi:10.1002/bit.260240512

McGhee, J. E., Julian, G. S., Detroy, R. W., & Bothast, R. J. (1982b). Ethanol production by immobilized Saccharomyces cerevisiae, Saccharomyces uvarum, and Zymomonas mobilis. *Biotechnology and Bioengineering, 24*(5), 1155-1163. doi:10.1002/bit.260240512

McGhee, J. E., St Julian, G., & Detroy, R. W. (1982). Continuous and static fermentation of glucose to ethanol by immobilized Saccharomyces cerevisiae cells of different ages. *Appl Environ Microbiol, 44*(1), 19-22.

Melaina, M. W. (2007). Turn of the century refueling: A review of innovations in early gasoline refueling methods and analogies for hydrogen. *Energy Policy, 35*(10), 4919-4934. doi:https://doi.org/10.1016/j.enpol.2007.04.008

Meng, F., Ibbett, R., de Vrije, T., Metcalf, P., Tucker, G., & McKechnie, J. (2019). Process simulation and life cycle assessment of converting autoclaved municipal solid

waste into butanol and ethanol as transport fuels. *Waste Manag, 89*, 177-189. doi:10.1016/j.wasman.2019.04.003

Meunier, J. R., & Choder, M. (1999). Saccharomyces cerevisiae colony growth and ageing: biphasic growth accompanied by changes in gene expression. *Yeast, 15*(12), 1159-1169. doi:10.1002/(sici)1097-0061(19990915)15:12<1159::aid-yea441>3.0.co;2-d

Miceli, M. V., Jiang, J. C., Tiwari, A., Rodriguez-Quinones, J. F., & Jazwinski, S. M. (2011). Loss of mitochondrial membrane potential triggers the retrograde response extending yeast replicative lifespan. *Front Genet, 2*, 102. doi:10.3389/fgene.2011.00102

Miles, S., Li, L., Davison, J., & Breeden, L. L. (2013). Xbp1 directs global repression of budding yeast transcription during the transition to quiescence and is important for the longevity and reversibility of the quiescent state. *PLoS Genet, 9*(10), e1003854. doi:10.1371/journal.pgen.1003854

Miličević B., B. J., Ačkar Đ., Miličević R., Jozinović A., Jukić H., Babić V., Šubarić D. . (2017). Sparkling wine production by immobilised yeast fermentation. *Czech J. Food Sci., 35*, 171-179.

Mináriková, L., Kuthan, M., Řičicová, M., Forstová, J., & Palková, Z. (2001). Differentiated Gene Expression in Cells within Yeast Colonies. *Exp Cell Res, 271*(2), 296-304. doi:https://doi.org/10.1006/excr.2001.5379

Mizunuma, T. (1986). Soy saucelike production. *Bimonthly J. Microorg., 2*, 35.

Mohagheghi, A., Evans, K., Chou, Y.-C., & Zhang, M. (2002). SESSION 3-BIOPROCESS RESEARCH AND DEVELOPMENT-Cofermentation of Glucose, Xylose, and Arabinose by Genomic DNA-Integrated Xylose/Arabinose Fermenting Strain of Zymomonas mobilis AX101. *Applied Biochemistry and Biotechnology-Part A-Enzyme Engineering and Biotechnology, 98*, 885-898.

Mohd Azhar, S. H., Abdulla, R., Jambo, S. A., Marbawi, H., Gansau, J. A., Mohd Faik, A. A., & Rodrigues, K. F. (2017). Yeasts in sustainable bioethanol production: A review. *Biochemistry and Biophysics Reports, 10*, 52-61. doi:https://doi.org/10.1016/j.bbrep.2017.03.003

Monod, J. (1950). La technique de culture continue: theorie et applications.

Montarras, D., L'Honore, A., & Buckingham, M. (2013). Lying low but ready for action: the quiescent muscle satellite cell. *Febs j, 280*(17), 4036-4050. doi:10.1111/febs.12372

Moreno-Garcia, J., Garcia-Martinez, T., Mauricio, J. C., & Moreno, J. (2018). Yeast Immobilization Systems for Alcoholic Wine Fermentations: Actual Trends and Future Perspectives. *Front Microbiol, 9*, 241. doi:10.3389/fmicb.2018.00241

Mortimer, R. K., & Johnston, J. R. (1959). Life span of individual yeast cells. *Nature, 183*(4677), 1751-1752.

Mortimer, R. K., & Johnston, J. R. (1986). Genealogy of principal strains of the yeast genetic stock center. *Genetics, 113*(1), 35-43.

Muller, N. A., Wijnen, C. L., Srinivasan, A., Ryngajllo, M., Ofner, I., Lin, T., . . . Maloof, J. N. (2016). Domestication selected for deceleration of the circadian clock in cultivated tomato. *48*(1), 89-93. doi:10.1038/ng.3447

Mutturi, S., & Lidén, G. (2013). *Effect of Temperature on Simultaneous Saccharification and Fermentation of Pretreated Spruce and Arundo* (Vol. 52).

Myers, J. A., Curtis, B. S., & Curtis, W. R. (2013). Improving accuracy of cell and chromophore concentration measurements using optical density. *BMC Biophysics, 6*(1), 4. doi:10.1186/2046-1682-6-4

Nagarajan, S., Kruckeberg, A. L., Schmidt, K. H., Kroll, E., Hamilton, M., McInnerney, K., . . . Rosenzweig, F. (2014). Uncoupling reproduction from metabolism extends chronological lifespan in yeast. *Proc Natl Acad Sci U S A, 111*(15), E1538-1547. doi:10.1073/pnas.1323918111

Nanalyze. (2017). Retrieved from http://www.nanalyze.com/2017/03/electric-cars-usa/

Naouri, P., Bernet, N., Chagnaud, P., Arnaud, A., Galzy, P., & Rios, G. (2007). *Bioconversion of L-malic acid into L-lactic acid using a high compacting multiphase reactor (HCMR)* (Vol. 51).

Nasri, M., Sayadi, S., Barbotin, J. N., Dhulster, P., & Thomas, D. (1987). Influence of immobilization on the stability of pTG201 recombinant plasmid in some strains of Escherichia coli. *Appl Environ Microbiol, 53*(4), 740-744.

Nasri, M., Sayadi, S., Barbotin, J. N., & Thomas, D. (1987). The use of the immobilization of whole living cells to increase stability of recombinant plasmids in escherichia coli. *J Biotechnol, 6*(2), 147-157. doi:https://doi.org/10.1016/0168-1656(87)90052-6

Naydenova, V., Badova, M., Vassilev, S., Iliev, V., Kaneva, M., & Kostov, G. (2014). Encapsulation of brewing yeast in alginate/chitosan matrix: lab-scale optimization of lager beer fermentation. *Biotechnology, biotechnological equipment, 28*(2), 277-284. doi:10.1080/13102818.2014.910373

Nedović, V., Gibson, B., Mantzouridou, T. F., Bugarski, B., Djordjević, V., Kalušević, A., . . . Yilmaztekin, M. (2015). Aroma formation by immobilized yeast cells in fermentation processes. *Yeast (Chichester, England), 32*(1), 173-216. doi:10.1002/yea.3042

Neganova, I., & Lako, M. (2008). G1 to S phase cell cycle transition in somatic and embryonic stem cells. *J Anat, 213*(1), 30-44. doi:10.1111/j.1469-7580.2008.00931.x

Newbold, A., Martin, B. P., Cullinane, C., & Bots, M. (2014). Detection of apoptotic cells using propidium iodide staining. *Cold Spring Harb Protoc, 2014*(11), 1202-1206. doi:10.1101/pdb.prot082545

News, N. P. (2004).

Nichols, N. N., & Bothast, R. J. (2008). Production of Ethanol from Grain. In W. Vermerris (Ed.), *Genetic Improvement of Bioenergy Crops* (pp. 75-88). New York, NY: Springer New York.

Norton, S., & D'Amore, T. (1994). Physiological effects of yeast cell immobilization: Applications for brewing. *Enzyme and Microbial Technology, 16*(5), 365-375. doi:https://doi.org/10.1016/0141-0229(94)90150-3

Norton, S., Watson, K., & D'Amore, T. (1995). Ethanol tolerance of immobilized brewers' yeast cells. *Appl Microbiol Biotechnol, 43*(1), 18-24.

Novick, A., & Szilard, L. (1950a). Description of the chemostat. *Science, 112*(2920), 715-716.

Novick, A., & Szilard, L. (1950b). Experiments with the Chemostat on spontaneous mutations of bacteria. *Proc Natl Acad Sci U S A, 36*(12), 708-719.

Nowak, M. A., Tarnita, C. E., & Wilson, E. O. (2010). The evolution of eusociality. *Nature, 466*(7310), 1057-1062. doi:10.1038/nature09205

Nunokawa, Y., and Hirotsune, M. . (1993). Production of soft sake by an immobilized yeast reactor system. In T. T. A. Tanaka, T. Kobayashi (Ed.), *Industrial Applications of Immobilized Biocatalysts* (pp. 235-253): New York and Basel: Marcel Dekker, Inc.

Nussinovitch, A. (2010). Bead Formation, Strengthening, and Modification. In A. Nussinovitch (Ed.), *Polymer Macro- and Micro-Gel Beads: Fundamentals and Applications* (pp. 27-52). New York, NY: Springer New York.

Nussinovitch, A. (2010). *Polymer Macro- and Micro-Gel Beads: Fundamentals and Applications*: Springer New York.

O'Brien, D. J., & Craig, J. C. (1996). Ethanol production in a continuous fermentation/membrane pervaporation system. *Applied Microbiology and Biotechnology, 44*(6), 699-704. doi:10.1007/bf00178605

Oberto, J., Breuil, N., Hecker, A., Farina, F., Brochier-Armanet, C., Culetto, E., & Forterre, P. (2009). Qri7/OSGEPL, the mitochondrial version of the universal Kae1/YgjD

protein, is essential for mitochondrial genome maintenance. *Nucleic Acids Research, 37*(16), 5343-5352. doi:10.1093/nar/gkp557

Ohta, K., Beall, D., Mejia, J., Shanmugam, K., & Ingram, L. (1991). Genetic improvement of Escherichia coli for ethanol production: chromosomal integration of Zymomonas mobilis genes encoding pyruvate decarboxylase and alcohol dehydrogenase II. *Appl. Environ. Microbiol., 57*(4), 893-900.

Okasha, S. (2006). *Evolution and the Levels of Selection*: Clarendon Press.

Olderoy, M. O., Xie, M., Andreassen, J. P., Strand, B. L., Zhang, Z., & Sikorski, P. (2012). Viscoelastic properties of mineralized alginate hydrogel beads. *J Mater Sci Mater Med, 23*(7), 1619-1627. doi:10.1007/s10856-012-4655-x

Oliver, J. D. (2005). The viable but nonculturable state in bacteria. *The Journal of Microbiology, 43*(1), 93-100.

Orlandi, I., Ronzulli, R., Casatta, N., & Vai, M. (2013). Ethanol and Acetate Acting as Carbon/Energy Sources Negatively Affect Yeast Chronological Aging. *Oxid Med Cell Longev, 2013*, 10. doi:10.1155/2013/802870

Oud, B., Guadalupe-Medina, V., Nijkamp, J. F., de Ridder, D., Pronk, J. T., van Maris, A. J., & Daran, J. M. (2013). Genome duplication and mutations in ACE2 cause multicellular, fast-sedimenting phenotypes in evolved Saccharomyces cerevisiae. *Proc Natl Acad Sci U S A, 110*(45), E4223-4231. doi:10.1073/pnas.1305949110

Ouwerx, C., Velings, N., Mestdagh, M., & Axelos, M. (1998). Physico-chemical properties and rheology of alginate gel beads formed with various divalent cations. *Polymer Gels and Networks, 6*(5), 393-408.

Ouwerx, C., Velings, N., Mestdagh, M. M., & Axelos, M. A. V. (1998). Physico-chemical properties and rheology of alginate gel beads formed with various divalent cations. *Polymer Gels and Networks, 6*(5), 393-408. doi:https://doi.org/10.1016/S0966-7822(98)00035-5

Palkova, Z., Devaux, F., Icicova, M., Minarikova, L., Le Crom, S., & Jacq, C. (2002). Ammonia pulses and metabolic oscillations guide yeast colony development. *Mol Biol Cell, 13*(11), 3901-3914. doi:10.1091/mbc.e01-12-0149

Palkova, Z., & Vachova, L. (2006). Life within a community: benefit to yeast long-term survival. *FEMS Microbiol Rev, 30*(5), 806-824. doi:10.1111/j.1574-6976.2006.00034.x

Palková, Z., & Váchová, L. (2003). Ammonia signaling in yeast colony formation *International Review of Cytology* (Vol. 225, pp. 229-272): Academic Press.

Palkova, Z., Vachova, L., Gaskova, D., & Kucerova, H. (2009). Synchronous plasma membrane electrochemical potential oscillations during yeast colony development and aging. *Mol Membr Biol, 26*(4), 228-235. doi:10.1080/09687680902893130

Palkova, Z., Wilkinson, D., & Vachova, L. (2014). Aging and differentiation in yeast populations: elders with different properties and functions. *FEMS Yeast Res, 14*(1), 96-108. doi:10.1111/1567-1364.12103

Panchal, C. J., Bast, L., Russell, I., & Stewart, G. G. (1988). Repression of xylose utilization by glucose in xylose-fermenting yeasts. *Can J Microbiol, 34*(12), 1316-1320. doi:10.1139/m88-230

Pandey, A., Nigam, P., Soccol, C. R., Soccol, V. T., Singh, D., & Mohan, R. (2000). Advances in microbial amylases. *Biotechnol Appl Biochem, 31 (Pt 2)*, 135-152. doi:10.1042/ba19990073

Pardee, A. B. (1974). A restriction point for control of normal animal cell proliferation. *Proc Natl Acad Sci U S A, 71*(4), 1286-1290.

Park, J. K., & Chang, H. N. (2000). Microencapsulation of microbial cells. *Biotechnology Advances, 18*(4), 303-319. doi:https://doi.org/10.1016/S0734-9750(00)00040-9

Pasha, C., Kuhad, R., & Rao, L. V. (2007). Strain improvement of thermotolerant Saccharomyces cerevisiae VS3 strain for better utilization of lignocellulosic substrates. *J Appl Microbiol, 103*(5), 1480-1489.

Pate, R., Klise, G., & Wu, B. (2011). Resource demand implications for US algae biofuels production scale-up. *Applied Energy, 88*(10), 3377-3388. doi:https://doi.org/10.1016/j.apenergy.2011.04.023

Pentz, J., Taylor, B. P., & Ratcliff, W. C. (2015). Apoptosis in snowflake yeast: Novel trait, or side effect of toxic waste? *bioRxiv*. doi:10.1101/029918

Pereira, F. B., Gomes, D. G., Guimarães, P. M. R., Teixeira, J. A., & Domingues, L. (2012). Cell recycling during repeated very high gravity bio-ethanol fermentations using the industrial Saccharomyces cerevisiae strain PE-2. *Biotechnol Lett, 34*(1), 45-53. doi:10.1007/s10529-011-0735-0

Perrone, G. G., Tan, S. X., & Dawes, I. W. (2008). Reactive oxygen species and yeast apoptosis. *Biochim Biophys Acta, 1783*(7), 1354-1368. doi:10.1016/j.bbamcr.2008.01.023

Petralia, R. S., Mattson, M. P., & Yao, P. J. (2014). Aging and longevity in the simplest animals and the quest for immortality. *Ageing Res Rev, 16*, 66-82. doi:10.1016/j.arr.2014.05.003

Pimentel, D. (1991). Ethanol fuels: Energy security, economics, and the environment. *Journal of Agricultural and Environmental Ethics, 4*(1), 1-13. doi:10.1007/bf02229143

Piper, P. W., Harris, N. L., & MacLean, M. (2006). Preadaptation to efficient respiratory maintenance is essential both for maximal longevity and the retention of replicative potential in chronologically ageing yeast. *Mech Ageing Dev, 127*(9), 733-740. doi:10.1016/j.mad.2006.05.004

Plessas, S., Bekatorou, A., Koutinas, A. A., Soupioni, M., Banat, I. M., & Marchant, R. (2007a). Use of Saccharomyces cerevisiae cells immobilized on orange peel as biocatalyst for alcoholic fermentation. *Bioresour Technol, 98*(4), 860-865. doi:10.1016/j.biortech.2006.03.014

Plessas, S., Bekatorou, A., Koutinas, A. A., Soupioni, M., Banat, I. M., & Marchant, R. (2007b). Use of Saccharomyces cerevisiae cells immobilized on orange peel as biocatalyst for alcoholic fermentation. *Bioresour Technol, 98*(4), 860-865. doi:https://doi.org/10.1016/j.biortech.2006.03.014

Powers, R. W., 3rd, Kaeberlein, M., Caldwell, S. D., Kennedy, B. K., & Fields, S. (2006). Extension of chronological life span in yeast by decreased TOR pathway signaling. *Genes Dev, 20*(2), 174-184. doi:10.1101/gad.1381406

Qazizada, M. E. (2016). Design of a Batch Stirred Fermenter for Ethanol Production. *Procedia Engineering, 149*, 389-403. doi:https://doi.org/10.1016/j.proeng.2016.06.684

Qin, H., & Lu, M. (2006). Natural variation in replicative and chronological life spans of Saccharomyces cerevisiae. *Exp Gerontol, 41*(4), 448-456. doi:https://doi.org/10.1016/j.exger.2006.01.007

Queller, D. C., Ponte, E., Bozzaro, S., & Strassmann, J. E. (2003). Single-Gene Greenbeard Effects in the Social Amoeba Dictyostelium discoideum. *Science, 299*(5603), 105-106. doi:10.1126/science.1077742

Queller, D. C., & Strassmann, J. E. (2009). Beyond society: The evolution of organismality. *Philosophical Transactions of the Royal Society of London B: Biological Sciences, 364*(1533), 3143-3155. doi:10.1098/rstb.2009.0095

Qun, J., Shanjing, Y., & Lehe, M. (2002). Tolerance of immobilized baker's yeast in organic solvents. *Enzyme and Microbial Technology, 30*(6), 721-725. doi:https://doi.org/10.1016/S0141-0229(02)00048-0

Qureshi, A. S., Zhang, J., & Bao, J. (2015). Cellulosic ethanol fermentation using Saccharomyces cerevisiae seeds cultured by pretreated corn stover material. *Appl Biochem Biotechnol, 175*(6), 3173-3183. doi:10.1007/s12010-015-1480-y

Ramachandra Rao, S., & Ravishankar, G. A. (2000). Vanilla flavour: production by conventional and biotechnological routes. *Journal of the Science of Food and Agriculture, 80*(3), 289-304. doi:doi:10.1002/1097-0010(200002)80:3<289::AID-JSFA543>3.0.CO;2-2

Ratcliff, W. C., Denison, R. F., Borrello, M., & Travisano, M. (2012). Experimental evolution of multicellularity. *Proceedings of the National Academy of Sciences, 109*(5), 1595-1600. doi:10.1073/pnas.1115323109

Ratcliff, W. C., Fankhauser, J. D., Rogers, D. W., Greig, D., & Travisano, M. (2015). Origins of multicellular evolvability in snowflake yeast. *Nat Commun, 6*, 6102. doi:10.1038/ncomms7102

Ratcliff, W. C., Hawthorne, P., & Libby, E. (2015). Courting disaster: How diversification rate affects fitness under risk. *Evolution, 69*(1), 126-135. doi:10.1111/evo.12568

Ratcliff, W. C., Herron, M., Conlin, P. L., & Libby, E. (2017). Nascent life cycles and the emergence of higher-level individuality. *Philos Trans R Soc Lond B Biol Sci, 372*(1735). doi:10.1098/rstb.2016.0420

Ratcliff, W. C., Herron, M. D., Howell, K., Pentz, J. T., Rosenzweig, F., & Travisano, M. (2013). Experimental evolution of an alternating uni- and multicellular life cycle in Chlamydomonas reinhardtii. *Nat Commun, 4*, 2742. doi:10.1038/ncomms3742

Ratcliff, W. C., Pentz, J. T., & Travisano, M. (2013). Tempo and mode of multicellular adaptation in experimentally evolved *Saccharomyces cerevisiae*. *Evolution, 67*(6), 1573-1581. doi:10.1111/evo.12101

Ratcliff, W. C., & Travisano, M. (2014). Experimental Evolution of Multicellular Complexity in Saccharomyces cerevisiae. *BioScience, 64*(5), 383-393. doi:10.1093/biosci/biu045

Restoration, O. o. R. a. (2013). Retrieved from https://response.restoration.noaa.gov/oil-and-chemical-spills/significant-incidents/exxon-valdez-oil-spill

Ribeiro, G. F., Corte-Real, M., & Johansson, B. (2006). Characterization of DNA damage in yeast apoptosis induced by hydrogen peroxide, acetic acid, and hyperosmotic shock. *Mol Biol Cell, 17*(10), 4584-4591. doi:10.1091/mbc.e06-05-0475

Riccardi, C., & Nicoletti, I. (2006). Analysis of apoptosis by propidium iodide staining and flow cytometry. *Nat Protoc, 1*, 1458. doi:10.1038/nprot.2006.238

Richard, P. (2003). The rhythm of yeast. *FEMS Microbiol Rev, 27*(4), 547-557.

Roberts, G. A. F. (1992). *Chitin chemistry*. London: Macmillan.

Rosebrock, A. P., & Caudy, A. A. (2017). Metabolite Extraction from Saccharomyces cerevisiae for Liquid Chromatography-Mass Spectrometry. *Cold Spring Harb Protoc, 2017*(9), pdb.prot089086. doi:10.1101/pdb.prot089086

Roukas, T. (1994). Ethanol production from nonsterilized carob pod extract by free and immobilized Saccharomyces cerevisiae cells using fed-batch culture. *Biotechnology and Bioengineering, 43*(3), 189-194. doi:doi:10.1002/bit.260430302

Roukas, T., & Kotzekidou, P. (1996). Continuous production of lactic acid from deproteinized whey by coimmobilized lactobacillus casei and lactococcus lactis cells in a packed-bed reactor. *Food Biotechnology, 10*(3), 231-242. doi:10.1080/08905439609549916

Rymowicz, W., Fatykhova, A. R., Kamzolova, S. V., Rywińska, A., & Morgunov, I. G. (2010). Citric acid production from glycerol-containing waste of biodiesel industry by Yarrowia lipolytica in batch, repeated batch, and cell recycle regimes. *Applied Microbiology and Biotechnology, 87*(3), 971-979. doi:10.1007/s00253-010-2561-z

Sabba, F., Terada, A., Wells, G., Smets, B. F., & Nerenberg, R. (2018). Nitrous oxide emissions from biofilm processes for wastewater treatment. *Appl Microbiol Biotechnol, 102*(22), 9815-9829. doi:10.1007/s00253-018-9332-7

Santos, A. L. S. D., Galdino, A. C. M., Mello, T. P. d., Ramos, L. d. S., Branquinha, M. H., Bolognese, A. M., . . . Roudbary, M. (2018). What are the advantages of living in a community? A microbial biofilm perspective! *Memorias do Instituto Oswaldo Cruz, 113*(9), e180212-e180212. doi:10.1590/0074-02760180212

Sauer, M., & Mattanovich, D. (2016). Non-genetic impact factors on chronological lifespan and stress resistance of baker's yeast. *Microbial Cell, 3*(6), 232-235. doi:10.15698/mic2016.06.504

Sayadi, S., Nasri, M., Berry, F., Barbotin, J. N., & Thomas, D. (1987). Effect of temperature on the stability of plasmid pTG201 and productivity of xylE gene product in recombinant Escherichia coli: development of a two-stage chemostat with free and immobilized cells. *J Gen Microbiol, 133*(7), 1901-1908. doi:10.1099/00221287-133-7-1901

Segale, L., Giovannelli, L., Mannina, P., & Pattarino, F. (2016). Calcium Alginate and Calcium Alginate-Chitosan Beads Containing Celecoxib Solubilized in a Self-Emulsifying Phase. *Scientifica (Cairo), 2016*, 8. doi:10.1155/2016/5062706

Shalsh, F., Ibrahim, A., Mohammed, A., & Meor Hussin, A. S. (2016). *Optimization of the Protoplast Fusion Conditions of Saccharomyces cerevisiae and Pichia stipitis for Improvement of Bioethanol Production from Biomass* (Vol. 9).

Shibata, K., Amemiya, T., Kawakita, Y., Obase, K., Itoh, K., Takinoue, M., . . . Yamaguchi, T. (2018). Promotion and inhibition of synchronous glycolytic oscillations in yeast by chitosan. *Febs j, 285*(14), 2679-2690. doi:10.1111/febs.14513

Silk, J. B., Alberts, S. C., & Altmann, J. (2003). Social bonds of female baboons enhance infant survival. *Science, 302*(5648), 1231-1234. doi:10.1126/science.1088580

Silva, D. P., Nogueira, D. S., & De Marco, P., Jr. (2016). Contrasting patterns in solitary and eusocial bees while responding to landscape features in the Brazilian cerrado: A multiscaled perspective. *Neotrop Entomol*. doi:10.1007/s13744-016-0461-3

Sirianuntapiboon, S., Jeeyachok, N., & Larplai, R. (2005). Sequencing batch reactor biofilm system for treatment of milk industry wastewater. *J Environ Manage, 76*(2), 177-183. doi:https://doi.org/10.1016/j.jenvman.2005.01.018

Sleight, S. C., Bartley, B. A., Lieviant, J. A., & Sauro, H. M. (2010). Designing and engineering evolutionary robust genetic circuits. *Journal of Biological Engineering, 4*(1), 1-20. doi:10.1186/1754-1611-4-12

Slininger, P. J., Thompson, S. R., Weber, S., Liu, Z. L., & Moon, J. (2011). Repression of xylose-specific enzymes by ethanol in Scheffersomyces (Pichia) stipitis and utility of repitching xylose-grown populations to eliminate diauxic lag. *Biotechnology and Bioengineering, 108*(8), 1801-1815. doi:10.1002/bit.23119

Smith, D. L., Jr., McClure, J. M., Matecic, M., & Smith, J. S. (2007). Calorie restriction extends the chronological lifespan of Saccharomyces cerevisiae independently of the Sirtuins. *Aging Cell, 6*(5), 649-662. doi:10.1111/j.1474-9726.2007.00326.x

Smith, T. W. (1999). Aristotle on the conditions for and limits of the common good. *The American Political Science Review, 93*(3), 625-636. doi:10.2307/2585578

Smrdel, P., Bogataj, M., & Mrhar, A. (2008). The influence of selected parameters on the size and shape of alginate beads prepared by ionotropic gelation. *Scientia Pharmaceutica, 76*(1), 77-90.

Smrdel, P., Bogataj, M., Podlogar, F., Planinšek, O., Zajc, N., Mazaj, M., . . . Mrhar, A. (2006). Characterization of calcium alginate beads containing structurally similar drugs. *Drug development and industrial pharmacy, 32*(5), 623-633.

Sobering, A. K., Jung, U. S., Lee, K. S., & Levin, D. E. (2002). Yeast Rpi1 Is a Putative Transcriptional Regulator That Contributes to Preparation for Stationary Phase. *Eukaryot Cell, 1*(1), 56-65. doi:10.1128/EC.1.1.56-65.2002

Spencer, J. F., Spencer, D. M., & Reynolds, N. (1988). Genetic manipulation of non-conventional yeasts by conventional and non-conventional methods. *J Basic Microbiol, 28*(5), 321-333.

Spencer, S. L., Cappell, S. D., Tsai, F. C., Overton, K. W., Wang, C. L., & Meyer, T. (2013). The proliferation-quiescence decision is controlled by a bifurcation in CDK2 activity at mitotic exit. *Cell, 155*(2), 369-383. doi:10.1016/j.cell.2013.08.062

Sprinzak, D., & Elowitz, M. B. (2005). Reconstruction of genetic circuits. *Nature, 438*(7067), 443-448.

Sreenath, H. K., & Jeffries, T. W. (2000). Production of ethanol from wood hydrolyzate by yeasts. *Bioresour Technol, 72*(3), 253-260. doi:https://doi.org/10.1016/S0960-8524(99)00113-3

Steen, E. J., Kang, Y., Bokinsky, G., Hu, Z., Schirmer, A., McClure, A., . . . Keasling, J. D. (2010). Microbial production of fatty-acid-derived fuels and chemicals from plant biomass. *Nature, 463*(7280), 559-562. doi:10.1038/nature08721

Stouthamer, A. H. (1973). A theoretical study on the amount of ATP required for synthesis of microbial cell material. *Antonie van Leeuwenhoek, 39*(1), 545-565. doi:10.1007/bf02578899

Strassmann, J. E., Gilbert, O. M., & Queller, D. C. (2011). Kin discrimination and cooperation in microbes. *Annu Rev Microbiol, 65*, 349-367. doi:10.1146/annurev.micro.112408.134109

Strassmann, J. E., Zhu, Y., & Queller, D. C. (2000). Altruism and social cheating in the social amoeba Dictyostelium discoideum. *Nature, 408*(6815), 965-967.

Stumpferl, S. W., Brand, S. E., Jiang, J. C., Korona, B., Tiwari, A., Dai, J., . . . Jazwinski, S. M. (2012). Natural genetic variation in yeast longevity. *Genome Res, 22*(10), 1963-1973. doi:10.1101/gr.136549.111

Suarez-Mendez, A. C., Sousa, A., Heijnen, J. J., & Wahl, A. (2014). Fast "Feast/Famine" Cycles for Studying Microbial Physiology Under Dynamic Conditions: A Case Study with Saccharomyces cerevisiae. *Metabolites, 4*(2). doi:10.3390/metabo4020347

Sun, S., Luo, Y., Cao, S., Li, W., Zhang, Z., Jiang, L., . . . Wu, W.-M. (2013). Construction and evaluation of an exopolysaccharide-producing engineered bacterial strain by protoplast fusion for microbial enhanced oil recovery. *Bioresour Technol, 144*, 44-49. doi:https://doi.org/10.1016/j.biortech.2013.06.098

Sun, Z.-J., Lv, G.-J., Li, S.-Y., Xie, Y.-B., Yu, W.-T., Wang, W., & Ma, X.-J. (2007). Probing the role of microenvironment for microencapsulated Sacchromyces cerevisiae under osmotic stress. *J Biotechnol, 128*(1), 150-161. doi:10.1016/j.jbiotec.2006.09.001

Suzuki, S. W., Onodera, J., & Ohsumi, Y. (2011). Starvation induced cell death in autophagy-defective yeast mutants is caused by mitochondria dysfunction. *PLoS One, 6*(2), e17412. doi:10.1371/journal.pone.0017412

Swinnen, E., Ghillebert, R., Wilms, T., & Winderickx, J. (2014). Molecular mechanisms linking the evolutionary conserved TORC1-Sch9 nutrient signalling branch to lifespan regulation in Saccharomyces cerevisiae. *FEMS Yeast Res, 14*(1), 17-32. doi:10.1111/1567-1364.12097

Taherzadeh, M. J., Millati, R., & Niklasson, C. (2001). Continuous cultivation of dilute-acid hydrolysates to ethanol by immobilized Saccharomyces cerevisiae. *Appl Biochem Biotechnol, 95*(1), 45-57.

Taipa, M. A., Cabral, J. M., & Santos, H. (1993). Comparison of glucose fermentation by suspended and gel-entrapped yeast cells: An in vivo nuclear magnetic resonance study. *Biotechnol Bioeng, 41*(6), 647-653. doi:10.1002/bit.260410607

Takka, S., & Gürel, A. (2010). Evaluation of chitosan/alginate beads using experimental design: formulation and in vitro characterization. *AAPS PharmSciTech, 11*(1), 460-466. doi:10.1208/s12249-010-9406-z

Takubo, K., Nagamatsu, G., Kobayashi, Chiharu I., Nakamura-Ishizu, A., Kobayashi, H., Ikeda, E., . . . Suda, T. (2013). Regulation of Glycolysis by Pdk Functions as a Metabolic Checkpoint for Cell Cycle Quiescence in Hematopoietic Stem Cells. *Cell Stem Cell, 12*(1), 49-61. doi:10.1016/j.stem.2012.10.011

Talebnia, F., Niklasson, C., & Taherzadeh, M. J. (2005). Ethanol production from glucose and dilute-acid hydrolyzates by encapsulated S. cerevisiae. *Biotechnol Bioeng, 90*(3), 345-353. doi:10.1002/bit.20432

Talebnia, F., & Taherzadeh, M. J. (2006). In situ detoxification and continuous cultivation of dilute-acid hydrolyzate to ethanol by encapsulated S. cerevisiae. *J Biotechnol, 125*(3), 377-384. doi:10.1016/j.jbiotec.2006.03.013

Talebnia, F., & Taherzadeh, M. J. (2007). Physiological and morphological study of encapsulated Saccharomyces cerevisiae. *Enzyme and Microbial Technology, 41*(6), 683-688. doi:https://doi.org/10.1016/j.enzmictec.2007.05.020

Talukder, A. A., Easmin, F., Mahmud, S. A., & Yamada, M. (2016). Thermotolerant yeasts capable of producing bioethanol: isolation from natural fermented sources, identification and characterization. *Biotechnology & Biotechnological Equipment, 30*(6), 1106-1114. doi:10.1080/13102818.2016.1228477

Tang, Y.-Q., An, M.-Z., Zhong, Y.-L., Shigeru, M., Wu, X.-L., & Kida, K. (2010). Continuous ethanol fermentation from non-sulfuric acid-washed molasses using traditional stirred tank reactors and the flocculating yeast strain KF-7. *J Biosci Bioeng, 109*(1), 41-46. doi:https://doi.org/10.1016/j.jbiosc.2009.07.002

Taniguchi, M., Tohma, T., Itaya, T., & Fujii, M. (1997). Ethanol production from a mixture of glucose and xylose by co-culture of Pichia stipitis and a respiratory-deficient mutant of Saccharomyces cerevisiae. *Journal of Fermentation and Bioengineering, 83*(4), 364-370. doi:https://doi.org/10.1016/S0922-338X(97)80143-2

Tantirungkij, M., Izuishi, T., Seki, T., & Yoshida, T. (1994). Fed-batch fermentation of xylose by a fast-growing mutant of xylose-assimilating recombinant Saccharomyces cerevisiae. *Applied Microbiology and Biotechnology, 41*(1), 8-12.

Tataridis, P., Ntagas, P., Voulgaris, I., & Nerantzis, E. (2005). *Production of sparkling wine with immobilized yeast fermentation* (Vol. 1).

TeBeest, D. O. (2012). *Microbial control of weeds*: Springer Science & Business Media.

Techaparin, A., Thanonkeo, P., & Klanrit, P. (2017). High-temperature ethanol production using thermotolerant yeast newly isolated from Greater Mekong Subregion. *Brazilian Journal of Microbiology, 48*(3), 461-475. doi:https://doi.org/10.1016/j.bjm.2017.01.006

Technology, L. E. (2011). *Biofuels International*.

Teng, X., & Hardwick, J. M. (2013). Quantification of genetically controlled cell death in budding yeast *Necrosis* (pp. 161-170): Springer.

Terán Hilares, R., Ienny, J. V., Marcelino, P. F., Ahmed, M. A., Antunes, F. A. F., da Silva, S. S., & Santos, J. C. d. (2017). Ethanol production in a simultaneous saccharification and fermentation process with interconnected reactors employing hydrodynamic cavitation-pretreated sugarcane bagasse as raw material. *Bioresour Technol, 243*, 652-659. doi:https://doi.org/10.1016/j.biortech.2017.06.159

Thomas, P., Sekhar, A. C., Upreti, R., Mujawar, M. M., & Pasha, S. S. (2015). Optimization of single plate-serial dilution spotting (SP-SDS) with sample anchoring as an assured method for bacterial and yeast cfu enumeration and single colony isolation from diverse samples. *Biotechnology Reports, 8*, 45-55. doi:https://doi.org/10.1016/j.btre.2015.08.003

Thorne, B. L. (1997). Evolution of eusociality in termites. *Annual Review of Ecology and Systematics, 28*, 27-54.

Tong, Z., Chen, Y., Liu, Y., Tong, L., Chu, J., Xiao, K., . . . Chu, X. (2017). Preparation, Characterization and Properties of Alginate/Poly(gamma-glutamic acid) Composite Microparticles. *Mar Drugs, 15*(4). doi:10.3390/md15040091

Travisano, M., & Velicer, G. J. (2004). Strategies of microbial cheater control. *Trends Microbiol, 12*(2), 72-78. doi:10.1016/j.tim.2003.12.009

Trivers, R. (1971). *The Evolution of Reciprocal Altruism* (Vol. 46).

Tsang, F., & Lin, S.-J. (2015). Less is more: Nutrient limitation induces cross-talk of nutrient sensing pathways with NAD(+) homeostasis and contributes to longevity. *Frontiers in biology, 10*(4), 333-357. doi:10.1007/s11515-015-1367-x

Tsuruta, H., Paddon, C. J., Eng, D., Lenihan, J. R., Horning, T., Anthony, L. C., . . . Newman, J. D. (2009). High-Level Production of Amorpha-4,11-Diene, a Precursor of the Antimalarial Agent Artemisinin, in <italic>Escherichia coli</italic>. *PLoS One, 4*(2), e4489. doi:10.1371/journal.pone.0004489

Turnbull, L., Toyofuku, M., Hynen, A. L., Kurosawa, M., Pessi, G., Petty, N. K., . . . Whitchurch, C. B. (2016). Explosive cell lysis as a mechanism for the biogenesis of bacterial membrane vesicles and biofilms. *Nat Commun, 7*, 11220. doi:10.1038/ncomms11220

University, N. D. S. (2010).

Unrean, P., & Khajeeram, S. (2015). Model-based optimization of Scheffersomyces stipitis and Saccharomyces cerevisiae co-culture for efficient lignocellulosic ethanol production. *Bioresources and Bioprocessing, 2*(1), 41. doi:10.1186/s40643-015-0069-1

Vachova, L., Cap, M., & Palkova, Z. (2012). Yeast colonies: a model for studies of aging, environmental adaptation, and longevity. *Oxid Med Cell Longev, 2012*, 601836. doi:10.1155/2012/601836

Váchová, L., Čáp, M., & Palková, Z. (2012). Yeast Colonies: A Model for Studies of Aging, Environmental Adaptation, and Longevity. *2012*, 601836. doi:10.1155/2012/601836

Vachova, L., Hatakova, L., Cap, M., Pokorna, M., & Palkova, Z. (2013). Rapidly developing yeast microcolonies differentiate in a similar way to aging giant colonies. *Oxid Med Cell Longev, 2013*, 102485. doi:10.1155/2013/102485

Vachova, L., Kucerova, H., Devaux, F., Ulehlova, M., & Palkova, Z. (2009). Metabolic diversification of cells during the development of yeast colonies. *Environ Microbiol, 11*(2), 494-504. doi:10.1111/j.1462-2920.2008.01789.x

Vachova, L., & Palkova, Z. (2005). Physiological regulation of yeast cell death in multicellular colonies is triggered by ammonia. *J Cell Biol, 169*(5), 711-717. doi:10.1083/jcb.200410064

Vachova, L., & Palkova, Z. (2011). Aging and longevity of yeast colony populations: metabolic adaptation and differentiation. *Biochem Soc Trans, 39*(5), 1471-1475. doi:10.1042/bst0391471

Váchová, L., & Palková, Z. (2018). How structured yeast multicellular communities live, age and die? *FEMS Yeast Res, 18*(4). doi:10.1093/femsyr/foy033

Vancanneyt, M., De Vos, P., Maras, M., & De Ley, J. (1990). Ethanol Production in Batch and Continuous Culture from Some Carbohydrates with Clostridium thermosaccharolyticum LMG 6564. *Systematic and Applied Microbiology, 13*(4), 382-387. doi:https://doi.org/10.1016/S0723-2020(11)80237-7

Vautrin, E., & Vavre, F. (2009). Interactions between vertically transmitted symbionts: Cooperation or conflict? *Trends Microbiol, 17*(3), 95-99. doi:10.1016/j.tim.2008.12.002

Ventola, C. L. (2015). The antibiotic resistance crisis: part 1: causes and threats. *Pharmacy and therapeutics, 40*(4), 277.

Verbelen, P. J., De Schutter, D. P., Delvaux, F., Verstrepen, K. J., & Delvaux, F. R. (2006). Immobilized yeast cell systems for continuous fermentation applications. *Biotechnol Lett, 28*(19), 1515-1525. doi:10.1007/s10529-006-9132-5

Verduyn, C., Postma, E., Scheffers, W. A., & van Dijken, J. P. (1990). Energetics of Saccharomyces cerevisiae in anaerobic glucose-limited chemostat cultures. *J Gen Microbiol, 136*(3), 405-412. doi:10.1099/00221287-136-3-405

Verrills, N. M. (2006). Clinical proteomics: present and future prospects. *Clin Biochem Rev, 27*(2), 99-116.

Vidoli, R., Yamazaki, H., Nasim, A., & Veliky, I. A. (1982). A novel procedure for the recovery of hybrid products from protoplast fusion. *Biotechnol Lett, 4*(12), 781-784. doi:10.1007/bf00131152

Visser, W., Scheffers, W. A., Batenburg-van der Vegte, W. H., & van Dijken, J. P. (1990). Oxygen requirements of yeasts. *Appl Environ Microbiol, 56*(12), 3785-3792.

Vos, T., Hakkaart, X. D., de Hulster, E. A., van Maris, A. J., Pronk, J. T., & Daran-Lapujade, P. (2016). Maintenance-energy requirements and robustness of Saccharomyces cerevisiae at aerobic near-zero specific growth rates. *Microb Cell Fact, 15*(1), 111. doi:10.1186/s12934-016-0501-z

Wade, M. J., Wilson, D. S., Goodnight, C., Taylor, D., Bar-Yam, Y., de Aguiar, M. A. M., . . . Zee, P. (2010). Multilevel and kin selection in a connected world. *Nature, 463*(7283), E8-E9.

Wang, N., Adams, G., Buttery, L., Falcone, F. H., & Stolnik, S. (2009). Alginate encapsulation technology supports embryonic stem cells differentiation into insulin-producing cells. *J Biotechnol, 144*(4), 304-312. doi:https://doi.org/10.1016/j.jbiotec.2009.08.008

Wang, Y., & Dohlman, H. G. (2004). Pheromone signaling mechanisms in yeast: a prototypical sex machine. *Science, 306*(5701), 1508-1509. doi:10.1126/science.1104568

Wang, Y., Liu, C. L., Storey, J. D., Tibshirani, R. J., Herschlag, D., & Brown, P. O. (2002). Precision and functional specificity in mRNA decay. *Proc Natl Acad Sci U S A, 99*(9), 5860-5865. doi:10.1073/pnas.092538799

Wasko, B. M., & Kaeberlein, M. (2014). Yeast replicative aging: a paradigm for defining conserved longevity interventions. *FEMS Yeast Res, 14*(1), 148-159. doi:10.1111/1567-1364.12104

Watanabe, I., Miyata, N., Ando, A., Shiroma, R., Tokuyasu, K., & Nakamura, T. (2012). Ethanol production by repeated-batch simultaneous saccharification and fermentation (SSF) of alkali-treated rice straw using immobilized Saccharomyces cerevisiae cells. *Bioresour Technol, 123*, 695-698. doi:10.1016/j.biortech.2012.07.052

Webb, K. J., Xu, T., Park, S. K., & Yates, J. R., 3rd. (2013). Modified MuDPIT separation identified 4488 proteins in a system-wide analysis of quiescence in yeast. *J Proteome Res, 12*(5), 2177-2184. doi:10.1021/pr400027m

Webber, R. E., & Shull, K. R. (2004). Strain Dependence of the Viscoelastic Properties of Alginate Hydrogels. *Macromolecules, 37*(16), 6153-6160. doi:10.1021/ma049274n

Wei, M., Fabrizio, P., Hu, J., Ge, H., Cheng, C., Li, L., & Longo, V. D. (2008). Life span extension by calorie restriction depends on Rim15 and transcription factors downstream of Ras/PKA, Tor, and Sch9. *PLoS Genet, 4*(1), e13. doi:10.1371/journal.pgen.0040013

Wei, M., Madia, F., & Longo, V. D. (2011). Studying age-dependent genomic instability using the S. cerevisiae chronological lifespan model. *J Vis Exp*(55). doi:10.3791/3030

Werner-Washburne, M., Braun, E., Johnston, G. C., & Singer, R. A. (1993). Stationary phase in the yeast Saccharomyces cerevisiae. *Microbiol Rev, 57*(2), 383-401.

Westman, J. O., Bonander, N., Taherzadeh, M. J., & Franzen, C. J. (2014). Improved sugar co-utilisation by encapsulation of a recombinant Saccharomyces cerevisiae strain in alginate-chitosan capsules. *Biotechnol Biofuels, 7*, 102. doi:10.1186/1754-6834-7-102

Westman, J. O., Manikondu, R. B., Franzen, C. J., & Taherzadeh, M. J. (2012). Encapsulation-induced stress helps Saccharomyces cerevisiae resist convertible Lignocellulose derived inhibitors. *Int J Mol Sci, 13*(9), 11881-11894. doi:10.3390/ijms130911881

Westman, J. O., Mapelli, V., Taherzadeh, M. J., & Franzén, C. J. (2014). Flocculation Causes Inhibitor Tolerance in Saccharomyces cerevisiae for Second-Generation Bioethanol Production. *Appl Environ Microbiol, 80*(22), 6908-6918. doi:10.1128/AEM.01906-14

Westman, J. O., Taherzadeh, M. J., & Franzen, C. J. (2012). Proteomic analysis of the increased stress tolerance of saccharomyces cerevisiae encapsulated in liquid core alginate-chitosan capsules. *PLoS One, 7*(11), e49335. doi:10.1371/journal.pone.0049335

Westman, J. O., Taherzadeh, M. J., & Franzén, C. J. (2012). Proteomic analysis of the increased stress tolerance of saccharomyces cerevisiae encapsulated in liquid core alginate-chitosan capsules. *PLoS One, 7*(11), e49335-e49335. doi:10.1371/journal.pone.0049335

White, F. H., & Portno, A. D. (1978). CONTINUOUS FERMENTATION BY IMMOBILIZED BREWERS YEAST. *Journal of the Institute of Brewing, 84*(4), 228-230. doi:doi:10.1002/j.2050-0416.1978.tb03878.x

Wilkinson, D., Marsikova, J., Hlavacek, O., Gilfillan, G. D., Jezkova, E., Aalokken, R., . . . Palkova, Z. (2018). Transcriptome Remodeling of Differentiated Cells during Chronological Ageing of Yeast Colonies: New Insights into Metabolic Differentiation. *Oxid Med Cell Longev, 2018*, 4932905. doi:10.1155/2018/4932905

Willaert, R., & Nedovic, V. A. (2006). Primary beer fermentation by immobilised yeast—a review on flavour formation and control strategies. *Journal of Chemical Technology & Biotechnology, 81*(8), 1353-1367. doi:doi:10.1002/jctb.1582

Williams, D., & Munnecke, D. M. (1981). The production of ethanol by immobilized yeast cells. *Biotechnology and Bioengineering, 23*(8), 1813-1825. doi:doi:10.1002/bit.260230809

Wilson, E. O. (1971). The insect societies. *The insect societies.*

Wilson, E. O., & Hölldobler, B. (2005). Eusociality: Origin and consequences. *Proc Natl Acad Sci U S A, 102*(38), 13367-13371. doi:10.1073/pnas.0505858102

Wojdyla, B. (2013). Retrieved from http://www.popularmechanics.com/cars/hybrid-electric/a11687/four-things-to-know-about-e15-15096134/

Won, K. Y., Kim, Y. S., & Oh, K. K. (2012). Comparison of bioethanol production of simultaneous saccharification & fermentation and separation hydrolysis & fermentation from cellulose-rich barley straw. *Korean Journal of Chemical Engineering, 29*(10), 1341-1346. doi:10.1007/s11814-012-0019-y

Woo, J.-W., Roh, H.-J., Park, H.-D., Ji, C.-I., Lee, Y.-B., & Kim, S.-B. (2007). Sphericity optimization of calcium alginate gel beads and the effects of processing conditions on their physical properties. *Food Science and Biotechnology, 16*(5), 715-721.

Xinhua. (2016). Retrieved from http://news.xinhuanet.com/english/2016-01/25/c_135043964.htm

Yague, P., Lopez-Garcia, M. T., Rioseras, B., Sanchez, J., & Manteca, A. (2012). New insights on the development of Streptomyces and their relationships with secondary metabolite production. *Curr Trends Microbiol, 8*, 65-73.

Ylitervo, P., Franzen, C. J., & Taherzadeh, M. J. (2011). Ethanol production at elevated temperatures using encapsulation of yeast. *J Biotechnol, 156*(1), 22-29. doi:10.1016/j.jbiotec.2011.07.018

Yomano, L., York, S., & Ingram, L. (1998). Isolation and characterization of ethanol-tolerant mutants of Escherichia coli KO11 for fuel ethanol production. *Journal of Industrial Microbiology and Biotechnology, 20*(2), 132-138.

Yoon, G. S., Lee, T. S., Kim, C., Seo, J. H., & Ryu, Y. W. (1996). *Characterization of alcohol fermentation and segregation of protoplast fusant of Saccharomyces cerevisiae and Pichia stipitis* (Vol. 6).

You, L., Cox, R. S., Weiss, R., & Arnold, F. H. (2004). Programmed population control by cell-cell communication and regulated killing. *Nature, 428*(6985), 868-871.

Youssef, K. A., Ghareib, M., & Khalil, A. A. (1989). Production of ethanol by alginate-entrapped Saccharomyces cerevisiae strain "14-12". *Indian J Exp Biol, 27*(2), 121-123.

Zaldivar, J., Nielsen, J., & Olsson, L. (2001). Fuel ethanol production from lignocellulose: a challenge for metabolic engineering and process integration. *Appl Microbiol Biotechnol, 56*(1-2), 17-34.

Zarrinpar, A., Park, S.-H., & Lim, W. A. (2003). Optimization of specificity in a cellular protein interaction network by negative selection. *Nature, 426*(6967), 676-680. doi:http://www.nature.com/nature/journal/v426/n6967/suppinfo/nature02178_S1.html

Zegerman, P., & Diffley, J. F. X. (2009). DNA replication as a target of the DNA damage checkpoint. *DNA repair, 8*(9), 1077-1088. doi:10.1016/j.dnarep.2009.04.023

Zhang, M., Xiao, Y., Zhu, R., Zhang, Q., & Wang, S.-L. (2012). Enhanced thermotolerance and ethanol tolerance in Saccharomyces cerevisiae mutated by high-energy pulse electron beam and protoplast fusion. *Bioprocess and Biosystems Engineering, 35*(9), 1455-1465. doi:10.1007/s00449-012-0734-0

Zhang, Y., Wang, C., Wang, L., Yang, R., Hou, P., & Liu, J. (2017). Direct bioethanol production from wheat straw using xylose/glucose co-fermentation by co-culture of two recombinant yeasts. *J Ind Microbiol Biotechnol, 44*(3), 453-464. doi:10.1007/s10295-016-1893-9

Zhao, J., & Xia, L. (2010). Ethanol production from corn stover hemicellulosic hydrolysate using immobilized recombinant yeast cells. *Biochemical Engineering Journal, 49*(1), 28-32. doi:https://doi.org/10.1016/j.bej.2009.11.007

Zhu, J. Q., Li, X., Qin, L., Li, W. C., Li, H. Z., Li, B. Z., & Yuan, Y. J. (2016). In situ detoxification of dry dilute acid pretreated corn stover by co-culture of xylose-utilizing and inhibitor-tolerant Saccharomyces cerevisiae increases ethanol production. *Bioresour Technol, 218*, 380-387. doi:10.1016/j.biortech.2016.06.107

Zimmermann, A., Kainz, K., Hofer, S., Pendl, T., Carmona-Gutierrez, D., & Madeo, F. (2018). Yeast as a tool to identify anti-aging compounds. *FEMS Yeast Res, 18*(6). doi:10.1093/femsyr/foy020

Zorova, L. D., Popkov, V. A., Plotnikov, E. Y., Silachev, D. N., Pevzner, I. B., Jankauskas, S. S., . . . Zorov, D. B. (2018). Mitochondrial membrane potential. *Anal Biochem, 552*, 50-59. doi:10.1016/j.ab.2017.07.009